DURBAN UNIVERSITY OF TECHNOLOGY
INYUVESI YASETHEKWINI YEZOBUCHWEPHESHE

ENHANCED BIOHYDROGEN PRODUCTION FROM CARBOHYDRATE-RICH WASTEWATER THROUGH ANAEROBIC FERMENTATION

Submitted in fulfilment of the requirements for Master of Engineering degree in Chemical Engineering at the Durban University of Technology

By
Boldwin Mutsvene (21649785)

2020

Supervisor…… Date…….

Dr. M. Chetty

Co-Supervisor……. Date…….

Dr. S.K.K. Pillai

Co-Supervisor……. Date…….

Prof. F. Bux

DECLARATION

I **BOLDWIN MUTSVENE** declare that:

i. The research reported in this thesis, except where otherwise indicated, is my original work.

ii. This thesis has not been submitted for any degree or examination at any other university.

iii. This thesis does not contain other persons' data, pictures, graphs or other information unless specifically acknowledged as being sourced from other persons.

iv. This thesis does not contain other persons' writing unless specifically acknowledged as being sourced from other researchers. Where other written sources have been quoted, then:

   a. their words have been re-written, but the general information attributed to them has been referenced;

   b. where their exact words have been used, their writing has been placed inside quotation marks, and referenced.

v. Where I have reproduced a publication of which I am an author, co-author, or editor, I have indicated in detail which part of the publication was actually written by myself alone and have fully referenced such publications.

vi. This thesis does not contain text, graphics or tables copied and pasted from the Internet, unless specifically acknowledged, and the source being detailed in the thesis and in the References sections.

Signed: _____

ABSTRACT

In recent times, the world has faced serious problems emanating from the use of fossil fuels which are detrimental to the environment at large. On the other hand, due to the industrial boom, many industries produce wastewater that is harmful to the environment hence, carbohydrate-rich industrial wastewater can be advantageously used to reduce impact on the environment. If subjected to anaerobic fermentation, organic wastewater has the potential to produce renewable energy sources that have less impact on the environment, including biohydrogen, which has little or no carbon footprint. While reducing the impact of the problems caused by the disposal of wastewater to the environment, the biological methods also offer a solution to the detrimental effects of fossil fuels and their after use effects. The study was mainly based on environmental protection and clean, renewable alternative energy production by generating biohydrogen from organic industrial wastewater as a substrate. Anaerobic digestion has been extensively studied, but dark fermentation, which is an emerging technology within anaerobic digestion that involves the production of hydrogen from carbohydrate-rich substrates, has less information documented regarding this technology. This technology is crucial in the because it forecasts beyond fossil fuel usage and is accompanied with long-term economic expansion and energy security as there are many reservations about fossil fuel reserves and their high risk of exploitation.

Biohydrogen potential tests (BHP) were performed on five different wastewater streams (yeast, alcohols, brewery, sugar, and dairy industries) to determine the stream with the best hydrogen potential. Rigorous characterisation of various wastewater streams was conducted; the main parameters of interest were COD, BOD, VS, TS, pH, among others. The BHP tests were conducted in triplicates in 600 mL Schott bottles charged independently with various wastewater streams and inoculated by the seed sludge from a local wastewater treatment plant at the different substrate to biomass ratios. The highest hydrogen composition was recorded with the brewery wastewater, which had 40.1% H_2 in the off-gas as analysed by the gas chromatograph; and the minimum was found in alcohol wastewater, 21.4%. The Kepner-Tregor decision-making tool was conducted to determine the most suitable stream for the scaled-up reactor. A conclusion to use the brewery wastewater in the scaled-up Anaerobic Baffled Reactor (ABR) was reached.

Four 10 L Anaerobic Baffled Reactors were used as the scaled-up reactors to optimise operating conditions for the production of biohydrogen using the brewery wastewater. Design-Expert software, under response surface methodology, was used to produce the matrix of combinations of the experimental runs by varying temperature (32-38℃), batch time (4-16 h), and pH (3.5-7.5); in total 20 runs were formulated.

The highest hydrogen production rate of 18.16 mL/h and the hydrogen yield of 30.98 mmol/gCOD were observed at temperature, batch time, and pH of 35℃, 4-10 h, and 5, respectively. The optimum operating conditions were determined to be a temperature of 36℃, batch time of 10.2 h, and a pH of 5.6. A predictive model, quadratic polynomial in nature, was developed after an intensive analysis of variance, a regression coefficient between predicted and actual hydrogen production rates was found to be 0.92.

A system was run on optimum conditions to validate the developed mathematical model. The maximum hydrogen potential rate (HPR) determined in this study was 6.11% higher than the predicted value. The validation runs were also performed as control experiments for comparison between a system with nanoparticles and a system without nanoparticles with regards to the HPR. 25.37% H_2 and 21.85% H_2 were determined for with magnetite nanoparticle system and a system without nanoparticles, respectively. The experiments with nanoparticles garnered 44% higher HPR (23.41 mL/h) than a system without nanoparticles.

ACKNOWLEDGEMENTS

First and foremost, I would love to express my sincere and hearty thanks to the Lord God Almighty for leading me throughout my studies and the opportunity to be at this institution and in the Department of Chemical Engineering. Secondly, I would like to make a special mention of my supervisor Dr. M. Chetty for her guidance throughout the whole study, I thank her so much for sharpening my engineering skills, and without her experience and knowledge, this project would not have had substance. God bless you so much.

My profound gratitude is again forwarded to the Institute for Water and Wastewater Technology (IWWT) family, particularly Prof. F. Bux and Dr. S. Kumari, for their permission, mentorship, and assistance in the conduction of experiments at IWWT. My heartfelt thanks go to Ismail, Krieveshin, Precious, and other fellow students at IWWT, I am indebted to them.

I would also significantly extend my vigorous and cheerful gratitude and honour to my family members, especially my parents Mr. and Mrs. Mutsvene, for their invaluable moral and emotional support throughout my project. I also make a special mention to my wife for her invaluable moral support.

Last but not least, I would have done injustice if I do not mention my academic friends and fellow engineers Sheriff, Eric, Teleleni Haikela, Chiodza, and Elvis Ganda, among others. Their help, contribution, and constructive criticism made this project to be a success.

DEDICATION

I dedicate this project to my nephew Kyle Tavonga Mutsvene and my wife Vimbainashe Cynthia Makowa Mutsvene

TABLE OF CONTENTS

LIST OF FIGURES

LIST OF TABLES

ACRONYMS AND NOMENCLATURE

μ_m	Maximum specific growth rate, h^{-1}
ABR	Anaerobic Baffled Reactors
ANN	Artificial Neural Network
ANOVA	Analysis of variance
AP	Adequate Precision
APHA	American Public Health Association
ARB	Anode-Respiring Bacteria
ATP	Adenosine Triphosphate
BBD	Box and Behnken Design
BHP	Biochemical Hydrogen Potential
BOD	Biochemical Oxygen Demand
BT	Batch Time
C_B	COD/BOD ratio
CCD	Central Composite Design
CFD	Computational Fluid Dynamics
CH_3COOH	Acetate molecule
COD	Chemical Oxygen Demand
COD_{total}	Total Chemical Oxygen Demand (G/L)
CSTR	Completely Stirred Tank Reactor
D	Depth of the reactor.
DEWATS	Decentralised Wastewater Treatment Systems
DFS	Dark Fermentative System
Dm	Doehlert Matrix
DSW	Designed Synthetic Wastewater
DVS	Dissolved Volatile Solids
Emf	Electromotive Force

Fd	Ferredoxin
Fd_{red}	Reduced Ferredoxin
Gc	Gas Chromatograph
H	Cumulative Hydrogen Volume Generated (Ml),
HPB	Hydrogen Producing Bacteria
HPR	Hydrogen Production Rate
HRT	Hydraulic Retention Time
K_i	Inhibition Constant, G-Cod L^{-1}
K_m	Dissociation Constant
MABR	Modified Anaerobic Baffled Reactor
MB	Methanogenic Bacteria
MEC	Microbial Electrolysis Cell
m_i	Mass of sugar 1, sugar 2, sugar 3, etc. in the substrate (g).
M_i	Molar mass of sugar 1, sugar 2, sugar 3, etc. in the substrate (g/mol).
m_s	Maintenance Coefficient, g-COD g-VSS^{-1}
MSW	Municipal Solid Waste
NADH	Nicotinamide Adenine Dinucleotide (hydrogen)
nm	Nanometres
nNP	Without nanoparticles
NP	With nanoparticles
OLR	Organic Loading Rate
ORP	Oxidation-Reduction Potential
P	Potential of hydrogen formation (ml),
P	Pressure of the operating system, Pa
PBR	Packed Bed Reactor
PMEC	Photosynthetic Microbial Electrochemical Cell
PNS	Photosynthetic Non-Sulphur

PSB	Photosynthetic Bacteria
R	Hydrogen production rate, mM h^{-1}
R	Universal gas constant, Pa. m^3/ (mol.K)
R_m	The highest rate of formation (mL/h) and
RSM	Response Surface Methodology
R-squared	Denotes the R^2 value
S	Substrate concentration, g-COD L^{-1}
SDR	Substrate Degradation Rate
SHPR	Specific Hydrogen Production Rate
SMP	The Soluble Metabolite Products
S_o	Initial substrate concentration, g-COD L^{-1}
SS	Suspended Solids
t	Fermentation time, h
T	Temperature of the system, K
TCD	Thermal Conductivity Detector
TDS	Total Dissolved Solids
TON	Total Oxidisable Nitrogen
TS	Total Solids
TSG	Total Sugar
TSS	Total Suspended Solids
TVS	Total Volatile Solids
UASB	Upflow Anaerobic Sludge Blanket
v	Specific substrate degradation rate, g-COD $gVSS^{-1}$ h^{-1}
V	Volume of the reactor
VFA	Volatile Fatty Acid
VHPR	Volumetric Hydrogen Production Rate
v_m	Maximum specific substrate degradation rate, gCOD.gCODgVSS^{-1} h^{-1}

VS	Volatile Solids
VSS	Volatile Suspended Solids (g/L)
V_{subs}	Volume of the substrate (litres)
WAS	Waste Activated Sludge
X_m	Maximum attainable biomass concentration, gVSS L^{-1}
X_o	Initial biomass concentration, g-VSS L^{-1}
$Y_{x/S}$	Maximum yield coefficient, g-VSS g-COD^{-1}
λ	Lag phase (h).

PREFACE

Outputs

Conferences participated

Mutsvene, B., and Chetty, M. 2018. Enhanced biohydrogen production from carbohydrate-rich wastewater through anaerobic fermentation. The South African Institution of Chemical Engineers In collaboration with The Institution of Chemical Engineers, August 17, UKZN, Durban, South Africa.

Mutsvene, B., Bux, F., Chetty, M., and Sheena-Kumari. 2018. Biohydrogen Potential of Industrial Wastewater. Oral presentation. Proceedings of the 21st Conference on Process Integration, Modelling and Optimisation for Energy Saving and Pollution Reduction, 25-29 August, Prague, Czech Republic.

Mutsvene, B., Bux, F., Chetty, M., and Sheena-Kumari. 2019. Enhanced biohydrogen production from industrial wastewater through dark fermentation in an Anaerobic Baffled Reactor. 6th South African Young Water Professionals (YWP-ZA) Biennial Conference, 20-22 October 2, Durban ICC, South Africa.

CHAPTER ONE

INTRODUCTION

1.1 Problem statement

The global economy has been largely impacted by the use of fossil fuels, which have been overly consumed as an energy source. Today, requirements of global energy are primarily met through the combustion of fossil fuels, contributing to 80% of the world's energy consumption (Biresselioglu and Yelkenci 2016; Covert, Greenstone and Knittel 2016). The global energy demand has exponentially grown while there is a decrease in fossil fuel reserves (Owusu and Asumadu-Sarkodie 2016; Musa *et al.* 2018). Additionally, the motivation to explore alternative sources of energy that are renewable and environmentally friendly has been propagated by environmental contamination caused by the use of fossil fuel and its decrease in reserves or finite nature (Bauer *et al.* 2016). On the other hand, the wastewater, which is carbohydrate-laden, has several negative impacts on the environment if discharged untreated. Some of the problems encountered are a decline in the surface water quality (Elahi *et al.* 2017), the nitrates in the groundwater increase (Katz 2019), and irritating impact from malodour and spray drift (Poddar and Sahu 2017). There has been an increasing appetency for the employment of renewable fuels, not only in a bid to minimise dependence on fossil fuels but also to ameliorate on the damage caused by fossil fuels on the environment. This motivated the idea of creating and finding alternative sources of fuel. Hydrogen (H_2), being a highly-priced fuel to the industry, has become a favourite energy source and is regarded as an alternative fuel (Vinoth Kanna and Paturu 2018; Hoffmann 2019).

The hydrogen technology has been of interest and relevant to renewable energy topic that has gained popularity globally. Hydrogen being a clean source of energy (releases only water instead of greenhouse gases upon combustion), is characterised with a high energy density of about 120 MJ/kg (Kan and Strezov 2018). Different from fossil fuels, hydrogen is free from CO_2, CO, SO_x and NO_x emissions releasing water as the only by-product upon combustion, thus significantly lowering the greenhouse effects. Hydrogen is a potential primary energy source of the future, and electricity generation by the use of fuel cells can be adopted (Rohendi *et al.* 2018).

One of the most attractive methods of hydrogen production is biological hydrogen generation from organic waste material by the action of microorganisms because hydrogen has a limited number of environmental threats (Kapdan *et al.* 2009; Veeravalli *et al.* 2019). Biological processes mainly involve photosynthetic hydrogen generation (photofermentation), fermentative hydrogen production (dark fermentation) and biophotolysis of water using cyanobacteria and algae (Kumar *et al.* 2018). Dark fermentation is considered as a practically achievable process because it produces biohydrogen from carbohydrate-rich substrates including organic waste materials and biomass. However, the process has relatively low biohydrogen yield, since biohydrogen is generated as an intermediate of the biomethanation process (Turhal, Turanbaev and Argun 2019). As an intermediate, hydrogen can be further reduced to methane, propionate, and acetate by hydrogen-consuming bacteria (HCB) during dark fermentation leading to low H_2 yield (Kumar *et al.* 2018).

Producing hydrogen through the anaerobic process is preferable in terms of cost and feasibility—biologically produced hydrogen results in a win-win solution (Bolatkhan *et al.* 2019). Besides being a clean fuel, it also solves the problem of industrial waste. By using these industrial wastes as a substrate for producing hydrogen, the wastes being dumped and treated will be reduced into something more beneficial, and it also contributes to renewable extraction of clean gas (Vinoth Kanna and Paturu 2018). This is also in line with the environmental management systems, ISO 14001:2015 which postulates that application of farsighted methods to guard the environment against damage and destruction, such as sustainable resource use and climate change alleviation. A focus on life cycle assessment to ensure consideration of environmental aspects from development to end-of-life.

Critical factors in fermentative hydrogen generation are feed concentration, temperature, pH, hydraulic retention time (HRT), bacterial population among other vital factors (Gokfiliz-Yildiz and Karapinar 2018; Karapinar *et al.* 2019). Experiments have been performed to study the probability of hydrogen generation using carbohydrate-rich wastes from different industries, coupled with the wastewater treatment strategy (Veeravalli *et al.* 2019).

The high cost of suitable feedstock for hydrogen production has led to the use of biomass as feedstock. According to a study by Kotay and Das (2008), a conclusion was reached that industrial waste could become a crucial and significant source of renewable hydrogen. However, processes involved in using the low-cost waste biomass require a much more expensive and complicated procedure compared to the derivation of hydrogen from natural gas. Although using biomass as a substrate in producing hydrogen is a breakthrough in technology today, its low hydrogen conversion efficiency and low yield of biohydrogen are questionable

(Turhal, Turanbaev and Argun 2019). However, this can be overcome by the use of microbial consortia which can increase the yield apart from improving operating parameters and reactor design.

Therefore, this research aims to increase the biohydrogen production rate from carbohydrate-rich industrial wastewater by optimising operating parameters and the use of metallic oxide nanoparticles in dark fermentation in an anaerobic baffled reactor (ABR). An ABR was used because of its satisfactory heat and mass transfer properties in comparison to reactors such as the (Upflow anaerobic sludge blanket) UASBs and packed bed reactor (PBR). The ABR is much easier to operate more than the UASBs and PBR.

The magnetite nanoparticles have excellent physical and chemical properties that alter the surface characteristics of the microbes involved, increasing the surface area and activity of the hydrogen-producing bacteria (HPB) (Taherdanak, Zilouei and Karimi 2015; Kumar *et al.* 2019). The increased activity has a direct impact on the hydrogen production rate (HPR).

Carbohydrate-rich industrial wastewater is a feedstock that is readily available, cheap and abundant, with a high concentration of carbohydrates which are highly biodegradable. Biohydrogen and biomethane production are produced using similar techniques and infrastructure, but hydrogen production is slowly taking precedence due to a host of reasons. Hydrogen has a broader scope of industrial applications in comparison to methane. Hydrogen is used for the manufacturing of useful chemicals such as fertilisers, hydrogenation of oils, among other chemicals, whereas methane is mainly used as a fuel (Gupta, Basile and Veziroglu 2016). Hydrogen also has the edge over methane because of its high energy density that is superior to that of methane (about three times higher in calorific value) and hydrogen only produces water upon combustion. Hence, the carbon footprint is significantly reduced by the adoption of hydrogen as an alternative renewable source.

This study focused on characterising five wastewater streams to determine the stream with best hydrogen potential, after which it was used as the substrate in the scaled-up reactors. In the scaled-up reactor, operating parameters such as temperature, batch time and pH were optimised for the highest HPR. The optimum conditions were later adopted to test the effect of metallic oxide nanoparticles on HPR. A model based on the data collected was developed, validated and calibrated.

1.2 Aim and objectives

1.2.1 Aim

The aim of the study is to enhance biohydrogen production from carbohydrate-rich industrial wastewater through an improved dark fermentation process using an anaerobic baffled reactor.

1.2.2 Objectives

The aim above is satisfied by the following specific objectives succinctly not in order of priority:

1. Characterise various industrial wastewater streams to determine the most suitable wastewater stream for the dark fermentation process.
2. Optimise hydrogen production from the selected wastewater stream by dark fermentation in an ABR.
3. Develop and apply mathematical models for fermentative hydrogen production from the selected wastewater stream.
4. Evaluate the effect of metallic oxide nanoparticles on the hydrogen production rate.

1.3 Hypotheses and Key Questions

The hypothesis is stated as follows:

Dark fermentation of organic-rich industrial wastewater to produce biohydrogen, using modified bioreactors, is a cost effective and sustainable method, in comparison to physicochemical and other biological methods.

The key questions that are going to be addressed in proving the hypothesis are:

1. Is biohydrogen production from industrial wastewater a technically feasible process?
2. Which process variables have a great impact on the yields and production rates of the dark fermentation process?
3. What are the environmental implications of the dark fermentation process?

1.4 Thesis structure

Chapter 1: Introduces the whole project. It gives a summary of the entire project. It highlights why and how the project was done. The background information on the project is also documented in this chapter.

Chapter 2: This chapter reviewed the literature for both previous and current similar works from scientific investigations on the effectiveness of biohydrogen production methods. It provided some concepts to understand the impact of the current research. This chapter also presents the equations and theory used from the selected method to compute components of various mathematical models.

Chapter 3: Extensive characterisation of various wastewater streams was conducted, and the best substrate in terms of biohydrogen production was selected with some other non-technical factors considered.

Chapter 4: This chapter saw the optimisation of hydrogen production by dark fermentation in an ABR. Operating factors were studied, and the best conditions for hydrogen production for a specific substrate were determined.

Chapter 5: The effects of metal oxide nanoparticles were studied on the optimised operating conditions. Particular attention was given to the improvement of the rate of hydrogen production. Magnetite nanoparticles were used in the investigation.

Chapter 6: A correlation between input variables and product formation was determined in the form of a statistical regression model.

Chapter 7: This chapter presented the conclusion and recommendations reached to produce biohydrogen based on the experimental results.

CHAPTER TWO

LITERATURE REVIEW

2.1 Introduction

Fossil fuel combustion by automobiles and coal-fired power industries is a major contributor to the release of greenhouse gases into the environment (Farrauto, Deeba and Alerasool 2019). The effects of increased greenhouse gas emissions are global warming which leads to ocean acidification, smog pollution, ozone depletion as well as changes to plant growth and nutrition levels. Therefore, there is a need for alternative energy that is less polluting, affordable, sustainable, and environmentally friendly. Hydrogen is a clean and environmentally friendly source of fuel that releases only water upon combustion instead of polluting greenhouse gases (Rohendi *et al.* 2018).

Food, beverages, and chemical processing plants' wastewater pose environmental problems. These waste streams can undergo aerobic treatment, but this method is energy-intensive as there is a need to pump air or oxygen into the treatment system (Yang *et al.* 2018b). Alternatively, wastes can be anaerobically processed to produce methane, hydrogen, carbon dioxide and others in minute quantities such as hydrogen sulphide. The anaerobic treatment has been shown to be less energy-intensive as some of the processes since high energy requirements such as aeration are eliminated from the process. Anaerobic treatment is known to produce energy carriers in the form of methane and hydrogen dependent upon conditions employed. The production of biohydrogen may be more lucrative than biomethanation if bioreactors like the ones employed in biomethane production are also used because of the high commercial value that hydrogen possesses (Reith, Wijffels and Barten 2003). Additionally, hydrogen has an energy density that is between 120 and 142 MJ/kg, nearly triple that of methane which has 55.5 MJ/kg (Soccol *et al.* 2016; Kan and Strezov 2018).

Most of the methods for generating hydrogen do not satisfy the dual benefits of producing energy and reducing the waste load (e.g. electrolysis, electrical cracking of dilute acids into oxygen and hydrogen or chemical methods which involve reforming of hydrocarbons into H_2) (Soccol *et al.* 2016). Most importantly, these methods are energy-intensive and require significant inputs of power customarily derived from the combustion of fossil fuels (Ueno, Otsuka and Morimoto 1996; Patel and Ayers 2019). Thus, these cannot be qualified as renewable sources of energy because they use conventional unclean sources of energy.

Microbial production of hydrogen from organic wastes is an important emerging branch of bioenergy generation. In recent surveys carried out, it was discovered that there is a tremendous increase in the demand for hydrogen globally, with an increase of 12% per annum and there is an estimated market contribution of hydrogen of 8-10% by 2025 (Parihar *et al.* 2017).

2.2 Biological methods of hydrogen production

Basically, there are six significant and well-documented types of biological processes that are responsible for hydrogen generation. These methods are biophotolysis, water-gas shift, microbial electrolysis cell, photofermentation, dark fermentation and combined dark & photofermentation as discussed in the followings sub-sections (Parihar *et al.* 2017; Łukajtis *et al.* 2018; Sołowski 2018).

2.2.1 Direct and Indirect biophotolysis

Several scientific documentations have been reported on the base work for erecting renewable hydrogen-producing systems through 'biophotolysis'. Biophotolysis is the generation of biohydrogen through the photosynthetic breaking of water into hydrogen and oxygen by microbes in the presence of light (Han, Kim and Shin 2005). Direct biophotolysis is carried out by green algae, whereas indirect biophotolysis is carried out by and cyanobacteria (Schopf 2014). Biophotolysis depends on light and is kinetically slow.

In direct biophotolysis, water is first split into oxygen and hydrogen with light being the energy source and protons are reduced to produce hydrogen. Nitrogenase and hydrogenase enzymes that exist in different kinds of algae catalyse this reaction. Das and Veziroglu (2008) stated that hydrogenase action was observed in *Chlorella fusca, Scenedesmus obliquus, Platymonas subcordiformis,* and *Chlorococcum littorale.* However, green algae which lack hydrogenase activity such as *Dunaliella salina* and *Chlorella vulgaris* were additionally considered (Das and Veziroglu 2008). In indirect biophotolysis, cyanobacteria first fix carbon dioxide from the air to synthesise sugars as intermediate products and those produced sugars are utilised in the subsequent reaction to generate biohydrogen and carbon dioxide (Ni *et al.* 2006). Both reactions proceed in the presence of light. This reaction needs water as the only raw material, sunlight as the source of energy and oxygen is evolved as a by-product. It is very desirable from an environmental protection point of view (Ni *et al.* 2006). *Anabaena, Oscillataria, Oscillatoria, Calothrix, Chlamidomonas* are strains, among others, of

cyanobacteria which produce biohydrogen via indirect biophotolysis (Argun, Kargi and Kapdan 2009; Nath and Das 2014).

The evolution of oxygen negatively influences the nitrogenase and hydrogenase enzymes that are responsible for biohydrogen generation. Argun (2010) revealed rates of 0.07 mmol H_2 /h.L and 0.355 mmol H_2 /h.L for both direct and indirect biophotolysis which are very low when contrasted to photofermentation and dark fermentation rates of 145-160 mmol H_2 /h.L and 77 mmolH_2/h.L, respectively. Currently, hydrogen generation rate by *Anabaena sp*. is significantly less than that produced in dark fermentation or photofermentation (Masukawa, Mochimaru and Sakurai 2002; Tsygankov *et al.* 2002; Zhang *et al.* 2017).

2.2.2 Water-gas-shift

Certain photoheterotrophic microbes of the *Rhodospirillaceae* species can grow in darkness utilising carbon monoxide as the only carbon source to form Adenosine triphosphate (ATP) and synchronously evolve hydrogen and carbon dioxide. The water-gas-shift reaction that is responsible for the oxidation of carbon monoxide to carbon dioxide to produce hydrogen is illustrated in Equation 2.1 (Das and Veziroglu 2008).

$$CO + H_2O \rightarrow H_2 + CO_2 \qquad 2.1$$

2.2.3 Microbial electrolysis cell (MEC)

MEC is a novel technique that capitalises on the combination of microbial metabolism and electrochemistry to produce hydrogen. As illustrated in Figure 2.1 anode-respiring bacteria (ARB) from genera of *Desulfuromonas, Pseudomonas, Escherichia, Geobacter, Shewanella, Klebsiella, and Clostridium* attach to the anode to oxidise simple organic substances (that is, butyrate, lactate, ethanol, acetate, and propionate) and migrate electrons to the conductive solid (Zilouei and Taherdanak 2015).

Conduction via an external electric circuit effectively enables electrons to reach the cathode, resulting in reaction with water to generate hydrogen at the cathode. Acetate which is an electron donor has a more positive standard potential (-0.28 V) than hydrogen (-0.41 V). Thus the effective theoretical electromotive force (EMF) applied for generating hydrogen is -0.13 V. To cater for energy losses taking place in the MEC, the applied EMF should be higher than 0.13 V and typically ranges from 0.6 – 1.2 V (Bensaid, Ruggeri and Saracco 2015). MEC gave significantly high hydrogen yields as the efficiency of hydrogen production was between 68%

and 92% from a wide variety of substrates such as glucose, lactate, propionate, or acetate (Lee, Li and Noike 2010; Bensaid, Ruggeri and Saracco 2015).

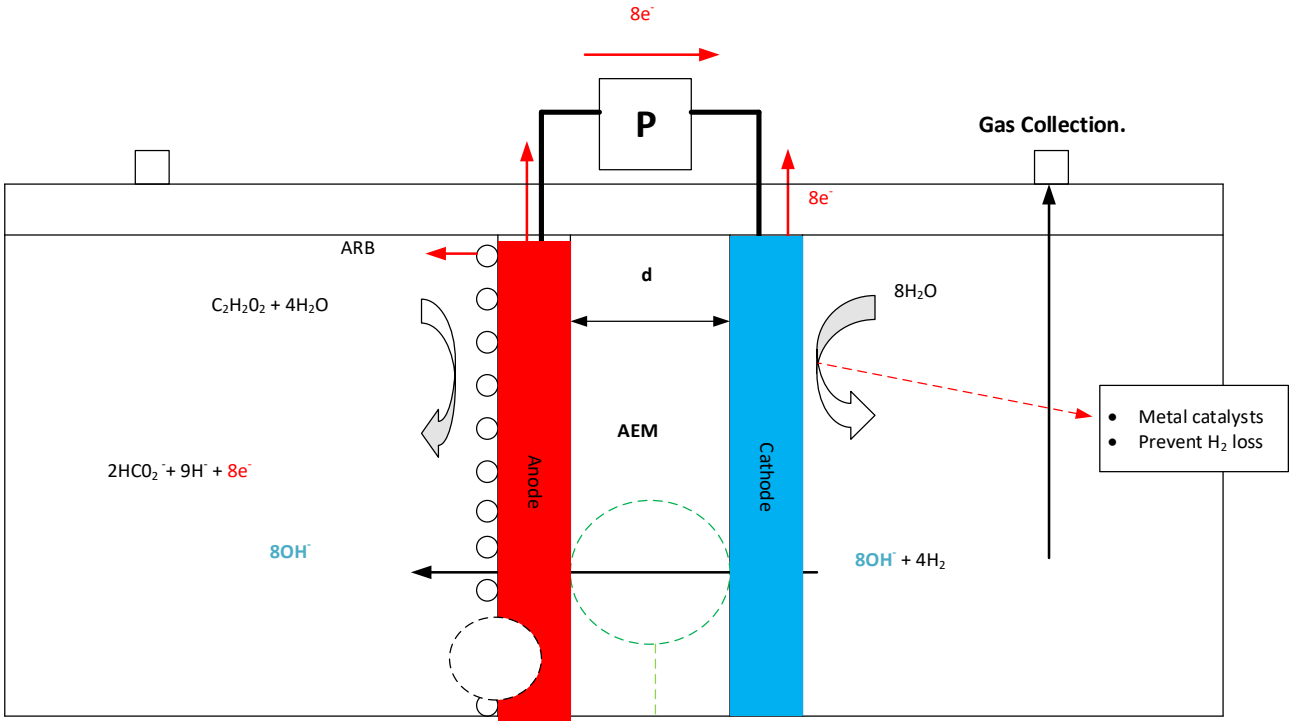

Figure 2.1 Microbial electrolysis cell electrolysis for the production of hydrogen
Source: Zilouei and Taherdanak (2015)

2.2.4 Dark fermentative hydrogen production

Anaerobic bacteria utilise carbohydrate-rich material as the only source of energy and electrons to produce hydrogen (Hawkes *et al.* 2007). Hydrogen production reactions (Equations 2.2 and 2.3) are fast, and these systems do not need solar energy, thus, qualify to be used for the treatment of wastewater by employing large bioreactors (Sung 2004).

$$\text{Glucose} + 2H_2O \rightarrow 2\ \text{Acetate} + 2CO_2 + 4H_2 \qquad \Delta G = -184.2\ \text{kJ} \qquad 2.2$$

$$\text{Glucose} \rightarrow \text{Butyrate} + 2CO_2 + 2H_2 \qquad \Delta G = -257.1\ \text{kJ} \qquad 2.3$$

Dark fermentative conditions do not allow a further breakdown of the remaining organic metabolites (short-chain fatty acids). Nonetheless, biohydrogen generation through dark fermentation requires less time, a smaller volume of the digester and low construction capital costs (Chandra 2015; Ghimire *et al.* 2015).

If developed, hydrogen fermentative processes from organic wastes would be of relatively low-cost as compared to anaerobic production of methane (between $3.79 -7.58/GJ) as they would employ similar reactors (Kotay and Das 2008). Hence, dark fermentation of organic

wastes could compete with hydrogen derived from fossil fuel, providing a reasonable avenue to industrial biohydrogen generation (Kotay and Das 2008; Saratale *et al.* 2008). Nevertheless, for over three decades aback several studies on biohydrogen generation from organic wastes have put the focus on the use of photosynthetic bacteria (Archana, Sasikala and Ramana 2003). Soon, highly digestible wastewaters will appear to be the most probable target for hydrogen synthesis.

pH control, thermal treatment, and HRT control of the treatment system were used for enriching the culture of hydrogen producers such as *Clostridia* (Wang and Yin 2017). The process has a dual advantage of generating environmentally clean energy in the form of hydrogen gas and synchronously stabilising the waste. Thus, the developed dark fermentative technology to generate hydrogen could lower the growing energy problem, while eliminating pollution problems resulting from an immoderate use of fossil fuels (El-Shafie, Kambara and Hayakawa 2019). The economic feasibility of many processes using hydrogen as an energy source or as raw materials could be enhanced by the dark fermentation technology (Demirbas 2009). Producing biohydrogen by dark fermentation is easier, and a wider range of carbohydrates, mainly industrial organic waste material can be used.

2.2.5 Photofermentative hydrogen production

In this case (different form biophotolysis), the photosynthetic bacteria use organic substrates such as short-chain organic acids, alcohols, etc. for hydrogen generation. In comparison to biophotolysis, the photosynthetic microbes need much less free energy (+8.5 kJ/mol hydrogen for lactate) to generate hydrogen. In addition, organic substances can be completely decomposed (Basak and Das 2017). Various photosynthetic microbes that are purple non-sulphur bacteria (PNS), which belong to the *Rhodosprillacae* species as exemplified by *R. sphaeroides-RV, R. capsulatus, R. sphaeroides*, and *R. palustris* can generate biohydrogen from various types of volatile organic acids in the presence of light (Miyamoto 1997; Basak and Das 2017).

Nitrogenases are the main catalysts during photofermentation and need nitrogen depleted environment for effective biohydrogen generation (Yokoi *et al.* 1998; Kapdan and Kargi 2006). NH_4-N concentration over 45 mg/L was observed to hinder biohydrogen generation when dark fermentation effluent of wheat solution substrate was utilised by the photosynthetic bacteria (Yokoi *et al.* 1998). As Equation 2.4 shows, in theory, only four molecules of hydrogen are generated for every molecule of acetic acid.

$CH_3COOH + 2H_2O$ + 'light energy' → $4H_2 + 2CO_2$ $\Delta G^o = +208$ kJ 2.4

Because of a positive change in Gibbs free energy, the reaction does not spontaneously proceed unless energy is outsourced externally for the reaction to proceed. Briefly, PNS microbes use organic acids as electron donors and transfer the electrons to the nitrogenase enzyme by ferredoxin. Protons are reduced by the nitrogenase using ATP and hydrogen is produced (Manish and Banerjee 2008). PNS microorganisms require a strict operating environment during the fermentative process. Optimum temperature and pH range for these microbes are 30-37℃ and 6.7- 7.3, respectively (Basak and Das 2017).

The source of the light also affects the generation of hydrogen. These photosynthetic bacteria prefer emergent light with wavelengths ranging between 400 -1000 nm because the highest absorption of light was observed at 522 and 860 nm (Lata *et al.* 2007). Other than daylight, different types of simulated light sources, for example, halogen, fluorescent, and tungsten could be used (Akkerman *et al.* 2002; Kayahan, Eroglu and Koku 2017). Various wastewater streams containing the short-chain fatty acids such as dark fermentation effluents can be used as the feed stream for the photofermentative hydrogen production, this, in turn, reduces raw material cost (Basak and Das 2017).

2.2.6 Combined dark and photofermentation

This approach is in practice, but little has been done, and there is limited literature on this technology (Reungsang *et al.* 2018). Dark and photofermentation is a two-stage fermentation process that can either be combined or sequential as a method of fermentative hydrogen production (Zhang *et al.* 2019a). Digestion of volatile fatty acids (VFAs) from dark fermentation synchronically enhances biohydrogen yield per mole of carbohydrate (Cheng *et al.* 2013). Equation 2.5 states that it is possible to produce 12 moles of hydrogen for every mole of glucose digested when dark fermentation and photofermentation are hybridised; if and only if, acetic acid is the VFA present (Yang, Guo and Liu 2010; Cheng *et al.* 2013). Additionally, when the appropriate environment is provided, organic acids produced during the dark fermentative process could be readily consumed by PNS microbes.

$C_6H_{12}O_6 + 6H_2O$ + light energy → $12H_2 + 6CO_2$ $\Delta G^0 = +3.2$ kJ 2.5

The conversion of glucose to hydrogen and carbon dioxide by hybrid fermentation is represented in Figure 2.2. As illustrated in that route, light energy is crucial for PNS microbes because conversion from organic acids is thermodynamically unfavourable (Uyar *et al.* 2009;

Cheng *et al.* 2013). Figure 2.2 also shows the formation of hydrogen through the acetate (-44 Kcal) and butyrate (-61 Kcal) pathways is thermodynamically feasible, whereas the formate pathway (+33 Kcal) is not thermodynamically feasible.

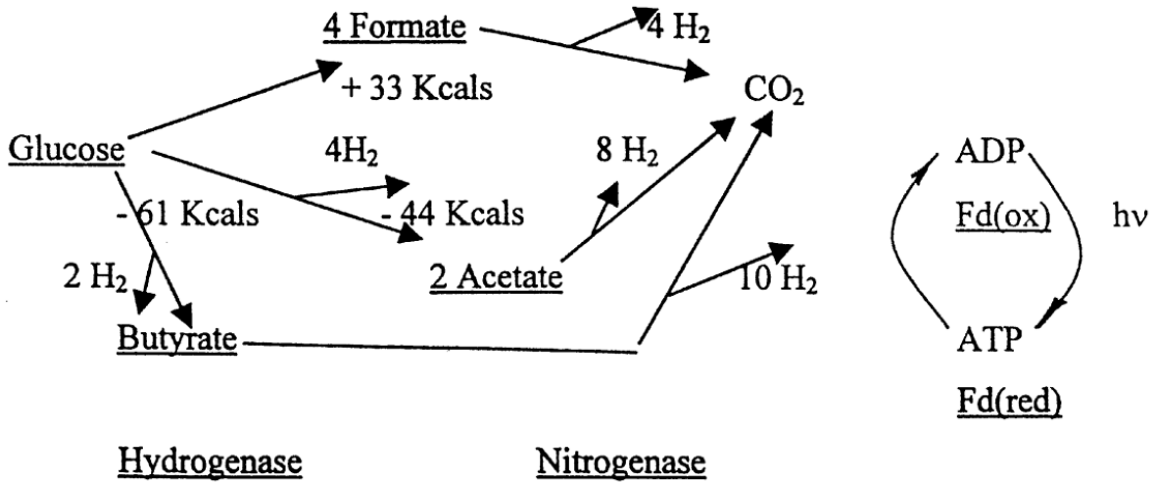

Figure 2.2 Hydrogen formation from glucose in combined dark and photofermentation
Adapted from Das and Veziroglu (2008)

For effective combined fermentation, appropriate operating conditions such as oxidation-reduction potential (ORP), pH, temperature, light source, lighting regime, light intensity, the ratio of dark to light fermentative microbes, the supplement of necessary nutrients and trace elements need to be regulated (Niño-Navarro *et al.* 2020). The selection of the appropriate culture is also equally important (Cheng *et al.* 2013). To record viable dark /photofermentation, PNS microbes must adapt to the acidic environment during the growth phase before inoculation. Various operating systems for dark-photofermentation, for example, the batch system in suspended culture, or immobilised PNS microorganisms with suspended dark fermentative microbes are well documented (Reungsang *et al.* 2018).

2.2.7 Summary of the methods for biohydrogen production

Table 2.1 summarises the advantages and disadvantages of the biological methods of hydrogen production as discussed in Section 2.2.

Table 2.1 Pros and Cons of biological hydrogen production

Biological method	Pros	Cons
Biophotolysis	Uses solar energy with no carbon fixation as an intermediate to directly produce hydrogen form water.	Production of hydrogen is commercially infeasible, because hydrogenase and nitrogenase are can be poisoned by oxygen from biophotolysis. Generation of explosive from hydrogen–oxygen mixtures are possible hence expensive photobioreactors are required.
Water-gas-shift	Reduction in atmospheric CO. Comparatively low energy demands	Difficult in microbial consortium concentration. Slow cellular growth Serious gas-liquid mass transfer limitation
Microbial electrolysis cell	Fast and efficient.	Requires constant replacement of the cathode, thereby attracting more costs.
Photofermentation	A wide spectral light energy can be used by these bacteria. Can be used for a wide range of wastes	Nitrogenase enzymes are inhibited by oxygen and light conversion efficiency is low.
Dark fermentation	A variety of carbon sources can be used as Substrate. It produces valuable metabolites such as butyric, lactic, acetic acids as by-products	Relatively lower hydrogen yield. At higher hydrogen yield, process becomes thermodynamically unfavourable.
Combined Dark-Photofermentation	Two stage fermentation can improve the overall yield of hydrogen	Requires continuous light source which is difficult for large scale processes.

Source: Oh *et al.* (2005); Pandu and Joseph (2012); Fatima, Kumar and Singh (2018); Pareek *et al.* (2020)

2.3 Metabolism of fermentative hydrogen production

Fermentation is an anaerobic process in which hydrogen can be obtained from carbohydrate-rich substrates. This process is easier and cheaper than other biological methods and allows them to have a high rate of hydrogen generation. However, its bottleneck is inferior hydrogen yield due to the creation of reduced organic compounds (Lee, Salerno and Rittmann 2008).

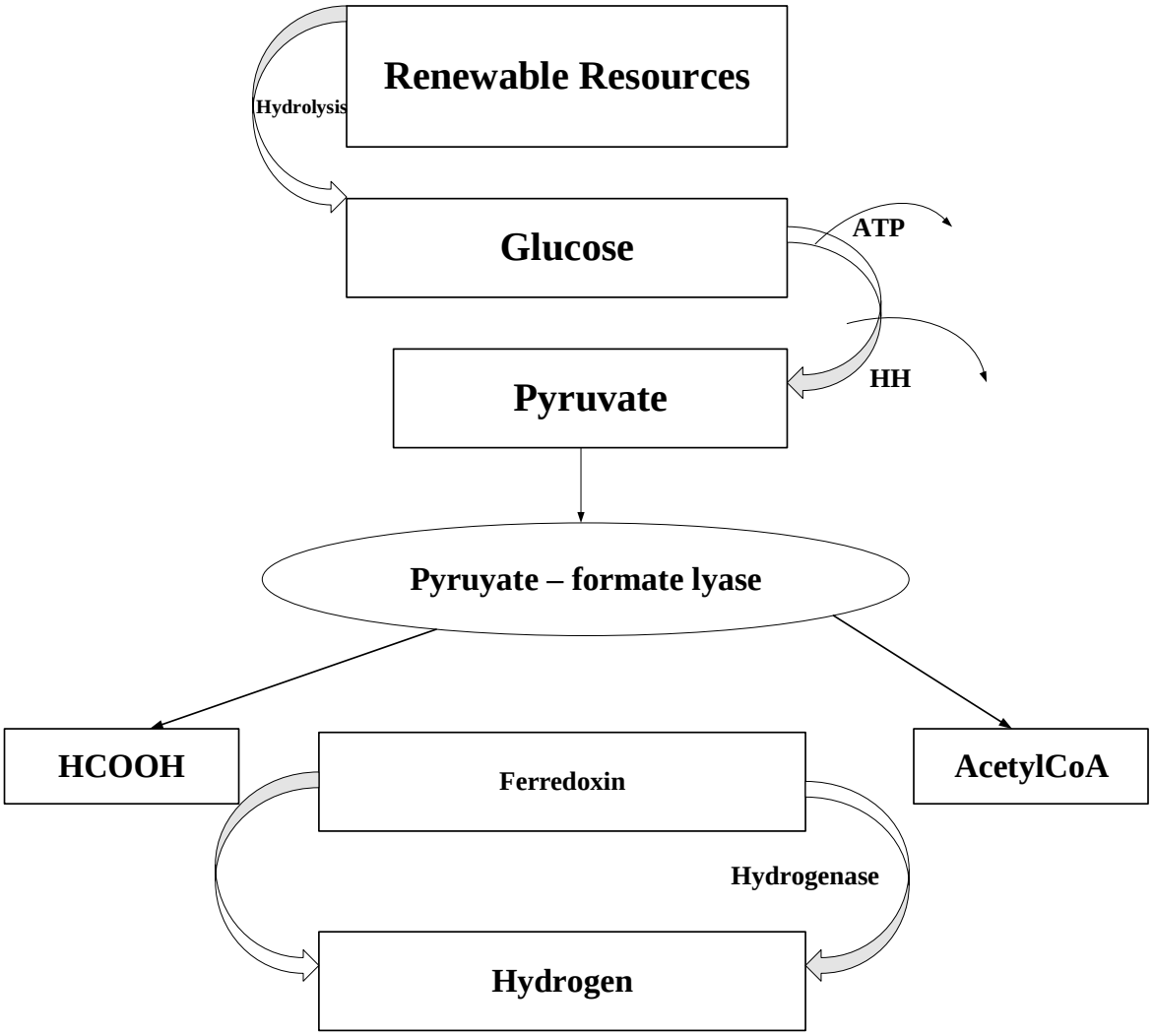

Figure 2.3 A schematic route for conversion of renewables to hydrogen through fermentation
Source: (Hallenbeck 2015).

During glycolysis, as shown in Figure 2.3, carbohydrates are decomposed to pyruvate, and its further fermentation depends on the type of bacteria (Hallenbeck 2015). In the presence of facultative anaerobes (*Enterobacter, E. Coli, Klebsiella*), pyruvate is converted through pyruvate-formate lyase to acetyl-CoA and formate. An increase in the formate concentration

leads to a pH drop and induction of the formate-hydrogen lyase, which catalyses its break down into CO_2 and H_2 (Bisaillon, Turcot and Hallenbeck 2006).

One glucose mole can be decomposed into two formate moles, so the maximum hydrogen production yield is 2 mol/mol glucose (Hallenbeck 2015). Strict anaerobes (obligates – *Clostridium* and *Ethanoligenens)* transform pyruvate into acetyl-CoA and CO_2 and synthesise reduced ferredoxin (Fd_{red}), which migrates electrons to [Fe-Fe] leading to hydrogenase catalysing hydrogen formation (McInerney and Gieg 2004). More quantities of H_2 can also be generated due to the action of NADH-ferredoxin oxidoreductase, resulting in the oxidation of NADH (Nicotinamide adenine dinucleotide) and production of reduced ferredoxin, which can be subsequently used for proton reduction (Hallenbeck 2015). If glycolysis results in the production of two moles of NADH, one could potentially gain two extra moles of hydrogen from this pathway. Therefore, *Clostridium* bacteria can produce 4 mol H_2/mol glucose (Angenent *et al.* 2004; Hallenbeck 2015). The redox potential of hydrogen (-0.42 V, at pH 7) is, however, much less as compared to NADH/NAD pair potential (-0.32 V), hence, at low hydrogen partial pressure (normally less than 0.001 atm), it is possible to produce hydrogen utilising electrons from NADH (Angenent *et al.* 2004; Hallenbeck 2015).

From an evolutionary point of view, fermentation is a process that enables organisms to gather energy (ATP) through substrate-level phosphorylation, a thermodynamically controlled process. A conclusion was made that regardless of the environmental pH, the three reactions in which ATP is created have large negative values of free energy: glycolysis, acetate production, and butyrate production. In fermentation, reducing power (in the form of NADH) is created as well. Oxygenation of NADH also takes place during the production of lactate, propionate, ethanol, and butyrate. Therefore, fermentative bacteria often conduct a mixed acid fermentation, during which succinate, acetate, ethanol, butyrate, lactate, formate, as well as acetone, butanol of butanediol can be produced (Lee, Salerno and Rittmann 2008; Murarka *et al.* 2008; Hallenbeck 2015). Increased acetate and butyrate resulted in low cell growth rate, substrate consumption rate, and hydrogen production rate. Butyrate significantly inhibited the growth of bacteria as compared to acetate (Khanal *et al.* 2004; Elbeshbishy *et al.* 2017).

The ratio of products is dependent on the type of microorganisms used, the substrate and the conditions of the process (Cai *et al.* 2011). In practice, hydrogen production efficiency is almost two times lower than its theoretical value (Lee, Salerno and Rittmann 2008; Wang and Wan 2009; Hallenbeck 2015). The goal of future research should be increasing this efficiency

through minimising the number of organic products and streaming electrons into then hydrogen production pathway (Lee, Li and Noike 2010). The biogas produced from dark fermentation is a mixture of gases, mainly containing H_2 and CO_2, but CH_4, CO and H_2S may also be found in the mixture depending on reactor configurations and substrates (Hussy *et al.* 2003; Najafpour, Younesi and Mohamed 2004; Hussy *et al.* 2005; Temudo, Kleerebezem and van Loosdrecht 2007).

2.4 Feedstocks for dark fermentation

The most efficient feedstocks for hydrogen generation utilising the dark fermentative system are carbohydrates, such as glucose, sucrose, and starch (Hallenbeck 2005; Hawkes *et al.* 2007; Lin, Chang and Hung 2008), as well as arabinose (Abreu *et al.* 2012), xylose (Ngo, Nguyen and Bui 2012) and glycerol (Seifert *et al.* 2009). However, pure substrates are costly, so for industrial-scale hydrogen production to be profitable, cheap waste products such as sludge from sewage (Massanet-Nicolau *et al.* 2010), solid municipal waste (Dong *et al.* 2009), molasses (Li *et al.* 2007) and wastewater originating from breweries (Han *et al.* 2012), olive oil production (Ntaikou *et al.* 2009) or palm oil production (Vijayaraghavan and Ahmad 2006) have to be used. Over the past few years, first-generation biofuels have been produced from energetic plants, such as oilseed rape or soybean. Nevertheless, their cultivation is controversial because it requires high-quality soil, which could be potentially used to grow food. This problem could be avoided by using second-generation biofuels, e.g. hydrogen generated from plants such as sweet sorghum, switchgrass and silver grass which can grow on land otherwise less desirable from an agricultural point of view, as well as from lignocellulosic residues produced by the pulp and paper industry (Magnusson *et al.* 2008). It is worth remembering, however, that such substrates contain complex polymers: cellulose, hemicellulose and lignin and therefore require pretreatment to dispose of lignin and change the structure of cellulose, which facilitates biodegradation of these waste products by cellulolytic microorganisms but simultaneously increases the costs of hydrogen production.

From a pollution control and resource recovery point of view, it would be ideal if one can convert polluted wastewater into hydrogen energy. With this effect, there is dire need to consider various industries that discharge vast amounts of organic loaded streams of wastewater that are economically feasible and easy to digest. Not all industries produce organic wastewater that is easily and readily digestible; hence wastewater streams are grouped

according to their putrescibility potential (Lay 2000; Ginkel, Sung and Lay 2001; Logan *et al.* 2002; Zhao *et al.* 2019).

Table 2.1 shows various carbohydrate-rich industrial wastewater streams with different composition of organic material subjected under dark fermentation and closely similar operating conditions. Although in some cases the reactor configuration was different, the yields and production rates of biohydrogen indicate performing streams using the dark fermentation process.

Table 2.2 Yields and rates of biohydrogen from various wastewater steams

Wastewater stream (COD in mg/L)	Mode of operation	SHPR mL/g VSS.h	VHPR mL/L.hr	Hydrogen yield $Mol_{H_2}/mol_{substrate}$	Reference
Dairy	Batch	55		1.60	(Mizuno *et al.* 2000)
Dairy	Fed-batch		22.66[b1]	16.8[b2]	(Mohan, Babu and Sarma 2007)
Pulp and paper	Batch	17		0.70	(Lin, Wu and Wang 2013)
Sugar beet	Continuous	25	0.125	1.7-1.9	(Hussy *et al.* 2005)
Brewery	Batch	143		2.03	(Lin *et al.* 2012)
Sugar factory	Continuous	122	0.1332	1.45	(Ueno, Otsuka and Morimoto 1996)
Sugar and ethyl alcohol	PBR			102[a]	(Hafez, Nakhla and El Naggar 2010)
Yeast manufacturing	Continuous		466.8 [d1]	16.5 [d2]	(Łukajtis *et al.* 2018)
Fisheries		87	0.16875	0.98	(Van Ginkel and Logan 2005)
Distillery	Fed-batch		26[c1]	6.98[c2]	(Mohan *et al.* 2008)
Palm oil	Continuous			1.28	(Vijayaraghavan and Ahmad 2006)
Olive oil	Batch			0.94	(Ntaikou *et al.* 2009)
Rice Winery	Continuous		$9.5*10^{-2}$	0.31	(Yu *et al.* 2002)
Sewage Sludge	Batch			1.7	(Lin and Chang 2019)
Glucose	Continuous (immobilised)			2.3	(Kumar and Das 2000)

SHPR: specific hydrogen production; VHPR: volumetric hydrogen production rate

PBR: Packed bed reactor, [a] $L\text{-}H_2/kg$ COD
[b1] mol H_2/m^3-d [b2] mol $H_2/kg\ COD_R$-d
[c1] mol H_2/m^3-d [c2] mol $H_2/kg\ COD_R$-d
[d1] cm^3/d [d2] cm^3 H_2/g waste

2.5 Operational parameters

There are two categories of factors to be considered during the production of hydrogen biologically. These are the environmental factors such as pH & alkalinity, temperature, nutrient availability, volatile acid, toxic materials, the concentration of the substrate, and the basic factors such as bacteria, food, hydrogen & carbon dioxide partial pressure, and contact time (Prajapati *et al.* 2013). These factors have a strong influence on the selection of reaction routes.

2.5.1 Hydrogen and carbon dioxide partial pressure

The cumulative effect of hydrogen and carbon dioxide in dark fermentation leads to inhibition of their evolution, and this results in the formation of more soluble metabolites.

2.5.1.1 Hydrogen partial pressure

The routes of biohydrogen generation are responsive to the hydrogen partial pressure (H_{pp}), as this factor is rate-limiting, especially during dark fermentation because the activity of hydrogenase is highly likely to drop due to feedback inhibition (Chandrasekhar, Lee and Lee 2015). To maintain H_{pp} at balance, inert gases (such as argon, nitrogen, etc.) are sparged into the headspace of the reactor, and increased hydrogen yield is evident (Van Groenestijn *et al.* 2002; Chandrasekhar, Lee and Lee 2015). This also helps to dispose of carbon dioxide, which could potentially take part in acetogenesis and consuming the hydrogen generated (Hawkes *et al.* 2007; Massanet-Nicolau *et al.* 2010). In a study conducted by Bastidas-Oyanedel *et al.* (2012), it was observed that flushing reactor with N_2 in headspace increased hydrogen production yield from 1.01 to 3.26 mol H_2/mol glucose at pH 4.5 and nitrogen gas flushing rate of 58.4 L/d. The increase in hydrogen yield was because of low hydrogen partial pressure which controlled the thermodynamics of the system and simultaneously lactate homoacetogenesis reactions, NADH hydrogenase, and lactate hydrogenase was affected as they take part in hydrogen production.

Continuous hydrogen production requires H_{pp} of 60 kPa at 55℃ (Lee and Zinder 1988; Rajhi *et al.* 2016), 20 kPa at 70℃ (Van Niel *et al.* 2002), and for kPa at 98℃ under standard conditions (Adams 1990; Levin, Pitt and Love 2004). Conditions which favour the production of hydrogen are however less influenced by hydrogen concentration as the temperature increases (Tamagnini *et al.* 2002).

It is imperative to minimise the partial pressure of hydrogen in the reaction system. One method of preventing excessive hydrogen partial pressure is to introduce an external gas sparger. Kim *et al.* (2006) showed that adding nitrogen and carbon dioxide into the reaction system influences hydrogen production and reduction of H_{pp} had a beneficial influence on fermentation.

Another investigation indicated that hydrogen yield at higher nitrogen purging rate would be simultaneously higher than without purging (Kraemer and Bagley 2008). This technique would, however, introduce a necessary, but unwanted cost owing to the dilution caused by nitrogen and thus, recovery of hydrogen would be difficult (Ghimire *et al.* 2015). Therefore, introducing nitrogen into the reactor regulates the H_{pp}. This method, however, presents the dilution effect in the overall biogas production and poses problems of separation and low concentration of desired gaseous products.

2.5.1.2 Carbon dioxide partial pressure

If there is a high concentration of carbon dioxide in the system, the formation of succinate or fumarate is favoured, and these metabolites have a high affinity of electrons and thus consume electrons that could have otherwise been used to reduce hydrogen ions to form hydrogen. The overall production of hydrogen is significantly reduced (Wang *et al.* 2018)

It is well documented that venting off carbon dioxide improves the generation of hydrogen in the dark fermentative process (Tanisho, Kuromoto and Kadokura 1998; Wang *et al.* 2018), resulting in the yield of hydrogen doubling. Carbon dioxide partial pressure was also found to have an inhibitory effect on dark fermentation, thus removal of carbon dioxide by purging in argon brought forth improvement in the production of hydrogen. In the research conducted by Chandrasekhar, Lee and Lee (2015), methane gas was purged to reduce the hydrogen and carbon dioxide concentration in the liquid phase. Gas purging significantly increased hydrogen production by 88% as compared to a quoted figure of 63%. Mizuno *et al.* (2000) documented a 68% increase in hydrogen production after purging with nitrogen gas. This behaviour could be directly credited to the reduction of partial pressures of hydrogen and carbon dioxide.

2.5.2 Culture pH and inoculation

Inoculum is introduced into the digester to give a lively source of microorganisms during start-up (Foucault 2011). The use of inoculum in a biochemical process is extremely important as it will

speed up the process, improve stability and increase the formation of biogas. At first, the substrate is used as an inoculum in a digester for days or even months to grow microorganisms and populate as much as possible.

pH is a key parameter to control biohydrogen synthesis as it impacts on the action of hydrogenase (Dabrock, Bahl and Gottschalk 2019), microbial communities' structure and their metabolic activity thereby modifying the spectrum of products (Ye *et al.* 2007; Guo *et al.* 2010). In another study, the optimum pH value during fermentative hydrogen production ranged from 3 to 9 (Lee, Miyahara and Noike 2002; Gadhamshetty *et al.* 2015) and greatly depended on the type of the substrate and inoculum (Wang and Wan 2009). If food wastes were used as the substrate, the optimal pH value was about 5-6, whereas if the substrate were crop residues and animal manure, pH oscillated around 7 (Guo *et al.* 2010).

While investigating *C. tyrobutyricum* ATCC 25755 (Zhu and Yang 2004), it was observed that a change in pH affected the expression level of various enzymes. Enzymes responsible for creating butyrate and using up lactate were strongly expressed at pH 6.3, while other enzymes responsible for creating acetate, and lactate at pH 5. However, this schema looks different for other organisms, such as *C. butyricum* CGS5 (Chen, Nakthong and Chen 2005), for which an opposite relation was observed: the highest butyrate production rate took place at pH 5.5 and dropped as pH increased to 6.5. Therefore, while applying different microorganisms, it is necessary to check how pH affects the fermentation process (Cai *et al.* 2011).

In a low pH environment, there is the conversion of pyruvate to VFAs associated with hydrogen generation, whereas a neutral pH supports methanogenesis by its respective microorganisms (Chandrasekhar, Lee and Lee 2015). Maintenance of pH at around 6.0 saw high production of hydrogen, but an extremely low pH (less than 4.5) hampered the ability of the microbial community to generate hydrogen (Chandrasekhar, Lee and Lee 2015; Penniston and Gueguim Kana 2018). Solventogenesis affects fermentative pathways in an alkaline micro-condition (Mohan and Reddy 2013).

2.5.3 Temperature

Hydrogen production can proceed using mesophilic bacteria (*Clostridium, Enterobacter*); 25-40℃, thermophiles (*Caldicellulosiruptor, Thermoanaerobacterium*); 40-65℃, extreme thermophiles (*Caldicellulosiruptor saccharolyticus*); 65-80℃ or hyperthermophiles

(*Thermotoga*); >80°C. In mixed culture, a change in the process temperature may affect the dominant bacteria culture. Karadag and Puhakka (2010) observed a change in the dominant culture from *Clostridium* in a mesophilic environment to *Thermoanaerobacterium* in the thermophilic environment. A comparison of the parameters suggests that hydrogen generation efficiency, as well as its fraction in biogas, was higher under thermophilic and hyperthermophilic conditions than that in mesophilic conditions (Shin, Youn and Kim 2004; Valdez-Vazquez *et al.* 2005). This is because hyperthermophilic microbes are less affected by the H_{pp}, which causes a metabolic shift to non-hydrogen generation routes, such as solvent formation and due to high temperature, fermentation is less susceptible to contamination with other cultures. Confirmation was made by Shin, Youn and Kim (2004) and Valdez-Vazquez *et al.* (2005), who did not notice any activity of methanogens even though the inoculum was not pretreated.

On the whole, the advantages of operating outside the mesophilic range are not conspicuous (Levin, Pitt and Love 2004; Elbeshbishy *et al.* 2017). From an engineering viewpoint, a disadvantage of a thermophilic process is that a reactor must be heated up to the desired temperature and since the volumetric production rate of hydrogen is low, and adoption of much larger reaction vessels than those employed in mesophilic fermentation, thus increasing the costs (Hallenbeck 2015). Most of the hydrogen dark fermentative studies at the laboratory scale were done using mesophilic microbes because are easy to operate and have maximum specific growth rates (Chandrasekhar, Lee and Lee 2015; Dessì *et al.* 2018). In another study, the effect of temperature on dark fermentation using a mixed culture was investigated. A maximum yield of hydrogen of 319 mL/gCOD was recorded by increasing the temperature from 35 to 45°C, whereas a decrease in yield (182 mL/gCOD) was observed when temperatures were raised from 45 to 55°C (Tang *et al.* 2018). Temperature can alter the byproducts spectrum; hence, it can also be optimised to shift the metabolic pathways towards acetate and butyrate production away from alcohol or solventogenesis (Vijayaraghavan, Mohd and Mohd 2006; de Souza Moraes *et al.* 2019).

2.5.4 Hydraulic retention time (HRT)

HRT also modulates selection of microorganisms for a process, and this is because microorganisms have different growth rates with different behaviour under mechanical dilution due to continuous volumetric circulation, and therefore, there must be a balance on the microorganisms selected and their ability to withstand the mechanical dilution (Palomo-Briones

et al. 2019). A prolonged time of fermentation does not favour hydrogen generation as the metabolism shifts from the acidogenic phase to the methanogenic phase. Shorter HRT restricts the rate of growth of the methanogens (Chandrasekhar, Lee and Lee 2015). For acceptable hydrogen yield, the most conducive HRT ranged from 8 to 14 hours for a wide variety of feed streams (Mamimin and Prasertsan 2011; Chandrasekhar, Lee and Lee 2015; Hallenbeck 2015). By keeping short HRTs (2-10 h), suppression of the methanogenic phase was effective (Ren *et al.* 2011; Chandrasekhar, Lee and Lee 2015). However, for attractive hydrogen production, many factors affect the HRT, including the type of the feed, the type of microbes, the system redox condition, and the OLR, among others (Kirli and Karapinar 2018). A short HRT decreases the efficiency in substrate use for the dark fermentation process and consequently reduces the efficiency during a downstream process of photofermentation (Mamimin and Prasertsan 2011; Chandrasekhar, Lee and Lee 2015). However, the effects of pH and HRT are interrelated that no dedicated research has isolated the effect of these two parameters.

2.5.5 Nutrients

Nutritional supplement (with the source of carbon present) for microbial growth is pivotal in increasing hydrogen production. In a study, Lin and Lay (2012) substantiated that at the carbon to nitrogen ratio of 47, the production rate and productivity of hydrogen was 270 mmol H_2/L.d and 4.8 mol H_2/mol sucrose, respectively (Chandrasekhar, Lee and Lee 2015). For a mixed culture, the highest generation potential of 291.4 mL (equivalent to 3.25 mmol), the highest hydrogen yield of 298.8 mL/g of glucose (3.33 mmol H_2/g of glucose) and the highest mean hydrogen generation rate of 8.5 mL/h were attained at ammonia concentration of 0.1g of N/L (Wang and Wan 2009; Chandrasekhar, Lee and Lee 2015). However, if nitrogen exceeds the optimum amount, the intracellular pH of microbes used for hydrogen production was affected, and nitrogenase activity was also inhibited (Chandrasekhar, Lee and Lee 2015). Furthermore, the high composition of nitrogen effectuated ammonification, and this was not favourable for hydrogen generation (Kotay and Das 2008; Chandrasekhar, Lee and Lee 2015).

Zhu *et al.* (2008) examined the impact of ammonium concentration on entrapped, suspended cultures of *R. sphaeroides* and *C. butyricum*, as well as entrapment of those microbes in the form of co-culture in batch experiments. Glucose (50 mM) was fed, and the ammonium concentration was varied between 1 to10 mM. Ammonium strongly inhibited hydrogen generation in suspended cultures compared to those entrapped. However, after ammonium was used up in the suspended

culture, biohydrogen production recuperated. The maximum cumulative hydrogen generation was acquired by suspended *R. sphaeroides* (380 mL hydrogen), entrapped *R. sphaeroides* (367 mL hydrogen), entrapped *C. butyricum* (66 mL hydrogen) and entrapped co-culture (106 mL hydrogen) (Zhu *et al.* 2008; Elbeshbishy *et al.* 2017).

2.5.6 Substrate-to-biomass ratio (S/X)

Food-to-microorganism (F/M) ratio (for continuous systems) is an essential operational and design parameter in anaerobic digestion. It is also known as the substrate-to-biomass ratio (S/X) (for batch systems). Optimisation of substrate utilisation and biomass formation helps to achieve system equilibrium. The S/X ratio oversees the biodegradation of organic material (Nasr *et al.* 2015).

The F/M ratio in this review was characterised as the initial ratio of COD contained in the wastewater stream to the VSS contained in the inoculum with each parameter multiplied by their respective volumes when the batch fermentation runs begin. The amount of substrate and seed were calculated based on a substrate-to-biomass (S/X) ratio using the Equation 2.5 (Nasr *et al.* 2015; Reddy 2016).

$$\frac{S}{X} = \frac{V_{substrate} * COD_{total}}{V_{seed} * VSS} \qquad 2.5$$

Where $V_{substrate}$ is the volume of substrate (L)

COD_{total} is the total chemical oxygen demand (g/L)

V_{seed} is the volume of seed (L)

VSS is the volatile suspended solids (g/L)

For batch anaerobic digestion, hydrogen generation can be regulated by altering the initial S/X ratio. From a study done by Kotay and Das (2008), the impact of the F/M on the generation rate of hydrogen during the 44 hours mesophilic fermentation is shown in Figure 2.4. Various patterns of biohydrogen production rate were evident when the S/X ratio was shifted from 1 to 10. The maximum hydrogen generation rate was 19.8 mL/h; this was registered after the first 12 hours of fermentation at an F/M of 5.

The second highest peak (17.6 mL/h at F/M of 6) appeared at the 12^{th} hour, as depicted in Figure 2.4. Such peak trends may be ascribed to the inhibition of hydrogen-producing microorganisms resulting from the formation of VFAs and the quick reduction of pH in the first 12 hours (Ginkel, Sung and Lay 2001; Lee, Miyahara and Noike 2002). After adjustment of microbes to the acidic

conditions, hydrogen generation might be supported if the substrate was supplied (Elbeshbishy *et al.* 2017).

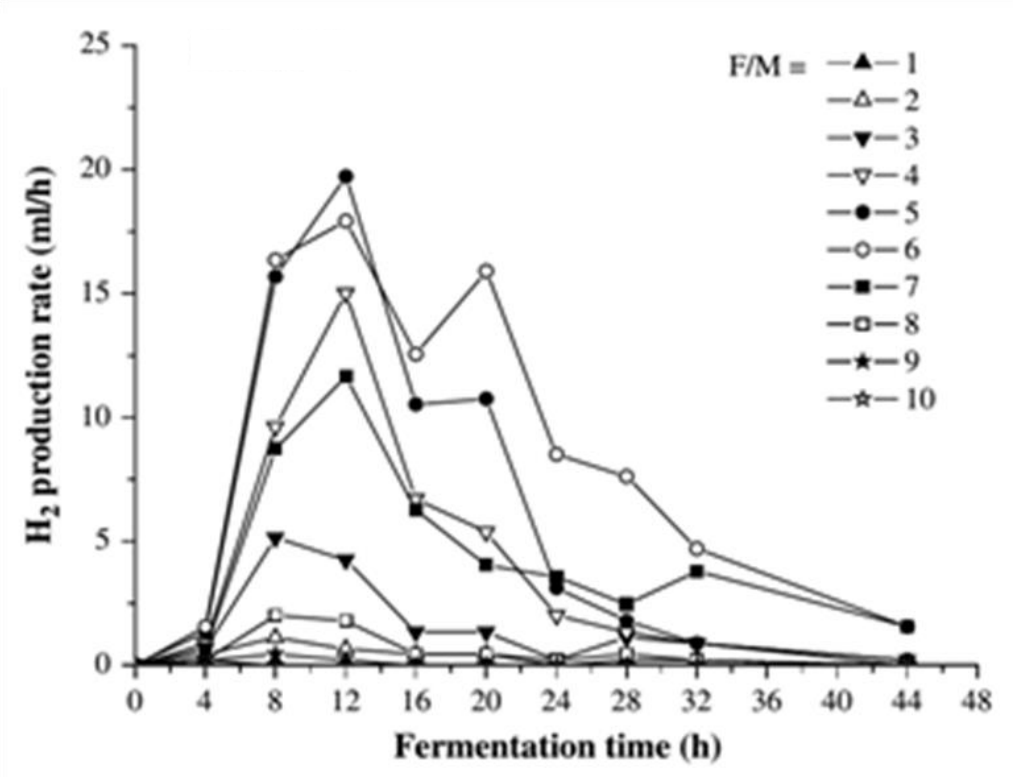

Figure 2.4 Effect of F/M on HPRs over 44-hour mesophilic fermentation.

Source: (Lee, Miyahara and Noike 2002)

2.5.7 Other methods to improve hydrogen production

2.5.7.1 Metabolic Shift

Dark fermentation is also followed by the generation of short-chain acids as metabolites, as shown in Figure 2.5; however, the fermentative microbes are limited in further digesting these acids. There is a sharp drop in pH of the culture, which is attributed to acids accumulation, and subsequently, this inhibits biological hydrogen generation (Nath and Das 2014). At pH lower than 5, microbes cannot be sustained, thus introducing a method to lower production of acid or to follow specific biological pathways that reduce the concentration of protons in the cell exterior proportional to the pH of culture (Nath and Das 2014).

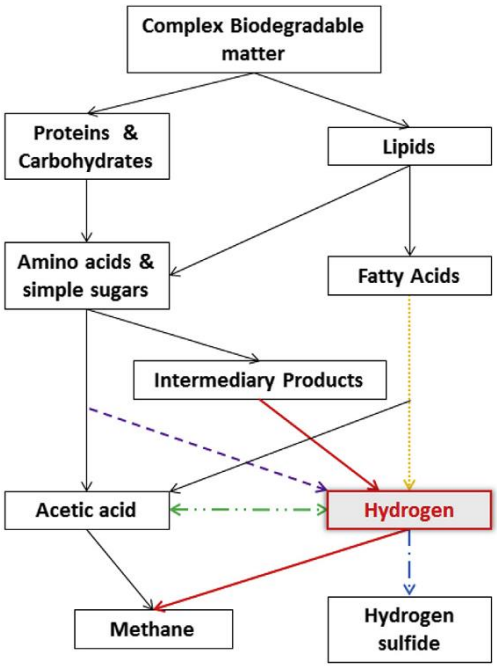

Figure 2.5 Suggested routes for hydrogen production and consumption.

Source: Nath and Das (2014)

Blockage of the generation of these acids through redirection of metabolic routes may be another effective way to improve hydrogen production (Bansal, Singhal and Singh 2012). One of the major drawbacks in facultative microbes generating hydrogen involves the disposal of overabundance reducing products of fermentation (Ginkel, Sung and Lay 2001). The overabundance reducing products could be discarded through proton reduction, as illustrated in Equation 2.6, encouraged by hydrogenases and electron carriers, thus prompting the synthesis of hydrogen in microorganisms such as *E. aerogens* and *E. cloacae*. Considering this, it is reasonable to account for the biohydrogen generation as a technique to dispose of electrons discharged in oxidative metabolism by the action of hydrogenases, resulting in sped up the reaction (Hallenbeck and Benemann 2002; Adams and Stiefel 2014).

$$2\bar{e} + 2H^+ \rightarrow H_2 \qquad 2.6$$

Additional to VFAs, dark fermentation also involves the production of alcohols. These reduced products, such as lactate, butanol and ethanol, have additional hydrogen atoms that are not released as gas (Levin, Pitt and Love 2004). Thus, alcohol production accompanies correspondingly low yields of hydrogen. For maximal hydrogen yield, microbial metabolic processes should be shifted

from alcohols and short-chain acids (lactate) towards volatile fatty acids (Levin, Pitt and Love 2004; Hawkes *et al.* 2007).

Hydrogenase, which comprises of two subunits, corporates with NADH (reducing equivalent) on the cytoplasmic end and with protons on the periplasmic end. NADH is typically formed by the breaking down of glucose to pyruvate through glycolysis. Oxidation of NADH is involved in the changing of pyruvate to butyric acid, lactic acid, butanediol and ethanol. If the production of these acidic and alcoholic metabolic products could be inhibited, this would see the concentration of NADH increasing (Kumar and Das 2001). This, in turn, augments hydrogen yield by oxidising NADH. The yields were recorded to have improved from 2.7 to 3.8 mol/mol glucose by inhibiting the routes of organic acid formation utilising the proton-suicide technique with sodium bromide and sodium bromate (Kumar and Das 2001). A comparative improvement of hydrogen yield using *E. aerogenes* was recorded by inhibiting the production of acidic and alcoholic metabolic products by both the proton-suicide technique and allyl alcohol (Nath and Das 2014). *C. pasteurianum* has limited growth under low pH conditions and is a classic hydrogen producer and VFA. Still, its glucose metabolism can be transformed from hydrogen generation and towards the production of solvents by keeping glucose at high concentrations (12% w/v). This can be achieved by introducing carbon monoxide (hydrogenase inhibitor) and by limiting iron (Levin, Pitt and Love 2004; Hawkes *et al.* 2007). HRT likewise, pronouncedly affects balance in metabolism. *Clostridia* generate hydrogen and VFAs in the logarithmic growth phase, and sped-up alcohol formation happens in the late growth phase (Lay 2000).

In batch experiments with municipal solid waste (MSW) mixture and pretreated sludge inoculum, VFAs and hydrogen formation began after a lag of 2.3 days, followed by propanol/butanol formation on days 3.2 and 4 as hydrogen evolution dwindled (Ginkel, Sung and Lay 2001). Comparative generation of alcohols after the peak of VFA/hydrogen generation was observed in another batch examination utilising heat-treated seed sludge and micro-crystalline cellulose (Lay 2000).

Table 2.2 succinctly parades the methods and techniques that are in practice to improve the yield and hydrogen production rates. Advantages and disadvantages of the cited methods have also been articulated in Table 2.2.

Table 2.3 Summary of methods and parameters to increase hydrogen production yield and rates.

Strategy	**Advantages**	**Possible drawbacks**
Utilising thermophilic strains	High temperature supports hydrogen generation	Extra energy to heat the reactor is required, high costs
Optimisation of bioprocess factors	Could bolster hydrogen generation yields and/or rates	Generally low cost, simple bioreactors needed
Removal of side reactions	Channels more reduction to hydrogen	The strain should be genetically amenable
Decrease H_{pp}	Enhances yields in *Clostridial* -type fermentations	Production of dilute gas – high purification costs
Provide more active hydrogenase	Enhances hydrogen generation rates	No demonstration of restriction of active enzyme quantity

Source: (Chandrasekhar, Lee and Lee 2015; Łukajtis et al. 2018; Romão et al. 2019)

2.6 Bioreactors

Bioreactor configuration is of prime importance in hydrogen generation as it influences the microenvironment of the reactor, its established hydrodynamic behaviour, the prevailing microorganism population, and their contact with the substrate. For research purposes, batch reactors are used most frequently, because they are flexible and are easy to operate. However, industrial-scale hydrogen production requires a continuous-flow bioreactor (Waligórska 2012).

2.6.1 Basic bioreactor selection criteria

To select the best reactor configuration, the following factors are considered (Pirsaheb *et al.* 2015):

- Microorganism and biochemical qualities of the cellular framework (mammalian, plant, microbial).
- Hydrodynamic properties of the reaction vessel.
- Heat and mass transfer properties of the reactor.

- Product formation and cell development kinetics.
- Cell system's genetical stability properties.
- Regulation of the reactor conditions (Both micro- and macro-environment).
- Effect of the reactor design on downstream processes such as product separation.
- The scaling-up potential of the bioreactor.

2.6.2 Anaerobic baffled reactor (ABR)

The ABR, was initially created at Stanford University by McCarty (1981); Bachmann, Beard and McCarty (2015), and has various focal points, such as desirable resilience to hydraulic and organic shocks, improved biomass residence time, reduced sludge yields, and the capacity to isolate the different phases of anaerobic catabolism longitudinally towards the downside of the reactor. ABR is a series of up-flow anaerobic sludge blanket reactors (UASBs), it uses a series of vertical baffles to force the medium to flow under and over them as it passes from inlet to outlet, the wastewater has intimacy with huge quantities of activated biomass, while the reactor effluent has fewer solids than the influent (Krishna, Kumar and Kumar 2009).

The advantages cause a transformation in the microbial populace, and permits improved defence against poisonous substances and are highly resistant to the alterations in environmental factors, for example, pH and temperature (Baloch, Akunna and Collier 2007; Liu, Ren and Wan 2007; Huajun *et al.* 2008). Additionally, it has a straightforward outline and inexpensive construction, appropriate for application in industry, and it has superior oil and COD reduction than UASBs during the treatment of 'stubborn' organic wastewater (Kuşçu and Sponza 2006; Krishna, Kumar and Kumar 2008; Saritpongteeraka and Chaiprapat 2008; Zhu *et al.* 2008).

The ABR configuration employs a chain of baffles to coerce carbohydrate-rich wastewater to flow in a zig-zag manner (or through) the baffles as it moves in the reactor from one end to the other, as shown in Figure 2.6 (McCarty and Bachmann 1992; Barber and Stuckey 2009). Even though they are not standard on larger scales, the ABRs have several merits over other well-established reactors, as summarised underneath (Pirsaheb *et al.* 2015; Li, Nan and Gao 2016). Maybe, the most exceptional benefit of the ABR is that it can divide methanogenesis and acidogenesis longitudinally down the reactor, enabling the bioreactor to carry on as a two-stage system with low costs and related control problems (Yang *et al.* 2018a).

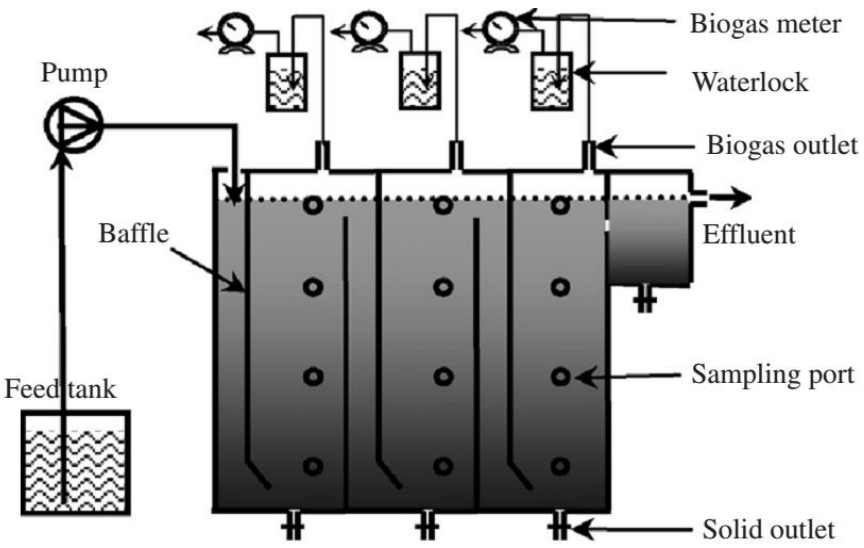

Figure 2.6 Schematic diagram of the ABR system.

Source: Saritpongteeraka and Chaiprapat (2008)

The methanogenic and acidogenic activity can be increased in a two-phase operation by a factor reaching four as the acidogens accumulate in the primary stage (Mengmeng *et al.* 2009), and diverse microbial consortia can develop under more favourable environment. The merits of the two-stage system have been broadly archived (Ke, Shi and Fang 2005). Qualities of the ABR design at the pilot/full-scale incorporate the prerequisite to constructing shallow reaction vessels to maintain permissible gas up the flow and liquid velocities, and issues with maintenance of evenly distributed influent (Barber and Stuckey 2009; Li, Nan and Gao 2016).

The anaerobic reactor is accompanied by several merits, as well as some demerits that are summarised as follows:

Advantages

- High resistance to organic and hydraulic loads.
- Little or no electricity is needed.
- Reduced working expenses.
- Prolonged operational life.
- High Biochemical Oxygen Demand (BOD) removal.
- Reduced sludge generation; the sludge is stabilised.
- Reasonable area requirement (can be assembled underground).
- Simple.

Disadvantages

- Prolonged start-up period.
- Needs expert design and development.
- The reduced diminishment of pathogens and nutrients.
- Effluent and sludge need downstream treatment and/or proper release.
- Requires programme for faecal sludge management.
- Requires flushing water.
- Clear guidelines for the bioreactor design are not available in the literature.

2.6.3 Effect of effluent recycle

There is significant evidence that recycling of effluent stream lowers the COD reduction efficiency as the reaction system approaches a totally blended system, and thus the mass transfer driving force for substrate removal decreases even though there is a small increment in the loading rate (Barber and Stuckey 2009). The impact of increasing recycle ratios and loading rates on performance is summarised in Table 2.3. Chynoweth, Srivastra and Conrad (2015) observed a constructive outcome of recycling 20% of the effluent when the methane yield improved by more than 30% (the same is also possible for hydrogen). The recycled stream mitigated the problems of a drop in pH created by large amounts of VFAs in the primary stage of the reactor and discourages gelatinous microbial development at the reactor's inlet for the treatment of recalcitrant protein-carbohydrate wastewater (Nachaiyasit and Stuckey 1997). Another advantage of recycling is the weakening of poisons, and inhibition of substrate is reduced in the influent (Barber and Stuckey 2009; Hamawand 2015).

Table 2.4 Merits and demerits of effluent recycle in the ABR

Merits	**Demerits**
Increased front pH	An overall reduction in efficiency
Reduced substrate inhibition and influent toxicity	High solids loss
Possibility of high loading rates	Large hydraulic dead space
Improved biomass substrate/ contact	Disturbance of the microbial consortia and bioflocs
	Supports one-phase digestion

Source: (Chynoweth, Srivastra and Conrad 2015; Hamawand 2015)

2.7 Immobilisation of cells

A system of immobilised microbes is progressively utilised at both the laboratory and industrial scale as an option to upgrade the activity of microorganisms in the fermentative processes. In comparison to free cells, cells immobilisation offers many advantages, for example, reusability, ease of solids and liquids separation, low contamination risk, increased microbe density, improved metabolic activity, and enhanced stability in operation (Singh and Wahid 2015).

Cell immobilisation has been recognised as the physical localisation of feasible microbes to a specific predetermined space to confine their free movement and keep up hydrodynamic behaviour which varies from the surroundings while keeping up their catalytic potency for prolonged and steady utilisation (Pandey 2011; Mohammadi *et al.* 2012; Sekoai and Daramola 2018).

Immobilisation generally describes a broad spectrum of cells or the particles entrapment or attachment (Calvo *et al.* 1997; Solé *et al.* 2019). Basically, it applies to all classes of biological catalysts, including cell organelles, enzymes, plant cells, and animal. At present, various types of immobilisation are widely applied, not only in biotechnology, but also in food, environmental, biosensor industries, and pharmaceuticals (Peinado *et al.* 2005).

Immobilisation of cells has surfaced as an option for immobilisation of enzymes (Rehm, Chen and Rehm 2018; Solé *et al.* 2019). Cell immobilisation containing certain enzymes has additional advantages such as complete removal of costly and lengthy methods for enzymes purification and separation. It is imperative to increase their range of utilisation by allowing simple products' separation and purification from reactants and effective catalyst recovery (Martins *et al.* 2013). In comparison to immobilised enzymes, immobilised cells present new alternatives because of their use as water-insoluble, natural carriers of needed enzyme activities (Sagir *et al.* 2017).

For microbial cell immobilisation, they can be applied to range from industrial to environmental systems. Microbes held on a carrier can be reused in subsequent processes; thus, there is significant cost reduction, as there is no replenishment of the biocatalyst (Park and Chang 2000; Mrudula and Shyam 2012)

Application in biotechnology has been on the increase with practical use in various fields because nanoparticles have shown contact with microbes even at reduced concentration. Conversely, some nanoparticles portray antimicrobial behaviour by closely interacting with the microbes, causing membrane disruption, also raising environmental concerns in as far as their disposal is concerned (Neal 2008).

In another view, some microbes tend to manipulate the nanoparticles positively, especially under anaerobic conditions, by enabling efficient migration of electrons to their respective acceptors. Intracellular or extracellular nanoparticles can be synthesised by reducing metal ions for the bio-formation of nanomaterials of varied chemical composition or morphologies (Korbekandi, Iravani and Abbasi 2009; Dinesh *et al.* 2012). The nanoparticles have well-exhibited advantages because of their ability to speedily react with the electron donors, improving the kinetics of the reaction as biocatalysts, and thus enhancing the activity of microorganisms (Xu *et al.* 2012). The highest hydrogen yield of 149.8 mL/gVS was observed with starch (5370 mg/L COD) as the substrate when iron (37.5 mg/L) and nickel (37.5 mg/L) nanoparticles were used (Taherdanak, Zilouei and Karimi 2015).

2.7.1 Support materials

The support is critical, hence the decision on their selection are pivotal during the preparation of the immobilisation process (Martins *et al.* 2013). For wastewater treatment, support materials should be non-toxic, insoluble, non-biodegradable, non-polluting, lightweight; mechanically, and chemically stable, flexible, highly diffusive, simple, having high biomass retention, selective, having a minimum attachment of other microbes and relatively inexpensive (Leenen *et al.* 1996; Martins *et al.* 2013).

The carriers are categorised as organic polymers and inorganic material. Inorganic carriers are thermostable and can resist biological degradation; thus, these were selected to immobilise microorganisms (Cassidy, Lee and Trevors 1996; Verma *et al.* 2013). Natural polymers of alginate and carrageenan are the regularly utilised polymers but are unstable in wastewater as compared to manufactured polymers (Bashan *et al.* 2002; Moreno-Garrido 2008). Alginates are known for easy handleability, non-toxicity to the environment, and humans; and the entrapped microbes are safe for human use, accessible in bulk, and low cost (Wannapokin *et al.* 2019).

2.7.2 Methods for immobilisation of microbial cells

Cells immobilisation can exist artificially or through natural processes (Ramakrishna and Prakasham 1999; Sagir *et al.* 2017). To date, several immobilisation techniques have been documented, and these are covalent coupling, entrapment, encapsulation, and adsorption (Mallick 2002). The types of immobilisation can be categorised as ‘passive’ (using the natural propensity

of microbes to attach to surfaces naturally or synthetically and grow on them) and 'active' (flocculant agents, chemical attachment, and gel encapsulation) (Sagir *et al.* 2017).

2.7.2.1 Covalent bonding/Cross-linking

This technique depends on covalent bonds formed between cells supported by a binding agent and activated inorganic support. For cross-linking, chemical restructuring of the surface is vital. Covalent bonding is efficient and durable to enzymes, but it is scarcely used in cell immobilisation (Ramakrishna and Prakasham 1999; Sagir *et al.* 2017).

2.7.2.2 Entrapment

Entrapment cannot be reversed where immobilised cells are trapped in a support material. This strategy offers a defensive screen around the immobilised cells, guaranteeing their long feasibility during the process and storage in polymers (Gorecka and Jastrzębska 2011). Entrapment as a technique has been widely examined in immobilisation of cell. The matrices utilised are carrageenan, alginate, epoxy resin, cellulose, agar, and its derivatives, gelatine, photo cross-linkable resins, polyurethane, collagen, polyacrylamide, polyester, and polystyrene (Kumar *et al.* 2016a; Sagir *et al.* 2017). Microbial entrapment in permeable polymer carrier was regularly employed to trap the microbes from solutions with suspension and then acquire the immobilised microbes. The polymer matrix utilised in this technique restricting microbes has a permeable structure, and thus there is easy diffusion of pollutants and different metabolites through the matrix. In this technique, a considerable measure of permeable polymers can entrap microbes under surrounding conditions (Verma *et al.* 2013).

Techniques of entrapment depend on the incorporation of cells within an inflexible network to avoid diffusion of cells into the surrounding medium with substrate penetration still allowed. Mechanical strength is high for entrapment, but also has loopholes, such as leakage of cells, immobilisation expenses, diffusion restrictions, deactivation during immobilisation and abrasion of support material during use. Reduced loading capacity is also a drawback, as biological catalysts should be included in the support system (Krekeler, Ziehr and Klein 1991; Song *et al.* 2008).

2.7.2.3 Encapsulation

Encapsulation, as a technique for immobilisation of cells, is also irreversible. The membrane limits biocatalysts but freely float in the core space (Gorecka and Jastrzębska 2011). The membrane is semi-porous, selective to freely flowing nutrients and substrates (cells as biocatalysts), holding the

cells inside. The proper size of membrane pores determines this principle and has to be adjusted to the size of the core material. One of the significant advantages of micro-encapsulation is the constrained access to the interior of the microcapsule, for it preserves the biological catalyst from the unfavourable surroundings. Like many other immobilisation methods, it prevents the leakage of biocatalyst and improves the efficiency of the process (Park and Chang 2000). Microbial enclosure in a polymer gel was ensured by the encapsulation method (Sheu *et al.* 1998; Kumar *et al.* 2016a).

2.7.2.4 Adsorption

This method is hinged upon the physical collaboration between the carrier surfaces, and the microorganisms, and is simple, cheap, effective, and reversible. The immobilisation of microbes on properly selected adsorbents excites metabolism of microbes, preserves cells from harmful components, and maintains their physiological action (Martins *et al.* 2013).

Apart from the existing drawbacks related to entrapment, adsorption gives an immediate interaction between the immobilised cells and nutrients; thus, eradicating such problems (Chu *et al.* 2009). Adsorption as a method which includes the transfer of the cells from the bulk phase to the support surface, adhesion of cells then follows, and subsequent colonisation of the surface of the support (Martins *et al.* 2013).

Adsorption involves weak forces; however, they are strong enough to enable efficient binding. Bond formation involves several forces such as the van der Waals forces, hydrogen bonds and hydrophobic & ionic interactions. Both electrostatics and hydrophobicity regulate the cell-support adhesion, which is an important control step in the immobilisation of cells on the matrix (Hsu *et al.* 2004; Gorecka and Jastrzębska 2011).

As opposed to ceramics, straw, and wood chips; adequate supporting surfaces for adsorption are provided by the fibrous matrices (Talabardon, Schwitzguébel and Péringer 2000; Chu *et al.* 2009) because they have large contact area, void volume, permeability, and mechanical strength; reduced drop in pressure decreased diffusion challenges and low toxicity; increased loading, durability & biodegradability; readily available and inexpensive (Huang and Yang 1998). Their natural orientation also enables them to entrap more cells as compared to other materials (Kumar *et al.* 2016a; Kumar *et al.* 2018).

2.7.3 Previous work on cell immobilisation

In recent times, a considerable amount of work was done to immobilise cells in a bid to increase their microbial activities (Farghali *et al.* 2019). Nanoparticles are classified into four, being assessed as functional materials for water and wastewater treatment, for example, carbonaceous nanomaterial, zeolite nanomaterials, metal-containing nanoparticles, and dendrimers. Because of their enhanced surface area to volume ratio, nanoparticles exhibit a favourable outcome as compared to other methods used in water and wastewater treatment (Stoimenov *et al.* 2002; Dinesh *et al.* 2012). Beyond an uncertainty, the nanotechnological method is one of the best techniques for the treatment of water and wastewater, but to this date, there is limited knowledge on the impact to the environment, transportation, and toxic nature of nanoparticles (Colvin 2003; Kumar *et al.* 2019).

2.7.3.1 Biodegradation of organic matter by immobilised cells

Figure 2.7 shows the time course of lactose degradation by free cells and coated cells (Colvin 2003). Both coated and free cells showed complete utilisation of lactose in 4 hours. However, the coated cells showed 90% of lactose utilisation in the first 2 hours, whereas free cells could utilise only 60% lactose during the same time. The degradation rate of lactose for coated cells and uncoated cells was 1.4 ppm/min and 0.32 ppm/min, respectively.

.

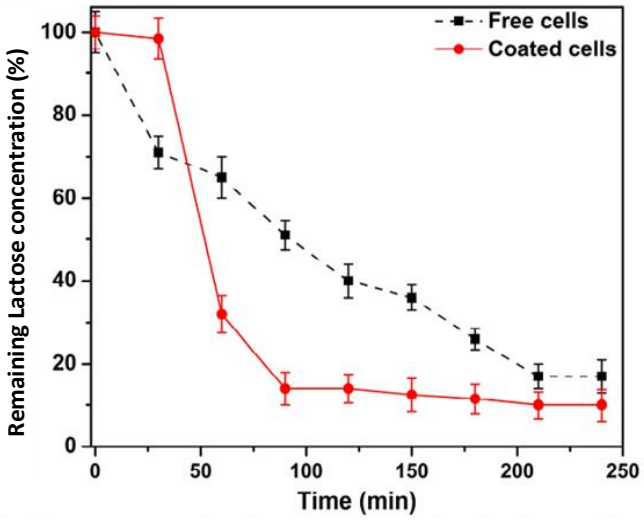

Figure 2.7 Time course of lactose degradation by free and magnetite nanoparticles coated cells.

Source: (Brar et al. 2015)

This increase in degradation activity of coated cells could be attributed to the increase in membrane permeability due to the coating of the bacterial surface with magnetite nanoparticles. From an industrial perspective, coated cells will take half the time as compared to free cells to complete the task, significantly reducing cost and labour (Brar *et al.* 2015).

2.7.3.2 Metal nanoparticles

Lately, nanotechnology has been employed in several customary products and procedures because nanoparticles introduce new physical and chemical characteristics. Previously, only gold nanoparticles at very low concentration (108 mmol/L) were examined to reveal their impact on the generation of hydrogen by biological methods, with a 56% performance improvement registered (Colvin 2003; He, Chen and Evans 2007; Bagchi *et al.* 2012). The researchers conclusively revealed that gold nanoparticles would function as ‘‘electron sinks’’ because they have a high affinity for electrons which promote the reduction of protons to form hydrogen molecules. They acted parallel to hydrogenases that naturally accomplish this metabolic pathway in cells. Other metals interact with microbes under ambient conditions.

Gold and Nickel are regarded as metals which interact with the microorganisms for their antimicrobial activity (Sotiriou and Pratsinis 2010; Bagchi *et al.* 2012; Reddy 2016). Palladium is typically involved because it strongly interacts with hydrogen molecules in chemical reactions (Klavsyuk *et al.* 2011). Iron is an essential metal and serves as a cofactor for hydrogenase processes. In this investigation, the impact of nanoparticles of about 2–3 nm for three metals (palladium, silver, copper) and one iron oxide was studied with pure *C. butyricum* culture, and a 43% increase in hydrogen production rate was observed (Lee, Li and Noike 2010; Xu *et al.* 2012).

2.7.3.3 Iron concentration

Iron is crucial in the formation of hydrogenase by electron transport to generate more hydrogen. In the presence of iron, the iron-sulphur protein in ferredoxin that acts as an electron carrier to oxidise pyruvate to acetyl-CoA and carbon dioxide and as a proton reducer to molecular hydrogen directs acidogenic metabolism. However, in iron-deficient conditions, flavodoxin replaces ferredoxin as an electron transporter, thus reducing the possibility of hydrogen production. Therefore, it is essential to supplement iron into fermentative hydrogen production to improve ferredoxin activity (Lee, Miyahara and Noike 2002). One of the studies conducted demonstrating the supplement of 25 mg/L of iron resulted in enhanced hydrogen yield with 391 to 408 mL/g of

glucose utilised. In addition, it was reported that increased iron concentration could also negatively affect hydrogen production (Zhang *et al.* 2018).

Recent studies have also focused on factors such as the effect of external iron concentration which have shown to diminish hydrogenase activity under depleted iron concentration in the media (Lee, Miyahara and Noike 2002). Further tests showed that using nanoparticles improves the bioactivity of hydrogen producers (Han *et al.* 2012; Zhao, Li and Astruc 2013). Nanoparticles have an affinity for electrons which enable further reduction of protons to hydrogen resulting in a higher hydrogen production rate (Beckers *et al.* 2013). Nanoparticles can be classified according to their material of construction, that is, metallic, semi-conductor and polymeric nanoparticles (Liu, Ren and Wan 2007). Using nanoparticles can enhance chemical reaction rates which can increase hydrogen production rate during fermentation (Gadhe and Gupta 2007; Kim, Yang and Logan 2018).

2.7.4 Enhancing biohydrogen production with nanoparticles

Nanoparticles have recently obtained much attention to bumper the activity of hydrogen generating microbes (Han *et al.* 2011). Nanoparticles can be synthesised by sputtering to chemical vapour deposition and most popular micro-emulsion technique. The micro-emulsion technique is a useful wet chemical method that is dependent on the nature of the surfactant to participate in self-assembly into a micelle. Synthesising such structures are advantageous because of their protective and magnetic properties (Carpenter 2001). Nanoparticles, for example, gold, iron, and metal oxides have shown to improve the kinetics of the bioprocess through their ability to react with electron donors and increase the activity of microbes under anaerobic environments (Zhang and Shen 2007; Xu *et al.* 2012; Beckers *et al.* 2013). Metal oxides and metallic nanoparticles have gained interest because of low cost and their unique physical and chemical properties. Iron nanoparticles have shown much potential for hydrogen production as iron is easily available as it is a common metal. Since iron has a low standard redox potential, it can be readily oxidised by water. According to the chemical Equation 2.7, iron reacts once in contact with water to produce hydrogen gas under ambient conditions, when one mole of iron reacts, a mole of hydrogen is produced (Reardon 1995; Zhang *et al.* 2018).

$$Fe^{0} + 2H_2O \rightarrow Fe^{+2} + + 2OH^{-} + H_2 \qquad 2.7$$

Iron oxide nanoparticles can be represented in various forms such as magnetite (Fe_3O_4), hematite (α-Fe_2O_3) and maghemite (γ-Fe_2O_3) (Teja and Koh 2009; Nasr *et al.* 2015). Researchers have

proposed that an interaction between iron oxides' nanoparticles and hydrogen producers exists, thus causing a rapid rate of hydrogen evolution (Han *et al.* 2011). The claim states that nanoparticles would behave as 'electron sinks' that would further reduce protons to hydrogen (Mu and Chen 2011). Investigations using hematite nanoparticles found that an optimum concentration of 200 mg/L yielded 3.21 mol H_2/mol sucrose (Han *et al.* 2011; Kumar *et al.* 2018). Maghemite nanoparticles have also been explored by using actual starch wastewater to enhance hydrogen production rate in a mixed culture system. Results showed that cultures immobilised with nanoparticles had an increased yield of hydrogen when compared to unaltered cells (Nasr *et al.* 2015; Kumar *et al.* 2019).

2.8 Statistical modelling for the dark fermentation process.

An endeavour was made to build up a unified model for the fixed-film reactors and for the ABR to forecast reactor efficiency and effectiveness. Within each compartment for one loading, the concentration of active microbes was determined, and the data related to the same feeding rates as with the 'fixed-film' model (Mohammadi *et al.* 2017). The second model, named 'the dispersed growth' model, had outcomes that did not give a sensible explanation of the data because diffusional restrictions were disregarded (Niz *et al.* 2019).

Bachmann, Beard and McCarty (2015) carried out additional work utilising the 'fixed-film' model on baffled reactors with an influent substrate whose strength was 8 gCOD/L. The model foresaw the behaviour that follows a decline in treatment effectiveness with:

i. diminishing input concentration at steady feeding rates,
ii. an upsurge in the loading of organics at constant inlet concentration, and
iii. an increment in the recycling ratio at a steady HRT because the reactor approaches well-blended behaviour.

Reactor effectiveness was enhanced by decreasing substrate concentration at constant HRT.

Nachaiyasit and Stuckey (1997) came up with a 'spherical' model employing Monod kinetics joined with substrate molecular diffusion into the biomass aggregates if:

i. The concentration of the substrate can be explained by one parameter, COD,
ii. Biomass quantities can be satisfactorily depicted by a solitary parameter, VSS,
iii. The biomass concentration is uniform under balanced growth and,
iv. The important bioreactions happen at steady pH and temperature.

The computation of essential model components, for example, the thickness of the diffusion layer, and liquid-phase mass transfer coefficient obeyed the procedures suggested by Bachmann, Beard and McCarty (2015). Generally, the model forecast better COD removal than was determined in experimental runs and was largely exact for higher loading rates (between 9.6 and 18 gCOD/L.d with HRT of 20 h) than at small residence time (10.5 h HRT with an influent composition of 4g COD/l) but demonstrated substantial non-conformities for the primary compartments in some of the simulations (Barber and Stuckey 2009). Likewise, with past models, certain patterns showed up in the outcomes such as a reduction in removal efficiency with increase in circulating load, reducing HRTs (at fixed substrate concentrations), and increasing substrate concentrations (at fixed HRT). However, the previous planar fixed-film equations provided a nearer fit than the spherical model. Considering the discoveries of a sensitivity analysis that showed floc flowrate and surface area greatly influenced the model predictions, modification to the model was done with the surface area as the fitting parameter (Li, Nan and Gao 2016).

2.8.1 Kinetics of substrate consumption

Substrate utilisation kinetics customarily described by a generalised Leudeking-Piret-like relationship combined with Logistic mass balance on COD utilisation comprised of substrate consumption for maintenance of cells and formation of biomass in Equation 2.8 (Don and Shoparwe 2010):

$$S = S_o - \frac{X_o X_m e^{\mu_m t}}{Y_{X/S}(X_m - X_0 + X_0 e^{\mu_m t})} + \frac{X_0}{Y_{X/S}} - \frac{X_m m_s}{\mu_m} ln \frac{X_m - X_0 + X_0 e^{\mu_m t}}{X_m} \quad 2.8$$

Where S_o = initial substrate concentration

S = Substrate concentration, g-COD L^{-1}

X_o = Initial biomass concentration, g-VSS L^{-1}

X_m = Maximum attainable biomass concentration, gVSS L^{-1}

μ_m = Maximum specific growth rate, h^{-1}

Y_{xS} = Maximum yield coefficient, g-VSS g-COD^{-1}

m_s = Maintenance coefficient, g-COD g-VSS^{-1}

t = Fermentation time, h

The values of Y_{xS} and m_s were estimated by nonlinear curve fitting of Equation 2.9. Additionally, the specific degradation rate (v), which depends on the substrate, was predicted using the Michaelis-Menten model.

$$v = \frac{v_m S}{k_m + S} \quad 2.9$$

Where v = Specific substrate degradation rate, g-COD $gVSS^{-1}$ h^{-1}

v_m = Maximum specific substrate degradation rate, gCOD g-COD $gVSS^{-1}$ h^{-1}

k_m = Dissociation constant

The Lineweaver-Burk linearised model was used to predict the kinetic constants v_m and k_m.

2.8.2 Kinetics of product formation

A modified version of the Gompertz relationship as shown in Equation 2.10 was employed for analysing the hydrogen and the VFA production profiles during batch fermentation as described by (Gadhe, Sonawane and Varma 2014).

$$H = P \exp\left\{-exp\left[\frac{R_m e}{P}(\lambda - t) + 1\right]\right\} \quad 2.10$$

Where H is the cumulative hydrogen volume generated (mL), P is potential of hydrogen formation (ml), R_m the highest rate of formation (mL/h) and λ the lag phase (h). The values of P, R_m and λ were determined by finding the best fit from the hydrogen generation data for Gompertz equation using the MATLAB R2010a with Optimisation Toolbox 2.1 (Pradhan *et al.* 2016). The highest SHPR (mL/ (g-VSS·d)) was computed by determining the quotient of R_m and the primary sludge's VSS. The hydrogen yield (mL/g substrate) was also computed by finding the quotient of P, and the substrate concentration in wastewater.

Furthermore, the influence of substrate concentration on hydrogen production rate (HPR) in the batch test under optimised conditions was analysed using modified Andrew's model as follows :

$$R = \frac{kS}{k_S + S + S^2/K_I} \quad 2.11$$

Where R = Hydrogen production rate, mM h^{-1}

K_I = Inhibition constant, g-COD L^{-1}

The HPR was computed as described by Wang and Wan (2009) and a nonlinear relationship between R and S was evaluated using Equation 2.11.

2.9 Role of optimisation of operating parameters in the improvement of Biohydrogen production

For the development of economically sound bioprocesses, it is crucial to optimise the operating conditions of the fermentation process. The optimisation is pivotal in the development of any fermentative process because of its impact on the economics and feasibility of the process. Optimisation can be described as the regulation of a process at or around its optimal points to realise maximum productivity in an economical way and simultaneously not compromising quality of products and the process at large (Hitit, Lazaro and Hallenbeck 2017; Bryson 2018). Upon scaling up to commercial level, process optimisation helps to reduce the cost relative to the benefits. Optimisation of any process is of paramount importance in commercial-scale of production, with particularity in biotechnology where even small improvements can be of utmost importance on a commercial scale (Reddy *et al.* 2008).

Quantity and quality of the product are affected by several parameters including the genetical make-up of the fermentation microbes, operating conditions, physiological conditions, nature of the substrate and reactor configuration (Prakasham *et al.* 2007; Rao *et al.* 2008). Process parameters need to be treated with care as they have the propensity to influence the microbial consortia required for the dark fermentation process which synchronously influences the stability of the fermentation process (Prakasham *et al.* 2007; Krakat, Schmidt and Scherer 2010). The same rules also govern the production of hydrogen through dark fermentation; it is also influenced by the nature of the substrate and its concentration, the pH and the orientation of the reactor, so as other operating conditions such as temperature (Fan *et al.* 2004; Wang and Wan 2009), and the nature of the inoculum (Lee, Miyahara and Noike 2002; Gadhamshetty *et al.* 2015).

A more robust process for commercial use is built upon optimisation, and it has been considered as one of the most critical techniques to improve the dark fermentation process (Prakasham *et al.* 2009). There is a need to use statistical techniques to optimise the operational factors that influence the fermentative production of biohydrogen. The experimental design is essential in optimising the dark fermentation process because of its complexity, and it is affected by several factors; thus, an appropriate design of experiments must be adopted to study the effects of these critical factors (Nath and Das 2011).

A model delineates the relationship between the key variables and quantitatively elucidates the behaviour of a production system. The model creates an entry point for analysis, design and operation of the bioreactor (Nawawi *et al.* 2011; Faloye 2015). The purpose of modelling and optimisation was to improve the biohydrogen production process by using different modelling methods (Wang and Wan 2009). Statistical methods such as RSM and Artificial Neural Network (ANN) have recently gained popularity. They have been on the rise in as far as their adoption is concerned, because of the loopholes of the other optimisation methods (Mukherjee, Chakraborty and Dutta 2019).

The design of experiments is widely employed to control the effects of input factors in several processes. Its main advantage lies in reducing the number of experiments preserving, the quality of research and in turn, saves time and resources. Additionally, analysis of the observations is without difficulties realised, and experimental errors are to a kept minimum. Statistical methods measure the effects of change in operating variables and their interactions on the process (GE 2005; Kaminari *et al.* 2005). The three steps used in experimental design included statistical design experiments, estimation of coefficient through a mathematical model and analysis of the model's applicability (GE 2005; Dashamiri *et al.* 2017).

2.9.1 Response Surface Methodology (RSM)

It is well documented that if the goal of a study is to optimise the process parameters, the second-order, with care, must be used. The second-order models are very flexible since they resort to the estimation of the response surface in the vicinity and can assume a broad range of functional form (Akhbaria *et al.* 2019). There is substantial evidence that demonstrates the success of second-order models in dealing with real-life response surface problems (Thakur, Tandon and Jadhav 2017). Owing to these reasons, the second-order models are frequently used to approximate the actual response surfaces in comparison to the first-order models. The widely popular second-order models include the central composite design (CCD), the Doehlert Matrix design (DM) and the Box and Behnken Design (BBD) (Madondo 2018; Veljković *et al.* 2018).

RSM is mostly adopted in formulating new products, in improving existing product design, in optimising processes, in developing and improving processes (Montgomery 2017; Sadati, Chinnam and Nezhad 2018). The RSM has a unique ability to set up an experiment that achieves the maximum number of dependent variables on the response surface with the minimum possible

number of observations (Domínguez *et al.* 2016; Argun and Onaran 2017). The principal aim of RSM is the estimation of the area and the optimal point of the area that gives the desired properties in a design consisting of several parameters that affect the result in an experiment (Domínguez *et al.* 2016). RSM involves planning operations strategically in a bid to investigate the experimental region of process variables and optimisation methods using experimental modelling techniques to establish the correlation between the input variables and the output parameters (response) (Tunçay *et al.* 2017; Gokfiliz-Yildiz and Karapinar 2018; Mishra *et al.* 2018; Sağır, Yucel and Hallenbeck 2018). For multi-response problems, the solution is evaluated in stages, that is, modelling and optimisation after collection of data (Sadati, Chinnam and Nezhad 2018; Majdi, Esfahani and Mohebbi 2019).

The output factors are predicted by the polynomial quadratic equation to establish a relationship between the response variables and the input variables (independent). The general form taken by the quadratic equation is as follows (Mu, Wang and Yu 2006; Ulhiza, Puad and Azmi 2018; Zhang *et al.* 2019b):

$$R = C_0 + \sum_{i=1}^{k} C_i I_i + \sum_{i=1}^{k} C_{ii} I_i^2 + \sum_{i=1}^{k} \sum_{j=1}^{k} C_{ij} I_i I_j \qquad 2.12$$

Where I_i is the independent variables which influence the response variable R, C_0 is the offset term (intercept), C_i is the i^{th} linear coefficient, C_{ii} is the quadratic coefficient, and C_{ij} is the ij^{th} interaction coefficient. Equation 2.12 can be used to determine optimum values for a corresponding set of input variables by partially deriving the model response with respect to individual input variables and equated to zero (Majdi, Esfahani and Mohebbi 2019).

CHAPTER THREE

WASTEWATER CHARACTERISATION AND SUBSTRATE SELECTION FOR BIOHYDROGEN PRODUCTION

3.1 Introduction

It is almost impossible to avoid the generation of wastes from human activities, and a more significant portion of the waste ends up as wastewater. Many factors affect the quality and quantity of wastewater that are discharged from different industries. The wastewater characteristics are mainly influenced by the behaviour, and process type of the industry in question, as well as the technical framework by which industries comply with (Dickenson *et al.* 2011; Xiaoxin *et al.* 2019).

The feasibility of biological hydrogen production from different industrial (organic-rich) wastewater streams was examined theoretically by applying relevant chemical equations and practically through batch experiments in Schott bottles (Hwang *et al.* 2004; Carrillo-Reyes *et al.* 2019). However, there is a deficiency of information on hydrogen potential of several industrial wastewater streams under similar operating conditions such as temperature, time, digester configuration, inoculum, among other factors. Thus, this chapter focuses on discussing ways of characterising wastewater streams from different industries and selection of the stream with the highest hydrogen potential together with other non-technical factors.

3.2 Methodology

Five streams (yeast, alcohols, brewery, sugar and dairy industries) were chosen for characterisation, and theoretical hydrogen potential was calculated based on the properties found. Preliminary batch experiments were also run to determine the stream with the highest hydrogen potential. The selected sample had no consistent characteristics (since processes differ in operation every time), although the values of the monitor parameters were closely related.

3.2.1 Sampling and transportation

Samples were collected from five different industries around Durban (names of the companies are not be disclosed), whose effluent was rich in organic material and stored to maintain and mimic their original state as in the source plant or effluent section. Specific care was taken to avoid contamination of samples. Thus, samples were stored in secure places to prevent conditions which could alter the parameters of the sample (Ntaikou *et al.* 2009; Van Loosdrecht *et al.* 2016)**.** Identification of possible organic-rich wastewater streams was influenced by the research from literature and synchronous consultation of the factories running the same processes in and around Durban. This helped to reduce the number of streams to be characterised.

The quality control and quality affirmation measures were performed by discarding the samples whose properties deviated from the expected properties as determined on the first sampling day. The onsite quality control parameters were pH, conductivity, dissolved oxygen, total dissolved solids, and salinity as measured by a calibrated YSI instrument (YSI 556MPS, Yellow Springs, USA). The sampling protocol was established considering industry administration practices and variety in peak times of operation. Plant cleaning and non-operational periods were avoided as it would not give an accurate representation of the wastewater discharged by the processes in question. The sampling schedule was used to capture effluent from an industry when it is effectively producing wastewater. For this survey, commingling was assumed to have occurred, as the goal of this review was to decide on a suitable wastewater stream for attractive biohydrogen production. Sampling was done every week.

After the sampling process, the samples were set in an iced cooler and were instantly transported to the laboratory for analysis. Each laboratory parameter to be tested had a specific container, holding time and collection methodology that was followed during sampling. To lessen this adjustment of samples drawn for solids determination, samples were stored at 4°C. Samples were not permitted to freeze (Dong *et al.* 2009). Although specimens were kept in this way for up to 48 hours for settleable solids and up to seven days for different solids tests, it was profoundly prescribed that characterisation start inside 24 to 36 hours of sample gathering (Clesceri *et al.* 2005).

3.2.2 Analytical methods

The constituents of a wastewater stream are of paramount importance, especially in processes such as fermentation. Thus, the following parameters were determined: COD, BOD, TS, Volatile solids (VS), pH, Oxidation-reduction potential (ORP), DO, Total dissolved solids (TDS), Suspended solids (SS), Conductivity, Nitrites, Nitrates, Ammonium, and Total Oxidisable Nitrogen (TON). All samples were analysed as described in the Standard Methods for the Examination of Water and Wastewater and Standard Methods for water and effluent analysis (Ademoroti 1996; APHA 2005; Clesceri *et al.* 2005). Where examination was not instantly conceivable, the samples were refrigerated at 4℃ to repress biodegradation.

3.2.2.1 COD and BOD characterisation

When analysing for BOD, the wastewater sample, or a proper dilution, was incubated for five days at 20℃ in darkness in a thermostat incubator cabinet (Manometric BOD Measuring Devices-OxiTop ® IS 12). For high BOD range 22.7 mL of the sample were put in the brown sample bottles (nominal volume 510 mL), a magnet stirrer was also inserted and closed with a rubber quiver. 2 sodium hydroxide pellets were placed into the rubber quiver and tightly closed with constant shaking throughout the 5-day testing period. The diminishment in the concentration of dissolved oxygen during the incubation period yields a measure of the BOD (Jirka and Carter 1975; Jouanneau *et al.* 2014). Dilution was made with potable water.

For soluble COD determination, the sample was filtered to under 0.45 µm, and 1.5 mL of the substrate was charged to a vial with acidified potassium chromate (2.5 mL $K_2Cr_2O_7$ and 3.5 mL H_2SO_4). The contents of the vials were digested for 2 hours at 150℃ using a Hach COD Reactor (45600-02)(APHA 2005). After digestion, the samples were filtered to under 0.45 µm, diluted with distilled water accordingly. COD was determined using the Spectroquant Pharo 300 Spectrophotometer (320-1100 nm, EMD Millipore, 1007060001) at a wavelength of 620 nm and results are shown in Appendix A, Table A3, A4 and Appendix D, Figure D3. A blank was run every time to zero the instrument.

3.2.2.2 Solids determination

Detailed methodology on characterisation was presented in the handbook for water and wastewater characterisation (APHA 2005), and intricate calculations and determination on characterisation are

shown in Appendix A1. 'Total solids' was the material remaining in a vessel after a sample was evaporated and subsequently dried at 103-105℃ in a furnace. Total solids is a combination of 'total suspended solids', that is filtration residue and 'total dissolved solids', as referred to the filtrate (APHA 2005).

A homogenous sample of wastewater was evaporated in a dish of known mass and put in the furnace at 103-105℃ to dryness until a constant mass was achieved. The change in mass of the solids and dish in comparison to the empty dish amounts to the total solids (TS) (APHA 2005).

A homogenous wastewater sample was passed through a glass fibre filter with 0.45μm pore size without the organic binder. The filtrate was evaporated in a weighed dish, then dried at 180℃ until a constant weight was achieved. Total dissolved solids (TDS), was then determined as the change in mass of the dish and solids in relationship to the empty dish (APHA 2005).

A homogenous measured sample was filtered with the help of a vacuum pump, through a pre-weighed standard laboratory glass fibre filter. The glass fibre filter was dried at 103-105℃ after filtration, desiccated, and reweighed. The change in mass of the filter and solids relative to the independent filter represented the total suspended solids (TSS) (APHA 2005).

Solids that remained after the analysis for TS, TDS or TSS were ignited at 550 ±25℃ to a constant mass. The change in mass due to ignition represented the volatile part of the solids. The difference in mass of the support vessel and ash which remained after ignition relative to an empty dish represented the fixed solids (APHA 2005).

3.2.3 Seed sludge and pretreatment

The seed sludge was taken from the anaerobic digester at Amanzimtoti wastewater treatment plant and was observed to contain a consortium of microorganisms. A known volume of the seed sludge collected was fed into a heat resistant glassware and heated in an autoclave at 121℃ for 15 min to select hydrogen-producing bacteria through thermal pretreatment method (Kumar *et al.* 2016b). The pretreated sludge was left to cool down before mixing with the wastewater. The pretreated seed sludge was characterised for VSS before and after mixing with the substrate.

3.2.4 Experimental setup for the BHP tests

Anaerobic biogasification potential assay, also known as BHP tests, were conducted in 600 mL Schott bottles. The pretreated seed sludge and the substrates were mixed based on volumes and

fed into the Schott bottles for anaerobic digestion. Pretreated sludge was used as inocula with a substrate-to-biomass ratio ranging from 4-20:1 in all the batch tests using different wastewater streams as carbon sources. The reactors were flushed at the start with nitrogen gas for 3 min to vent off the air and to ensure strict anaerobic conditions within the bottles (Jia *et al.* 2019). All the reactors were manually shaken for up to a minute before taking measurements of the biogas produced to avoid or minimise stratification of the medium and this also gave assurance of sufficient mixing and agitation of the substrate. The initial pH of the media was between 4 and 7.5 and was not controlled or maintained during the experiments (Penniston and Gueguim Kana 2018). The tests were run at atmospheric pressure and 35 ± 0.5℃ in a thermostatically controlled water bath.

Only the volume of the substrate was a variable; all other parameters and operational conditions were held constant, as per the literature conditions (Ghimire *et al.* 2015; Dessì *et al.* 2018). The samples from different streams were not diluted, and no supplementary nutrients were added.

3.2.5 Decision-making tool for substrate selection

The ranking technique was used to determine the best substrate for the biohydrogen production using the dark fermentation, and this is called the Kepner-Tregoe technique (K-T). The alternatives are identified as a possible solution for ill-structured problems (Guth *et al.* 2016). K-T analysis involved giving weight to the various factors which need consideration in substrate selection with the factor having high value commensurably given a high score and low-rated factors corresponding given low scores. The most critical factor is ranked 10, and the least important can be as low as 1. Each wastewater stream was rated for each factor, and the score (evaluation) was the product of the weighting and the rating. The substrate stream with the highest score was, therefore chosen (Kepner and Tregoe 1976; Parker and Moseley 2017).

3.3 Theoretical hydrogen calculation

3.3.1 Percentage of hydrogen yield

When predicting the amount of hydrogen that a specific source (wastewater stream) can produce, it is imperative to consider the biochemical reactions routes taken and the products formed. The following balanced equation predicted the anaerobic digestion process, and its derivation

applicable to various substrates is illustrated (Rittmann and McCarty 2012). During anaerobic digestion, part of the organic matter is converted into biomass (characteristic formula $C_5H_7O_2N$) and the other into energy (products) (Kim and Cui 2017).

The degree of production of a specific substrate can be predicted by the following relationship. Equation 3.1 is based on both practical and theoretical production of hydrogen from digestible hydrocarbons (Guo *et al.* 2010; Kothari *et al.* 2017).

An assumption was made that all the carbohydrates (hexoses and pentoses) were digested to only carbon dioxide and hydrogen, disregarding the intermediate routes taken by these biological reactions (Catal 2016; Ravndal *et al.* 2018). This was done to estimate the maximum possible hydrogen that can be produced by a particular wastewater stream with all the other factors held constant. The yield of hydrogen was then computed using the relationship of hydrogen created practically and the theoretical biohydrogen prediction. Equations 3.1 and 3.2 require the knowledge of the constituent quantities of sugars in a sample. To estimate the theoretical yields of biohydrogen, the glucose biotransformation reaction is widely accepted as a reference (Liu and Chen 2018).

$$\%\, H_2\ yield = 100\,\frac{\boldsymbol{PV}}{\boldsymbol{RT}}\sum_{\boldsymbol{i=1}}^{\boldsymbol{k}}\frac{\boldsymbol{M_i}}{\boldsymbol{r_i m_i}}\ , where\ k = 1,2,3, \ldots \qquad 3.1$$

Where $\mathbf{r_i = x_i + 0.5\ y_i - z_i}$ (for i =1, 2, 3…) = stoichiometric ratio of hydrogen produced theoretically from sugar 1, sugar 2, sugar 3, etc. in the substrate (refer to Equations 3.3 and 3.4).

m_i = mass of sugar 1, sugar 2, sugar 3, etc. in the substrate (g).

M_i = molar mass of sugar 1, sugar 2, sugar 3, etc. in the substrate (g/mol).

R = universal gas constant

P = pressure of the operating system

T = temperature of the system

The maximum ideal yield would be (y/2 + x – z) mol H_2/ mol carbohydrate. In practice, this value is unachievable as different reaction pathways are taken based on the microbial activity in an individual system (Ferreira *et al.* 2018)

3.3.2 Maximum possible volume of hydrogen produced

For known simple carbohydrates in a sample, the total volume, V_t resulting from different sugars in a substrate is given by the following relationship in Equation 3.2:

$$V_t = \sum_{i=1}^{k} \frac{r_i m_i RT}{PM_i} = \boldsymbol{\frac{RT}{P} \sum_{i=1}^{k} \frac{r_i m_i}{M_i}}, where\ k = 1,2,3, \ldots \quad 3.2$$

The total volume will then be used to determine the total mass or number of moles hydrogen gas produced at a given set of conditions.

3.3.3 Volume of hydrogen from a known COD/BOD ratio

This section outlines the relationship between volume hydrogen produced and COD/BOD ratio. Any carbohydrate oxidation is calculated using the theoretical chemical equation of conversion of carbohydrates of any nature to water and carbon dioxide given in Equation 3.3 as follows (Catal 2016):

$$C_x H_y O_z + (x + \frac{y}{4} - \frac{z}{2}) O_2 \rightarrow x CO_2 + \frac{y}{2} H_2 O \quad 3.3$$

Hydrogen evolved is calculated using the theoretical chemical equation of conversion of carbohydrates of any nature through the acetic pathway as given in Equation 3.4:

$$C_x H_y O_z + (2x - z) H_2 O \rightarrow \frac{1}{2} x\ CH_3 COOH + \frac{1}{2} x\ CO_2 + (\frac{y}{2} + x - z) H_2 \quad 3.4$$

The relationship in Equations 3.5 gives the volume of hydrogen (in mL) gas produced with the knowledge of COD, BOD (in mg/L) and volume of the substrate (in litres) (Buitrón *et al.* 2019).

$$V_{hydrogen}(mL) = \boldsymbol{\frac{31.25\ (COD) V_{subs} RT}{C_B P} \sum_{i=1}^{k} \frac{r_i}{j_i}}\ for\ i = 1,2,3 \ldots \quad 3.5$$

Or in Equation 3.6 (in mL per litre of the reactor)

$$\frac{V_{hydrogen}}{\boldsymbol{V_{subs}}}(mL/\boldsymbol{L_{reacto}}) = \frac{\boldsymbol{31.25\ (BOD)RT}}{\boldsymbol{P}}\sum_{\boldsymbol{i=1}}^{\boldsymbol{k}}\frac{\boldsymbol{r_i}}{\boldsymbol{j_i}}\ for\ i = 1,2,3\ \ldots \qquad 3.6$$

Where: j = x + 0.25y – 0.5 z (refer to Equation 3.3)

r = x + 0.5 y - z

C_B = COD/BOD ratio

V_{subs} = volume of the substrate (litres)

NB: The relationship shown in Equation 3.5 is independent of masses of constituent sugars and their molar masses. However, it is important to know the COD, BOD, and chemical equations of the constituent sugars in a certain sample.

3.4 Results and data analysis

3.4.1 Summary of wastewater characteristics

The characterisation yielded the results, as shown in Table 3.1. Various properties were determined based on their importance in determining the biohydrogen potential of the respective streams. The standard deviations were calculated and presented against the averages of triplicate trials for every characteristic and every wastewater stream. The notable critical properties were the COD, BOD, pH, volatile solids (VS) salts and TS, among others, for reasons elucidated anywhere else (Ravndal *et al.* 2018).

From Table 3.1, it is visible that the yeast wastewater stream had the highest COD value of 12277±269 mg/L comparable to a study conducted by Pirsaheb *et al.* (2018) with the COD ranging between 13000 and 16000 mg/L. This was followed by the brewery stream (6767±232 mg/L) which was accompanied by a similar study by Gluck, Phan and Patnode (2018) with COD ranging between 4000 and 6000 mg/L. The least was the sugar wastewater stream with 1766±150 mg/L and concurred with a study conducted by Assawamongkholsiri *et al.* (2018) with stable COD from 1250-2400 mg/L. Interestingly, the sugar wastewater stream had the lowest COD/BOD ratio of 1.45, making it is easier to digest anaerobically. In contrast, the dairy wastewater had the highest COD/BOD ratio of 5.36, making it difficult to digest anaerobically.

The dairy wastewater stream registered the highest DO of 50.3%, and the brewery stream had 2.5% making it less toxic to the anaerobes as compared to the dairy stream. pH was lowest in the sugar wastewater stream with a pH value of 3.72, and the highest among the five streams was the alcohols wastewater stream with a pH of 7.79. low pH values below 4.5 render the hydrogen-producing microbes ineffective, and high pH above 6.5 would also hamper productivity by the HPBs as they operate within a specific pH range (Chandrasekhar, Lee and Lee 2015; Łukajtis *et al.* 2018)

Table 3.1 Characteristics of wastewater streams in summary.

Wastewater stream / Property	Sugar Industry	Alcohols	Dairy	Brewery	Yeast
COD	1766±150	4561±229	10571±239	6767±232	12277±269
BOD	1215±99	1108±48	1974±212	3118±188	4376±145
TS	2 846±105	14 095±698	17 245±1896	5503±308	1014±74
TSS	1 856.47±76	9196.91±616	10 974±586	3592±237	593±46
TDS	989.53±80	4898.09±302	6271±467	1911±263	421±26
VS	2 558.21±178	6257±411	3483±173	2189±140	439±37
pH	3.72 ±0.25	7.79±0.78	7.02±1	5.77±0.26	5.92±0
pH mV	170.5±16	-19.3±7.22	-99.3±29	0.8±0.11	49.5±6
ORP mv	-57±15	-96.7±10	-32.9±4	-65.9±10	-126.1±17
DO	0.39±0.13 (3.9%)	1.25±0.04 (7.7%)	5.12±1 (50.3%)	0.19± 0.05 (2.5%)	0.62±0.06 (6.6%)
Conductivity C/ µS/cm	4910±236	739±52	538±42	2508±256	13 291491
Nitrites	0.07±0.01	0.15±0.02	0.05±0.02	0.04±0.01	0.03±0.01
Nitrates	0.34±0.01	0.51±0.04	0.43±0.07	1.41±0.17	0.48±0.08
Ammonium	0.39±0.05	0.41±0.05	0.71±0.12	0.87±0.05	0.82±0.12
TON	0.59±0.07	0.66±0.05	0.38±0.08	0.53±0.03	0.45±0.06
Phosphate	23.21±0.74	53.81±3.49	0.64±0.07	15.34±0.88	1.63±0.15
Sulphate	18.27±1.12	45.62±2.95	0.57±0.09	28.40±1.69	3.41±0.59
Colour	Dark yellow	Beige	Cloudy	Brown	Reddish-brown

The results summarised in this section are averages of the tests done with their respective standard deviations as shown in Table 3.1.

3.4.2 Biohydrogen potential test results

The hydrogen potential for the seed sludge alone was tested to determine its effect on the overall hydrogen production. Seed sludge produced an infinitesimally small amount of gas under mesophilic conditions 5 mL/day from the 550 mL of the digested medium. Thus, it can be concluded that under mesophilic conditions, the hydrocarbon material in the seed sludge did not contribute any gas volume during the dark fermentation. Therefore, the biogas produced was the direct determination from the respective wastewater streams. In another study, hydrogen production at 37g TS/L of natural microflora was recorded as 80.62 mL $H_2/L_{reactor}$. However, there was a significant increase to 351.12 mL $H_2/L_{reactor}$ at the same conditions when the fruit mixture was inoculated with the heat-treated anaerobic sludge. Still, the independent inoculum did not produce any biogas (Turhal, Turanbaev and Argun 2019).

Plate 3.1 shows the experimental setup for the BHP tests conducted in 600 mL Schott bottles with various wastewater streams.

Plate 3.1 Set up for preliminary batch experiments

Figure 3.1 shows the production of biogas over time, under similar conditions. The graph was constructed from averages of triplicate runs for dark fermentation tests. From Figure 3.1, it is evident that high gas production rates were experienced in the first 3-5 hours as the hydrogen

producers are expected to be more dominant than the hydrogen consumers. The hydrogen evolved per litre of wastewater streams in question varied widely under the set test conditions. The brewery wastewater had the highest biogas production rate with 58.0 mL of the biogas produced in the first hour, and hydrogen constituted 24% of the off-gas as reported by the results from GC ((Shimadzu GC-2014, Japan). In the first 8 hours, a total of 137.0 mL of biogas and a corresponding cumulative hydrogen composition of 40.1% was recorded (see Appendix G, Table G4). These values are slightly lower than a study done by Tena, Perez and Solera (2019) where the 243 mL of hydrogen was produced for thermally pretreated inoculum.

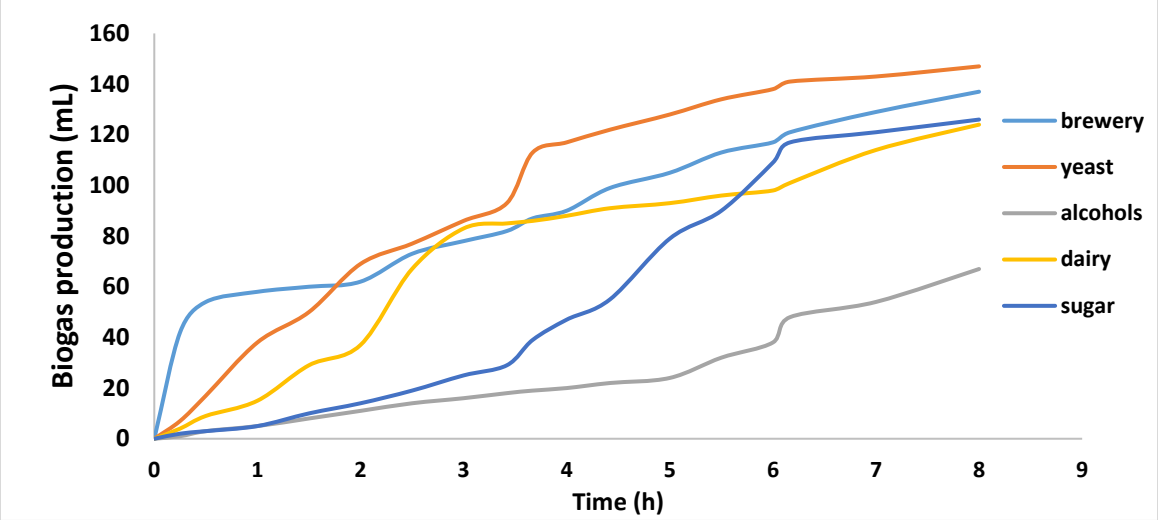

Figure 3.1 Biogas production in preliminary batch experiments

The alcohols wastewater had the lowest rate of production of biogas which reached 38.0 mL after 6 hours of the test with 8% hydrogen being reported by the GC. 67.0 mL was the cumulative total after 8 hours, and that constituted about 21.4% H_2. The other three streams produced biogas and hydrogen at fair rates in comparison to the brewery substrate; dairy cumulatively recorded 36.4% of hydrogen after 8 hours of operation, yeast: 25.1% and sugar: 32.9%. The balance was carbon dioxide in all the cases as verified by the GC analysis (no methane was produced) and it was in tandem with a study conducted by Koupaie *et al.* (2019) in which there was zero methane reported on the GC as a result of total inhibition of the methane producers during the pretreatment process. These differences in hydrogen generation were largely orchestrated by the initial COD and BOD concentrations. Streams with low COD/BOD ratios (less than 2.5) produced higher hydrogen

concentrations, except for the dairy stream. A low COD/BOD ratio represents a greater availability of digestible material in a sample (Zainal *et al.* 2018). Therefore the brewery (2.17) and the sugar (1.45) industrial wastewaters produced high yields biogas than all the other samples. There was however, an anomaly with the dairy wastewater (COD/BOD of 5.36) which registered a high HPR (3.9 mL H_2/h.). A possible explanation is that a high concentration of dissolved solids (6271 mg/L) have constituents that are readily biodegradable material, despite having a high concentration of carbon material which is usually difficult to digest biologically. Further studies need to be done to fully comprehend these results (Van Ginkel, Oh and Logan 2005; Mishra *et al.* 2016). The complexity of various wastewater streams could also have contributed to the anomalies presented in the biogas production distribution, as shown in a similar study by Ghimire *et al.* (2018) where 10% TS produced the largest substrate conversion of 2.901 (±0.143) mM metabolites/g TS, while the lowest was recorded for 30% TS as 1.435± 0.013 mM metabolites/g TS. The alcohols wastewater contains sizeable molecular weight compounds in comparison to simple sugars as evidenced by its high particulate nature. Large molecules need to be cleaved first into smaller molecules (typically less than $1.66*10^{-21}$ g) for them to be effectively digested by the microbes (Confer and Logan 1997; Abubackar *et al.* 2019).

3.4.2.1 Gas Chromatography results

Table 3.2 highlights the characteristics of the gaseous products ran on gas chromatography (Shimadzu GC-2014, Japan) outfitted with a thermal conductivity detector (TCD), 1.8m * 2.1mm stainless steel Porapak Q column with nitrogen as the carrier gas at 30 mL/min. The injector, oven and detector temperatures were set at 120℃, 50℃ and 250℃, respectively. The chromatograms were manually integrated, and the composition of component gases was determined accordingly.

The dominant components of the offgas were hydrogen and carbon dioxide, as illustrated in Table 3.2. Methane gas was produced in a few instances, but it was below detectable amounts as the peaks at the methane retention times were giving extremely insignificant areas. A summary of the GC results is presented in Table 3.2 and Figure 3.2.

Table 3.2 A summary of the GC results for different substrates' gas production

GC parameter	Peak*	Standard	Different streams' S/X ratios				
			Alcohols	**Brewery**	**Yeast**	**Dairy**	**Sugar**
Retention time	1	**0.723**	0.716	0.738	0.726	0.714	0.719
	2	**1.124**	-	-	-	-	-
	3	**1.843**	1.821	1.797	1.804	1.833	1.827
Area	1	**251358.3**	19325.6	32619.2	22299.6	26759.5	29 583.70
	2	**148921.5**	0	0	0	0	0
	3	**102754.2**	70980.9	48725.4	66543.4	46755.6	60336.4
Percentage composition (%)	1	**100**	21.4	40.1	25.1	36.4	32.9
	2	**100**	0.0	0.0	0.0	0.0	0.0
	3	**100**	78.6	59.9	74.9	63.6	67.1

*Peak 1, 2 and 3 represent hydrogen, methane, and carbon dioxide, respectively.

Number of moles, n, of biogas in a sample is determined as follows:

$$n = \frac{A}{A_{std}} * n_{std} * \frac{V_{reactor\ gas}}{V_{sample\ injected}} \qquad 3.6$$

Where A & A_{std} = areas of sample and standard, respectively

$V_{reactor\ gas}$ = total volume of the gas

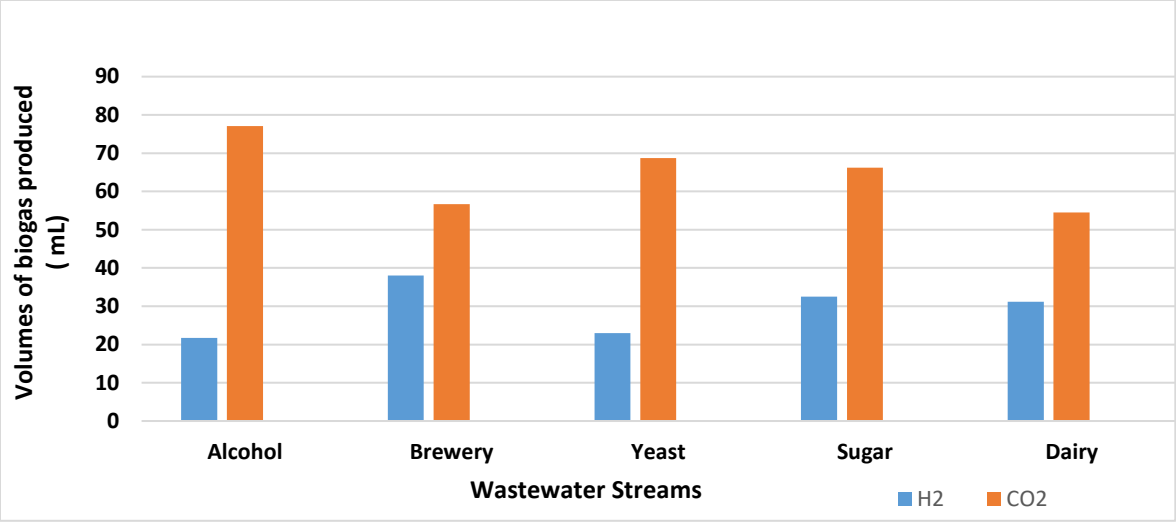

Figure 3.2 Volumes of gases produced in preliminary dark fermentation tests

The BHP tests were carried out on various industrial streams, and the following conclusions have been drawn as shown in Figure 3.2. Methane was not detected (infinitesimally small) for the gas collected within the first 8 hours of running the experiments for all industrial wastewater samples. In a similar study, Nualsri, Reungsang and Plangklang (2016) had the same observation registering 45-55% hydrogen and the remainder was carbon dioxide. The gas composition of hydrogen was below 50% in all the cases, and the balance of the gases as carbon dioxide. In a few instances, infinitesimally small amounts of H_2S were detected after 24 hours of operation and were considered negligible in this study. The brewery wastewater was found to have the best hydrogen potential in comparison to the other streams. It is recommended that further tests be carried out on a larger scale with the optimised parameters for the best possible yield of hydrogen and production rates.

3.5 Substrate selection

Several factors are considered when selecting the best substrate for biohydrogen production through dark fermentation as shown in Table 3.3. The major criteria for the selection of waste materials to be used in biohydrogen production are the availability, cost, carbohydrate content and biodegradability. The best substrate in its most natural state was favoured, in the field of engineering cost is also a vital factor to consider.

Table 3.3 Levels of the importance of factors affecting the selection of suitable substrate for fermentation

FACTOR	LEVEL OF IMPORTANCE (on a scale of 1- 10)	EXPLANATION
Sample availability	10	Steady acquisition of wastewater is crucial for the smooth running of the experiments and their availability is also a function of time. Substrate's source proximity is pivotal.
Initial COD/BOD	10	Influent COD/BOD ratio shows the potential of a specific substrate. Small ratios (less than 1.5) are preferred.
Chemical Analysis	9	Anaerobic reactions are sensitive to the chemical composition of the substrates such as sulphur, nitrogen, phosphorus. Balance of these chemicals is pivotal for the smooth operation of fermentation processes.
Solids Analysis	8	The solids content plays a crucial role in fermentation; characteristics such as VSS, TS and particle size affect the bioreactions directly.
Digestibility	10	Anaerobic reactions are hinged upon ease of biodegradability of the substrates.
Toxicity	9	Source of the substrate should be evaluated for any possible poisons as this has a detrimental impact on the whole process. Toxins may arise from cleaning of vessels or some enhancement strategies to the product.
Proximity to research centres	7	Wastewater is laden with microbes which may degrade the substrate when introduced to favourite conditions, especially during transportation; thus, laboratories should be close for experiments and analysis.
Legislation	6	Consent of publication of results from in-question industries.
Irritation Considerations	8	Impact of the effluent upon disposal to the environment and people nearby. Ease of getting rid of toxicants and irritants is of high value.

Table 3.4 Substrate selection by Kepner −Tregoe (KT) methodology

CRITERION	IMPORTANCE LEVEL, W	TYPE OF THE INDUSTRY BEING INVESTIGATED									
		Yeast		Sugar		Alcohols		Brewery		Dairy	
		P	S	P	S	P	S	P	S	P	S
Samples availability	10	6	60	8	80	8	80	10	100	8	80
Initial COD/BOD	10	8	80	8	80	6	60	10	100	9	90
Chemical analysis	9	7	63	8	72	6	54	8	72	7	63
Solids analysis	8	7	56	8	64	6	48	8	64	7	56
Digestibility	10	8	80	9	90	6	60	9	90	8	80
Toxicity	9	7	63	8	72	7	63	9	81	7	63
Proximity to research centres	7	7	49	6	42	7	49	7	49	7	49
Legislation	6	4	24	5	30	5	30	5	30	5	30
Irritation Considerations	8	7	56	7	56	7	56	7	56	7	56
Total	**675**		**531**		**586**		**500**		**642**		**567**
Percentage /%	**100**		78.7		86.8		74.1		95.1		84.0

Where P = points attained

S = P*W = Score attained

K-T is a decision-making tool that seeks to evaluate the factors regarded as crucial in the evaluation of a decision (Kepner and Tregoe 1976; Parker and Moseley 2017). This technique involves looking at similar processes to give weighting to various parameters under comparison that is, quantifying qualitative features of the decision-making parameters. From the results of the KT- decision analysis in Table 3.4, the substrate stream from the **brewery industrial wastewater** was found to be the most suitable feed for this study.

The KT framework is preferred mainly by researchers because of its systematic approach and well-defined outline of critical factors, creating less bias and more clarity around decisions. The KT process was designed to be flexible and modified for unique scenarios. Therefore, this study considered the KT process to be a reasonable technique (Guth *et al.* 2016).

In the subsequent sections, a thorough analysis of the brewery industrial water will be microscopically conducted; conclusions and recommendations in the enhancing of fermentative biohydrogen production will be drawn from this substrate stream.

3.6 Summary

The preliminary experiments were conducted in Schott bottles at fixed operating conditions of temperature 35℃ and batch time of 8 hours in all the cases. The wastewater streams investigated were the dairy, brewery, yeast, alcohols and the sugar industries. The highest COD value was found in yeast industry wastewater (12277±269 mg/L) and the lowest in the sugar industry wastewater (1766±150 mg/L). It is, however, the brewery wastewater, COD of 6767±232 mg/L that had the highest average hydrogen in the biogas (40.1%), dairy (36.4%), sugar (32.9%) yeast (25.1%) and alcohols industrial wastewater (21.4%). The best substrate selection was based on the Kepner-Tregor analysis tool, which is based on both quantitative and qualitative analyses of the wastewater streams. The brewery wastewater was determined to be the best stream among the five streams investigated.

CHAPTER FOUR

OPTIMISATION OF THE DARK FERMENTATION OPERATING CONDITIONS IN AN ANAEROBIC BAFFLED REACTOR

4.1 Introduction

Operating conditions such as temperature, pH and residence time play a crucial role in the dark fermentation processes as they significantly alter the rate of production, yields and reaction pathways (Bastidas-Oyanedel *et al.* 2019). This then introduces the dire need to regulate operating conditions within the range that confers favourable outcomes. Optimisation of operating conditions alone without the support of a suitable reactor may not be as effective as expected, hence this study adopted the use of the anaerobic baffled reactor (ABR), which is highly defined by its satisfactory heat and mass transfer properties (Sayedin, Kermanshahi-pour and He 2019). This chapter aims at determining the optimal conditions for lucrative fermentative hydrogen production. The parameters of interest were the batch time, pH and the temperature among others as they have a greater effect on the dark fermentation process in comparison to other parameters beyond the scope of this study (Kirli and Karapinar 2018; Muhialdin *et al.* 2019; Ziara *et al.* 2019)

The drawback of biohydrogen production by dark fermentation is that, in the dark, only enzymatic bacteria produce relatively small quantities of biohydrogen, usually lower than 30% stoichiometric (based on 12 mol-H_2 / mol-glucose) (Yang, Guo and Liu 2010; Cheng *et al.* 2013). Thus there was a need to focus more on improving the rate of hydrogen production than the yield since it has a thermodynamic limit. For this reason, more effort was devoted to maximising the rate of hydrogen production with a partial sacrifice to the conversion efficiency.

In this chapter, dark fermentation experiments which were performed on brewery wastewater are discussed. A series of fermentation runs were performed to determine the optimum conditions for attractive hydrogen production yield and rate. Laboratory-scale dark fermentation tests play an especially important part in the optimisation of this biological hydrogen-producing technology. Such tests are often used in investigations of the effect of HRT, temperature, hydrogen partial pressure, nutrients, culture pH and biomass immobilisation on the efficiency of the dark fermentation technology before it can be employed on an industrial scale (Jimenez *et al.* 2015).

In the view that the objective of the investigation was to acquire data, efficiency in research may be well-defined as the amount of valuable data acquired per unit cost. This logical, efficient method speeds up the solution of the investigational projects by allowing predictions to be made before all experimental trials are completed. One method for improving this research efficiency is that of the statistically designed (Rai, Mohanty and Bhargava 2016; Whitcomb and Anderson 2016). The technique requires less experimental runs, saves time, allows flexibility to assign the levels of variables and gives closer confirmation of the output response towards the set goals (Oliveira *et al.* 2017).

Response Surface Methodology (RSM), (Central Composite Design (CCD)) was adopted because of its prowess in integrating both statistical and mathematical, and is of significant use for the analytical exercises of problems and modelling wherein a dependent or response variable is affected by many input variables. The chief objective of the loophole is optimising the response variable (Whitcomb and Anderson 2016). It was also employed for its exceptional ability to determine the optimum conditions for HPR. Most of the control strategies use either COD or VFA as a control variable, whereas the measurement of hydrogen has not been widely exploited (Jimenez *et al.* 2015).

4.2 Methodology

4.2.1 Seed sludge

Anaerobic sludge acquired from a local wastewater treatment plant was used as the inoculum for the dark fermentation experiments. The seed sludge was pretreated by heat shock method to the spore-forming hydrogen-producing bacteria (HPB) and synchronously suppressing methanogenic bacteria by autoclaving it at 121℃ for 15 min (HL-341, Cameroon) (Lay 2000; Clesceri *et al.* 2005; Chandra 2015; Ghimire *et al.* 2015). The pretreated sludge was characterised mainly for volatile solids (VS), salts content and pH among other properties by adopting standard methods (APHA 2005).

The hydrogen production potential of the seed sludge was determined elsewhere in the previous chapter. 2 L of the pretreated anaerobic culture (prepared as above) was charged to the 10.5 L ABRs in proportion with the substrate, depending on the target substrate-to-biomass ratio (S/X)

which fell in the region of 2-3 in all the cases, as shown in Appendix C, Table C5. For about 24 hours before charging into the reactor the seed sludge and the substrate separately were incubated at 32℃ for acclimatisation of the microbes and to raise the temperature of the substrate close to the operating temperatures before charging the reactor.

The quantity of gas evolved was determined at atmospheric conditions by the water displacement method is graduated 1 L glass tubes, as shown in Figure 4.1, was charged with acidic water at a pH of three or less to prevent the dissolution of the gas units (Müller, Frommert and Jörg 2004; Walker *et al.* 2009).

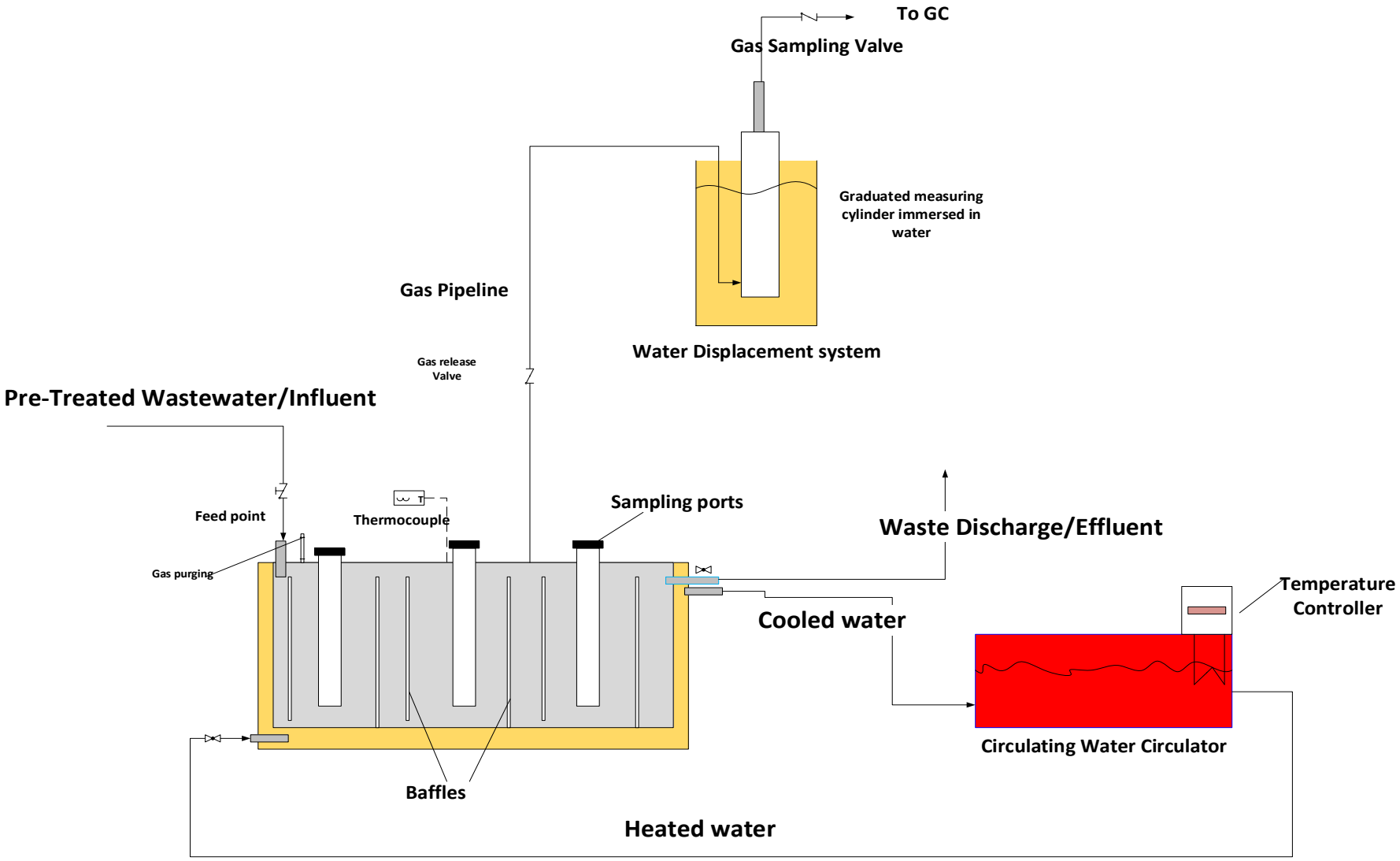

Figure 4.1 Gas collection in a water displacement setup

4.2.2 Wastewater samples

Samples were drawn from different industrial effluent streams, and the most attractive stream with the highest hydrogen potential was selected, as shown in sub-section 3.5**.** The samples were collected from the brewery, and some spot tests on pH, alkalinity, conductivity and oxidation-reduction potential (ORP) were done. The collected samples for the substrate were then stored in a cold room at 4℃; all other tests such as COD, VS, VFA were done within 48 hours before significant degradation transpired. The substrate collected was run in the digesters at various set conditions within a week of collection to avert huge difference in characteristics from the day of sampling to the time of experimentation (Clesceri *et al.* 2005; Chandra 2015).

The brewery wastewater stream had on average the following characteristics: TDS, 1911±263 mg/L; TS, 5503±78 mg/L; COD, 5744±78 mg/L; BOD, 3118±118 mg/L, pH 6.5±0.3 nitrates, 1.5±0.01 mg/L; phosphate, 15.3±0.08 mg/L; sulphate, 28.4±0.11 mg/L, the conductivity of 2508±256 C/µS/cm, was used as substrate.

4.2.3 Experimental methodology

4.2.3.1 Reactor design and configuration

Four identical ABRs were used with 10.5 L working volume and 4 L of the headspace, equipped with a 9 L capacity external heating jacket. The reactors were constructed with Perspex material because of its ability to withstand the desired operating conditions. Each reactor was covered with aluminium foil to create five opaque faces (to assure dark conditions) and one transparent front face (with detachable foil) for observations as shown in Figure 4.2.

The volume and the depth of the reactors should be known depending on the space limitation, the other dimensions were derived from the known volume of the digester and the depth that meets the required upward fluid velocity, with minimum biomass washout. The following empirical formulae were used to design the ABR.

$$Breath = \frac{1.2}{3} * D \quad (4.1)$$

$$Length = 3.5 * \frac{V}{D^2} \quad (4.2)$$

Where D = the depth of the reactor. V = volume of the reactor

Detailed specifications and design of the ABR are shown in Appendix B (Appendix B2 and Table B1**.** The reactors (14 L each, with a working volume of 10.5 L) contained standing and vertical suspended plates (acting as baffles) which compartmentalised each vessel into three equal sections; 3-sequential compartments (Gutterer, Ulrich and Reuter 2009).

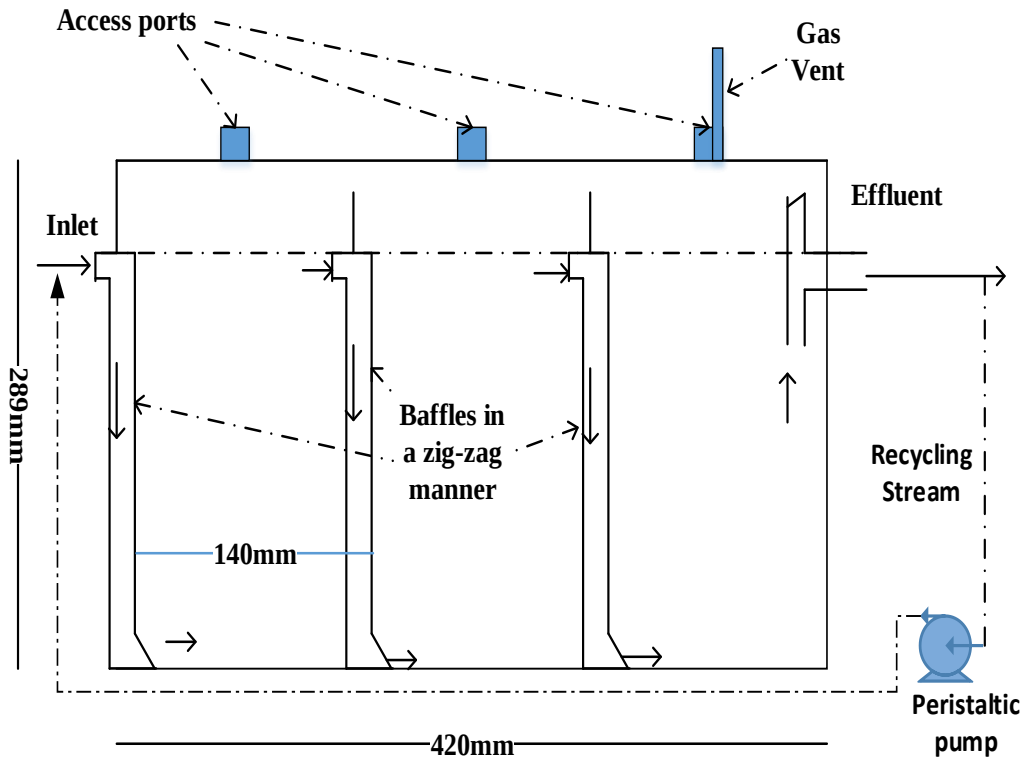

Figure 4.2 Two-dimensional representation of the ABR and its dimension.

All the experiments were operated in batch mode with a total/working volume of 14 L/10.5 L at S/X ratio of 2-3. The temperature of the reaction volume was varied between 33 and 37°C, (since the temperature was a variable in this study, in the mesophilic range) using a circulating water heating bath as the reactors were outfitted with heating jackets. Plate 4.1 shows the pictorial setup of the bioreactors in the laboratory, and the four reactors were all thermostatically controlled by a single circulating water bath to maintain the reaction temperature.

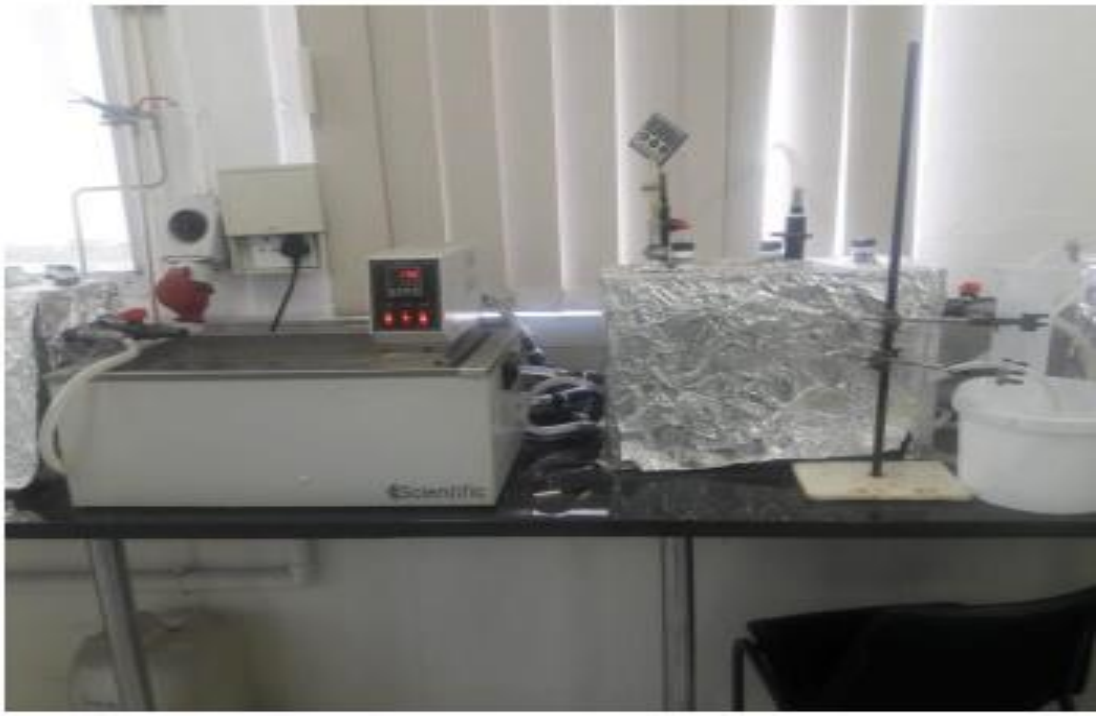

Plate 4.1 Experimental set up ABRs in the laboratory.

4.2.3.2 Medium preparation and characterisation

The pH of the substrate was set in the range 3.5 to 6.5 after mixing the wastewater with the seed culture because it was also a variable. Initial pH was balanced and regulated accordingly by adding 3 M HCl acid or 2 M NaOH unless otherwise stated all chemicals used in this study were analytical grade and purchased from Sigma Aldrich. Organic loading was not adjusted as all the samples collected lied within the same range of 5.74±0.078 kg COD/m^3.

Before the feeding of the reactors, the reaction chamber was cleaned by completely discharging the effluent for the previous runs. The temperature of the circulating water was set at the predetermined run temperature about 2 hours before feeding the reactors. The substrate and the inoculum were mixed in appropriate volumetric ratios to balance the desired S/X ratios. The pH was also normalised in the same equalisation tank before charging to match the run pH under vigorous agitation. A variable peristaltic pump was used to charge the ABR, after which the headspaces of the reactor was flushed with nitrogen gas for 5 min to ensure and maintain the anaerobic environment (Jia *et al.* 2019), pH was not regulated during the course of the runs; thus final pH values were determined after the run time (Penniston and Gueguim Kana 2018).

After purging the reactors with nitrogen gas and the set temperature for the reactor had been reached as detected by the temperature probe dipped in the reactor, the clock was then started. The reactors were hand shaken vigorously before taking volumetric readings. All the experimental runs were conducted in duplicate, for repeatability and reproducibility purposes. Upon completion of each run, the effluent was collected and analysed for VFAs, final COD and final pH determination.

A calibrated pH meter (Jenway, Model 3020) was used to determine pH, after which the samples were centrifuged (12 000 rpm for 12 min) and analysed for COD and VFAs. The HACH TNT 812 kits were used to determine the total VFA quoted as acetic acid using the HACH® (Model 3900) spectrometer, this shows the microenvironment and bioprocesses of the dark fermentation. The samples for COD analysis, after centrifugation, were filtered to 0.45 µm, proper reagents were applied using the open reflux method as stated in APHA (2005) and a calibrated Jenway photometer (7200) was used to determine the absorbance of the digested sample whose COD content was found by substituting in the calibration equation, 620 nm shown in Figure D3. High optical density samples were diluted before analysis on the photometer. Organic loading (kg COD/m^3) based on COD and substrate utilisation (kg COD_R /m^3) were determined to examine the trends of COD removal during dark fermentation.

4.2.3.3 Gas composition determination

The gas vent valve was left open during the entire operation, and it was closed when the batch time had elapsed. The volume of the gas collected through the water displacement system was observed and recorded, as shown in Figure 4.1. Samples of gases were withdrawn from the gas collecting cylinders for assaying with the gas chromatograph (GC-2014 Shimadzu, Japan). 150 mL gas-tight 'septum port gas sampling tubes or gas bombs' were used to sample the collected gas from the reactor cylinders to the GC before analysis. A 100 µL gas-tight syringe was used to extract the sample from the gas bomb. The GC was equipped with a TCD, a 1.8 m by 2 mm (i.d.) stainless steel column packed with Porapak Q (80/100 mesh). The injector, column, and detector temperature were set at 120℃, 40℃ and 250℃, respectively, with nitrogen as the carrier gas at a flow rate of 20 mL/min. The areas determined by the GC were used to calculate the percentage composition of represented gases.

4.2.3.4 Combination of experimental runs

Experimental run combination of variables (matrix) was planned using a Design Expert 11 software (StatEase Inc, Minneapolis, Minnesota, USA).

This software is notable for its credibility and effectiveness in designing experimental combinations. Each numeric factor is varied over five levels: plus, or minus alpha (axial points), plus or minus 1 (factorial points) and the centre point. The centre point was repeated five times to test the repeatability of the experiments. If categorical factors are added, the central composite design (CCD) will be duplicated for every combination of the categorical factor levels. This technique also shows the relative significance of process factors as well as their interactions, something not readily available with other methods (Rai, Mohanty and Bhargava 2016).

Table 4.1 illustrates how the experimental runs were conducted and their corresponding combinations. Table 4.1 consists of 3 input variables and three output responses. The responses were also shown with their corresponding standard deviations.

Table 4.1 Combination of experimental runs

	Input variables			**Output responses**		
Run	**Batch time (h)**	**Temp (ºC)**	**pH**	**H_2 production rate (mL/h)**	**COD removal efficiency %**	**VFA profile (mg/L)**
1	6	33.0	3.5	2.98±0.37	17.66±1.19	302±9
2	14.0	33.0	3.5	2.30±0.09	40.25±2.36	327±10
3	6.0	37.0	3.5	4.40±0.45	20.91±1.03	456±13
4	14.0	37.0	3.5	3.79±0.27	46.20±2.03	353±11
5	6.0	33.0	6.5	8.56±0.66	15.76±0.79	493±15
6	14.0	33.0	6.5	5.54±0.04	50.99±0.15	212±7
7	6.0	37.0	6.5	13.70±1.01	37.37±1.58	53416
8	14.0	37.0	6.5	13.26±0.49	60.81±0.51	581±18
9	3.3	35.0	5.0	2.11±0.01	18.03±1.38	330±1
10	16.7	35.0	5.0	7.47±0.06	55.46±0.79	130±4
11	10.0	32.0	5.0	6.72±0.11	34.49±1.63	424±13
12	10.0	38.0	5.0	12.07±0.86	56.57±0.46	480±14
13	10.0	35.0	2.5	0.94±0.08	25.83±0.30	234±7
14	10.0	35.0	7.5	5.73±0.50	39.68±0.75	143±5
15	10.0	35.0	5.0	17.20±1.43	43.88±1.20	676±21
16	10.0	35.0	5.0	14.37±1.81	41.40±2.08	639±19
17	10.0	35.0	5.0	18.16±0.62	49.90±0.17	724±22
18	10.0	35.0	5.0	14.94±1.12	46.11±0.63	733±23
19	10.0	35.0	5.0	15.67±1.24	45.03±1.61	700±21
20	10.0	35.0	6.5	15.99±0.73	37.95±0.28	666±20

4.3 Results and discussion on the ABR

This section highlights the whole experimentation process before it is analysed in detail in the forthcoming sub-sections. Table 4.2 shows a summary of the results as extracted from the averages of raw data in Table 4.1.

Table 4.2 Summary of results of the experiments

Name	Units	Type	Low	High
Batch time	h	Factor	3.3	16.7
Temperature	**ºC**	Factor	32.0	38.0
pH		Factor	2.5	7.5
Hydrogen yield	mL/h	Response	0.94	18.16
COD removal efficiency	%	Response	15.76	60.81
VFA profiling	mg/L	Response	130	733

The batch digestion experiments were run in a maximum time of 16.7 hours and a minimum of 3.3 hours. A lag phase was evident at the beginning of all runs lying between 0 and 2 hours. The use of activated inocula and the abundance of soluble, biodegradable materials in the brewery wastewater stream could be the reason for the low lag time being registered, and this is in tandem with a study that was done by Turhal, Turanbaev and Argun (2019) with the adaptation time dropping from 55 to 25 hours in a system that was inoculated with the seed sludge. Those runs which stretched to about 2 hours of lag time might have been orchestrated by microbes adjusting to the new environment and production of enzymes required for their growth, maintenance, and metabolism. The biogas in this study was produced normally, and no unexpected severe trends were noticeable. The composition of biogas in the experiments showed hydrogen contents ranging between 0 and 22% depending on the input variables, as shown in Table 4.1 and raw data in Appendix C, Table C1.

Table 4.3 shows the relationship that exists between the hydrogen yields and hydrogen production rate for various sets of operating conditions.

Table 4.3 Relationship between hydrogen production rates and hydrogen yields

Run	Batch time (h)	Temperature (ºC)	pH	Hydrogen production rate (mL/h)	Hydrogen yield (mL/gCOD)
1	6	33.0	3.5	2.98±0.37	182.09
2	14.0	33.0	3.5	2.30±0.09	146.53
3	6.0	37.0	3.5	4.40±0.45	230.76
4	14.0	37.0	3.5	3.79±0.27	209.88
5	6.0	33.0	6.5	8.56±0.66	595.89
6	14.0	33.0	6.5	5.54±0.04	278.16
7	6.0	37.0	6.5	13.70±1.01	402.39
8	14.0	37.0	6.5	13.26±0.49	549.08
9	3.3	35.0	5.0	2.11±0.01	76.87
10	16.7	35.0	5.0	7.47±0.06	417.71
11	10.0	32.0	5.0	6.72±0.11	350.40
12	10.0	38.0	5.0	12.07±0.86	383.58
13	10.0	35.0	2.5	0.94±0.08	67.75
14	10.0	35.0	7.5	5.73±0.50	268.33
15	10.0	35.0	5.0	17.20±1.43	728.15
16	10.0	35.0	5.0	14.37±1.81	745.99
17	10.0	35.0	5.0	18.16±0.62	654.45
18	10.0	35.0	5.0	14.94±1.12	582.78
19	10.0	35.0	5.0	15.67±1.24	646.28
20	10.0	35.0	6.5	15.99±0.73	757.52

The hydrogen yield and rate generally improved with temperature and pH. The highest HPR, 18.16 mL/h was registered at the batch time of 10 h, pH of 5 and a temperature of 35℃, corresponding to a yield of 654.54 mL/gCOD, although the highest yield was recorded as 757.52 mL/gCOD at batch time of 10 h, pH of 5.0 and a temperature of 35℃. The highest COD removal efficiency (60.81%) was recorded at batch time of 14 h, pH of 6.5 and a temperature of 33℃. The highest VFA concentration, 733 mg/L was recorded at a batch time of 10 h, pH of 5 and a temperature of 35℃. Hydrogen and carbon dioxide were the only gaseous products except for runs 1, 6 and 17 where methane was evident 30.13%, 22.14% and 12.41%, respectively. This could be because of the pretreatment method for the inoculum applied, which does not selectively activate the hydrogen producers. Remnant methane producers (homoacetogens and lactate producers, e.g. *Sporolactobacillus* spp.) can withstand the harsh conditions introduced during the pretreatment of the inoculum (Kraemer and Bagley 2007; Cisneros-Pérez *et al.* 2015; Castelló *et al.* 2020). At exceptionally low pH values, the HPR was infinitesimally small, with the lowest recorded as 0.94

mL/h at a pH of 2.5, and this synchronously affected the production of VFAs (234 mg/L). The lowest values of VFA were recorded when the batch time (16.7 h) was high or when the pH was high (7.5), 130 and 143 mg/L, respectively.

4.4 Effects of input parameters on the performance of the dark fermentation

The input factors analysed were temperature, batch time and pH, while output responses analysed were the HPR, COD removal efficiency and VFA concentration in the effluent.

4.4.1 Effect of temperature on output responses

Temperature is a significant parameter in dark fermentation processes, hence the careful choice of the operating range was pivotal and as such a range of 32-38℃ (Hallenbeck 2015). However, effective biohydrogen production is only within a narrow range of temperature (35-37℃), especially in the mesophilic reactions, even though the HPB grow in a wide range of temperatures (Mu *et al.* 2006). According to Mu *et al.* (2006), the HPBs are physiologically active at a certain point of incubation temperature or with a narrow range of temperature. Figure 4.3 A-C shows the relationship of temperature towards individual responses. The temperature (with respect to HPR) p-value was $0.0126 < 0.05$ which shows that the parameter is significant in the production of biohydrogen although there was poor correlation (0.267) between HPR and different levels of temperature which cements the notion that microbes are highly active within a narrow range of temperature, if not a specific value (Łukajtis *et al.* 2018).

In relationship with temperature alone, from Figure 4.3, the highest recorded biohydrogen production rate was 18.16 mL/h (654.45 mL/gCOD) at 35℃ and the lowest of 0.95 mL/h at the same temperature with both scenarios demarcated by different operating pH. This could have been an effect of the microenvironment of the microbes. The production rate of hydrogen at the extremes of the temperature range of the experiment were 6.72 mL/h and 12.07 mL/h for the lower limit and the upper limit, respectively. This a clear indication that temperature is a pivotal parameter in biohydrogen production because temperatures outside the appropriate range will restrain hydrogen generation at lucrative rates (Mu *et al.* 2006).

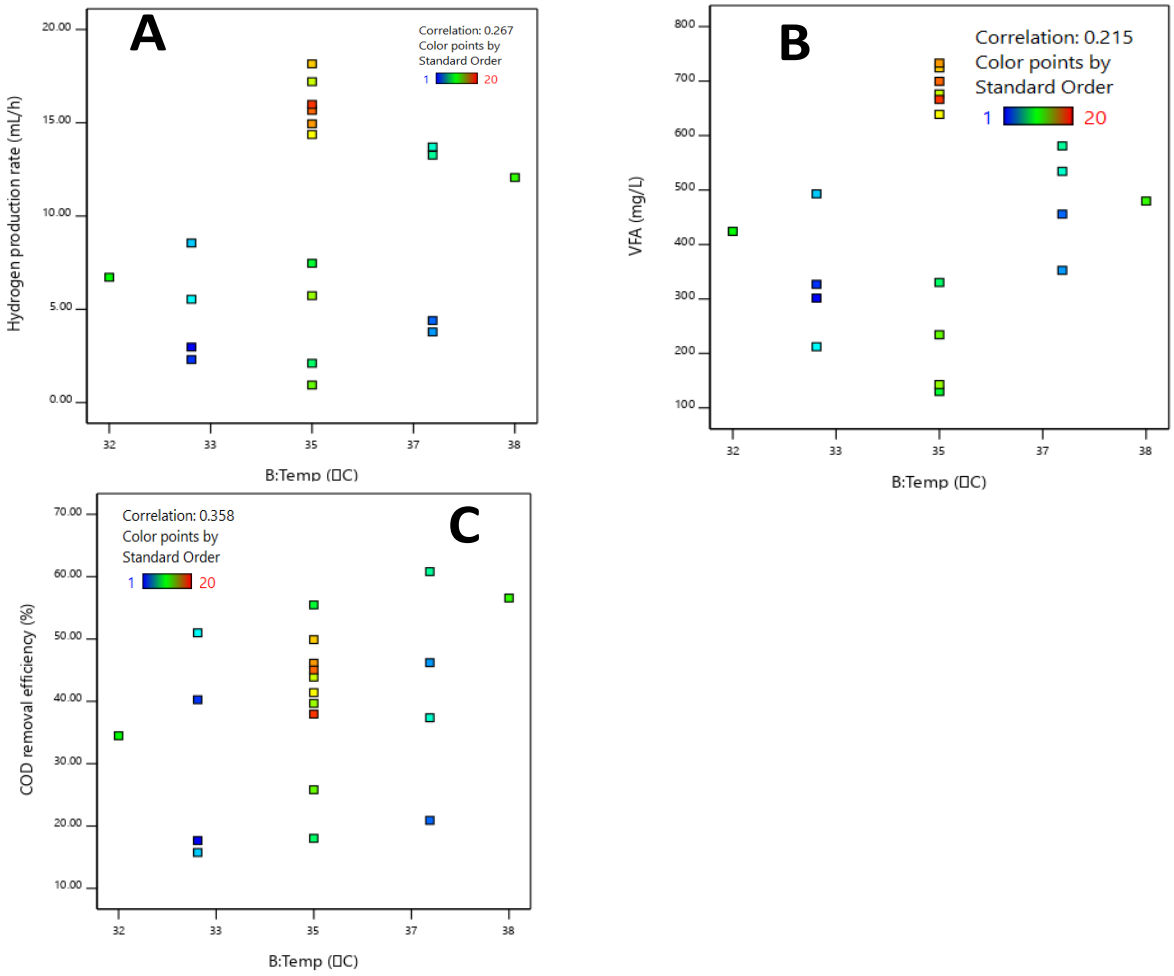

Figure 4.3 Response factors with respect to temperature (**A= HPR vs Temp; B= VFA vs Temp; C = COD vs Temp)**

Highest concentrations of VFAs (above 600 mg/L) were recorded at high temperatures from 35-37℃ signifying the high activity of the HBPs as evidenced by high concentrations of VFAs for this particular wastewater stream. This is one of the indicators that the reaction is following the desired reaction pathways which bring about enhanced biohydrogen production as reported in the literature (Yang, Guo and Liu 2010; Cheng *et al.* 2013). The highest noted VFA concentration was 733 mg/L at 35℃. The p-value was 0.1318 > 0.05 and a very low positive correlation coefficient of 0.215, as shown in Figure 4.3 B, which is a clear indicator that the temperature and VFA alone are not directly related hence other factors' interactions need to be looked at.

The COD removal efficiency, Figure 4.3 C, was high towards the upper limit of the selected range with 60.81% at an incubation temperature of 37℃. This could have been attributed to the increased

activity of the microbes at elevated temperatures resulting in pronounced degradation of the organic material in the wastewater and the COD removal efficiencies recorded in this study are in conformity with the ones determined elsewhere (Rajhi *et al.* 2016; Ertugay and Acar 2017). 0.004 (below 0.05) was the determined p-value insinuating significant correlation between the two parameters in question.

In comparison with another study, the effect of temperature on dark fermentation using mixed culture was investigated, and a maximum yield of hydrogen of 319 mL/gCOD (twice as low as this study) was recorded by increasing the temperature from 35 to 45℃, whereas a decrease in yield (182 mL/gCOD) was observed when the temperature was raised from 45 to 55℃ (Tang *et al.* 2018).

4.4.2 Effect of pH on output variables

It must be noted that optimal initial pH depends on the type of strains of the mixed microflora. Furthermore, the type of substrate undoubtedly affects the optimum pH, as reported in the literature (Wang and Wan 2009). Volumetric HPR and VFA concentration were highly pronounced in the acidic conditions, and the highest Figures were recorded at pH of 5.0, that is 18.16 mL/h and 733 mg/L, respectively. High COD removal was supported by a microenvironment that is slightly acidic and close to neutrality pH, 60.81% COD removal was recorded at a pH of 6.5 as shown in Figure 4.4 A-C.

As observed, hydrogen yield and production rate were low at pH values below 4.5, with the lowest HPR and yield noted at a pH of 2.5, 0.94 mL/h and 2.7 mmol/gCOD, respectively. After a pH of 5.5, there was a sharp decrease in the HPR and the yield, 5.73 mL/h and 10.97 mmol/gCOD. This behaviour may have been caused by increased osmotic pressure which then redirects the HPBs into metabolic pathways away from biohydrogen generation to stabilise their microenvironment. At higher pH, above 6.5, rapid production of hydrogen may be hampered by the production of fatty acids and these may affect the buffering capacity of the system and the hydrogen production potential is lowered in the long run. On the other side of the coin, low initial pH environment (below 4), the HPBs would need more time to acclimatise to the environment, which has adverse effects on hydrogen yield and the production rate (Ginkel, Sung and Lay 2001; Fang and Liu 2002; Khanal *et al.* 2004).

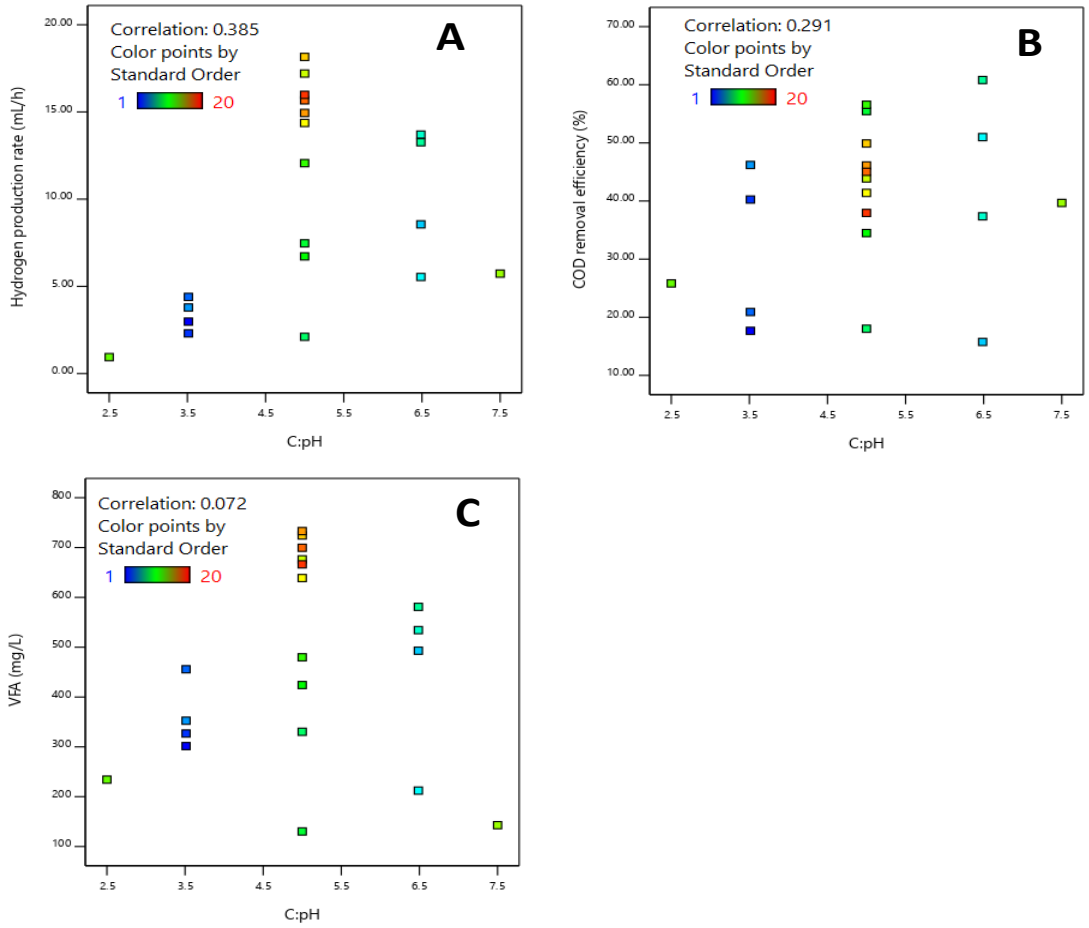

Figure 4.4 The relationship between pH and response variables (A= HPR vs pH; B= VFA vs pH; C = COD vs pH)

In this study, favourable HPR was observed at pH values between 5.0 and 5.5, which is in close agreement with what other researchers have found in dark fermentation (Lee, Salerno and Rittmann 2008; Łukajtis *et al.* 2018). This pH range was found to be optimal because it synchronously suppresses methanogenic activities in as much as it exalts the hydrogen producers. The average composition of hydrogen in the biogas produced at pH 5.0 was 21.22%, with corresponding COD removal efficiencies of 43.61% (absolute COD removal of 2465 mg/L on average), as shown in Appendix C, Table C3.

The VFA concentration was less pronounced towards the extremes of the selected pH ranges, that is 3.5 and 6.5, and it was high at pH 5.0. pH above 6.5 has a higher likelihood of supporting methanogenesis given a longer fermentation time. The HPB could also have not adapted to the elevated pH environment and would eventually be inhibited.

In the majority of the experimental runs, there was an average increase in pH except for a few cases where there was a drop from the initial set pH. It appeared in all the runs, and the pH endeavoured to approach the pH 5 from either side of the set limits. At initial pH below 4.5 microenvironments could not have been conducive for HPBs as evidenced by lag time in the region of 0-2 h. Nevertheless, after acclimatisation and self-adjustment to the pH conditions, biogenic hydrogen production gradually commenced. The soluble metabolites (on average, 326 mg/L) produced were not enough to cause an abrupt disturbance in the pH distribution.

At low initial pH, high total hydrogen production yields, but lower biohydrogen production rates were evident as shown in Table 4.4, and there would be a switch in metabolic pathway resulting in cessation of biohydrogen generation. This observation was found in another study when low pH environments affected the hydrogenase activity and the metabolic pathway of microorganisms (An *et al.* 2018).

Table 4.4 Initial pH and production rates and yields

Run	Initial pH	Final pH	Production rate, mL/h	Yield mmol/gCOD	SHPR (mL/h)/gCOD
1	3.5	3.89	2.98	7.45	30.35
2	3.5	4.45	2.30	5.99	10.47
3	3.5	3.73	4.40	9.44	38.46
4	3.5	5.10	3.79	8.58	14.99
5	6.5	5.21	8.56	24.37	99.31
6	6.5	6.10	5.54	11.38	19.87
7	6.5	5.10	13.70	16.46	67.06
8	6.5	5.90	13.26	22.46	39.22
9	5	4.39	2.11	3.14	23.29
10	5	6.45	7.47	17.08	25.01
11	5	5.21	6.72	14.33	35.04
12	5	5.19	12.07	15.69	38.36
13	2.5	3.61	0.94	2.77	6.78
14	7.5	7.15	5.73	10.97	26.83
15	5	5.36	17.20	29.78	72.81
16	5	5.03	16.63	30.51	74.60
17	5	4.91	18.16	26.76	65.44
18	5	4.79	14.94	23.83	58.28
19	5	4.87	15.67	26.43	64.63
20	5	5.26	15.99	30.98	75.75

Overall, it was discovered that the optimal pH for reliable hydrogen production lied within the acidic phase between 5.0 and 6.0 (Penniston and Gueguim Kana 2018). This falls within the range found by Zhao and Yu (2008), who studied the influence of pH ranging from 4.0 to 7.0 and reached a conclusion that the optimum pH was 5.5 accompanied by a production rate of 42–145 ml-H_2L^{-1} h^{-1} and a yield 24.48–83.85 mmol-H_2/gCOD which are in tandem with the findings in some experimental runs of this study as shown in Table 4.3.

4.4.3 Effect of batch time on the response variables

The time in which the medium spends in a reactor affects the overall performance of the dark fermentation system. Low batch times would not give optimum hydrogen production, and in some cases, no hydrogen production occurred at all due to inadequate time of digestion or biomass washout, with the other factors held constant (Zhu *et al.* 2018; Santiago *et al.* 2019). Higher operational times are also detrimental to biogas production as they would cause a resurgence of hydrogen consumers or methanogens which have the capacity to sporulate during pretreatment and improved the production of methane (Mamimin and Prasertsan 2011; Chandrasekhar, Lee and Lee 2015; Hallenbeck 2015).

From Appendix A, Figure 4.5 A, it is conspicuous that biohydrogen yields were low at smaller retention times (3.3 h and 6.6 h), with the lowest being 3.14 mmol/gCOD. A discrepancy was however noticed at a retention time of 10.0 h, where the all-time lowest hydrogen yield in this study was recorded (2.77 mmol/gCOD). For the runs conducted, highest yield and production rate were recorded at 10.0 h, as 30.98 mmol/gCOD and 18.16 mL/h, respectively.

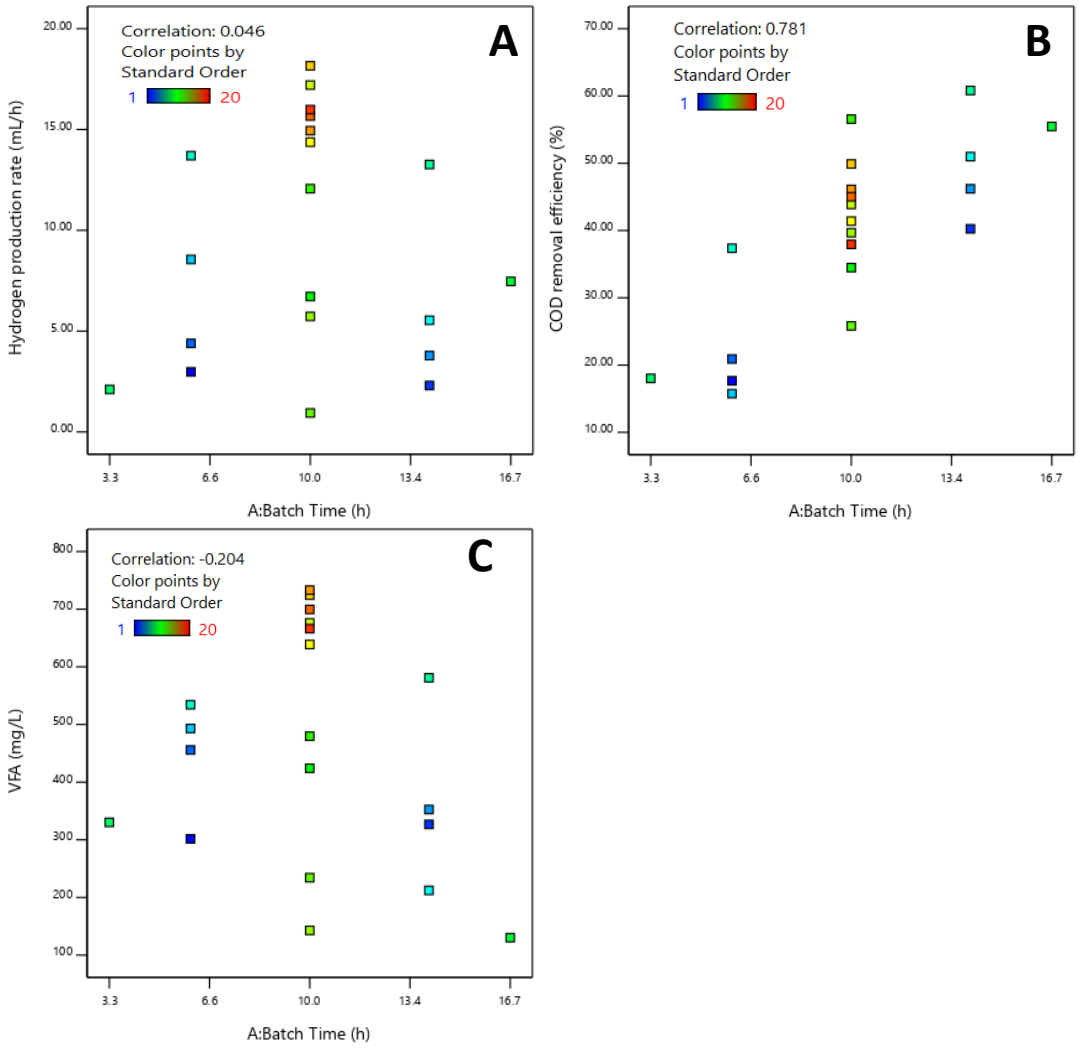

Figure 4.5 Batch time with respect to responses (A= HPR vs BT; B= VFA vs BT; C = COD vs BT)

Low hydrogen yields and rates were also evident at higher retention times above 13.4 h, 76.87 mL/gCOD and 2.11 mL/h. The interaction of other factors should also be considered to draw an informed conclusion. Owing to short retention times, methane was not detected, even though there is a possibility of the sporulating methanogens in the pretreatment methods being employed; however, 29.43, 21.63 and 12.17% of methane were recorded at the residence time of 14.0, 16.7 and 10.0 h, respectively. Under emerging favourable microenvironment, this agreed with some findings elsewhere (Lin and Jo 2003). Contrarily, the optimal retention times for hydrogen generation were inconsistent ranging from 8 to 12 hours as observed by Lin and Chang (2019) on hexose basis and 18 to 24 hours for wastewater from the brewery (Yu, Hu and Hong 2003; Fan,

Kan and Lay 2006). Higher production rates than the current study reported in literature could have been orchestrated by more convenient medium conditions.

The COD removal efficiency was high at increased batch times, that is, 60.81% at a retention time of 14.0 h (corresponding to actual removal of 3550.75 mg/L). A considerable amount of runs registered high COD removal efficiencies at around the retention time of 10.0 h. Perhaps, the microbes have had enough time to act on the organic material introduced. On the other hand, lowest COD removal efficiency (15.76%) was recorded at 6.0 h, and the expectation was to record the lowest removal at 3.3 h retention time since there was less contact time, superior counterpart input factors may have attributed to that discrepancy. The final VFA recorded followed the same trend as the HPR as exhibited in Appendix C, Figure 4.3 C.

4.4.4 Effect of organic loading on hydrogen yield

It is clearly documented that substrate concentration introduced in any anaerobic digestion system has either positive or detrimental effects on the overall performance of that system (Lay *et al.* 2010). High organic loading ameliorates hydrogen generation efficiency taking note of the loading threshold as going beyond the optimal range may have the substrate or product inhibiting the bioreaction. However, for the production of biohydrogen, there is no standard loading for optimal production efficiency because of the difference in nature of various substrates (Lay *et al.* 2010; Lin *et al.* 2012). From Figure 4.6 the effects of organic loading are shown with an average COD concentration of 5745±79 mg/L for all the experimental runs. The highest HPR was recorded between 5800 and 5850 mg/L COD which was the furthest extreme of the COD concentration introduced at a pH of 5.0 and batch time of 10.0, as shown in Appendix C3. High substrate concentrations were proportional to COD removal efficiencies (60.81%) and actual COD removal (3551 mg/L) at an initial COD of 5838 mg/L. An interesting observation was also made on the VFAs as they were moderately high (400-450 mg/L) at low initial pH runs and significantly high actual COD removed. This might have been engendered by the shift in metabolism of the involved bacteria towards soluble metabolites production instead of hydrogen generation.

Even though the hydrogen yields in this study, especially for low initial pH below optimal values, were a bit inferior to theoretically determined values because of VFA production and less of hydrogen generation (perhaps consumption) by possibly resurgent methanogens or hydrogen consumers. These results are not far off from those found in other studies for substrate

concentration of the same order (Lee, Salerno and Rittmann 2008). In some cases the lower end of the fed substrate concentration (5650 mg/L COD) and comparable HPRs as the upper limit (5850 mg/L), the same trend was applicable to actual COD removed and the COD removal efficiency.

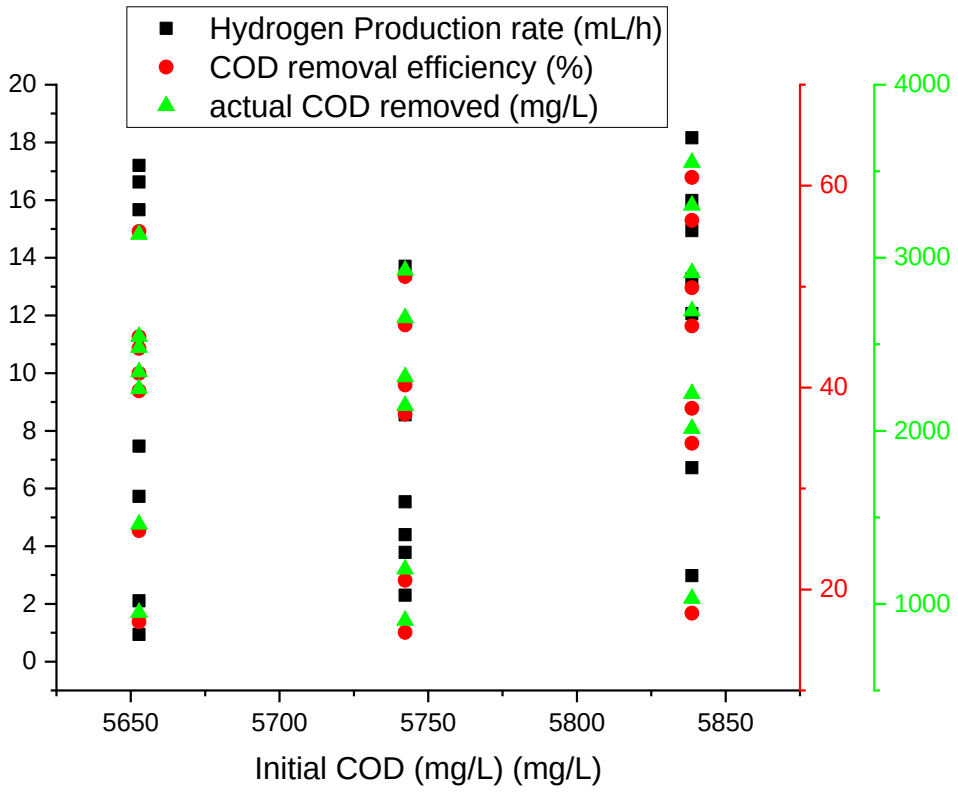

Figure 4.6 Effect of the initial COD on the performance of the dark fermentation

Thus, the initial substrate concentration must be kept at check to avert starvation of the microbes or inhibit the bioprocess by high influent organic loading. Consequently, this may lead to alteration in cell permeability, altered enzyme activity or even their dissociation (Elbeshbishy *et al.* 2017).

In this study, volumetric hydrogen yield of 757 mL/gCOD was found at initial concentration of 5838.67 mg/L, pH of 5.0 and absolute COD removal of 2215.81 mg/L (37.95%) which is in concordance with the findings by Fernandes *et al.* (2010) who recorded 612.5 mL/gCOD from an initial organic loading of 2500 mg/L COD. The general trend unearthed is that high substrate concentrations orchestrate high production rates and conversely lower yields of hydrogen.

4.4.5 Volatile acids and HPR

The knowledge of the concentration of the VFAs is of paramount importance in operation, maintenance, and control of the dark fermentation systems. Additionally, favourable amounts of VFAs would foster the employment of the dark fermentation effluent in the downstream photofermentation or biomethanation processes (Cheng *et al.* 2013).

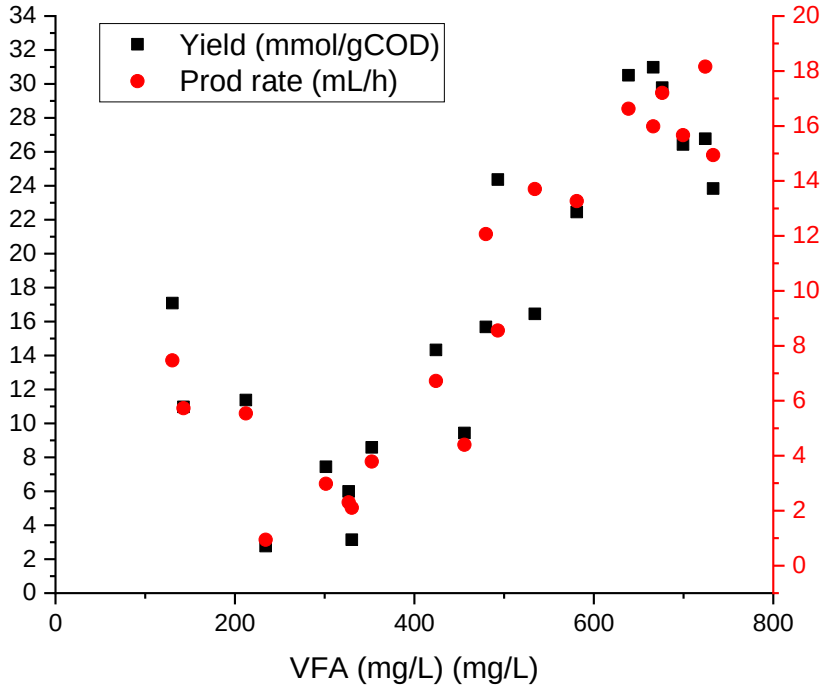

Figure 4.7 Effect of volatile fatty acids on the production rates and yields

Figure 4.7 shows the relationship that exists between VFAs and biohydrogen rate and yield. VFAs and hydrogen rate had a casual proportional relationship. HPR and yield were in tandem with VFA concentration in the effluent, the highest VFA effluent concentration (733 mg/L) accompanying a 14.94 H_2 mL/h production rate and a corresponding yield of 23.38 mmol/gCOD. The highest HPR (18.16 mL/h) was recorded when the effluent VFA concentration was 724 mg/L, and the lowest (0.94 mg/L) was found at 234 mg/L effluent VFA concentration. The VFA concentration was also exceptionally low in the cases where there was methane production during experiments, with VFA concentration in the effluent of 212 mg/L (5.54 mL/h and 11.38 mmol/gCOD), 130 mg/L(7.47

mL/h and 17.08 mmol/gCOD) and 143 mg/L (5.73 mL/h and 10.97 mmol/gCOD). In this study high VFA concentrations, in many cases, was accompanied by high production rates of hydrogen and yields. This could have been prompted by the acetate pathway which has a high potential of producing large quantities of the metabolites, but low enough to arrest the production of hydrogen as reported in the literature (Kraemer and Bagley 2007; Uyar *et al.* 2009). In the few cases when methane was produced, the short-chain fatty acids might have been digested in the methanogenic phase as there is a possibility of a resurgence of the acetoclastic methanogens (Saady 2013; Dahiya *et al.* 2015). The total VFA concentration needs to be kept at balance as it may also have detrimental effects on the overall system performance, with respect to biohydrogen production. Above a certain content of the VFAs (in this study above 730mg/L), there was a shift in metabolism and this affects the hydrogenase activity. This is highly likely the reason for a dip in biohydrogen production (Khanal *et al.* 2004). The tVFA recorded in this study was, however, significantly lower than recorded in other similar studies (Logan *et al.* 2002).

4.5 Interaction of variables

The preceding sections have endeavoured to analyse and discuss the findings of the study by inspection method and in this current section endeavours to reconcile the gap between the analysis by inspection and statistical analysis, incorporating interaction of variables there may be in the dark fermentation process for the selected operating conditions. Before optimum conditions were determined, rigorous analysis of variance (ANOVA) was conducted.

ANOVA assists in assessing the effects and interaction of input variables with respect to the chosen output response. Table 4.5 shows a fit summary of the credibility of levels of interaction, and the quadratic relationship was found to offer the best explanation on the interaction of variables. The quadratic relationship had the lowest and valid p-value; hence all the interaction assessments were based on it; this can also be bolstered by the adjusted R^2 value that is high (above 0.7).

Table 4.5 Fit summary of model interactions.

Source	Sequential P-value	Lack of Fit p-value	Adjusted R^2	Predicted R^2	
Linear	0.2692	0.0005	0.0645	-0.1109	
2FI	0.9470	0.0003	-0.1205	-0.6871	
Quadratic	**< 0.0001**	**0.0368**	**0.8677**	**0.5319**	**Suggested**
Cubic	0.1065	0.0534	0.9277	-1.8289	Aliased

The interactions could not be well explained by the linear, 2-factor interactions and the cubic forms as shown by high sequential p-value. Describing the impact of the main effects for each factor level without considering the levels of other factors must be conducted with caution. The significance of these interaction effects between the parameters in Table 4.6 is essential and is realised by conducting experiments using the method outlined in this manuscript.

Table 4.6 is a construct of the interaction of variables based on the quadratic relationship with respect to HPR.

Table 4.6 ANOVA for the significant variable in the matrix

Source	Sum of Squares	df	Mean Square	F-value	p-value	
Model	610.79	9	67.87	14.85	0.0001	Significant
A-Batch Time	1.34	1	1.34	0.2924	0.6005	
B-Temperature	44.89	1	44.89	9.82	0.0106	
C-pH	93.07	1	93.07	20.36	0.0011	
AB	0.8724	1	0.8724	0.1909	0.6715	
AC	0.5897	1	0.5897	0.1290	0.7269	
BC	12.42	1	12.42	2.72	0.1303	
A^2	205.29	1	205.29	44.91	< 0.0001	
B^2	66.39	1	66.39	14.53	0.0034	
C^2	264.91	1	264.91	57.96	< 0.0001	
Residual	45.71	10	4.57			
Lack of Fit	38.86	5	7.77	3.90	0.0808	not significant
Pure Error	6.62	5	1.32			
Cor Total	656.50	19				

The quadratic relationship F-value of 14.85 suggests as a logical consequence that the relationship is significant. There is only a 0.02% likelihood that an F-value of this magnitude could occur because of noise. P-values less than 0.0500 indicate model terms are significant (Natarajan, Suganthi and Periyanan 2016; Sahu, Mazumdar and Chaudhari 2019). In this study B, C, A^2, B^2, C^2 had significant effects and interaction on the HPR.

One of the best ways to envision the interaction and effects of input variables on the output responses is to synthesise a response surface plot. In this case, it was done by altering two independent variables within the set experimental range and holding the other at the central point. Effect of temperature-batch time interactions on HPR with pH fixed at its central point 5.0 was conducted.

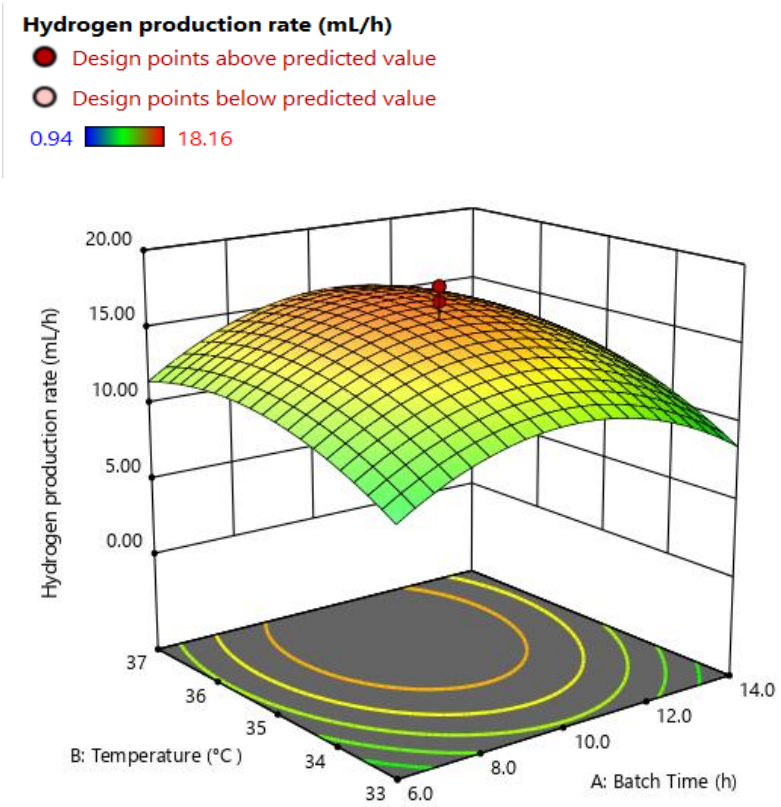

Figure 4.8 Surface plot of input variables in relationship to HPR.

As shown in Figure 4.8, it was determined that all parameters had interactions amongst themselves within the range of set limits of independent variables under study. According to the desirability assessment, the highest optimal production rate (17.054 mL/h) from operating an ABR would be

obtained at 10.0 h batch time, 35.0℃ incubation temperature and a pH of 5.0 while response surface shows 10.2 h batch time, 36.153℃ incubation temperature and a pH of 5.598 as shown in Figure 4.8; this was determined by the Design Expert software based on the quadratic form of interaction of parameters.

4.6 Optimal conditions for an enhanced production rate of hydrogen

Rigorous analysis of the performance of the ABR with respect to HPR has been conducted in precedent sections. Both inspection and statistical methods were exhausted to determine the optimal conditions for enhanced biohydrogen production carefully. A balance on the optimal conditions was made depending on the instruction given to the software. A software was instructed to optimise the system by maximising the HPR and keep all the other parameters in range, as shown in Table 4.7. Expected output responses were also predicted, and an experimental examination was done as discussed in the following chapter to confirm the anticipated results under the predicted optimal conditions.

Table 4.7 Factors considered for the experimental design software

Name	Unit	Goal	Lower Limit	Upper Limit
A: Batch Time	h	is in range	6	17
B: Temperature	**ºC**	is in range	33	37
C: pH		is in range	3.5	8
Hydrogen production rate	mL/h	maximise	0.941999	18.1581
COD removal efficiency	%	is in range	15.7556	60.8144
VFA	mg/L	is in range	130.25	733

In a bid to show the optimal conditions determined in this study, a pictorial representation, as shown in Figure 4.9, was made. The solutions found were in relation to the findings by other researchers, the optimum temperature was found to be 36℃ (Mu *et al.* 2006; Vijayaraghavan, Mohd and Mohd 2006; Elbeshbishy *et al.* 2017), batch time was determined to be 10.2 h (Ren *et al.* 2011; Chandrasekhar, Lee and Lee 2015; Lin and Chang 2019) and the pH of 5.6 (Dabrock, Bahl and Gottschalk 1992; Guo *et al.* 2010; Chandrasekhar, Lee and Lee 2015).

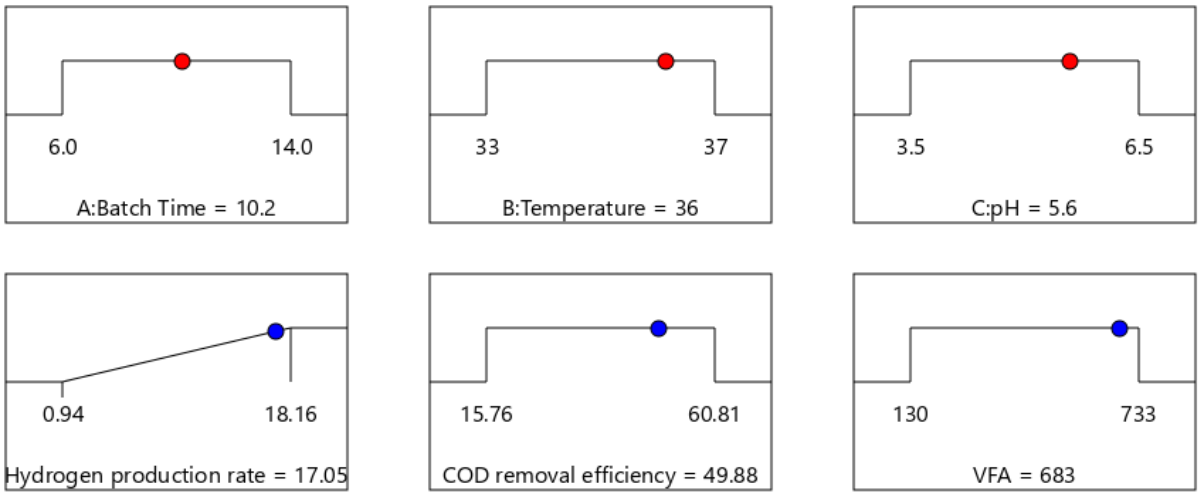

Figure 4.9 numerical solutions of the optimum conditions in an ABR

The quadratic regression relationship also predicted the output responses with an optimum expected HPR of 17.05 mL/ h which is twice as less as reported by Argun and Dao (2017) as 35.6 mLH_2/h and Eker and Sarp (2017) as 9.85 mLH_2/h. The prediction was accompanied by 49.88% COD removal efficiency and is comparable to other systems of similar nature (Khongkliang *et al.* 2017), where a maximum of 58% was observed. VFA concentration in the effluent of 683 mg/L was predicted to be the optimal concentration in the effluent stream.

4.7 Summary

The central composite design under the response surface methodology was used to determine the matrix for the experimental runs. In total, 20 runs were conducted characterised with various combination of experimental conditions. The maximum hydrogen composition in the biogas was recorded as 23.79% at the batch time of 14 h, temperature of 37℃ and a pH of 6.5. However, the highest HPR, 18.16 mL/h was registered at the batch time of 10 h, pH of 5 and a temperature of 35℃; the highest VFA concentration of 733 mg/L and the highest yield of 757.52 mL/gCOD at the same conditions. The highest COD removal efficiency (60.81%) was recorded at batch time of 14 h, pH of 6.5 and a temperature of 33℃. Hydrogen and carbon dioxide were the only gaseous products except for runs 1, 6 and 17 where methane was found to be 30.13%, 22.14% and 12.41%, respectively. The lowest HPR of 0.94 mL/h was recorded at a pH of 2.5, and this also affected the

production of VFAs (234 mg/L). The lowest values of VFA were recorded when the batch time (16.7 h) was high or when the pH was high (7.5), 130 and 143 mg/L, respectively. The determined optimum operating conditions were a batch time of 10.2 h, temperature of 36℃ and a pH of 5.6. The quadratic regression relationship also predicted the output responses with an optimum expected HPR of 17.05 mL/h. The model predicted a maximum of 49.88% COD removal efficiency, and in the experiments, the highest found was 58% using the optimum conditions determined.

CHAPTER FIVE

EFFECT OF NANOPARTICLES ON HYDROGEN PRODUCTION RATE

5.1 Introduction

Immobilisation of cells using metallic/ metal oxide nanoparticles has gained popularity in recent times because of its tendency to increase the rate of hydrogen production by altering the electron transfer pathways (Manohar, Kim and Karegoudar 2011; Elakkiya, Prabhakaran and Thirumarimurugan 2016). The hydrogenase enzyme is known to catalyse the dark fermentation process, and the Fe^{3+} make up the core structure of the hydrogenase enzyme. Hence, this orchestrated the study on the effect of nanoparticles on the production of biogas, mainly affecting the production rates by lowering the activation energies (Gadhe and Gupta 2007; Beaton *et al.* 2018). The iron ions have been previously reported to enhance the activity of hydrogenases, and the application of the nanoparticles (NPs) augments the activity of biohydrogen producing microbes (Wang and Wan 2008; Nasr *et al.* 2015; Beaton *et al.* 2018). However, the cells coated with magnetite nanoparticles can be easily separated using a magnetic field (Ali *et al.* 2016).

The effect of the NPs interacting with the hydrogenases brings about the immobilisation of cells, and the significant merits that immobilisation gives to whole cells are less sensitive to temperature and pH in comparison to free enzymes (Manohar, Kim and Karegoudar 2011; Elakkiya, Prabhakaran and Thirumarimurugan 2016).

The optimum conditions determined in the previous chapter were used in a comparative analysis between similar dark fermentation systems, with the control system having no nanoparticles charged to it. There is, however, a possibility that unoptimised conditions may give better production rates of hydrogen when charged together with nanoparticles, this is nevertheless beyond the scope of this study.

5.2 Experimental procedure and description of the equipment

5.2.1 Magnetite nanoparticles preparation

A reliable co-precipitation technique was used to synthesise the magnetic core based on literature accompanied by some modifications (Reddy *et al.* 2017). A total of 27.8 g of $FeSO_4.7H_2O$ and 79.6 g of $Fe_2(SO_4)_3$ were dissolved in 1000 mL of deionised water, $NH_3.H_2O$ was then added in drops to the solution under a water bath set at 65℃ and with lively agitated for 30 min. A pH of 12 for the aqueous solution was maintained. The mixture was left to age for 60 min. A permanent magnet was used for separation of the black solid and washed several times with distilled water until the pH reached 6.8–7.2. After drying at 60℃ for 24 h, the precipitate was pulverised. The final catalyst was stored in a desiccator (Hu *et al.* 2011; Mehndiratta *et al.* 2015). The average size was determined to be 50nm.

5.2.2 Operation of the ABR with nanoparticles.

In this exercise, the brewery wastewater and the seed sludge were used similar to the experimental runs performed previously in Chapter 4. The effect of magnetite nanoparticles on HPR was investigated in comparison to the same system without nanoparticles (nNP). The two separate operations were conducted in the ABR as described elsewhere in Chapter 4. Four identical reactors (R_1, R_2, R_3 and R_4) were used, with two (in duplicate) used with nanoparticles (NP) and the other two use as nNP system as the control. The operating temperature was set at 36℃, the pH at 5.6 and the batch time of 10.2 h as optimised in this study. The pH was controlled by dosing 3 M HCl or 5 M NaOH, whenever there was a slight deviation from the set point. The system with NP was charged with 200 mg/L of the magnetite nanoparticles, as was also reported in other studies elsewhere (Han *et al.* 2016; Reddy *et al.* 2017). The digesters were purged with nitrogen gas for 5 min to ensure anaerobic conditions. Samples before and after digestion were withdrawn in all cases to determine the COD, initial VS (APHA 2005), final VFA concentration using the TNT kits and spectrophotometer (DR3900, USA).

R1-R4 denote the reactors used under the same operating conditions, with R1 and R2 having the magnetite nanoparticles and duplication and R3 and R4 were the control reactors without the magnetite nanoparticles. Reactors R1 and R2 were collectively denoted by NP (with nanoparticles) and reactors R3 and R4 were denoted with nNP showing that the system had no nanoparticles.

The volume of the biogas was measured using the water displacement system, as described in the previous chapter. The quality of biogas was also assayed using the gas chromatography equipped with a TCD and packed column as described in the previous chapter. Gas volumes (by using a graduated measuring cylinder) and assaying of the biogas were done hourly to check for the rate of production of hydrogen.

5.3 Results and discussion

The effect of nanoparticles on the rate of production of biohydrogen was conducted using a substrate with an initial COD of 5623 mg/L which was fed to all the four identical reactors run at similar conditions as shown in Table 5.1.

NB: These values were a single determination of the gas produced; hence readings were not repeated and no deviation for a specific reactor.

Table 5.1 Biogas and hydrogen distribution for systems with and without nanoparticles

Time	**With nanoparticles**				**Without Nanoparticles**			
	Volume of biogas (mL)		**Composition of hydrogen (%)**		**Volume of biogas (mL)**		**Composition of hydrogen (%)**	
Reactor→ Time↓	**R1***	**R2***	**R1**	**R2**	**R3***	**R4***	**R3**	**R4**
0	0	0	0±0.00	0±0.00	0	0	0±0.00	0±0.00
1	237	201	0±0.00	0±0.00	196	205	0±0.00	0±0.00
2	539	493	9.87±0.12	10.7±0.24	489	504	6.74±0.04	5.94±0.10
3	617	598	16.87±0.17	17.99±0.17	561	550	14.46±0.21	13.96±0.17
4	707	682	19.32±0.20	20.24±0.22	647	669	16.7±0.11	15.58±0.19
5	866	842	22.03±0.51	23.21±0.17	728	741	16.57±0.22	17.93±0.20
6	904	902	24.37±0.12	23.55±0.59	794	782	18.02±0.19	19.32±0.31
7	943	913	23.69±0.47	24.77±0.35	821	813	19.56±0.17	18.86±0.22
8	951	926	23.14±0.32	25.76±0.63	843	830	21.23±0.13	18.95±0.24
9	951	928	25.84±0.50	24.18±0.54	848	842	22.03±0.21	20.85±0.05
10	955	928	24.77±0.45	25.85±0.29	850	842	22.24±0.15	20.89±0.10
10.2	955	928	25.02±0.45	25.72±0.62	852	844	22.66±0.15	21.16±0.09

5.3.1 Rate of the volume of biogas production in relation to nanoparticles

The nanoparticles, specifically the magnetite nanoparticles, have been extensively studied and their effects on the overall production rate biogas were explored in this study. From Figure 5.1 it is evident that in the first 2 hours, both systems with nanoparticles and without nanoparticles had closely similar production of biogas quantities. This could have been attributed to the slow acclimatisation of microbes in both cases (NP and nNP). After 2 hours of experimentation, a distinction between NP and nNP systems was conspicuous, as shown in Figure 5.1. The possible cause of this observation could be the immobilisation of the microorganisms on the surface of the magnetite NP, Abdelsalam *et al.* (2016) supported the same notion. The NPs have the capability to provide a high surface area of contact, thereby offering distinctively physicochemical properties (Nasr *et al.* 2015; Kumar *et al.* 2019). It should be noted that immobilisation is much more effective in continuous systems.

Note: nNP = without nanoparticles and NP = with nanoparticles

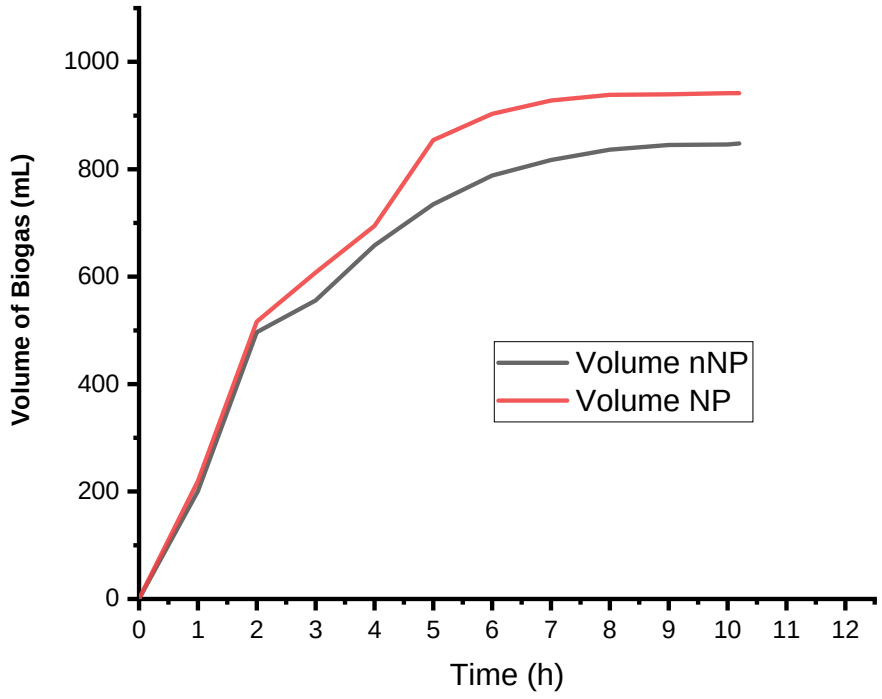

Figure 5.1 Effect of nanoparticles on the volume of biogas

After about 8 hours, the production of biogas slowed down, until it seized in a further 2 hours period as the digestible material had been depleted as evidenced by the reduction of COD from 5623 mg/L to about 2702 mg/L for NP and 2902 mg/L for nNP. Recalcitrant organic material would thermodynamically infeasible to digest; hence more stringent conditions need to be applied (Weiß *et al.* 2016). In another study, it was observed that optimum nanoparticle concentration enhanced the microbial (hydrogenase) activity by providing more surface area for biohydrogen production (Pugazhendhi *et al.* 2018).

5.3.2 The effect of magnetite nanoparticles on the composition of the biogas

The volume of biogas alone is not enough to be conclusive on the impact of the nanoparticles on the dark fermentation process for hydrogen production. Thus the gas produced was analysed to determine the percentage of hydrogen gas. Figure 5.2 shows the effect of nanoparticles with comparison to the control system nNP. The lag phases were similar on both occasions, after this period, there was a significant difference (although in the same order of magnitude) in the composition of hydrogen at a given time during the experiment. The NP system registered faster production of hydrogen than the nNP system with a minimum of 10.3% and 6.34%, whereas the maximum values were 25.37% and 21.85%, respectively. The NP laden system was more superior to the nNP counterpart, although in comparable ranges. The maximum hydrogen concentration for nNP was reached by the NP system only after 5 hours of operation, which then cements the positive effects the magnetite particles brought with respect to the production rate as was also postulated by Kumar *et al.* (2018)

This could be owing to the surface effects of the NPs which augments the activity of ferredoxin oxidoreductase by bolstering the rate of transfer of electrons from NADPH to Fe-Fe hydrogenases, henceforth synchronously increases the generation of hydrogen, as was documented by other researchers (Han *et al.* 2011; Eroglu and Melis 2016; Reddy *et al.* 2017). Furthermore, the NP have a higher propensity of attracting electrons and this further reduces the protons from H^+ to H_2, leading to an ‘electron sink’.

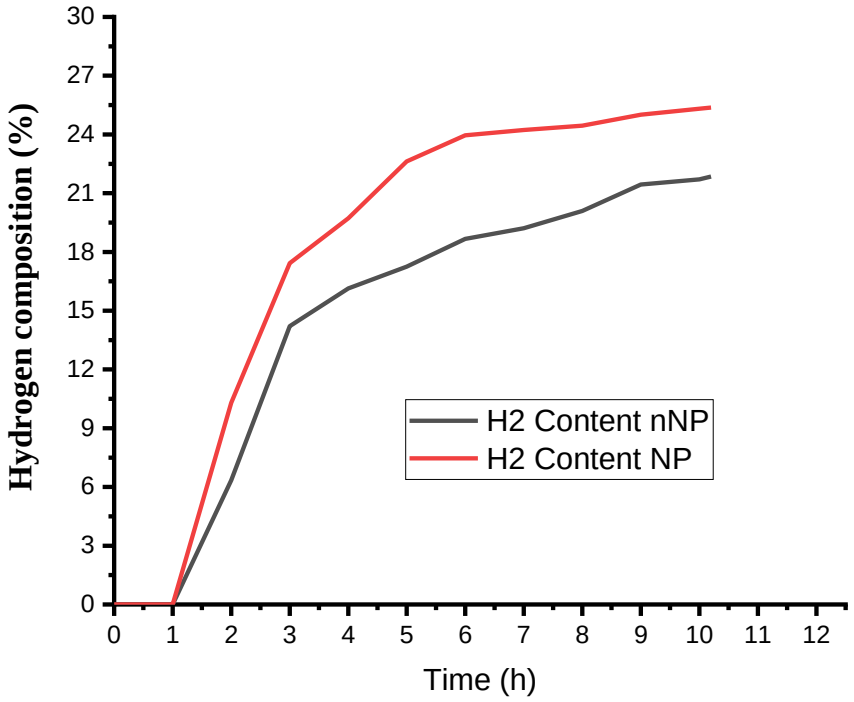

Figure 5.2 Composition of hydrogen in NP and nNP systems

Conversely, other researchers have found that the nanoparticles quantity charged in a reactor at higher concentrations may be toxic to the microbes and affect their growth This can be due to the toxicity effect of high nanoparticle concentration on the cell viability, such as cell wall penetration, cell wall breakage, and oxidative stress (Gadhe, Sonawane and Varma 2015; Pugazhendhi *et al.* 2018). This concept was, however, beyond the scope of this study, and it ought to be looked at in future studies for the same conditions.

5.3.3 Hydrogen Production Rate

The hourly production rate of hydrogen was examined to determine the effects of the nanoparticles on the rate of HPR in the dark fermentation process in an ABR. From Figure 5.3, the maximum HPR in nNP system was 26.53 mL/h at the 4th hour of operation, which was about 29% lower than the NP system after the same time. The NP system has had superior HPRs as compared to the nNP system for reasons explained in the above sections. There was an abnormal dip in the H_2 production rate in NP system (34.22 mL/h) at the 4th hour, before the rate picked up again to the maximum

value realised in this study, 38.62 mL/h. This could have been caused by a minor upset in the NP system as there was a slight increase in pH (6.1) at the 5th hour of operation, which could have been as a result of lack of continuous agitation in the reactor. The same dip was not noticed in the nNP system where the shaking of the reactors was done regularly. The maximum HPR registered in the NP system was about 44% higher than in nNP. This observation cements what other researchers have found about the effect of NPs on the general production rate of biohydrogen (Beckers *et al.* 2013).

Both elemental and ionic iron are crucial micronutrients in the formation of hydrogenase and other relevant enzymes, which almost all biohydrogenation requires by promoting the activity of the hydrogenases and the growth of microorganisms, thus increasing HPR, hydrogen content and slightly hydrogen yield, simultaneously decreasing the lag phase period (Wang and Wan 2008). Iron forms the metal part at the active site of hydrogenase enzymes that catalyses the reduction of protons to H_2 (Frey 2002; Kumar *et al.* 2019).

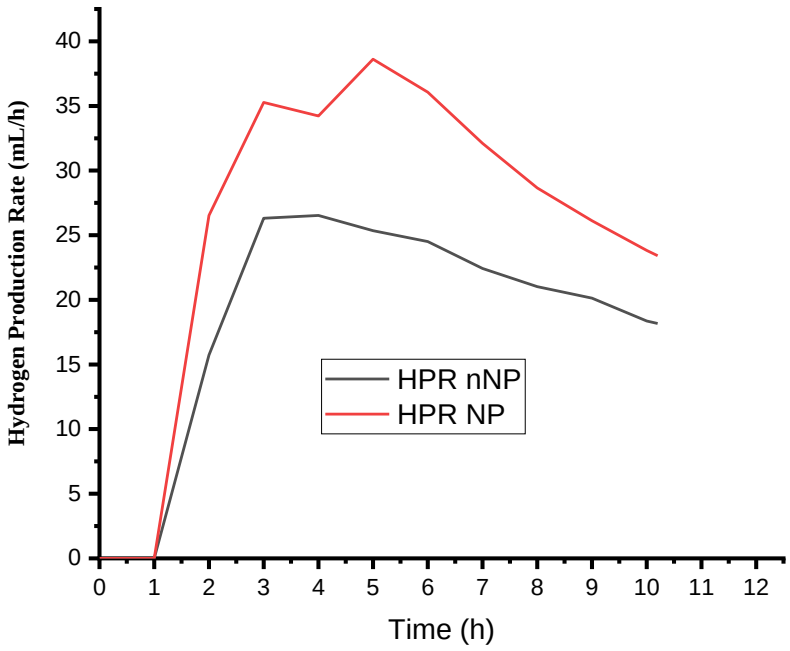

Figure 5.3 Production rates with respect to NP and nNP

When microorganisms are farther apart from each other, the transport of formate will be favoured, and if they are closer, hydrogen becomes more favourable (Giovannini *et al.* 2016).

5.3.4 Other output parameters

The effect of nanoparticles on the distribution of chiefly COD and VFA, among other parameters was examined. The initial COD in all the cases was 5623 mg/L. Table 5.2 shows the findings from the four reactors with respect to the final COD and VFA concentration. It was observed that the COD removal efficiency for the NP system was 51.95% average and that of the nNP system was 48.40%, and this is an indicator that the nanoparticles do not affect much the thermodynamics in the dark fermentation process but affects kinetics more. It was expected that the NP COD removal efficiency would be more superior to the nNP system, they were, however comparable as the magnetite nanoparticles affected the rate of COD removal. This also concords with the work done by Hou *et al.* (2012) whereby the NP and nNP systems would offset each other by less than 3.5% (144 and 149 mg/L, respectively).

More focus was placed on finding ways to increase the rate of COD removal, than the final COD removal. The COD removal efficiency is proportional to the biohydrogen production, given that all the operating conditions were optimised (Han and Shin 2004; Jha, Kana and Schmidt 2017).

Table 5.2 COD and VFAs based on nanoparticles

Parameter	Reactor	Run 1	Run 2	Run 3	Average	Removal efficiency	Overall average
COD	R1	2637	2661	2709	2669	52.53%	**2702**
	R2	2723	2704	2778	2735	51.36%	
	R3	2897	2942	2957	2932	47.86%	**2902**
	R4	2910	2847	2856	2871	48.94%	
VFA	R1	751	763	745	753		**788**
	R2	805	814	847	822		
	R3	641	665	644	650		**678**
	R4	701	716	701	706		

The knowledge on VFAs is of paramount importance as discussed earlier, elsewhere in this study. This enables the decision to be made on whether the effluent would be used for further downstream processes, especially with regards to photofermentation. By contrast, no significant alteration in metabolism was seen, with respect to the soluble metabolites distribution (Elbeshbishy *et al.* 2017). In this study, the NP system was, on average, 1.16 time higher than the nNP system, this is in an

agreement with another study done by Eduok *et al.* (2017) when the VFAs were 1.2 higher in the spiked bioreactors and visibly different (p =0.05) from the control set up.

5.4 Summary

A system with magnetite nanoparticles (NP) had superior HPR (23.41 mL/h) as compared to the control system without nanoparticles (nNP) (18.17 mL/h). The maximum HPR registered in the NP system was about 44% higher than in nNP. The NP system had COD removed from 5623 mg/L down to 2702 mg/L and 2902 mg/L for nNP. The highest composition of hydrogen in the biogas in NP was 25.37% and 21.85% in nNP, whereas the lowest was 10.3% in NP and 6.34% in nNP. The maximum HPR in nNP system was 26.53 mL/h at the 4th hour of operation, which was about 29% lower than the NP system after the same time. The COD removal efficiency for the NP system (51.95%) and that of the nNP system (48.40%). VFA concentration in the NP system (788 mg/L) was, on average, 1.16 time higher than the nNP system.

CHAPTER SIX

PREDICTIVE MODEL FOR FERMENTATIVE HYDROGEN PRODUCTION

6.1 Introduction

In this chapter, experimental work and existing models were used to investigate the relationship between the experimental performance of the ABR and existing mathematical models with respect to hydrogen yield and production rate. An in-depth theoretical and experimental analysis of the dark fermentation process was done, with temperature, batch time and pH as the variable parameters, while HPR, yield, COD removal efficiency and the VFA concentration where the output response. Modelling can be a useful tool used to understand and optimise a process, as experimental work in anaerobic digestion is time-consuming and costly.

Models are used to predict the behaviour of a certain reaction and in this study, a model generated by the software was used to validate the experiments. A mathematical model facilitates the interfusion and explanation of experimental findings, thus offering a deeper understanding of complex and dynamic systems such as biological communities. Mathematical modelling provides an account of relevant outcomes, such as HPR, yield, substrate utilisation and product generation; additionally, considering the influence of operating conditions, such as pH, temperature and operation time (Xie *et al.* 2016; Blanco, Oliveira and Zaiat 2019). Hence, the knowledge procured through the mathematical models can give room for determining more favourable operating conditions and microenvironment to achieve a lucrative performance of the dark fermentation process (Chezeau and Vial 2019; Frunzo *et al.* 2019). During dark fermentation COD, pH, HPR and some soluble metabolites change intermittently. Thus, mathematical and statistical have been suggested to describe the alterations as mentioned earlier (Zwietering *et al.* 1990; Blanco, Oliveira and Zaiat 2019).

6.2 Methods

The RSM employing the CCD was used to formulate the combination of experimental runs as this is a confirmation of the effectiveness of this method of optimising input parameters utilising statistical experimental design (Chaganti *et al.* 2012; Verma, Bishnoi and Gupta 2017; Wu 2019). CCD was preferred because of its ease of design as the alpha value used in synthesising the combination of experiments and experiment parameters is 1. By applying CCD, it led to an estimation of 10 significant coefficients after running 20 experiments (14 + 6 central points). This entails that some degrees of freedom were left out and this is very essential to help create a more reliable model, especially in situations where experimental accuracy can be affected (Rakić *et al.* 2014).

6.2.1 Statistical and mathematical analysis

After the data was collected based on the CCD matrix formulated, statistical and mathematical analyses were conducted based on the results observed, as shown in Table 4.1 in Chapter 4. The evaluation of the model was performed by the ANOVA using Design Expert 11 software (Statease, Inc. USA). The order of the model was determined by comparing the sequential and Lack of Fit p- values. The order of the equation obtained was solved using the method of Myers, Montgomery and Anderson-Cook (2016) to acquire the estimated optimum system conditions of the biohydrogen production rate for the RSM.

The most common models used are the linear, 2FI (two-factor interaction) and quadratic forms which are then evaluated by ANOVA to determine the order that has the best correlation between input parameters and selected output parameters (in this case the HPR). ANOVA evaluated the accuracy of the developed mathematical model. The ANOVA was then accompanied by the F-test to determine the significance of each term. High F-values ascertained that the developed mathematical model could explain the deviation in the output values. The corresponding p-values were used to assess if the F-values were large enough to signify statistical significance, the p-values should be lower than 0.05 to confirm significance in the model developed or otherwise (Maran *et al.* 2015). Experimental data from the 20 experimental runs were fitted into a second-order regression model which correlates the manipulated input variables to the predicted HPR, COD removal efficiency and VFA concentration.

6.2.2 Validation

After optimisation in the preceding chapters, the ABR was cleaned and reused with brewery industrial water and the inoculum for the local wastewater treatment plant that was used for the other 20 experimental runs as shown in Table 4.1. The validation was conducted in Chapter 5 with the system as the control for the investigation of nanoparticles on production rate (Donoso-Bravo *et al.* 2011). The experimental validation run was conducted in duplicate to obtain an average of the HPR, which was then compared with the HPR predicted by the mathematical model developed. In addition to the validation of the mathematical model, validation of optimised start-up conditions was performed. For that, the ABRs were inoculated with the same sewage sludge used in the 20 experiments.

6.3 Results and discussion

6.3.1 Significance of the ANOVA

Table 6.1 shows how the quadratic regression model was selected ahead of other sources such as the linear, 2FI and cubic models. The ANOVA was conducted to assess how significant was the reduced quadratic model based on experimental observations. It was found that the reduced quadratic model fitted better than the other models, hence on quadratic regression model was discussed in this chapter. The quadratic relationship has high predictive power between input and response factors.

Table 6.1 Fit summary of model sources for HPR

Source	Sequential P-value	Lack of Fit p-value	Adjusted R^2	Predicted R^2	
Linear	0.2692	0.0005	0.0645	-0.1109	
2FI	0.9470	0.0003	-0.1205	-0.6871	
Quadratic	**< 0.0001**	**0.0368**	**0.8677**	**0.5319**	**Suggested**
Cubic	0.1065	0.0534	0.9277	-1.8289	Aliased

The lowest p-value of 0.0001 for quadratic showed that the model was significant.

6.3.2 Model construction and interpretation

To determine the effects of the temperature, batch time and pH, the operating conditions matrix in tandem with their respective HPRs were subjected to regression analysis. Table 4.5 shows the

effect of terms in the final quadratic model and outlines if terms are significant or not to the regression model. The large F-values suggest that the variation in the response can be explained by the regression equation (Dahunsi *et al.* 2016). The F-value of 14.85 states that the model is significant, as explained in section 4.6. In this case, B, C, A^2, B^2, C^2 were significant model terms. Values greater than 0.1000 in the model were considered not significant (Parthiban *et al.* 2019). If there are many insignificant model terms (not counting those required to support hierarchy), model reduction may improve the model. The Lack of Fit F-value of 3.90 implies there is an 88% chance that a Lack of Fit F-value this large could occur due to noise (Singh and Jayswal 2018; Parthiban *et al.* 2019).

Table 6.2 Fit statistics

Std. Dev.	**2.14**		**R^2**	**0.9304**
Mean	9.41		**Adjusted R^2**	0.8677
C.V.%	22.73		**Predicted R^2**	0.5319
			Adequate Precision	10.9259

From Table 6.2, the predicted R^2 of 0.5319 is not as close to the adjusted R^2 of 0.8677 as expected since their margin is above 20%. This could have been attributed to a significant block effect or perhaps the model itself. The model also contains some insignificant terms leading to an inefficient model; hence they need to be struck out of the mathematical model (Tunçay *et al.* 2017). The removal of insignificant terms one by one in a stepwise manner (starting from largest insignificant to smallest insignificant term) is carried out to improve the quadratic model which produced higher 'R-square' or 'predicted R-square' value for the present model is 0.8677 and suggests how good the model predict the cumulative extraction yield. Confirmatory runs must be conducted to test the credibility of the empirical model. The margin between predicted R^2 and adjusted R^2 (33.5%) could have been due to the pH that was not regulated throughout the experimental run for the 20 trials and bacteria involved may not have a definite behaviour when they are disturbed because of the abrupt alterations in the system. Although influent COD was similar in order of magnitude (5745±78 mg/L) in all the cases, slight differences were depending on the day of collection of samples; thus, these differences might have had an impact on the extensive margin of the correlation coefficients, as found by Azman *et al.* (2016).

Adequate Precision measures the signal to noise ratio (Majdi, Esfahani and Mohebbi 2019). A ratio greater than 4 is desirable, and in this case, the ratio of 10.340 was recorded, and this shows adequacy in the signal. Thus, this model can be used to navigate the design space. By applying multiple regression analysis on the experimental results, the polynomial equation was obtained to describe the hydrogen production. Therefore, the quadratic model has the following coefficients, as presented in Table 6.3.

Table 6.3 Coefficients of the Terms of Actual Factors

Hydrogen production rate (HPR)	**= Parameter (Unit)**
-668.51153	
+3.57748	Batch Time (h)
+35.97802	Temperature (℃)
+6.71239	pH
+0.041279	Batch Time * Temperature (h℃)
-0.045250	Batch Time * pH (h)
+0.415308	Temperature * pH (℃)
-0.235889	Batch Time² (h^2)
-0.536583	Temperature² ($℃^2$)
-1.90553	pH²

The coefficients as presented in Table 6.3 can be used to construct the mathematical equation that follows which shows the response of HPR with respect to temperature, batch time and pH in different orders.

$$\boldsymbol{HPR} = -668.51153 + 3.57748\,\boldsymbol{A} + 35.97802\,\boldsymbol{B} + 6.71239\,\boldsymbol{C} + 0.041279\,\boldsymbol{A}*\boldsymbol{B} - 0.045250\,\boldsymbol{A}*\boldsymbol{C} + 0.415308\boldsymbol{B}*\boldsymbol{C} - 0.235889\boldsymbol{A}^2 - 0.504576\boldsymbol{B}^2 - 1.90553\boldsymbol{C}^2 \quad 6.1$$

Where A = Batch Time,

B = Temperature

C = pH

Equation 6.1 translated into actual terms under investigation, as shown in Equation 6.2.

$$\boldsymbol{HPR} = -668.51153 + 3.57748\,\boldsymbol{Batch\ Time} + 35.97802\,\boldsymbol{Temperature} + 6.71239\,\boldsymbol{pH} + 0.041279\,\boldsymbol{Batch\ Time} * \boldsymbol{Temperature} - 0.04525\,\boldsymbol{Batch\ Time} * \boldsymbol{pH} + 0.415308\,\boldsymbol{Temperature} * \boldsymbol{pH} - 0.235889\,\boldsymbol{Batch\ Time^2} - 0.536583\,\boldsymbol{Temperature^2} - 1.90553\boldsymbol{pH^2} \quad 6.2$$

The equation in terms of actual factors can be used to make predictions about the response for given levels of each factor. Here, the levels should be specified in the original units for each factor. This equation should not be used to determine the relative impact of each factor because the coefficients are scaled to accommodate the units of each factor, and the intercept is not at the centre of the design space.

6.3.3 Actual HPR with comparison to the predicted values

The model developed gave an erratic prediction of the HPR (mL/h), only a few predictions lied within 10% of the experimentally determined values, as shown in Table 6.4. Even the outcome at the centre points has not been acceptably consistent, giving rise to a low R^2 value of 0.53. This anomaly could have resulted from slightly different influent wastewater as it was collected on different days of plant operation and storing in the cold room for longer periods would compromise the nature of the wastewater. There was also a limitation of space to store larger volumes of wastewater. Another reason could be the uncontrolled pH during the experimentation, which might have disturbed the activity of hydrogenase enzymes which are responsible for hydrogen production (Wang and Wan 2009; Dabrock, Bahl and Gottschalk 2019). The lack of knowledge of the component sugars may also have dealt a major blow on the close conformation of the model. This difference in the behaviour of pH change in a system whose pH is not controlled is also a function of the difference in the initial COD concentration as shown in Table 4.1 and the raw data in Table C1 where influent was 5653 and 5839 mg/L distributed among runs 15 to 20, which happened to be the centre points of the matrix with the COD removal efficiencies ranging from 38 to 50% (Elbeshbishy *et al.* 2017).

Table 6.4 Actual and predicted HPR

	Input variables			H_2 production rate (mL/h)	
Run	**Batch time (h)**	**Temperature (℃)**	**pH**	**Actual**	**Predicted**
1	6	33.0	3.5	2.98±0.37	2.74
2	14.0	33.0	3.5	2.30±0.09	3.25
3	6.0	37.0	3.5	4.40±0.45	3.21
4	14.0	37.0	3.5	3.79±0.27	5.04
5	6.0	33.0	6.5	8.56±0.66	6.01
6	14.0	33.0	6.5	5.54±0.04	5.43
7	6.0	37.0	6.5	13.70±1.01	11.47
8	14.0	37.0	6.5	13.26±0.49	12.21
9	3.3	35.0	5.0	2.11±0.01	5.27
10	16.7	35.0	5.0	7.47±0.06	6.31
11	10.0	32.0	5.0	6.72±0.11	8.83
12	10.0	38.0	5.0	12.07±0.86	14.27
13	10.0	35.0	2.5	0.94±0.08	0.12
14	10.0	35.0	7.5	5.73±0.50	8.82
15	10.0	35.0	5.0	17.20±1.43	16.38
16	10.0	35.0	5.0	14.37±1.81	16.38
17	10.0	35.0	5.0	18.16±0.62	16.38
18	10.0	35.0	5.0	14.94±1.12	16.38
19	10.0	35.0	5.0	15.67±1.24	16.38
20	10.0	35.0	6.5	15.99±0.73	14.70

Figure 6.1 depicts the correlation that exists between the actual and predicted values of the HPR. A strong correlation between the actual and predicted values was determined, ascertaining that the model has reasonably high predictive power. Still, it needs to be treated with care as it does not consider the behaviour of microorganisms involved which may introduce an anomaly in the predictive nature of the model.

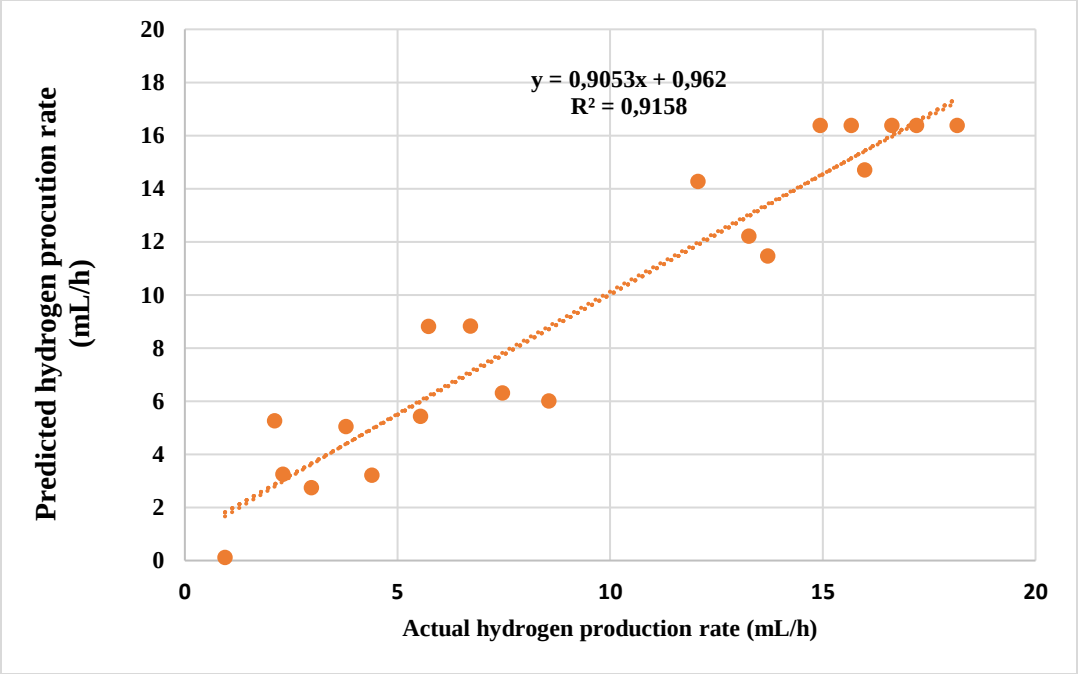

Figure 6.1 Correlation between actual and predicted HPR

6.3.4 Model validation at Controlled pH

After the development of the model, validation was done using optimum conditions as determined in the previous chapter. The model only considered initial pH values, and it was never maintained at the set point throughout the process, and there were significant changes in pH for some runs. For this reason, it might have reduced the predictive power and conformity of the model to the actual data.

To ascertain the predictive power of the quadratic regression model, the validation experiment was run at the optimal conditions determined previously by the software and by inspection. The operating conditions were a batch time of 10.2 h, temperature of 36℃ and pH of 5.6 (it was maintained throughout as discussed in the preceding chapters), the average production rate of hydrogen determined was 18.17 mL/h (optimum expected 17.05 mL/h). The quadratic model determined in this study managed to predict 17.37 mL/h HPR under the conditions as mentioned earlier, which was 4.42% deviant from the experimentally determined value. That shows that it is crucial to maintain the pH for any given set of operating conditions within the boundary conditions for the model to conform better to the experimental observations.

From experience gained in this research, although the model is exhibiting statistical robustness, it is believed that future microbial studies must consider the adaptation of biomass and its influence on the ABR performance under the operating conditions adopted in the adaptation period. Correction factors for use after adaptation of biomass will need to be employed. Conformity was also affected by modelling based only on COD, and the sugar analysis would improve the predictive power of models.

6.4 Conclusion

The quadratic model was adopted because it had the best p-value (<0.0001) and the R^2 value of 0.8677 as compared to other orders of models. However, there was a significant difference between the adjusted R^2 value and the predicted R^2 value, over 38% deviation. The average HPR determined was 18.17 mL/h (optimum expected 17.05 mL/h). The quadratic model (Equation 6.1) determined in this study managed to predict 17.37 mL/h HPR under the optimum conditions, which was 4.42% deviant from the experimentally determined value.

CHAPTER SEVEN

CONCLUSION AND RECOMMENDATIONS

7.1 Introduction

This study had its focus on characterising various wastewater streams (yeast, alcohols, brewery, sugar and dairy industries) and run them in preliminary batch experiments in a bid to determine the most suitable substrate for the scaled-up ABR. The brewery wastewater was determined to be the best among the five streams in question. The chosen stream was used for optimising the operating conditions in an ABR for an improved dark fermentation process. The optimised conditions were used to investigate the effect of nanoparticles in the dark fermentation process. A model quadratic model was finally developed and comparison between actual and predicted data was made.

7.2 Conclusion

The literature was extensively explored on the best practices of the production of biohydrogen from industrial wastewater through dark fermentation. The mesophilic range of operation was selected after a careful assessment of the available options.

- Several wastewater streams were chosen for the preliminary batch runs that were used to find the best wastewater stream for scaling up. The five streams (COD/BOD ratio) used were brewery (2.17), yeast manufacturing (2.81), alcohols manufacturing (4.11), dairy (5.36) and sugar manufacturing (1.45) wastewater streams. The dairy (36.4%), sugar (32.9%) and the brewery (40.1%) wastewater streams were found to have the best hydrogen potential for a specific set of operating conditions. However, not only yields and production rates of hydrogen were assessed to determine the best substrate, other non-technical aspects such as ease of availability, digestibility, legislation, disclosure policies among others were explored. Thus, the Kepner-Tregor Decision-making tool was utilised, and the brewery wastewater had the best index (95.1%) and was selected for the scaled-up ABR.
- After selection of the wastewater stream for the scaling up in the ABR, the brewery wastewater with initial COD averaging 5745 ± 78 mg/L was used. The operating

parameters were temperature ranging from 33 to 37℃, pH (3.5-6.5) and batch time (4-12 h). The highest hydrogen production rate, COD removal and VFA were recorded as 18.16 mL/h (26.76 mmol/gCOD), 60.81% and 733 mg/L, respectively, at different operating conditions. Design Expert 11 software was used as a tool to determine optimum operating conditions with 10.2 h, 36℃ and 5.6 as the optimal conditions for a batch time, operating temperature and pH, respectively. The surface plot and the contour plots helped to find the optimal region of operating parameters to maximise the hydrogen production rate among other outputs.

- Since the focus was deployed on the production rate more than the yield, the magnetite nanoparticles were used in a bid to bolster the rate of production of hydrogen operating at optimum conditions determined in this study. The control system without nanoparticles whose pH was maintained at the optimal point registered an overall production rate of 18.17 mL/h, whereas the test experiment with nanoparticles was graced with higher production rate than the system without nanoparticles, 23.41 mL/h (44% increase). There was an evident increase in the production rate when the magnetite nanoparticles were used, but not very satisfactory. The model developed had moderate predictive power.
- A predictive model for the hydrogen production rate was developed and assessed. The quadratic regression model was used to develop a model which conformed to the data casually. The adjusted correlation coefficient was 0.8677 and the predicted R^2 of 0.5319. The model selectively obeyed some operating conditions and had discrepancies for other conditions as pH of the reactors was not regulated, during the experiments. For confirmatory and validation experiments, pH was controlled, thus improved outputs were noticed.

7.3 Recommendations

For commercialisation of the dark fermentation using an ABR, there is still a need to explore a few other factors for the efficient and profitable running of the system. Some of the recommendations for future work related to this study are listed below:

- To avoid the use of inorganic chemicals (e.g. HCl and NaOH) to regulate the pH during fermentation, the synergistic interaction of various organic-rich wastewater streams that are either acidic or basic should be employed to make the entire process green.
- The use of nanoparticles such as ZnO, Ni, and Fe_3O_4 composite needs to be further studied in dark fermentation systems as this would bumper the yields of hydrogen and more importantly the hydrogen production rates.
- From the satisfactory effluent VFA concentrations found in this study, it is highly recommended to use the dark fermentation effluent for a downstream photofermentation process to improve on the efficiency of the wastewater treatment and harnessing energy.
- A two-stage process that combines biohydrogen and biomethane production could be studied extensively and be employed as a possible way for the enhancement of the efficiency of the dark fermentation systems.
- The ABR needs hydraulic agitation periodically to do away with dead zones and improve on its overall efficiency.
- Microbial analysis and its incorporation into mathematical models could be of paramount importance in developing models that conform to the actual operation of the dark fermentation process with fewer constraints.
- Specialised strains of bacteria useful in the conversion of recalcitrant organic material in wastewater streams could be genetically engineered in future studies as the microbes in use in recent studies are a consortium of various microbial communities and have different digestive power on various substrates. This manipulates the metabolic pathways of microbes and can improve the yields of hydrogen which are naturally difficult to enhance, hence more focus was on the production rate of hydrogen. Eventually, there will be a significant reduction in the cost of production for the whole process.
- The final effluent could be further assessed to check its nature and the possibility to be used in agro-based activities.

REFERENCES

Abdelsalam, E., Samer, M., Attia, Y., Abdel-Hadi, M., Hassan, H. and Badr, Y. 2016. Comparison of nanoparticles effects on biogas and methane production from anaerobic digestion of cattle dung slurry. *Renewable energy*, 87: 592-598.

Abreu, A. A., Karakashev, D., Angelidaki, I., Sousa, D. Z. and Alves, M. M. 2012. Biohydrogen production from arabinose and glucose using extreme thermophilic anaerobic mixed cultures. *Biotechnology for biofuels*, 5 (1): 1.

Abubackar, H. N., Keskin, T., Arslan, K., Vural, C., Aksu, D., Yavuzyılmaz, D. K., Ozdemir, G. and Azbar, N. 2019. Effects of size and autoclavation of fruit and vegetable wastes on biohydrogen production by dark dry anaerobic fermentation under mesophilic condition. *International Journal of Hydrogen Energy*, 44 (33): 17767-17780.

Adams, M. W. 1990. The metabolism of hydrogen by extremely thermophilic, sulfur-dependent bacteria. *FEMS Microbiology Letters*, 75 (2-3): 219-237.

Adams, M. W. and Stiefel, E. I. 2014. Biological hydrogen production: not so elementary. *Science*, 282 (5395): 1842-1843.

Ademoroti, C. 1996. *Standard method for water and effluent analysis, March prints and Consultancy*: Foludex press Ltd. Ibadan.

Akhbaria, A., Zinatizadehb, A. A., Vafaeifarda, M., Mohammadid, P., Zainala, B. S. and Ibrahima, S. 2019. Effect of operational variables on biological hydrogen production from palm oil mill effluent by dark fermentation using response surface methodology. *Desalination and Water Treatment*, 137: 101-113.

Akkerman, I., Janssen, M., Rocha, J. and Wijffels, R. H. 2002. Photobiological hydrogen production: photochemical efficiency and bioreactor design. *International Journal of Hydrogen Energy*, 27 (11): 1195-1208.

Ali, A., Hira Zafar, M. Z., ul Haq, I., Phull, A. R., Ali, J. S. and Hussain, A. 2016. Synthesis, characterization, applications, and challenges of iron oxide nanoparticles. *Nanotechnology, science and applications*, 9: 49.

An, Q., Wang, J.-L., Wang, Y.-T., Lin, Z.-L. and Zhu, M.-J. 2018. Investigation on hydrogen production from paper sludge without inoculation and its enhancement by Clostridium thermocellum. *Bioresource technology*, 263: 120-127.

Angenent, L. T., Karim, K., Al-Dahhan, M. H., Wrenn, B. A. and Domíguez-Espinosa, R. 2004. Production of bioenergy and biochemicals from industrial and agricultural wastewater. *TRENDS in Biotechnology*, 22 (9): 477-485.

APHA. 2005. Standard methods for the examination of water and wastewater. *American Public Health Association, American Water Works association, Water Environment Federation, Washington.*,

Archana, A., Sasikala, C. and Ramana, C. V. 2003. Augmentation of H_2 photoproduction in Rhodopseudomonas palustris by N-heterocyclic aromatic compounds. *Biotechnology letters*, 25 (1): 79-82.

Argun, H. 2010. Hydrogen gas production from waste ground wheat by dark and light fermentations. DEÜ Fen Bilimleri Enstitüsü.

Argun, H. and Dao, S. 2017. Bio-hydrogen production from waste peach pulp by dark fermentation: Effect of inoculum addition. *International Journal of Hydrogen Energy*, 42 (4): 2569-2574.

Argun, H., Kargi, F. and Kapdan, I. K. 2009. Microbial culture selection for bio-hydrogen production from waste ground wheat by dark fermentation. *International Journal of Hydrogen Energy*, 34 (5): 2195-2200.

Argun, H. and Onaran, G. 2017. Effects of N/C, P/C and Fe/C ratios on dark fermentative hydrogen gas production from waste paper towel hydrolysate. *International Journal of Hydrogen Energy*, 42 (22): 14990-15001.

Assawamongkholsiri, T., Reungsang, A., Plangkang, P. and Sittijunda, S. 2018. Repeated batch fermentation for photo-hydrogen and lipid production from wastewater of a sugar manufacturing plant. *International Journal of Hydrogen Energy*, 43 (7): 3605-3617.

Azman, N. F., Abdeshahian, P., Al-Shorgani, N. K. N., Hamid, A. A. and Kalil, M. S. 2016. Production of hydrogen energy from dilute acid-hydrolyzed palm oil mill effluent in dark fermentation using an empirical model. *International Journal of Hydrogen Energy*, 41 (37): 16373-16384.

Bachmann, A., Beard, V. L. and McCarty, P. L. 2015. Performance characteristics of the anaerobic baffled reactor. *Water Research*, 19 (1): 99-106.

Bagchi, B., Dey, S., Bhandary, S., Das, S., Bhattacharya, A., Basu, R. and Nandy, P. 2012. Antimicrobial efficacy and biocompatibility study of copper nanoparticle adsorbed mullite aggregates. *Materials Science and Engineering: C*, 32 (7): 1897-1905.

Baloch, M., Akunna, J. C. and Collier, P. J. 2007. The performance of a phase separated granular bed bioreactor treating brewery wastewater. *Bioresource technology*, 98 (9): 1849-1855.

Bansal, S. K., Singhal, Y. and Singh, R. 2012. Biohydrogen Production with Different Ratios of Kitchen Waste and Inoculum in Lab Scale Batch Reactor at Moderate Temperatures. In: *Chemistry of Phytopotentials: Health, Energy and Environmental Perspectives*. Springer, 213-216.

Barber, W. P. and Stuckey, D. C. 2009. The use of the anaerobic baffled reactor (ABR) for wastewater treatment: a review. *Water Research*, 33 (7): 1559-1578.

Basak, N. and Das, D. 2017. The prospect of purple non-sulfur (PNS) photosynthetic bacteria for hydrogen production: the present state of the art. *World Journal of Microbiology and Biotechnology*, 23 (1): 31-42.

Bashan, Y., Hernandez, J.-P., Leyva, L. A. and Bacilio, M. 2002. Alginate microbeads as inoculant carriers for plant growth-promoting bacteria. *Biology and Fertility of Soils*, 35 (5): 359-368.

Bastidas-Oyanedel, J.-R., Bonk, F., Thomsen, M. H. and Schmidt, J. E. 2019. The Future Perspectives of Dark Fermentation: Moving from Only Biohydrogen to Biochemicals. In: *Biorefinery*. Springer, 375-412.

Bastidas-Oyanedel, J.-R., Mohd-Zaki, Z., Zeng, R. J., Bernet, N., Pratt, S., Steyer, J.-P. and Batstone, D. J. 2012. Gas controlled hydrogen fermentation. *Bioresource technology*, 110: 503-509.

Bauer, N., Mouratiadou, I., Luderer, G., Baumstark, L., Brecha, R. J., Edenhofer, O. and Kriegler, E. 2016. Global fossil energy markets and climate change mitigation–an analysis with REMIND. *Climatic Change*, 136 (1): 69-82.

Beaton, S. E., Evans, R. M., Finney, A. J., Lamont, C. M., Armstrong, F. A., Sargent, F. and Carr, S. B. 2018. The structure of hydrogenase-2 from Escherichia coli: implications for H_2-driven proton pumping. *Biochemical Journal*, 475 (7): 1353-1370.

Beckers, L., Hiligsmann, S., Lambert, S. D., Heinrichs, B. and Thonart, P. 2013. Improving effect of metal and oxide nanoparticles encapsulated in porous silica on fermentative biohydrogen production by Clostridium butyricum. *Bioresource technology*, 133: 109-117.

Bensaid, S., Ruggeri, B. and Saracco, G. 2015. Development of a Photosynthetic Microbial Electrochemical Cell (PMEC) Reactor Coupled with Dark Fermentation of Organic Wastes: Medium Term Perspectives. *Energies*, 8 (1): 399-429.

Biresselioglu, M. E. and Yelkenci, T. 2016. Scrutinizing the causality relationships between prices, production and consumption of fossil fuels: A panel data approach. *Energy*, 102: 44-53.

Bisaillon, A., Turcot, J. and Hallenbeck, P. C. 2006. The effect of nutrient limitation on hydrogen production by batch cultures of Escherichia coli. *International Journal of Hydrogen Energy*, 31 (11): 1504-1508.

Blanco, V. M. C., Oliveira, G. H. D. and Zaiat, M. 2019. Dark fermentative biohydrogen production from synthetic cheese whey in an anaerobic structured-bed reactor: Performance evaluation and kinetic modeling. *Renewable energy*, 139: 1310-1319.

Bolatkhan, K., Kossalbayev, B. D., Zayadan, B. K., Tomo, T., Veziroglu, T. N. and Allakhverdiev, S. I. 2019. Hydrogen production from phototrophic microorganisms: reality and perspectives. *International Journal of Hydrogen Energy*, 44 (12): 5799-5811.

Brar, S. K., Zhang, T. C., Verma, M., Surampalli, R. Y. and Tyagi, R. D. 2015. Nanomaterials in the Environment. In: Proceedings of. American Society of Civil Engineers,

Bryson, A. E. 2018. *Applied optimal control: Optimization, estimation and control*. USA: Routledge.

Buitrón, G., Hernández-Juárez, A., Hernández-Ramírez, M. D. and Sánchez, A. 2019. Biochemical methane potential from lignocellulosic wastes hydrothermally pretreated. *Industrial Crops and Products*, 139: 111555.

Cai, G., Jin, B., Monis, P. and Saint, C. 2011. Metabolic flux network and analysis of fermentative hydrogen production. *Biotechnology advances*, 29 (4): 375-387.

Calvo, P., Remunan-Lopez, C., Vila-Jato, J. and Alonso, M. 1997. Novel hydrophilic chitosan-polyethylene oxide nanoparticles as protein carriers. *Journal of Applied Polymer Science*, 63 (1): 125-132.

Carpenter, E. E. 2001. Iron nanoparticles as potential magnetic carriers. *Journal of Magnetism and Magnetic Materials*, 225 (1): 17-20.

Carrillo-Reyes, J., Tapia-Rodríguez, A., Buitrón, G., Moreno-Andrade, I., Palomo-Briones, R., Razo-Flores, E., Juárez, O. A., Arreola-Vargas, J., Bernet, N. and Braga, A. F. M. 2019. A standardized biohydrogen potential protocol: An international round robin test approach. *International Journal of Hydrogen Energy*, 44 (237-247)

Cassidy, M., Lee, H. and Trevors, J. 1996. Environmental applications of immobilized microbial cells: a review. *Journal of Industrial Microbiology*, 16 (2): 79-101.

Castelló, E., Ferraz-Junior, A. D. N., Andreani, C., del Pilar Anzola-Rojas, M., Borzacconi, L., Buitrón, G., Carrillo-Reyes, J., Gomes, S. D., Maintinguer, S. I. and Moreno-Andrade, I. 2020. Stability problems in the hydrogen production by dark fermentation: Possible causes and solutions. *Renewable and Sustainable Energy Reviews*, 119: 109602.

Catal, T. 2016. Comparison of various carbohydrates for hydrogen production in microbial electrolysis cells. *Biotechnology & Biotechnological Equipment*, 30 (1): 75-80.

Chaganti, S. R., Kim, D.-H., Lalman, J. A. and Shewa, W. A. 2012. Statistical optimization of factors affecting biohydrogen production from xylose fermentation using inhibited mixed anaerobic cultures. *International Journal of Hydrogen Energy*, 37 (16): 11710-11718.

Chandra, R. 2015. Single-Stage Operation of Hybrid Dark-Photo Fermentation to Enhance Biohydrogen Production through Regulation of System Redox Condition: Evaluation with Real-Field Wastewater. 9540-9556.

Chandrasekhar, K., Lee, Y.-J. and Lee, D.-W. 2015. Biohydrogen production: Strategies to improve process efficiency through microbial routes. *International Journal of Molecular Sciences*, 16 (4): 8266-8293.

Chen, Y., Nakthong, C. and Chen, T. 2005. Improvement of laying hen performance by dietary prebiotic chicory oligofructose and inulin. *International Journal of Poultry Science*, 4 (2): 103-108.

Cheng, J., Xia, A., Su, H., Song, W., Zhou, J. and Cen, K. 2013. Promotion of hydrogen production by microwave-assisted treatment of water hyacinth with dilute sulphuric acid through combined dark fermentation and photofermentation. *Energy conversion and management*, 73: 329-334.

Chezeau, B. and Vial, C. 2019. Modeling and Simulation of the Biohydrogen Production Processes. In: *Biohydrogen*. Elsevier, 445-483.

Chu, Y.-F., Hsu, C.-H., Soma, P. K. and Lo, Y. M. 2009. Immobilization of bioluminescent Escherichia coli cells using natural and artificial fibers treated with polyethyleneimine. *Bioresource technology*, 100 (13): 3167-3174.

Chynoweth, D., Srivastra, V. and Conrad, J. 2015. Research study to determine the feasibility of producing methane gas from sea kelp. *Annual Report for General Electric Company, IGT Project*, 30502

Cisneros-Pérez, C., Carrillo-Reyes, J., Celis, L. B., Alatriste-Mondragón, F., Etchebehere, C. and Razo-Flores, E. 2015. Inoculum pretreatment promotes differences in hydrogen production performance in EGSB reactors. *International Journal of Hydrogen Energy*, 40 (19): 6329-6339.

Clesceri, L. S. G., Eaton, A. E., Rice, A. D., Franson, E. W. and Mary Ann, H. 2005. *Standard methods for the examination of water and wastewater*. Washington, DC: APHA, AWWA, WEF.

Colvin, V. L. 2003. The potential environmental impact of engineered nanomaterials. *Nature Biotechnology*, 21 (10): 1166-1170.

Confer, D. R. and Logan, B. E. 1997. Molecular weight distribution of hydrolysis products during the biodegradation of model macromolecules in suspended and biofilm cultures. II. Dextran and dextrin. *Water Research*, 31 (9): 2137-2145.

Covert, T., Greenstone, M. and Knittel, C. R. 2016. Will we ever stop using fossil fuels? *Journal of Economic Perspectives*, 30 (1): 117-138.

Dabrock, B., Bahl, H. and Gottschalk, G. 1992. Parameters affecting solvent production by Clostridium pasteurianum. *Appl. Environ. Microbiol.*, 58 (4): 1233-1239.

Dabrock, B., Bahl, H. and Gottschalk, G. 2019. Parameters affecting solvent production by Clostridium pasteurianum. *Applied and Environmental Microbiology*, 58 (4): 1233-1239.

Dahiya, S., Sarkar, O., Swamy, Y. and Mohan, S. V. 2015. Acidogenic fermentation of food waste for volatile fatty acid production with co-generation of biohydrogen. *Bioresource technology*, 182: 103-113.

Dahunsi, S., Oranusi, S., Owolabi, J. B. and Efeovbokhan, V. E. 2016. Mesophilic anaerobic co-digestion of poultry dropping and Carica papaya peels: Modelling and process parameter optimization study. *Bioresource technology*, 216: 587-600.

Das, D. and Veziroglu, T. N. 2008. Advances in biological hydrogen production processes. *International Journal of Hydrogen Energy*, 33 (21): 6046-6057.

Dashamiri, S., Ghaedi, M., Asfaram, A., Zare, F. and Wang, S. 2017. Multi-response optimization of ultrasound assisted competitive adsorption of dyes onto Cu (OH) 2-nanoparticle loaded activated carbon: central composite design. *Ultrasonics sonochemistry*, 34: 343-353.

de Souza Moraes, B., dos Santos, G. M., Delforno, T. P., Fuess, L. T. and da Silva, A. J. 2019. Enriched microbial consortia for dark fermentation of sugarcane vinasse towards value-added short-chain organic acids and alcohol production. *Journal of Bioscience and Bioengineering*, 127 (5): 594-601.

Demirbas, A. 2009. Biofuels securing the planet's future energy needs. *Energy conversion and management*, 50 (9): 2239-2249.

Dessì, P., Porca, E., Waters, N. R., Lakaniemi, A.-M., Collins, G. and Lens, P. N. 2018. Thermophilic versus mesophilic dark fermentation in xylose-fed fluidised bed reactors: Biohydrogen production and active microbial community. *International Journal of Hydrogen Energy*, 43 (11): 5473-5485.

Dickenson, E. R., Snyder, S. A., Sedlak, D. L. and Drewes, J. E. 2011. Indicator compounds for assessment of wastewater effluent contributions to flow and water quality. *Water Research*, 45 (3): 1199-1212.

Dinesh, R., Anandaraj, M., Srinivasan, V. and Hamza, S. 2012. Engineered nanoparticles in the soil and their potential implications to microbial activity. *Geoderma*, 173: 19-27.

Domínguez, J. R., González, T., Palo, P., Martín, J. S., Rodrigo, M. Á. and Sáez, C. 2016. Conductive-diamond electrochemical oxidation of a pharmaceutical effluent with high Chemical Oxygen Demand (COD). Kinetics and optimization of the process by Response Surface Methodology (RSM). *Environmental Engineering & Management Journal (EEMJ)*, 15 (1)

Don, M. M. and Shoparwe, N. F. 2010. Kinetics of hyaluronic acid production by Streptococcus zooepidemicus considering the effect of glucose. *Biochemical Engineering Journal*, 49 (1): 95-103.

Dong, L., Zhenhong, Y., Yongming, S., Xiaoying, K. and Yu, Z. 2009. Hydrogen production characteristics of the organic fraction of municipal solid wastes by anaerobic mixed culture fermentation. *International Journal of Hydrogen Energy*, 34 (2): 812-820.

Donoso-Bravo, A., Mailier, J., Martin, C., Rodríguez, J., Aceves-Lara, C. A. and Wouwer, A. V. 2011. Model selection, identification and validation in anaerobic digestion: a review. *Water Research*, 45 (17): 5347-5364.

Eduok, S., Ferguson, R., Jefferson, B., Villa, R. and Coulon, F. 2017. Aged-engineered nanoparticles effect on sludge anaerobic digestion performance and associated microbial communities. *Science of the Total Environment*, 609: 232-241.

Eker, S. and Sarp, M. 2017. Hydrogen gas production from waste paper by dark fermentation: Effects of initial substrate and biomass concentrations. *International Journal of Hydrogen Energy*, 42 (4): 2562-2568.

El-Shafie, M., Kambara, S. and Hayakawa, Y. 2019. Hydrogen production technologies overview. *Journal of Power and Energy Engineering*, 7 (01): 107.

Elahi, E., Zhang, L., Abid, M., Javed, M. T. and Xinru, H. 2017. Direct and indirect effects of wastewater use and herd environment on the occurrence of animal diseases and animal health in Pakistan. *Environmental Science and Pollution Research*, 24 (7): 6819-6832.

Elakkiya, M., Prabhakaran, D. and Thirumarimurugan, M. 2016. Methods of cell immobilization and its applications. *Methods*, 5 (4): 5429-5433.

Elbeshbishy, E., Dhar, B. R., Nakhla, G. and Lee, H.-S. 2017. A critical review on inhibition of dark biohydrogen fermentation. *Renewable and Sustainable Energy Reviews*, 79: 656-668.

Eroglu, E. and Melis, A. 2016. Microalgal hydrogen production research. *International Journal of Hydrogen Energy*, 41 (30): 12772-12798.

Ertugay, N. and Acar, F. N. 2017. Removal of COD and color from Direct Blue 71 azo dye wastewater by Fenton's oxidation: Kinetic study. *Arabian Journal of Chemistry*, 10: S1158-S1163.

Faloye, F. D. 2015. Optimisation of biohydrogen production inoculum development via hybrid pre-treatment techniques: semi pilot scale production assessment on agro waste (potato peels) (Doctoral Thesis).

Fan, K.-S., Kan, N.-r. and Lay, J.-j. 2006. Effect of hydraulic retention time on anaerobic hydrogenesis in CSTR. *Bioresource technology*, 97 (1): 84-89.

Fan, Y., Li, C., Lay, J.-J., Hou, H. and Zhang, G. 2004. Optimization of initial substrate and pH levels for germination of sporing hydrogen-producing anaerobes in cow dung compost. *Bioresource technology*, 91 (2): 189-193.

Fang, H. H. and Liu, H. 2002. Effect of pH on hydrogen production from glucose by a mixed culture. *Bioresource technology*, 82 (1): 87-93.

Farghali, M., Andriamanohiarisoamanana, F. J., Ahmed, M. M., Kotb, S., Yamashiro, T., Iwasaki, M. and Umetsu, K. 2019. Impacts of iron oxide and titanium dioxide nanoparticles on biogas production: Hydrogen sulfide mitigation, process stability, and prospective challenges. *Journal of environmental management*, 240: 160-167.

Farrauto, R. J., Deeba, M. and Alerasool, S. 2019. Gasoline automobile catalysis and its historical journey to cleaner air. *Nature Catalysis*, 2 (7): 603.

Fatima, S., Kumar, A. and Singh, R. K. 2018. Biohydrogen Production: A Potential Energy Resource. *International Journal of Advanced Engineering Science and Technological Research*, 4 (3): 1-10.

Fernandes, B. S., Peixoto, G., Albrecht, F. R., del Aguila, N. K. S. and Zaiat, M. 2010. Potential to produce biohydrogen from various wastewaters. *Energy for Sustainable Development*, 14 (2): 143-148.

Ferreira, T. B., Rego, G. C., Ramos, L. R., Soares, L. A., Sakamoto, I. K., de Oliveira, L. L., Varesche, M. B. A. and Silva, E. L. 2018. Selection of metabolic pathways for continuous hydrogen production under thermophilic and mesophilic temperature conditions in anaerobic fluidized bed reactors. *International Journal of Hydrogen Energy*, 43 (41): 18908-18917.

Foucault, L. J. 2011. Anaerobic Co-digestion of Chicken Processing Wastewater and Crude Glycerol from Biodiesel. Texas A & M University.

Frey, M. 2002. Hydrogenases: hydrogen-activating enzymes. *Biochemistry & Molecular Biology*, 3 (2-3): 153-160.

Frunzo, L., Fermoso, F., Luongo, V., Mattei, M. and Esposito, G. 2019. ADM1-based mechanistic model for the role of trace elements in anaerobic digestion processes. *Journal of environmental management*, 241: 587-602.

Gadhamshetty, V., Johnson, D. C., Nirmalakhandan, N., Smith, G. B. and Deng, S. 2015. Feasibility of biohydrogen production at low temperatures in unbuffered reactors. *International Journal of Hydrogen Energy*, 34 (3): 1233-1243.

Gadhe, A., Sonawane, S. S. and Varma, M. N. 2014. Kinetic analysis of biohydrogen production from complex dairy wastewater under optimized condition. *international journal of hydrogen energy*, 39 (3): 1306-1314.

Gadhe, A., Sonawane, S. S. and Varma, M. N. 2015. Enhancement effect of hematite and nickel nanoparticles on biohydrogen production from dairy wastewater. *International Journal of Hydrogen Energy*, 40 (13): 4502-4511.

Gadhe, J. B. and Gupta, R. B. 2007. Hydrogen production by methanol reforming in supercritical water: catalysis by in-situ-generated copper nanoparticles. *International Journal of Hydrogen Energy*, 32 (13): 2374-2381.

GE, P. 2005. *Box, WG Hunter, and JS Hunter. Statistics for Experimenters II*: Wiley, New York.

Ghimire, A., Frunzo, L., Pirozzi, F., Trably, E., Escudie, R., Lens, P. N. and Esposito, G. 2015. A review on dark fermentative biohydrogen production from organic biomass: process parameters and use of by-products. *Applied Energy*, 144: 73-95.

Ghimire, A., Trably, E., Frunzo, L., Pirozzi, F., Lens, P. N., Esposito, G., Cazier, E. A. and Escudié, R. 2018. Effect of total solids content on biohydrogen production and lactic acid accumulation during dark fermentation of organic waste biomass. *Bioresource technology*, 248: 180-186.

Ginkel, S. V., Sung, S. and Lay, J.-J. 2001. Biohydrogen production as a function of pH and substrate concentration. *Environmental science & technology*, 35 (24): 4726-4730.

Giovannini, G., Donoso-Bravo, A., Jeison, D., Chamy, R., Ruíz-Filippi, G. and Wouwer, A. V. 2016. A review of the role of hydrogen in past and current modelling approaches to anaerobic digestion processes. *International Journal of Hydrogen Energy*, 41 (39): 17713-17722.

Gluck, S. J., Phan, K. and Patnode, C. 2018. A solution for onsite treatment of low flow, high BOD brewery wastewater. *Proceedings of the Water Environment Federation*, 2018 (13): 2282-2294.

Gokfiliz-Yildiz, P. and Karapinar, I. 2018. Optimization of particle number, substrate concentration and temperature of batch immobilized reactor system for biohydrogen production by dark fermentation. *International Journal of Hydrogen Energy*, 43 (23): 10655-10665.

Gorecka, E. and Jastrzębska, M. 2011. Immobilization techniques and biopolymer carriers. *Biotechnology and Food Science*, 75 (1): 65-86.

Guo, X. M., Trably, E., Latrille, E., Carrere, H. and Steyer, J.-P. 2010. Hydrogen production from agricultural waste by dark fermentation: a review. *International Journal of Hydrogen Energy*, 35 (19): 10660-10673.

Gupta, R., Basile, A. and Veziroglu, T. N. 2016. *Compendium of hydrogen energy: hydrogen storage, distribution and infrastructure*. Woodhead Publishing.

Guth, R. M., Storey, P. E., Vitale, M., Markan-Aurora, S., Gordon, R., Prevost, T. Q., Dunagan, W. C. and Woeltje, K. F. 2016. Decision analysis for metric selection on a clinical quality scorecard. *American Journal of Medical Quality*, 31 (5): 400-407.

Gutterer, B., Ulrich, A. and Reuter, S. 2009. *Decentralised wastewater treatment systems (DEWATS) and sanitation in developing countries: a practical guide*. BORDA.

Hafez, H., Nakhla, G. and El Naggar, H. 2010. Waste-to-energy using a novel integrated biological process. In: Proceedings of *Fourteenth International Water Technology Conference*.

Hallenbeck, P. 2005. Fundamentals of the fermentative production of hydrogen. *Water Science and Technology*, 52 (1-2): 21-29.

Hallenbeck, P. C. 2015. Fermentative hydrogen production: principles, progress, and prognosis. *International Journal of Hydrogen Energy*, 34 (17): 7379-7389.

Hallenbeck, P. C. and Benemann, J. R. 2002. Biological hydrogen production; fundamentals and limiting processes. *International Journal of Hydrogen Energy*, 27 (11): 1185-1193.

Hamawand, I. 2015. Anaerobic digestion process and bio-energy in meat industry: A review and a potential. *Renewable and Sustainable Energy Reviews*, 44: 37-51.

Han, H., Cui, M., Wei, L., Yang, H. and Shen, J. 2011. Enhancement effect of hematite nanoparticles on fermentative hydrogen production. *Bioresource technology*, 102 (17): 7903-7909.

Han, J., Lee, D., Cho, J., Lee, J. and Kim, S. 2012. Hydrogen production from biodiesel byproduct by immobilized Enterobacter aerogenes. *Bioprocess and Biosystems Engineering*, 35 (1-2): 151-157.

Han, S.-K., Kim, S.-H. and Shin, H.-S. 2005. UASB treatment of wastewater with VFA and alcohol generated during hydrogen fermentation of food waste. *Process Biochemistry*, 40 (8): 2897-2905.

Han, S.-K. and Shin, H.-S. 2004. Performance of an innovative two-stage process converting food waste to hydrogen and methane. *Journal of the Air & Waste Management Association*, 54 (2): 242-249.

Han, W., Liu, Z., Fang, J., Huang, J., Zhao, H. and Li, Y. 2016. Techno-economic analysis of dark fermentative hydrogen production from molasses in a continuous mixed immobilized sludge reactor. *Journal of Cleaner Production*, 127: 567-572.

Hawkes, F. R., Hussy, I., Kyazze, G., Dinsdale, R. and Hawkes, D. L. 2007. Continuous dark fermentative hydrogen production by mesophilic microflora: principles and progress. *International Journal of Hydrogen Energy*, 32 (2): 172-184.

He, Y., Chen, Z. J. and Evans, A. C. 2007. Small-world anatomical networks in the human brain revealed by cortical thickness from MRI. *Cerebral Cortex*, 17 (10): 2407-2419.

Hitit, Z. Y., Lazaro, C. Z. and Hallenbeck, P. C. 2017. Hydrogen production by co-cultures of Clostridium butyricum and Rhodospeudomonas palustris: Optimization of yield using response surface methodology. *International Journal of Hydrogen Energy*, 42 (10): 6578-6589.

Hoffmann, P. 2019. *The forever fuel: the story of hydrogen*. 3 ed. Routledge.

Hou, L., Li, K., Ding, Y., Li, Y., Chen, J., Wu, X. and Li, X. 2012. Removal of silver nanoparticles in simulated wastewater treatment processes and its impact on COD and NH_4 reduction. *Chemosphere*, 87 (3): 248-252.

Hsu, A.-F., Jones, K. C., Foglia, T. A. and Marmer, W. N. 2004. Continuous production of ethyl esters of grease using an immobilized lipase. *Journal of the American Oil Chemists' Society*, 81 (8): 749-752.

Hu, S., Guan, Y., Wang, Y. and Han, H. 2011. Nano-magnetic catalyst KF/CaO–Fe3O4 for biodiesel production. *Applied Energy*, 88 (8): 2685-2690.

Huajun, F., Lifang, H., Dan, S., Chengran, F., Yonghua, H. and Dongsheng, S. 2008. Effects of operational factors on soluble microbial products in a carrier anaerobic baffled reactor treating dilute wastewater. *Journal of Environmental Sciences*, 20 (6): 690-695.

Huang, Y. and Yang, S. T. 1998. Acetate production from whey lactose using co-immobilized cells of homolactic and homoacetic bacteria in a fibrous-bed bioreactor. *Biotechnology and bioengineering*, 60 (4): 498-507.

Hussy, I., Hawkes, F., Dinsdale, R. and Hawkes, D. 2003. Continuous fermentative hydrogen production from a wheat starch co-product by mixed microflora. *Biotechnology and bioengineering*, 84 (6): 619-626.

Hussy, I., Hawkes, F., Dinsdale, R. and Hawkes, D. 2005. Continuous fermentative hydrogen production from sucrose and sugarbeet. *International Journal of Hydrogen Energy*, 30 (5): 471-483.

Hwang, M. H., Jang, N. J., Hyun, S. H. and Kim, I. S. 2004. Anaerobic bio-hydrogen production from ethanol fermentation: the role of pH. *Journal of Biotechnology*, 111 (3): 297-309.

Jha, P., Kana, E. and Schmidt, S. 2017. Can artificial neural network and response surface methodology reliably predict hydrogen production and COD removal in an UASB bioreactor? *International Journal of Hydrogen Energy*, 42 (30): 18875-18883.

Jia, X., Li, M., Zhu, J., Jiang, Y., Wang, Y. and Wang, Y. 2019. Enhancement split-phase hydrogen production from food waste during dark fermentation: Protein substances degradation and transformation during hydrothermal pre-treatments. *International Journal of Hydrogen Energy*, 44 (32): 17334-17345.

Jimenez, J., Latrille, E., Harmand, J., Robles, A., Ferrer, J., Gaida, D., Wolf, C., Mairet, F., Bernard, O. and Alcaraz-Gonzalez, V. 2015. Instrumentation and control of anaerobic digestion processes: a review and some research challenges. *Reviews in Environmental Science and Bio/Technology*, 14 (4): 615-648.

Jirka, A. M. and Carter, M. J. 1975. Micro semiautomated analysis of surface and waste waters for chemical oxygen demand. *Analytical chemistry*, 47 (8): 1397-1402.

Jouanneau, S., Recoules, L., Durand, M., Boukabache, A., Picot, V., Primault, Y., Lakel, A., Sengelin, M., Barillon, B. and Thouand, G. 2014. Methods for assessing biochemical oxygen demand (BOD): A review. *Water Research*, 49: 62-82.

Kaminari, N., Ponte, M., Ponte, H. and Neto, A. 2005. Study of the operational parameters involved in designing a particle bed reactor for the removal of lead from industrial wastewater—central composite design methodology. *Chemical Engineering Journal*, 105 (3): 111-115.

Kan, T. and Strezov, V. 2018. 13 Hydrogen Production. *Renewable Energy Systems from Biomass: Efficiency, Innovation and Sustainability*: 207.

Kapdan, I. K. and Kargi, F. 2006. Bio-hydrogen production from waste materials. *Enzyme and Microbial Technology*, 38 (5): 569-582.

Kapdan, I. K., Kargi, F., Oztekin, R. and Argun, H. 2009. Bio-hydrogen production from acid hydrolyzed wheat starch by photo-fermentation using different Rhodobacter sp. *International Journal of Hydrogen Energy*, 34 (5): 2201-2207.

Karadag, D. and Puhakka, J. A. 2010. Effect of changing temperature on anaerobic hydrogen production and microbial community composition in an open-mixed culture bioreactor. *International Journal of Hydrogen Energy*, 35 (20): 10954-10959.

Karapinar, I., Yildiz, P. G., Pamuk, R. T. and Gorgec, F. K. 2019. The effect of hydraulic retention time on thermophilic dark fermentative biohydrogen production in the continuously operated packed bed bioreactor. *International Journal of Hydrogen Energy*, 45 (5): 3524-3531.

Katz, B. G. 2019. Nitrate contamination in karst groundwater. In: *Encyclopedia of Caves*. Elsevier, 756-760.

Kayahan, E., Eroglu, I. and Koku, H. 2017. A compact tubular photobioreactor for outdoor hydrogen production from molasses. *International Journal of Hydrogen Energy*, 42 (4): 2575-2582.

Ke, S., Shi, Z. and Fang, H. H. 2005. Applications of two-phase anaerobic degradation in industrial wastewater treatment. *International journal of environment and pollution*, 23 (1): 65-80.

Kepner, C. H. and Tregoe, B. B. 1976. *The rational manager; a systematic approach to problem solving and decision making*. Princeton, New Jersey: Princeton Research Press.

Khanal, S. K., Chen, W.-H., Li, L. and Sung, S. 2004. Biological hydrogen production: effects of pH and intermediate products. *International Journal of Hydrogen Energy*, 29 (11): 1123-1131.

Khongkliang, P., Kongjan, P., Utarapichat, B., Reungsang, A. and Sompong, O. 2017. Continuous hydrogen production from cassava starch processing wastewater by two-stage thermophilic dark fermentation and microbial electrolysis. *International Journal of Hydrogen Energy*, 42 (45): 27584-27592.

Kim, D.-H., Han, S.-K., Kim, S.-H. and Shin, H.-S. 2006. Effect of gas sparging on continuous fermentative hydrogen production. *International Journal of Hydrogen Energy*, 31 (15): 2158-2169.

Kim, K.-Y., Yang, W. and Logan, B. E. 2018. Regenerable nickel-functionalized activated carbon cathodes enhanced by metal adsorption to improve hydrogen production in microbial electrolysis cells. *Environmental science & technology*, 52 (12): 7131-7137.

Kim, M. and Cui, F. 2017. A simplified stoichiometric kinetic model for estimating the concentration of reaction products in anaerobic digestion. *Environmental technology*, 38 (20): 2573-2580.

Kirli, B. and Karapinar, I. 2018. The effect of HRT on biohydrogen production from acid hydrolyzed waste wheat in a continuously operated packed bed reactor. *International Journal of Hydrogen Energy*, 43 (23): 10678-10685.

Klavsyuk, A., Kolesnikov, S., Smelova, E. and Saletsky, A. 2011. Molecular dynamics simulation of the formation of metal nanocontacts. *Physics of the Solid State*, 53 (11): 2356-2360.

Korbekandi, H., Iravani, S. and Abbasi, S. 2009. Production of nanoparticles using organisms. *Critical Reviews in Biotechnology*, 29 (4): 279-306.

Kotay, S. M. and Das, D. 2008. Biohydrogen as a renewable energy resource—prospects and potentials. *International Journal of Hydrogen Energy*, 33 (1): 258-263.

Kothari, R., Kumar, V., Pathak, V. V., Ahmad, S., Aoyi, O. and Tyagi, V. 2017. A critical review on factors influencing fermentative hydrogen production. *Front Bioscience*, 22: 1195-1220.

Koupaie, E. H., Azizi, A., Lakeh, A. B., Hafez, H. and Elbeshbishy, E. 2019. Comparison of liquid and dewatered digestate as inoculum for anaerobic digestion of organic solid wastes. *Waste management*, 87: 228-236.

Kraemer, J. T. and Bagley, D. M. 2007. Improving the yield from fermentative hydrogen production. *Biotechnology letters*, 29 (5): 685-695.

Kraemer, J. T. and Bagley, D. M. 2008. Optimisation and design of nitrogen-sparged fermentative hydrogen production bioreactors. *International Journal of Hydrogen Energy*, 33 (22): 6558-6565.

Krakat, N., Schmidt, S. and Scherer, P. 2010. Mesophilic fermentation of renewable biomass: does hydraulic retention time regulate methanogen diversity? *Appl. Environ. Microbiol.*, 76 (18): 6322-6326.

Krekeler, C., Ziehr, H. and Klein, J. 1991. Influence of physicochemical bacterial surface properties on adsorption to inorganic porous supports. *Applied Microbiology and Biotechnology*, 35 (4): 484-490.

Krishna, G. G., Kumar, P. and Kumar, P. 2008. Treatment of low strength complex wastewater using an anaerobic baffled reactor (ABR). *Bioresource technology*, 99 (17): 8193-8200.

Krishna, G. G., Kumar, P. and Kumar, P. 2009. Treatment of low-strength soluble wastewater using an anaerobic baffled reactor (ABR). *Journal of environmental management*, 90 (1): 166-176.

Kumar, G., Mathimani, T., Rene, E. R. and Pugazhendhi, A. 2019. Application of nanotechnology in dark fermentation for enhanced biohydrogen production using inorganic nanoparticles. *International Journal of Hydrogen Energy*, 44 (26): 13106-13113.

Kumar, G., Mudhoo, A., Sivagurunathan, P., Nagarajan, D., Ghimire, A., Lay, C.-H., Lin, C.-Y., Lee, D.-J. and Chang, J.-S. 2016a. Recent insights into the cell immobilization technology applied for dark fermentative hydrogen production. *Bioresource technology*, 219: 725-737.

Kumar, G., Shobana, S., Nagarajan, D., Lee, D.-J., Lee, K.-S., Lin, C.-Y., Chen, C.-Y. and Chang, J.-S. 2018. Biomass based hydrogen production by dark fermentation—recent trends and opportunities for greener processes. *Current opinion in biotechnology*, 50: 136-145.

Kumar, G., Zhen, G., Kobayashi, T., Sivagurunathan, P., Kim, S. H. and Xu, K. Q. 2016b. Impact of pH control and heat pre-treatment of seed inoculum in dark H2 fermentation: a feasibility report using mixed microalgae biomass as feedstock. *International Journal of Hydrogen Energy*, 41 (7): 4382-4392.

Kumar, N. and Das, D. 2000. Enhancement of hydrogen production by Enterobacter cloacae IIT-BT 08. *Process Biochemistry*, 35 (6): 589-593.

Kumar, N. and Das, D. 2001. Continuous hydrogen production by immobilized Enterobacter cloacae IIT-BT 08 using lignocellulosic materials as solid matrices. *Enzyme and Microbial Technology*, 29 (4): 280-287.

Kuşçu, Ö. S. and Sponza, D. T. 2006. Treatment efficiencies of a sequential anaerobic baffled reactor (ABR)/completely stirred tank reactor (CSTR) system at increasing p-nitrophenol and COD loading rates. *Process Biochemistry*, 41 (7): 1484-1492.

Lata, D., Chandra, R., Kumar, A. and Misra, A. 2007. Effect of light on generation of hydrogen by Halobacterium halobium NCIM 2852. *International Journal of Hydrogen Energy*, 32 (15): 3293-3300.

Lay, C.-H., Chen, C.-C., Lin, H.-C., Lin, C.-Y., Lee, C.-W. and Lin, C.-Y. 2010. Optimal pH and substrate concentration for fermentative hydrogen production from preserved fruits soaking solution. *J Environ Eng Manag*, 20: 35-41.

Lay, J. J. 2000. Modeling and optimization of anaerobic digested sludge converting starch to hydrogen. *Biotechnology and bioengineering*, 68 (3): 269-278.

Lee, D. Y., Li, Y. Y. and Noike, T. 2010. Influence of solids retention time on continuous H 2 production using membrane bioreactor. *International Journal of Hydrogen Energy*, 35 (1): 52-60.

Lee, H. S., Salerno, M. B. and Rittmann, B. E. 2008. Thermodynamic evaluation on H_2 production in glucose fermentation. *Environmental science & technology*, 42 (7): 2401-2407.

Lee, M. J. and Zinder, S. H. 1988. Hydrogen partial pressures in a thermophilic acetate-oxidizing methanogenic coculture. *Applied and Environmental Microbiology*, 54 (6): 1457-1461.

Lee, Y. J., Miyahara, T. and Noike, T. 2002. Effect of pH on microbial hydrogen fermentation. *Journal of Chemical Technology and Biotechnology*, 77 (6): 694-698.

Leenen, E. J., Dos Santos, V. A., Grolle, K. C., Tramper, J. and Wijffels, R. 1996. Characteristics of and selection criteria for support materials for cell immobilization in wastewater treatment. *Water Research*, 30 (12): 2985-2996.

Levin, D. B., Pitt, L. and Love, M. 2004. Biohydrogen production: prospects and limitations to practical application. *International Journal of Hydrogen Energy*, 29 (2): 173-185.

Li, J., Li, B., Zhu, G., Ren, N., Bo, L. and He, J. 2007. Hydrogen production from diluted molasses by anaerobic hydrogen producing bacteria in an anaerobic baffled reactor (ABR). *International Journal of Hydrogen Energy*, 32 (15): 3274-3283.

Li, S., Nan, J. and Gao, F. 2016. Hydraulic characteristics and performance modeling of a modified anaerobic baffled reactor (MABR). *Chemical Engineering Journal*, 284: 85-92.

Lin, C.-Y., Chang, C.-C. and Hung, C.-H. 2008. Fermentative hydrogen production from starch using natural mixed cultures. *International Journal of Hydrogen Energy*, 33 (10): 2445-2453.

Lin, C.-Y., Lay, C.-H., Sen, B., Chu, C.-Y., Kumar, G., Chen, C.-C. and Chang, J.-S. 2012. Fermentative hydrogen production from wastewaters: a review and prognosis. *International Journal of Hydrogen Energy*, 37 (20): 15632-15642.

Lin, C. and Lay, C. 2012. Carbon/nitrogen-ratio effect on fermentative hydrogen production by mixed microflora. *International Journal of Hydrogen Energy*, 29 (1): 41-45.

Lin, C. Y. and Chang, R. C. 2019. Hydrogen production during the anaerobic acidogenic conversion of glucose. *Journal of Chemical Technology & Biotechnology: International Research in Process, Environmental & Clean Technology*, 74 (6): 498-500.

Lin, C. Y. and Jo, C. H. 2003. Hydrogen production from sucrose using an anaerobic sequencing batch reactor process. *Journal of Chemical Technology & Biotechnology: International Research in Process, Environmental & Clean Technology*, 78 (6): 678-684.

Lin, Y., Wu, S. and Wang, D. 2013. Hydrogen-methane production from pulp & paper sludge and food waste by mesophilic–thermophilic anaerobic co-digestion. *International Journal of Hydrogen Energy*, 38 (35): 15055-15062.

Liu, H. and Chen, Y. 2018. Enhanced methane production from food waste using cysteine to increase biotransformation of l-monosaccharide, volatile fatty acids, and biohydrogen. *Environmental science & technology*, 52 (6): 3777-3785.

Liu, X.-l., Ren, N.-q. and Wan, C.-l. 2007. Hydrodynamic characteristics of a four-compartment periodic anaerobic baffled reactor. *Journal of Environmental Sciences*, 19 (10): 1159-1165.

Logan, B. E., Oh, S.-E., Kim, I. S. and Van Ginkel, S. 2002. Biological hydrogen production measured in batch anaerobic respirometers. *Environmental science & technology*, 36 (11): 2530-2535.

Łukajtis, R., Hołowacz, I., Kucharska, K., Glinka, M., Rybarczyk, P., Przyjazny, A. and Kamiński, M. 2018. Hydrogen production from biomass using dark fermentation. *Renewable and Sustainable Energy Reviews*, 91: 665-694.

Madondo, N. I. 2018. Optimization of anaerobic co-digestion of sewage sludge using bio-chemical substrates (Research). Master, Durban University of Technology.

Magnusson, L., Islam, R., Sparling, R., Levin, D. and Cicek, N. 2008. Direct hydrogen production from cellulosic waste materials with a single-step dark fermentation process. *International Journal of Hydrogen Energy*, 33 (20): 5398-5403.

Majdi, H., Esfahani, J. A. and Mohebbi, M. 2019. Optimization of convective drying by response surface methodology. *Computers and electronics in agriculture*, 156: 574-584.

Mallick, N. 2002. Biotechnological potential of immobilized algae for wastewater N, P and metal removal: a review. *Biometals*, 15 (4): 377-390.

Mamimin, C. and Prasertsan, P. 2011. Effect of temperature and initial pH on biohydrogen production from palm oil mill effluent: long-term evaluation and microbial community analysis. *Electronic Journal of Biotechnology*, 14 (5): 9-9.

Manish, S. and Banerjee, R. 2008. Comparison of biohydrogen production processes. *International Journal of Hydrogen Energy*, 33 (1): 279-286.

Manohar, S., Kim, C. and Karegoudar, T. 2011. Enhanced degradation of naphthalene by immobilization of Pseudomonas sp. strain NGK1 in polyurethane foam. *Applied Microbiology and Biotechnology*, 55 (3): 311-316.

Maran, J. P., Manikandan, S., Priya, B. and Gurumoorthi, P. 2015. Box-Behnken design based multi-response analysis and optimization of supercritical carbon dioxide extraction of bioactive flavonoid compounds from tea (Camellia sinensis L.) leaves. *Journal of Food Science and Technology*, 52 (1): 92-104.

Martins, S. C. S., Martins, C. M., Fiúza, L. M. C. G. and Santaella, S. T. 2013. Immobilization of microbial cells: A promising tool for treatment of toxic pollutants in industrial wastewater. *African Journal of Biotechnology*, 12 (28)

Massanet-Nicolau, J., Guwy, A., Dinsdale, R., Premier, G. and Esteves, S. 2010. Production of hydrogen from sewage biosolids in a continuously fed bioreactor: effect of hydraulic retention time and sparging. *International Journal of Hydrogen Energy*, 35 (2): 469-478.

Masukawa, H., Mochimaru, M. and Sakurai, H. 2002. Hydrogenases and photobiological hydrogen production utilizing nitrogenase system in cyanobacteria. *International Journal of Hydrogen Energy*, 27 (11): 1471-1474.

McCarty, P. 1981. One hundred years of anaerobic digestion, anaerobic digestion. *Elsevier Biomedical*, 34 (28): 123-142.

McCarty, P. L. and Bachmann, A. 1992. *Bioconversion reactor*: Google Patents.

McInerney, M. J. and Gieg, L. M. 2004. An overview of anaerobic metabolism. *Strict and facultatie anaerobes: medical and environmental aspects. Horiz Biosci, Norfolk*, 56: 27-66.

Mehndiratta, P., Jain, A., Singh, G. B., Sharma, S., Srivastava, S., Gupta, S. and Gupta, N. 2015. Magnetite nanoparticle aided immobilization of Pseudomonas sp. GBS. 5 for carbazole degradation. *Journal of Biochemical Technology*, 5 (4): 823-825.

Mengmeng, C., Hong, C., Qingliang, Z., Shirley, S. N. and Jie, R. 2009. Optimal production of polyhydroxyalkanoates (PHA) in activated sludge fed by volatile fatty acids (VFAs) generated from alkaline excess sludge fermentation. *Bioresource technology*, 100 (3): 1399-1405.

Mishra, P., Singh, L., Ab Wahid, Z., Krishnan, S., Rana, S., Islam, M. A., Sakinah, M., Ameen, F. and Syed, A. 2018. Photohydrogen production from dark-fermented palm oil mill effluent (DPOME) and statistical optimization: Renewable substrate for hydrogen. *Journal of Cleaner Production*, 199: 11-17.

Mishra, P., Thakur, S., Singh, L., Ab Wahid, Z. and Sakinah, M. 2016. Enhanced hydrogen production from palm oil mill effluent using two stage sequential dark and photo fermentation. *International Journal of Hydrogen Energy*, 41 (41): 18431-18440.

Miyamoto, K. 1997. *Renewable biological systems for alternative sustainable energy production*. Osaka, Japan: Food & Agriculture Organisation.

Mizuno, O., Dinsdale, R., Hawkes, F. R., Hawkes, D. L. and Noike, T. 2000. Enhancement of hydrogen production from glucose by nitrogen gas sparging. *Bioresource technology*, 73 (1): 59-65.

Mohammadi, M., Younesi, H., Najafpour, G. and Mohamed, A. R. 2012. Sustainable ethanol fermentation from synthesis gas by Clostridium ljungdahlii in a continuous stirred tank bioreactor. *Journal of Chemical Technology and Biotechnology*, 87 (6): 837-843.

Mohammadi, P., Ibrahim, S., Annuar, M. S. M., Khashij, M., Mousavi, S. A. and Zinatizadeh, A. 2017. Optimization of fermentative hydrogen production from palm oil mill effluent in an up-flow anaerobic sludge blanket fixed film bioreactor. *Sustainable Environment Research*, 27 (5): 238-244.

Mohan, S. V., Babu, V. L. and Sarma, P. 2007. Anaerobic biohydrogen production from dairy wastewater treatment in sequencing batch reactor (AnSBR): effect of organic loading rate. *Enzyme and Microbial Technology*, 41 (4): 506-515.

Mohan, S. V., Mohanakrishna, G., Ramanaiah, S. and Sarma, P. 2008. Simultaneous biohydrogen production and wastewater treatment in biofilm configured anaerobic periodic discontinuous batch reactor using distillery wastewater. *International Journal of Hydrogen Energy*, 33 (2): 550-558.

Mohan, S. V. and Reddy, M. V. 2013. Optimization of critical factors to enhance polyhydroxyalkanoates (PHA) synthesis by mixed culture using Taguchi design of experimental methodology. *Bioresource technology*, 128: 409-416.

Montgomery, D. C. 2017. *Design and analysis of experiments*. 9th ed. Arizona State University: John wiley & sons.

Moreno-Garrido, I. 2008. Microalgae immobilization: current techniques and uses. *Bioresource technology*, 99 (10): 3949-3964.

Mrudula, S. and Shyam, N. 2012. Immobilization of Bacillus megaterium MTCC 2444 by Ca-alginate entrapment method for enhanced alkaline protease production. *Brazilian Archives of Biology and Technology*, 55 (1): 135-144.

Mu, H. and Chen, Y. 2011. Long-term effect of ZnO nanoparticles on waste activated sludge anaerobic digestion. *Water Research*, 45 (17): 5612-5620.

Mu, Y., Wang, G. and Yu, H.-Q. 2006. Response surface methodological analysis on biohydrogen production by enriched anaerobic cultures. *Enzyme and Microbial Technology*, 38 (7): 905-913.

Mu, Y., Zheng, X.-J., Yu, H.-Q. and Zhu, R.-F. 2006. Biological hydrogen production by anaerobic sludge at various temperatures. *International Journal of Hydrogen Energy*, 31 (6): 780-785.

Muhialdin, B., Osman, F., Muhamad, R., Che Wan Sapawi, C., Anzian, A., Voon, W. and Hussin, A. 2019. Effects of sugar sources and fermentation time on the properties of tea fungus (kombucha) beverage. *International Food Research Journal*, 26 (2)

Mukherjee, R., Chakraborty, R. and Dutta, A. 2019. Comparison of optimization approaches (response surface methodology and artificial neural network-genetic algorithm) for a novel mixed culture approach in soybean meal fermentation. *Journal of Food Process Engineering*: e13124.

Müller, W.-R., Frommert, I. and Jörg, R. 2004. Standardized methods for anaerobic biodegradability testing. *Re/Views in Environmental Science & Bio/Technology*, 3 (2): 141-158.

Murarka, A., Dharmadi, Y., Yazdani, S. S. and Gonzalez, R. 2008. Fermentative utilization of glycerol by Escherichia coli and its implications for the production of fuels and chemicals. *Applied and Environmental Microbiology*, 74 (4): 1124-1135.

Musa, S. D., Zhonghua, T., Ibrahim, A. O. and Habib, M. 2018. China's energy status: a critical look at fossils and renewable options. *Renewable and Sustainable Energy Reviews*, 81: 2281-2290.

Myers, R. H., Montgomery, D. C. and Anderson-Cook, C. M. 2016. *Response surface methodology: process and product optimization using designed experiments*. John Wiley & Sons.

Nachaiyasit, S. and Stuckey, D. C. 1997. The effect of shock loads on the performance of an anaerobic baffled reactor (ABR). 2. Step and transient hydraulic shocks at constant feed strength. *Water Research*, 31 (11): 2747-2754.

Najafpour, G., Younesi, H. and Mohamed, A. R. 2004. Effect of organic substrate on hydrogen production from synthesis gas using Rhodospirillum rubrum, in batch culture. *Biochemical Engineering Journal*, 21 (2): 123-130.

Nasr, M., Tawfik, A., Ookawara, S., Suzuki, M., Kumari, S. and Bux, F. 2015. Continuous biohydrogen production from starch wastewater via sequential dark-photo fermentation with emphasize on maghemite nanoparticles. *Journal of Industrial and Engineering Chemistry*, 21: 500-506.

Natarajan, U., Suganthi, X. H. and Periyanan, P. 2016. Modeling and multiresponse optimization of quality characteristics for the micro-EDM drilling process. *Transactions of the Indian Institute of Metals*, 69 (9): 1675-1686.

Nath, K. and Das, D. 2011. Modeling and optimization of fermentative hydrogen production. *Bioresource technology*, 102 (18): 8569-8581.

Nath, K. and Das, D. 2014. Improvement of fermentative hydrogen production: various approaches. *Applied Microbiology and Biotechnology*, 65 (5): 520-529.

Nawawi, A., Husaini, M., Arshad, M. R. and Samad, Z. 2011. Optimization of underwater composite enclosure design using response surface methodology. *Indian Journal of Geo-Marine Sciences*, 40 (2): 222-226.

Neal, A. L. 2008. What can be inferred from bacterium–nanoparticle interactions about the potential consequences of environmental exposure to nanoparticles? *Ecotoxicology*, 17 (5): 362.

Ngo, T. A., Nguyen, T. H. and Bui, H. T. V. 2012. Thermophilic fermentative hydrogen production from xylose by Thermotoga neapolitana DSM 4359. *Renewable energy*, 37 (1): 174-179.

Ni, M., Leung, D. Y., Leung, M. K. and Sumathy, K. 2006. An overview of hydrogen production from biomass. *Fuel processing technology*, 87 (5): 461-472.

Niño-Navarro, C., Chairez, I., Christen, P., Canul-Chan, M. and García-Peña, E. 2020. Enhanced hydrogen production by a sequential dark and photo fermentation process: Effects of initial feedstock composition, dilution and microbial population. *Renewable energy*, 147: 924-936.

Niz, M., Etchelet, I., Fuentes, L., Etchebehere, C. and Zaiat, M. 2019. Extreme thermophilic condition: An alternative for long-term biohydrogen production from sugarcane vinasse. *International Journal of Hydrogen Energy*, 44 (41): 22876-22887.

Ntaikou, I., Kourmentza, C., Koutrouli, E., Stamatelatou, K., Zampraka, A., Kornaros, M. and Lyberatos, G. 2009. Exploitation of olive oil mill wastewater for combined biohydrogen and biopolymers production. *Bioresource technology*, 100 (15): 3724-3730.

Nualsri, C., Reungsang, A. and Plangklang, P. 2016. Biochemical hydrogen and methane potential of sugarcane syrup using a two-stage anaerobic fermentation process. *Industrial Crops and Products*, 82: 88-99.

Oh, Y.-K., Kim, Y.-J., Park, J.-Y., Lee, T. H., Kim, M.-S. and Park, S. 2005. Biohydrogen production from carbon monoxide and water byRhodopseudomonas palustris P4. *Biotechnology and Bioprocess Engineering*, 10 (3): 270.

Oliveira, J. V., Duarte, T., Costa, J., Cavaleiro, A. J., Pereira, M. and Alves, M. 2017. A design of experiments to assess methane production from anaerobic co-digestion of sewage sludge with lipid rich waste. In: Proceedings of *AD15-The 15th IWA World Conference on Anaerobic Digestion*. 451-454.

Owusu, P. A. and Asumadu-Sarkodie, S. 2016. A review of renewable energy sources, sustainability issues and climate change mitigation. *Cogent Engineering*, 3 (1): 1167990.

Palomo-Briones, R., Celis, L. B., Méndez-Acosta, H. O., Bernet, N., Trably, E. and Razo-Flores, E. 2019. Enhancement of mass transfer conditions to increase the productivity and efficiency of dark fermentation in continuous reactors. *Fuel*, 254: 115648.

Pandey, A. 2011. *Biofuels: alternative feedstocks and conversion processes*. Academic Press.

Pandu, K. and Joseph, S. 2012. Comparisons and limitations of biohydrogen production processes: a review. *International Journal of Advances in Engineering & Technology*, 2 (1): 342.

Pareek, A., Dom, R., Gupta, J., Chandran, J., Adepu, V. and Borse, P. H. 2020. Insights into renewable hydrogen energy: Recent advances and prospects. *Materials Science for Energy Technologies*, 3: 319-327.

Parihar, R. K., Kushwaha, P., Dwivedi, R. D. and Dangi, D. S. 2017. Production of biohydrogen gas from sewage wastewater by anaerobic fermentation process. *IJCS*, 5 (1): 35-38.

Park, J. and Chang, H. 2000. Microencapsulation of microbial cells. *Biotechnology advances*, 18 (4): 303-319.

Parker, J. S. and Moseley, J. D. 2017. Kepner-Tregoe decision analysis as a tool to aid route selection. Part 1. *Organic Process Research & Development*, 12 (6): 1041-1043.

Parthiban, A., Dhanasekaran, C., Sivaganesan, S. and Sathish, S. 2019. Modeling on surface cut quality of CO2 laser cutting for Austenitic Stainless steel sheet. In: Vijayan V, S. L. ed. Proceedings of *Materials Today: Proceedings on Recent Trends in Nanomaterials for Energy, Environmental and Engineering Applications*. ScienceDirect, 823-827.

Patel, P. and Ayers, K. 2019. Electrolysis for hydrogen production. *MRS Bulletin*, 44 (9): 684-685.

Peinado, R. A., Moreno, J. J., Maestre, O. and Mauricio, J. C. 2005. Use of a novel immobilization yeast system for winemaking. *Biotechnology letters*, 27 (18): 1421-1424.

Penniston, J. and Gueguim Kana, E. B. 2018. Impact of medium pH regulation on biohydrogen production in dark fermentation process using suspended and immobilized microbial cells. *Biotechnology & Biotechnological Equipment*, 32 (1): 204-212.

Pirsaheb, M., Mohamadi, S., Rahmatabadi, S., Hossini, H. and Motteran, F. 2018. Simultaneous wastewater treatment and biogas production using integrated anaerobic baffled reactor granular activated carbon from baker's yeast wastewater. *Environmental technology*, 39 (21): 2724-2735.

Pirsaheb, M., Rostamifar, M., Mansouri, A., Zinatizadeh, A. and Sharafi, K. 2015. Performance of an anaerobic baffled reactor (ABR) treating high strength baker's yeast manufacturing wastewater. *Journal of the Taiwan institute of chemical engineers*, 47: 137-148.

Poddar, P. K. and Sahu, O. 2017. Quality and management of wastewater in sugar industry. *Applied Water Science*, 7 (1): 461-468.

Pradhan, N., Dipasquale, L., d'Ippolito, G., Fontana, A., Panico, A., Lens, P. N., Pirozzi, F. and Esposito, G. 2016. Kinetic modeling of fermentative hydrogen production by Thermotoga neapolitana. *International Journal of Hydrogen Energy*, 41 (9): 4931-4940.

Prajapati, S. K., Kaushik, P., Malik, A. and Vijay, V. K. 2013. Phycoremediation coupled production of algal biomass, harvesting and anaerobic digestion: possibilities and challenges. *Biotechnology advances*, 31 (8): 1408-1425.

Prakasham, R., Brahmaiah, P., Sathish, T. and Rao, K. S. 2009. Fermentative biohydrogen production by mixed anaerobic consortia: impact of glucose to xylose ratio. *International Journal of Hydrogen Energy*, 34 (23): 9354-9361.

Prakasham, R., Rao, C. S., Rao, R. S., Lakshmi, G. S. and Sarma, P. 2007. l-asparaginase production by isolated Staphylococcus sp.–6A: design of experiment considering interaction effect for process parameter optimization. *Journal of Applied Microbiology*, 102 (5): 1382-1391.

Pugazhendhi, A., Shobana, S., Nguyen, D. D., Banu, J. R., Sivagurunathan, P., Chang, S. W., Ponnusamy, V. K. and Kumar, G. 2018. Application of nanotechnology (nanoparticles) in dark fermentative hydrogen production. *International Journal of Hydrogen Energy*,

Rai, A., Mohanty, B. and Bhargava, R. 2016. Supercritical extraction of sunflower oil: A central composite design for extraction variables. *Food chemistry*, 192: 647-659.

Rajhi, H., Puyol, D., Martínez, M. C., Díaz, E. E. and Sanz, J. L. 2016. Vacuum promotes metabolic shifts and increases biogenic hydrogen production in dark fermentation systems. *Frontiers of Environmental Science & Engineering*, 10 (3): 513-521.

Rakić, T., Kasagić-Vujanović, I., Jovanović, M., Jančić-Stojanović, B. and Ivanović, D. 2014. Comparison of Full Factorial Design, Central Composite Design, and Box-Behnken Design in Chromatographic Method Development for the Determination of Fluconazole and Its Impurities. *Analytical Letters*, 47 (8): 1334-1347.

Ramakrishna, S. and Prakasham, R. 1999. Microbial fermentations with immobilized cells. *Current Science*, 77 (1): 87.

Rao, C. S., Sathish, T., Mahalaxmi, M., Laxmi, G. S., Rao, R. S. and Prakasham, R. 2008. Modelling and optimization of fermentation factors for enhancement of alkaline protease production by isolated Bacillus circulans using feed-forward neural network and genetic algorithm. *Journal of Applied Microbiology*, 104 (3): 889-898.

Ravndal, K. T., Opsahl, E., Bagi, A. and Kommedal, R. 2018. Wastewater characterisation by combining size fractionation, chemical composition and biodegradability. *Water Research*, 131: 151-160.

Reardon, E. J. 1995. Anaerobic corrosion of granular iron: Measurement and interpretation of hydrogen evolution rates. *Environmental science & technology*, 29 (12): 2936-2945.

Reddy, K. 2016. Evaluation of biohydrogen production potential of sugarcane bagasse using activated sludge in a dark fermentation process (Full research). Master, Durban University of Technology.

Reddy, K., Nasr, M., Kumari, S., Kumar, S., Gupta, S. K., Enitan, A. M. and Bux, F. 2017. Biohydrogen production from sugarcane bagasse hydrolysate: effects of pH, S/X, Fe 2+, and magnetite nanoparticles. *Environmental Science and Pollution Research*, 24 (9): 8790-8804.

Reddy, L., Wee, Y.-J., Yun, J.-S. and Ryu, H.-W. 2008. Optimization of alkaline protease production by batch culture of Bacillus sp. RKY3 through Plackett–Burman and response surface methodological approaches. *Bioresource technology*, 99 (7): 2242-2249.

Rehm, F. B., Chen, S. and Rehm, B. H. 2018. Bioengineering toward direct production of immobilized enzymes: A paradigm shift in biocatalyst design. *Bioengineered*, 9 (1): 6-11.

Reith, J., Wijffels, R. H. and Barten, H. 2003. *Bio-methane and bio-hydrogen: status and perspectives of biological methane and hydrogen production*. Dutch Biological Hydrogen Foundation.

Ren, N., Guo, W., Liu, B., Cao, G. and Ding, J. 2011. Biological hydrogen production by dark fermentation: challenges and prospects towards scaled-up production. *Current opinion in biotechnology*, 22 (3): 365-370.

Reungsang, A., Zhong, N., Yang, Y., Sittijunda, S., Xia, A. and Liao, Q. 2018. Hydrogen from Photo Fermentation. In: *Bioreactors for Microbial Biomass and Energy Conversion*. Springer, 221-317.

Rittmann, B. E. and McCarty, P. L. 2012. *Environmental biotechnology: principles and applications*. Tata McGraw-Hill Education.

Rohendi, D., Rahmah, D. R., Yulianti, D. H., Amelia, I., Sya'baniah, N. F., Syarif, N. and Rachmat, A. 2018. A Review on Production of Hydrogen from Renewable Sources and Applications for Fuel Cell Vehicles. *International Journal of Sustainable Transportation*, 1 (2): 63-68.

Romão, B. B., Silva, F. T. M., de Barcelos Costa, H. C., do Carmo, T. S., Cardoso, S. L., de Souza Ferreira, J., Batista, F. R. X. and Cardoso, V. L. 2019. Alternative techniques to improve hydrogen production by dark fermentation. *3 Biotech*, 9 (1): 18.

Saady, N. M. C. 2013. Homoacetogenesis during hydrogen production by mixed cultures dark fermentation: unresolved challenge. *International Journal of Hydrogen Energy*, 38 (30): 13172-13191.

Sadati, N., Chinnam, R. B. and Nezhad, M. Z. 2018. Observational data-driven modeling and optimization of manufacturing processes. *Expert Systems with Applications*, 93: 456-464.

Sagir, E., Alipour, S., Elkahlout, K., Koku, H., Gunduz, U., Eroglu, I. and Yucel, M. 2017. Scale-up studies for stable, long-term indoor and outdoor production of hydrogen by immobilized Rhodobacter capsulatus. *International Journal of Hydrogen Energy*, 42 (36): 22743-22755.

Sağır, E., Yucel, M. and Hallenbeck, P. C. 2018. Demonstration and optimization of sequential microaerobic dark-and photo-fermentation biohydrogen production by immobilized Rhodobacter capsulatus JP91. *Bioresource technology*, 250: 43-52.

Sahu, O., Mazumdar, B. and Chaudhari, P. 2019. Electrochemical treatment of sugar industry wastewater: process optimization by response surface methodology. *International journal of environmental science and technology*, 16 (3): 1527-1540.

Santiago, S. G., Trably, E., Latrille, E., Buitrón, G. and Moreno-Andrade, I. 2019. The hydraulic retention time influences the abundance of Enterobacter, Clostridium, and Lactobacillus during the hydrogen production from food waste. *Letters in Applied Microbiology*,

Saratale, G. D., Chen, S.-D., Lo, Y.-C., Saratale, R. G. and Chang, J.-S. 2008. Outlook of biohydrogen production from lignocellulosic feedstock using dark fermentation–a review. *Journal of Scientific and Industrial Research*, 67 (11): 962-979.

Saritpongteeraka, K. and Chaiprapat, S. 2008. Effects of pH adjustment by parawood ash and effluent recycle ratio on the performance of anaerobic baffled reactors treating high sulfate wastewater. *Bioresource technology*, 99 (18): 8987-8994.

Sayedin, F., Kermanshahi-pour, A. and He, Q. S. 2019. Evaluating the potential of a novel anaerobic baffled reactor for anaerobic digestion of thin stillage: Effect of organic loading rate, hydraulic retention time and recycle ratio. *Renewable energy*, 135: 975-983.

Schopf, J. 2014. The fossil record: tracing the roots of the cyanobacterial lineage. *The Ecology of Cyanobacteria*: 13-35.

Seifert, K., Waligorska, M., Wojtowski, M. and Laniecki, M. 2009. Hydrogen generation from glycerol in batch fermentation process. *International Journal of Hydrogen Energy*, 34 (9): 3671-3678.

Sekoai, P. T. and Daramola, M. O. 2018. Effect of metal ions on dark fermentative biohydrogen production using suspended and immobilized cells of mixed bacteria. *Chemical Engineering Communications*, 205 (8): 1011-1022.

Sheu, D.-C., Li, S.-Y., Duan, K.-J. and Chen, C. W. 1998. Production of galactooligosaccharides by β-galactosidase immobilized on glutaraldehyde-treated chitosan beads. *Biotechnology Techniques*, 12 (4): 273-276.

Shin, H.-S., Youn, J.-H. and Kim, S.-H. 2004. Hydrogen production from food waste in anaerobic mesophilic and thermophilic acidogenesis. *International Journal of Hydrogen Energy*, 29 (13): 1355-1363.

Singh, L. and Wahid, Z. A. 2015. Enhancement of hydrogen production from palm oil mill effluent via cell immobilisation technique. *International Journal of Energy Research*, 39 (2): 215-222.

Singh, S. K. and Jayswal, S. 2018. Modeling and optimization of EDM Process Parameters on Machining of Inconel 686 using RSM. *International Journal of Applied Engineering Research*, 13 (11): 9335-9344.

Soccol, C. R., Brar, S. K., Faulds, C. and Ramos, L. P. 2016. *Green Fuels Technology*. Switzerland: Springer.

Solé, J., Caminal, G., Schürmann, M., Álvaro, G. and Guillén, M. 2019. Co-immobilization of P450 BM3 and glucose dehydrogenase on different supports for application as a self-sufficient oxidative biocatalyst. *Journal of Chemical Technology & Biotechnology*, 94 (1): 244-255.

Sołowski, G. 2018. Biohydrogen Production-Sources and Methods: A Review. *International Journal of Bioprocess & Biotechnological Advancements*,

Song, X., Zhao, Y., Wu, W., Bi, Y., Cai, Z., Chen, Q., Li, Y. and Hou, S. 2008. PLGA nanoparticles simultaneously loaded with vincristine sulfate and verapamil hydrochloride: systematic study of particle size and drug entrapment efficiency. *International Journal of Pharmaceutics*, 350 (1): 320-329.

Sotiriou, G. A. and Pratsinis, S. E. 2010. Antibacterial activity of nanosilver ions and particles. *Environmental science & technology*, 44 (14): 5649-5654.

Stoimenov, P. K., Klinger, R. L., Marchin, G. L. and Klabunde, K. J. 2002. Metal oxide nanoparticles as bactericidal agents. *Langmuir*, 18 (17): 6679-6686.

Sung, S. 2004. *Bio-hydrogen production from renewable organic wastes*. Golden Field Office, Golden, CO (US).

Taherdanak, M., Zilouei, H. and Karimi, K. 2015. Investigating the effects of iron and nickel nanoparticles on dark hydrogen fermentation from starch using central composite design. *International Journal of Hydrogen Energy*, 40 (38): 12956-12963.

Talabardon, M., Schwitzguébel, J.-P. and Péringer, P. 2000. Anaerobic thermophilic fermentation for acetic acid production from milk permeate. *Journal of Biotechnology*, 76 (1): 83-92.

Tamagnini, P., Axelsson, R., Lindberg, P., Oxelfelt, F., Wünschiers, R. and Lindblad, P. 2002. Hydrogenases and hydrogen metabolism of cyanobacteria. *Microbiology and Molecular Biology Reviews*, 66 (1): 1-20.

Tang, G.-L., Huang, J., Sun, Z.-J., Tang, Q.-q., Yan, C.-h. and Liu, G.-q. 2018. Biohydrogen production from cattle wastewater by enriched anaerobic mixed consortia: influence of fermentation temperature and pH. *Journal of Bioscience and Bioengineering*, 106 (1): 80-87.

Tanisho, S., Kuromoto, M. and Kadokura, N. 1998. Effect of CO 2 removal on hydrogen production by fermentation. *International Journal of Hydrogen Energy*, 23 (7): 559-563.

Teja, A. S. and Koh, P.-Y. 2009. Synthesis, properties, and applications of magnetic iron oxide nanoparticles. *Progress in Crystal Growth and Characterization of Materials*, 55 (1): 22-45.

Temudo, M. F., Kleerebezem, R. and van Loosdrecht, M. 2007. Influence of the pH on (open) mixed culture fermentation of glucose: a chemostat study. *Biotechnology and bioengineering*, 98 (1): 69-79.

Tena, M., Perez, M. and Solera, R. 2019. Effects of several inocula on the biochemical hydrogen potential of sludge-vinasse co-digestion. *Fuel*, 258: 116180.

Thakur, V., Tandon, M. and Jadhav, S. 2017. Optimization of key factors for enhanced fermentative biohydrogen production from water hyacinth by RSM. *Current Science (00113891)*, 113 (4)

Tsygankov, A., Fedorov, A., Kosourov, S. and Rao, K. 2002. Hydrogen production by cyanobacteria in an automated outdoor photobioreactor under aerobic conditions. *Biotechnology and bioengineering*, 80 (7): 777-783.

Tunçay, E. G., Erguder, T. H., Eroğlu, İ. and Gündüz, U. 2017. Dark fermentative hydrogen production from sucrose and molasses. *International Journal of Energy Research*, 41 (13): 1891-1902.

Turhal, S., Turanbaev, M. and Argun, H. 2019. Hydrogen production from melon and watermelon mixture by dark fermentation. *International Journal of Hydrogen Energy*, 44 (34): 18811-18817.

Ueno, Y., Otsuka, S. and Morimoto, M. 1996. Hydrogen production from industrial wastewater by anaerobic microflora in chemostat culture. *Journal of fermentation and bioengineering*, 82 (2): 194-197.

Ulhiza, T. A., Puad, N. I. M. and Azmi, A. S. 2018. Optimization of culture conditions for biohydrogen production from sago wastewater by Enterobacter aerogenes using Response Surface Methodology. *International Journal of Hydrogen Energy*, 43 (49): 22148-22158.

Uyar, B., Eroglu, I., Yücel, M. and Gündüz, U. 2009. Photofermentative hydrogen production from volatile fatty acids present in dark fermentation effluents. *International Journal of Hydrogen Energy*, 34 (10): 4517-4523.

Valdez-Vazquez, I., Ríos-Leal, E., Esparza-García, F., Cecchi, F. and Poggi-Varaldo, H. M. 2005. Semi-continuous solid substrate anaerobic reactors for H_2 production from organic waste: mesophilic versus thermophilic regime. *International Journal of Hydrogen Energy*, 30 (13): 1383-1391.

Van Ginkel, S. W. and Logan, B. 2005. Increased biological hydrogen production with reduced organic loading. *Water Research*, 39 (16): 3819-3826.

Van Ginkel, S. W., Oh, S.-E. and Logan, B. E. 2005. Biohydrogen gas production from food processing and domestic wastewaters. *International Journal of Hydrogen Energy*, 30 (15): 1535-1542.

Van Groenestijn, J., Hazewinkel, J., Nienoord, M. and Bussmann, P. 2002. Energy aspects of biological hydrogen production in high rate bioreactors operated in the thermophilic temperature range. *International Journal of Hydrogen Energy*, 27 (11): 1141-1147.

Van Loosdrecht, M. C., Nielsen, P. H., Lopez-Vazquez, C. M. and Brdjanovic, D. 2016. *Experimental methods in wastewater treatment*. IWA publishing.

Van Niel, E., Budde, M., De Haas, G., Van Der Wal, F., Claassen, P. and Stams, A. 2002. Distinctive properties of high hydrogen producing extreme thermophiles, Caldicellulosiruptor saccharolyticus and Thermotoga elfii. *International Journal of Hydrogen Energy*, 27 (11): 1391-1398.

Veeravalli, S. S., Shanmugam, S. R., Ray, S., Lalman, J. A. and Biswas, N. 2019. Biohydrogen Production From Renewable Resources. In: *Advanced Bioprocessing for Alternative Fuels, Biobased Chemicals, and Bioproducts*. Elsevier, 289-312.

Veljković, V. B., Veličković, A. V., Avramović, J. M. and Stamenković, O. S. 2018. Modeling of biodiesel production: Performance comparison of Box–Behnken, face central composite and full factorial design. *Chinese Journal of Chemical Engineering*,

Verma, A., Bishnoi, N. R. and Gupta, A. 2017. Optimization study for Pb (II) and COD sequestration by consortium of sulphate-reducing bacteria. *Applied Water Science*, 7 (5): 2309-2320.

Verma, M. L., Chaudhary, R., Tsuzuki, T., Barrow, C. J. and Puri, M. 2013. Immobilization of β-glucosidase on a magnetic nanoparticle improves thermostability: application in cellobiose hydrolysis. *Bioresource technology*, 135: 2-6.

Vijayaraghavan, K. and Ahmad, D. 2006. Biohydrogen generation from palm oil mill effluent using anaerobic contact filter. *International Journal of Hydrogen Energy*, 31 (10): 1284-1291.

Vijayaraghavan, K., Mohd, S. and Mohd, A. 2006. Trends in bio-hydrogen generation–A review. *Environmental Sciences*, 3 (4): 255-271.

Vinoth Kanna, I. and Paturu, P. 2018. A study of hydrogen as an alternative fuel. *International Journal of Ambient Energy*: 1-4.

Waligórska, M. 2012. Fermentative hydrogen production-process design and bioreactors. *Chemical and Process Engineering*, 33 (4): 585-594.

Walker, M., Zhang, Y., Heaven, S. and Banks, C. 2009. Potential errors in the quantitative evaluation of biogas production in anaerobic digestion processes. *Bioresource technology*, 100 (24): 6339-6346.

Wang, D., Duan, Y., Yang, Q., Liu, Y., Ni, B.-J., Wang, Q., Zeng, G., Li, X. and Yuan, Z. 2018. Free ammonia enhances dark fermentative hydrogen production from waste activated sludge. *Water Research*, 133: 272-281.

Wang, J. and Wan, W. 2008. Effect of Fe2+ concentration on fermentative hydrogen production by mixed cultures. *International Journal of Hydrogen Energy*, 33 (4): 1215-1220.

Wang, J. and Wan, W. 2009. Factors influencing fermentative hydrogen production: a review. *International Journal of Hydrogen Energy*, 34 (2): 799-811.

Wang, J. and Yin, Y. 2017. Principle and application of different pretreatment methods for enriching hydrogen-producing bacteria from mixed cultures. *International Journal of Hydrogen Energy*, 42 (8): 4804-4823.

Wannapokin, A., Cheng, Y.-T., Wu, S.-Z., Hsieh, P.-H. and Hung, C.-H. 2019. Co-immobilization of Nano-Metal and C. pasteurianum for Dark Fermentation Anaerobic Hydrogen Production. *International Journal of Environmental Science and Development*, 10 (11)

Weiß, S., Somitsch, W., Klymiuk, I., Trajanoski, S. and Guebitz, G. M. 2016. Comparison of biogas sludge and raw crop material as source of hydrolytic cultures for anaerobic digestion. *Bioresource technology*, 207: 244-251.

Whitcomb, P. J. and Anderson, M. J. 2016. *RSM simplified: optimizing processes using response surface methods for design of experiments*. CRC press.

Wu, Z. 2019. Mixed fermentation of Aspergillus niger and Candida shehatae to produce bioethanol with ionic-liquid-pretreated bagasse. *3 Biotech*, 9 (2): 41.

Xiaoxin, Z., Jin, H., Ling, L., Shuming, L., Yueping, W. and Xinheng, Z. 2019. Research on standards and regulations of the operation of wastewater treatment plants. In: Proceedings of *IOP Conference Series: Earth and Environmental Science*. IOP Publishing, 032028.

Xie, S., Hai, F. I., Zhan, X., Guo, W., Ngo, H. H., Price, W. E. and Nghiem, L. D. 2016. Anaerobic co-digestion: A critical review of mathematical modelling for performance optimization. *Bioresource technology*, 222: 498-512.

Xu, S., Liu, H., Fan, Y., Schaller, R., Jiao, J. and Chaplen, F. 2012. Enhanced performance and mechanism study of microbial electrolysis cells using Fe nanoparticle-decorated anodes. *Applied Microbiology and Biotechnology*, 93 (2): 871-880.

Yang, B., Xu, H., Wang, J., Yan, D., Zhong, Q. and Yu, H. 2018a. Performance evaluation of anaerobic baffled reactor (ABR) for treating alkali-decrement wastewater of polyester fabrics at incremental organic loading rates. *Water Science and Technology*, 77 (10): 2445-2453.

Yang, B., Xu, H., Yang, S., Bi, S., Li, F., Shen, C., Ma, C., Tian, Q., Liu, J. and Song, X. 2018b. Treatment of industrial dyeing wastewater with a pilot-scale strengthened circulation anaerobic reactor. *Bioresource technology*, 264: 154-162.

Yang, H., Guo, L. and Liu, F. 2010. Enhanced bio-hydrogen production from corncob by a two-step process: dark-and photo-fermentation. *Bioresource technology*, 101 (6): 2049-2052.

Ye, N. F., Lü, F., Shao, L. M., Godon, J. J. and He, P. J. 2007. Bacterial community dynamics and product distribution during pH-adjusted fermentation of vegetable wastes. *Journal of applied microbiology*, 103 (4): 1055-1065.

Yokoi, H., Mori, S., Hirose, J., Hayashi, S. and Takasaki, Y. 1998. H_2 production from starch by a mixed culture of Clostridium butyricum and Rhodobacter sp. M [h] 19. *Biotechnology letters*, 20 (9): 895-899.

Yu, H., Hu, Z. and Hong, T. 2003. Hydrogen production from rice winery wastewater by using a continuously-stirred reactor. *Journal of chemical engineering of Japan*, 36 (10): 1147-1151.

Yu, H., Zhu, Z., Hu, W. and Zhang, H. 2002. Hydrogen production from rice winery wastewater in an upflow anaerobic reactor by using mixed anaerobic cultures. *International Journal of Hydrogen Energy*, 27 (11): 1359-1365.

Zainal, B. S., Zinatizadeh, A. A., Chyuan, O. H., Mohd, N. S. and Ibrahim, S. 2018. Effects of process, operational and environmental variables on biohydrogen production using palm oil mill effluent (POME). *International Journal of Hydrogen Energy*, 43 (23): 10637-10644.

Zhang, J., Fan, C., Zhang, H., Wang, Z., Zhang, J. and Song, M. 2018. Ferric oxide/carbon nanoparticles enhanced bio-hydrogen production from glucose. *International Journal of Hydrogen Energy*, 43 (18): 8729-8738.

Zhang, Q., Wang, Y., Zhang, Z., Lee, D.-J., Zhou, X., Jing, Y., Ge, X., Jiang, D., Hu, J. and He, C. 2017. Photo-fermentative hydrogen production from crop residue: a mini review. *Bioresource technology*, 229: 222-230.

Zhang, T., Jiang, D., Zhang, H., Jing, Y., Tahir, N., Zhang, Y. and Zhang, Q. 2019a. Comparative study on bio-hydrogen production from corn stover: Photo-fermentation, dark-fermentation and dark-photo co-fermentation. *International Journal of Hydrogen Energy*,

Zhang, Y. and Shen, J. 2007. Enhancement effect of gold nanoparticles on biohydrogen production from artificial wastewater. *International Journal of Hydrogen Energy*, 32 (1): 17-23.

Zhang, Y., Zhang, T., Zhang, Z., Tahir, N. and Zhang, Q. 2019b. Biohydrogen production from Humulus scandens by dark fermentation: Potential evaluation and process optimization. *International Journal of Hydrogen Energy*, 45 (6): 3760-3768.

Zhao, C., Zhang, N., Zheng, H., Zhu, Q., Utsumi, M. and Yang, Y. 2019. Effective and long-term continuous bio-hydrogen production by optimizing fixed-bed material in the bioreactor. *Process Biochemistry*, 83: 55-63.

Zhao, P., Li, N. and Astruc, D. 2013. State of the art in gold nanoparticle synthesis. *Coordination Chemistry Reviews*, 257 (3): 638-665.

Zhao, Q.-B. and Yu, H.-Q. 2008. Fermentative H2 production in an upflow anaerobic sludge blanket reactor at various pH values. *Bioresource technology*, 99 (5): 1353-1358.

Zhu, G.-F., Li, J.-Z., Wu, P., Jin, H.-Z. and Wang, Z. 2008. The performance and phase separated characteristics of an anaerobic baffled reactor treating soybean protein processing wastewater. *Bioresource technology*, 99 (17): 8027-8033.

Zhu, K., Arnold, W. A., Sakkos, J., Davis, C. W. and Novak, P. J. 2018. Achieving high-rate hydrogen recovery from wastewater using customizable alginate polymer gel matrices encapsulating biomass. *Environmental Science: Water Research & Technology*, 4 (11): 1867-1876.

Zhu, Y. and Yang, S.-T. 2004. Effect of pH on metabolic pathway shift in fermentation of xylose by Clostridium tyrobutyricum. *Journal of Biotechnology*, 110 (2): 143-157.

Ziara, R. M., Miller, D. N., Subbiah, J. and Dvorak, B. I. 2019. Lactate wastewater dark fermentation: The effect of temperature and initial pH on biohydrogen production and microbial community. *International Journal of Hydrogen Energy*, 44 (2): 661-673.

Zilouei, H. and Taherdanak, M. 2015. Biohydrogen from lignocellulosic wastes. In: *Lignocellulose-based bioproducts*. Springer, 253-288.

Zwietering, M., Jongenburger, I., Rombouts, F. and Van't Riet, K. 1990. Modeling of the bacterial growth curve. *Applied and Environmental Microbiology*, 56 (6): 1875-1881.

APPENDICES

Appendix A: Wastewater Characterisation

A1: Sample calculations for characterisation.

The following are examples and representative of the calculations done to arrive at the average values:

Calculating total solids

$$mg\ total\frac{solids}{L} = \frac{(A-B)X1000\ mg}{sample\ volume, mL} \quad A1$$

Where: *A* = weight of dried residue (at 105℃) + dish, mg, and *B* = weight of dish, mg.

Calculating volatile solids

$$mg\ volatile\ solids = \frac{(A-B)\ X\ 1000}{V} \quad A2$$

Where:

A = weight of dried residue + dish, mg, B = weight of ignited solids (at 550℃), mg

V = volume of the sample used, mL

Calculating total dissolved solids

$$mg\ Total\ dissolvedsolids = \frac{(A-B)\ X\ 1000}{V} \quad A3$$

Where:

A = weight of dried residue + dish, mg, B = weight of dish, mg

V = volume of the sample used, mL

Calculating total suspended solids

$$mg\ Total\ suspended\ solids = \frac{(A - B)\ X\ 1000}{V} \qquad A2$$

Where:

A = weight of filter + dried residue, mg, B = weight of filter, mg

V = volume of the sample used, mL

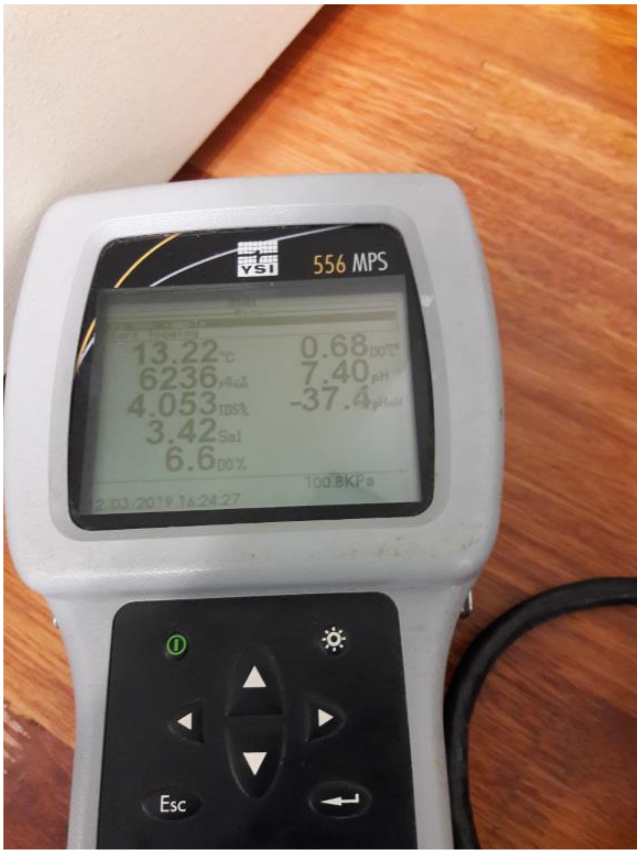

Figure A2: The YSI device measuring physical properties of the wastewater

Table A3: Gallery Automated Photometric Analyser results

Date 11/28/2017 User Dealer
Time 10:43:40PM Software version: 4.1

Sample/ctrl ID	Pat/Ctr/cAl	Test name		Test type	Result	Result unit	Result time	STAT	Status	Errors	Notes	Dilution 1 +	Manual dilution 1 +	Response	Blank
STD COD 0	A	COD >100	P	1.17159 mg/l	1/28/2016 23:43		MA		0		0.01163			0.05963	
STD COD 0	A	COD >100	P	1.17159 mg/l	1/28/2016 23:43		MA		0		0.01163			0.3031	
STD COD 100	A	COD >100	P	100.006 mg/l	1/28/2016 23:43		MA		0		0.04003			0.05963	
STD COD 100	A	COD >100	P	100.006 mg/l	1/28/2016 23:43		MA		0		0.04003			0.7844	
STD COD 250	A	COD >100	P	256.5925	mg/l	1/28/2016 23:43	MA			0		0.08501		0.05963	
STD COD 250	A	COD >100	P	256.5925	mg/l	1/28/2016 23:43	MA			0		0.08501		0.7844	
STD COD 500	A	COD >100	P	486.1348	mg/l	1/28/2016 23:43	MA			0		0.15096		0.05963	
STD COD 500	A	COD >100	P	486.1348	mg/l	1/28/2016 23:43	MA			0		0.15096		0.7844	
STD COD 750	A	COD >100	P	753.2449	mg/l	1/28/2016 23:43	MA			0		0.2277		0.05963	
STD COD 750	A	COD >100	P	753.2449	mg/l	1/28/2016 23:43	MA			0		0.2277		0.7844	
STD COD 1000	A	COD >100	P	1002.85 mg/l	1/28/2016 23:43		MA		0		0.29941			0.05963	
STD COD 1000	A	COD >100	P	1002.85 mg/l	1/28/2016 23:43		MA		0		0.29941			0.7844	
S-PO4-100	A	PHOS 1-25	P	0.43215 mg/l	11/22/2016 20:44		MA			99		0.03418 -0.0009			
S-PO4-100	A	PHOS 1-25	P	0.43215 mg/l	11/22/2016 20:44		MA			99		0.03418 -0.0009		0.20587	
S-PO4-100	A	PHOS 1-25	P	1.00036 mg/l	11/22/2016 20:44		MA			49		0.05508 -0.00103			
S-PO4-100	A	PHOS 1-25	P	1.00036 mg/l	11/22/2016 20:44		MA			49		0.05508 -0.00103			0.20587
NO2-0 A	Nitrite P	0.03497 mg/l		11/22/2016 20:44		MA		0		0.19375	-0.00053				
NO2-0 A	Nitrite P	0.03497 mg/l		11/22/2016 20:44		MA		0		0.19375	-0.00053			0.45818	
S-PO4-100	A	PHOS 1-25	P	2.55272 mg/l	11/22/2016 20:45		MA			19		0.11217 -0.00108			
S-PO4-100	A	PHOS 1-25	P	2.55272 mg/l	11/22/2016 20:45		MA			19		0.11217 -0.00108			0.20587
S-PO4-100	A	PHOS 1-25	P	5.10015 mg/l	11/22/2016 20:45		MA			9		0.20586 -0.00047			
S-PO4-100	A	PHOS 1-25	P	5.10015 mg/l	11/22/2016 20:45		MA			9		0.20586 -0.00047			0.20587
TON-High	A	TON High	P	0.40112 mg/l	11/22/2016 20:46		MA			39		0.16966 0.0001		0.05963	
TON-High	A	TON High	P	0.40112 mg/l	11/22/2016 20:46		MA			39		0.16966 0.0001		0.7844	
TON-High	A	TON High	P	1.14975 mg/l	11/22/2016 20:46		MA			19		0.23944 0.00874		0.05963	
TON-High	A	TON High	P	1.14975 mg/l	11/22/2016 20:46		MA			19		0.23944 0.00874		0.7844	
S-PO4-100	A	PHOS 1-25	P	12.37716	mg/l	11/22/2016 20:47		MA			3		0.47348 -0.0007		
S-PO4-100	A	PHOS 1-25	P	12.37716	mg/l	11/22/2016 20:47		MA			3		0.47348 -0.0007		0.20587
TON-High	A	TON High	P	1.93933 mg/l	11/22/2016 20:47		MA			9		0.31305 -0.00028			0.05963
TON-High	A	TON High	P	1.93933 mg/l	11/22/2016 20:47		MA			9		0.31305 -0.00028			0.7844
S-PO4-100	A	PHOS 1-25	P	25.03746	mg/l	11/22/2016 20:47		MA			1		0.93908 -0.00085		
S-PO4-100	A	PHOS 1-25	P	25.03746	mg/l	11/22/2016 20:47		MA			1		0.93908 -0.00085		0.205
TON-High	A	TON High	P	2.86473 mg/l	11/22/2016 20:47		MA			6		0.39931 -0.00052		0.05963	
TON-High	A	TON High	P	2.86473 mg/l	11/22/2016 20:47		MA			6		0.39931 -0.00052		0.7844	
NO2-STD A	Nitrite P	0.09776 mg/l		11/22/2016 20:48		MA		39		0.3351	-0.00128				
NO2-STD A	Nitrite P	0.09776 mg/l		11/22/2016 20:48		MA		39		0.3351	-0.00128			0.45818	
NH4-High	A	NH4 2-10	P	0.55741 mg/l	11/22/2016 20:48		MA			49		0.28114 0.00134		0.15672	
TON-High	A	TON High	P	4.01176 mg/l	11/22/2016 20:48		MA			4		0.50624 0.00039		0.05963	
TON-High	A	TON High	P	4.01176 mg/l	11/22/2016 20:48		MA			4		0.50624 0.00039		0.7844	
TON-High	A	TON High	P	4.99047 mg/l	11/22/2016 20:48		MA			3		0.59747 -0.0003			
TON-High	A	TON High	P	4.99047 mg/l	11/22/2016 20:48		MA			3		0.59747 -0.0003		0.7844	
NH4-High	A	NH4 2-10	P	1.20972 mg/l	11/22/2016 20:48		MA			9		0.85481 0.00139		0.15672	
NO2-STD A	Nitrite P	0.23423 mg/l		11/22/2016 20:49		MA		19		0.64231	-0.00111				
NO2-STD A	Nitrite P	0.23423 mg/l		11/22/2016 20:49		MA		19		0.64231	-0.00111			0.45818	
NO2-STD A	Nitrite P	0.49737 mg/l		11/22/2016 20:49		MA		9		1.23471	-0.00077				
NO2-STD A	Nitrite P	0.49737 mg/l		11/22/2016 20:49		MA		9		1.23471	-0.00077			0.45818	
NH4-High	A	NH4 2-10	P	1.97848 mg/l	11/22/2016 20:50		MA			4		1.53088 0.00168		0.15672	
NO2-STD A	Nitrite P	0.72208 mg/l		11/22/2016 20:50		MA		6		1.74058	-0.00125				
NO2-STD A	Nitrite P	0.72208 mg/l		11/22/2016 20:50		MA		6		1.74058	-0.00125			0.45818	
SO4-High	A	Sulphate H	P	15.14177	mg/l	11/22/2016 20:50		MA			24		0.13342 -0.00033		
SO4-High	A	Sulphate H	P	15.14177	mg/l	11/22/2016 20:50		MA			24		0.13342 -0.00033		0.303

Table A4: Summary of characterisation of various wastewater streams

Stream	**Sugar**					**Alcohols**					**Dairy**
Parameter	**1**	**2**	**3**	**Average**	**SD**	**1**	**2**	**3**	**Average**	**SD**	**1**
COD	1670.63	1978	1649.37	1766	150	4237.1	4724.7	4721.2	4561	229	10499
BOD	1341.28	1203	1100.72	1215	99	1097	1055	1172	1108	48	2161
TS	2838.28	2721.38	2978.34	2846	105	13723.2	13488.5	15073.3	14095	698	15975
TSS	1753.738	1936.34	1879.332	1856.47	76	8563.23	8995.38	10032.12	9196.91	616	10302.17
TDS	1102.34	932.4	933.85	989.53	80	5320.12	4744.72	4629.43	4898.09	302	6549
VS	2323.35	2754.87	2596.41	2558.21	178	5982.54	5951.06	6837.4	6257	411	3396
pH	3.41	4.01	3.74	3.72	0.25	7.12	8.89	7.36	7.79	0.78	6.52
pH mV	149.4	186.2	175.9	170.5	16	-27.6	-10	-20.3	-19.3	7.22	-78.17
ORP mv	-51	-77	-43	-57	15	-83.1	-103.7	-103.3	-96.7	10	-30.9
DO	0.23	0.54	0.4	0.39	0.13	1.31	1.21	1.23	1.25	0.04	4.66
Conductivity C/ µS/cn	5200	4621	4909	4910	236	698	707	812	739	52	549
Nitrites	0.06	0.06	0.09	0.07	0.01	0.13	0.14	0.18	0.15	0.02	0.04
Nitrates	0.36	0.33	0.33	0.34	0.01	0.46	0.54	0.53	0.51	0.04	0.51
Ammonium	0.42	0.32	0.43	0.39	0.05	0.35	0.48	0.4	0.41	0.05	0.72
TON	0.57	0.51	0.69	0.59	0.07	0.6	0.67	0.71	0.66	0.05	0.37
Phosphate	22.45	24.21	22.97	23.21	0.74	57.67	54.55	49.21	53.81	3.49	0.72
Sulphate	19.71	16.97	18.13	18.27	1.12	49.78	43.87	43.21	45.62	2.95	0.62
Colour				Dark yellow					Beige		

Table A4 continued

Stream	Dairy					Brewery					Yeast				
Parameter	**1**	**2**	**3**	**Average**	**SD**	**1**	**2**	**3**	**Average**	**SD**	**1**	**2**	**3**	**Average**	**SD**
COD	10499	10321	10893	10571	239	6439	6926	6936	6767	232	12231	11973	12627	12277	269
BOD	2161	2018	1743	1974	212	3383	2974	2997	3118	188	4181	4529	4418	4376	145
TS	15975	19425	16335	17245	1896	5291	5938.34	5279.66	5503	308	1043	912	1087	1014	74
TSS	10302.17	11237.4	11382.43	10974	586	3386	3466	3924	3592	237	619	528	632	593	46
TDS	6549	5732	6532	6271	467	2216	1943	1574	1911	263	395	457	411	421	26
VS	3396	3371	3682	3483	173	1992	2298	2277	2189	140	490	401	426	439	37
pH	6.52	7.56	6.98	7.02	1	5.52	5.66	6.13	5.77	0.26	6.36	5.32	6.08	5.92	0
pH mV	-78.17	-132.5	-87.23	-99.3	29	0.67	0.93	0.8	0.8	0.11	46.8	43.4	58.3	49.5	6
ORP mv	-30.9	-30.1	-37.7	-32.9	4	-53.5	-78.6	-65.6	-65.9	10	-115.5	-150.3	-112.5	-126.1	17
DO	4.66	5.76	4.94	5.12	1	0.14	0.26	0.17	0.19	0.05	0.65	0.53	0.68	0.62	0.06
Conductivity C/ µS/cn	549	492	573	538	42	2353	2869	2302	2508	256	13323	12674	13876	13291	491
Nitrites	0.04	0.04	0.07	0.05	0.02	0.04	0.033	0.047	0.04	0.01	0.037	0.025	0.028	0.03	0.01
Nitrates	0.51	0.37	0.41	0.43	0.07	1.23	1.64	1.36	1.41	0.17	0.44	0.41	0.59	0.48	0.08
Ammonium	0.72	0.59	0.82	0.71	0.12	0.82	0.93	0.86	0.87	0.05	0.89	0.65	0.92	0.82	0.12
TON	0.37	0.31	0.46	0.38	0.08	0.49	0.57	0.53	0.53	0.03	0.47	0.37	0.51	0.45	0.06
Phosphate	0.72	0.59	0.61	0.64	0.07	14.21	15.45	16.36	15.34	0.88	1.74	1.42	1.73	1.63	0.15
Sulphate	0.62	0.47	0.62	0.57	0.09	26.02	29.43	29.75	28.4	1.69	4.24	2.98	3.01	3.41	0.59
Colour				Cloudy					Brown					Reddish brown	

Appendix B: Anaerobic baffled reactor design

Various combinations were put in place the volume of interest was picked depending on the resources; the volume was accompanied by the respective dimensions.

Table B1: The Mathematical design for the ABR

V/Litres	D/m	B/m	L/m		L/m	D/m(V=10)	D/m(V=12)	D/m(V=15)	B/m(V=10)	B/m(V=12)	B/m(V=15)
10	0.2	0.08	0.875		0.3	0.3416	0.3742	0.4183	0.1366	0.1497	0.1673
12	0.2	0.08	1.05		0.33	0.3257	0.3568	0.3989	0.1303	0.1427	0.1595
15	0.2	0.08	1.3125		0.36	0.3118	0.3416	0.3819	0.1247	0.1366	0.1528
10	0.25	0.1	0.56		0.39	0.2996	0.3282	0.3669	0.1198	0.1313	0.1468
12	0.25	0.1	0.672		0.42	0.2887	0.3162	0.3536	0.1155	0.1265	0.1414
15	0.25	0.1	0.84		0.45	0.2789	0.3055	0.3416	0.1116	0.1222	0.1366
10	0.3	0.12	0.388889		0.48	0.2700	0.2958	0.3307	0.1080	0.1183	0.1323
12	0.3	0.12	0.466667		0.51	0.2620	0.2870	0.3208	0.1048	0.1148	0.1283
15	0.3	0.12	0.583333		0.54	0.2546	0.2789	0.3118	0.1018	0.1116	0.1247
10	0.35	0.14	0.285714		0.57	0.2478	0.2714	0.3035	0.0991	0.1086	0.1214
12	0.35	0.14	0.342857		0.6	0.2415	0.2646	0.2958	0.0966	0.1058	0.1183
15	0.35	0.14	0.428571		0.63	0.2357	0.2582	0.2887	0.0943	0.1033	0.1155
10	0.4	0.16	0.21875		0.66	0.2303	0.2523	0.2820	0.0921	0.1009	0.1128
12	0.4	0.16	0.2625		0.69	0.2252	0.2467	0.2758	0.0901	0.0987	0.1103
15	0.4	0.16	0.328125		0.72	0.2205	0.2415	0.2700	0.0882	0.0966	0.1080
					0.75	0.2160	0.2366	0.2646	0.0864	0.0947	0.1058
					0.78	0.2118	0.2320	0.2594	0.0847	0.0928	0.1038

B2: Drawings for the ABR design

Specifications of the Reactor

Effective volume of each compartment

140mm * 115.5mm * 210mm = 3 395 700mm^3 = **3.3957 Litres**

Effective reaction volume = 3 * 3.3957 = **10.1871 Litres ≈10L**

The volume of the heating jacket

472 * 123.5 * 20 + 2 (432 * 20 * 200 + 20 * 123.5 * 200) = 5 609 840mm^3

The volume of the heating jacket is approximately **5.61 Litres**

The volume of the headspace/freeboard

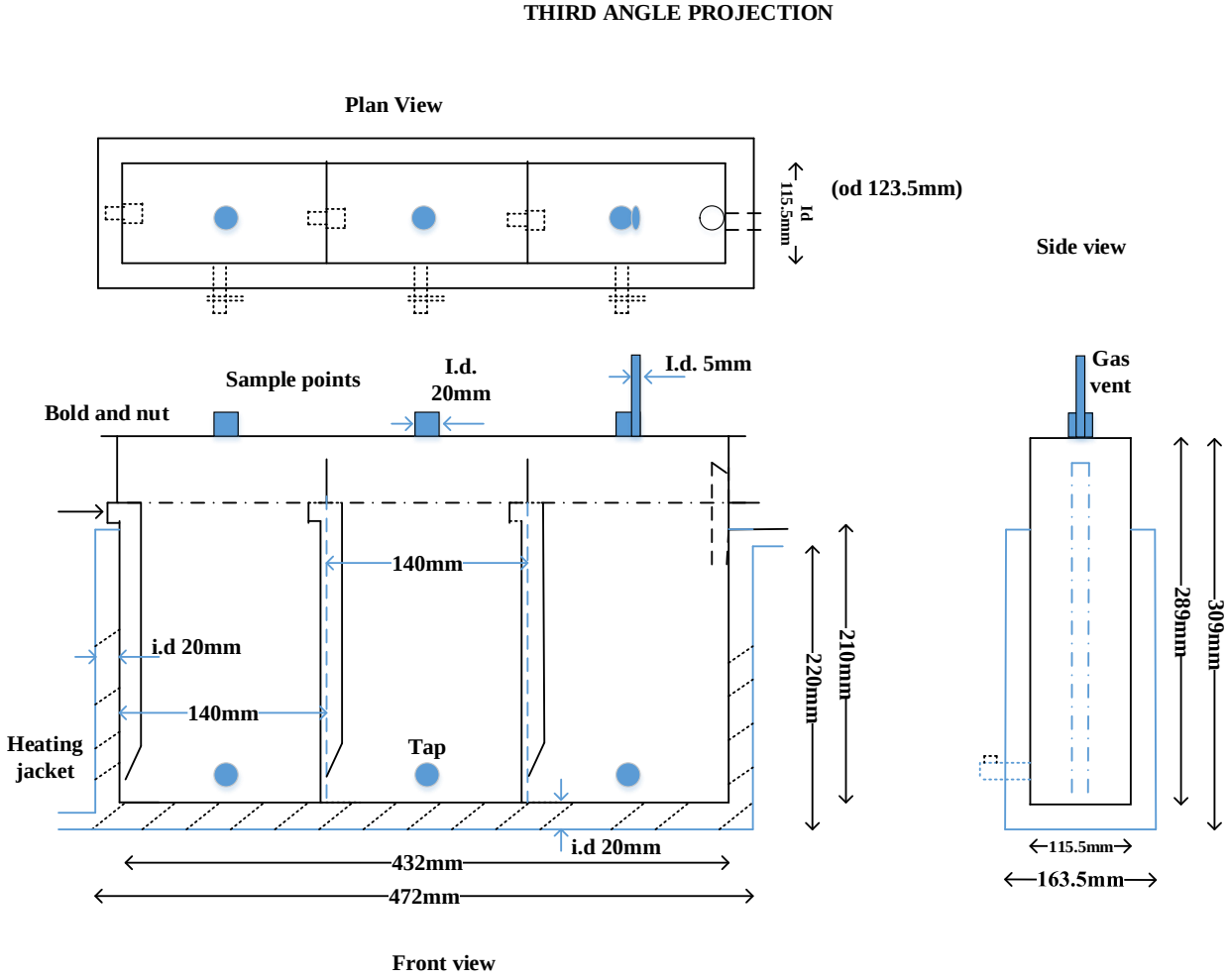

Figure B3 Orthogonal projection of the ABR

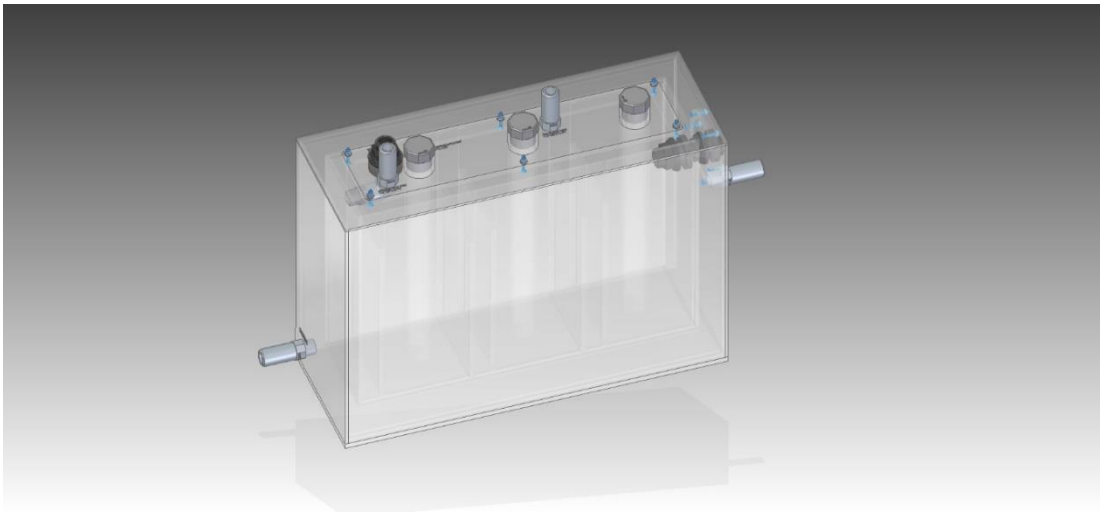

Figure B4: Isometric projection of the ABR

Appendix C: Raw data for optimisation

Table C1: Raw results of the biogas composition and the final COD and pH

Run/STD	BT (h)	Temp (°C	pH in	COD in		COD out		pH out		Biogas (mL)		% H2		% CH4		%CO2		Hydrogen Prod rate (mL/h)		
				1	2	1	2	1	2	1	2	1	2	1	2	1	2	1	2	Average
1	6	33	3.5	5838.67	5838.67	4856.67	4758.50	3.91	3.87	495	460	3.93	3.54	0.00	0.00	96.07	96.46	3.24	2.72	2.98
2	14	33	3.5	5742.22	5742.22	3335.00	3526.67	4.47	4.43	574	591	5.77	5.31	0.00	0.00	94.23	94.69	2.37	2.24	2.30
3	6	37	3.5	5742.22	5742.22	4500.00	4583.33	3.64	3.81	554	531	5.11	4.61	0.00	0.00	94.89	95.39	4.72	4.08	4.40
4	14	37	3.5	5742.22	5742.22	3171.67	3006.67	4.98	5.22	682	667	8.17	7.54	0.00	0.00	91.83	92.46	3.98	3.59	3.79
5	6	33	6.5	5742.22	5742.22	4805.56	4869.44	5.23	5.18	592	585	9.15	8.30	0.00	0.00	90.85	91.70	9.03	8.09	8.56
6	14	33	6.5	5742.22	5742.22	2820.00	2808.00	6.12	6.07	739	746	10.55	10.35	30.13	28.75	59.33	60.90	5.57	5.51	5.54
7	6	37	6.5	5742.22	5742.22	3660.75	3532.50	4.98	5.22	691	672	12.52	11.60	0.00	0.00	87.48	88.40	14.42	12.99	13.70
8	14	37	6.5	5838.67	5838.67	2266.67	2309.17	5.76	6.04	801	787	23.79	22.98	0.00	0.00	76.21	77.02	13.61	12.92	13.26
9	3.3	35	5	5652.78	5652.78	4757.50	4647.50	4.41	4.37	239	264	2.90	2.64	0.00	0.00	97.10	97.36	2.10	2.11	2.11
10	16.7	35	5	5652.78	5652.78	2485.83	2549.17	6.30	6.60	987	1084	12.64	11.51	22.14	21.12	65.22	67.37	7.47	7.47	7.47
11	10	32	5	5838.67	5838.67	3892.50	3757.50	5.23	5.19	747	761	9.10	8.73	0.00	0.00	90.90	91.27	6.79	6.65	6.72
12	10	38	5	5838.67	5838.67	2516.67	2555.00	5.07	5.31	856	840	14.81	13.64	0.00	0.00	85.19	86.36	12.68	11.45	12.07
13	10	35	2.5	5652.78	5652.78	4205.00	4180.83	3.62	3.59	538	521	1.86	1.69	0.00	0.00	98.14	98.31	1.00	0.88	0.94
14	10	35	7.5	5652.78	5652.78	3440.00	3380.00	6.98	7.32	702	673	8.67	7.99	12.41	11.93	78.92	80.08	6.09	5.38	5.73
15	10	35	5	5652.78	5652.78	3220.00	3124.17	5.38	5.33	844	831	21.58	19.48	0.00	0.00	78.42	80.52	18.22	16.19	17.20
16	10	35	5	5652.78	5652.78	3229.17	3395.83	4.91	5.15	837	793	21.40	19.35	0.00	0.00	78.60	80.65	17.91	15.34	16.63
17	10	35	5	5838.67	5838.67	2932.33	2918.40	4.93	4.89	853	867	21.80	20.44	0.00	0.00	78.20	79.56	18.60	17.72	18.16
18	10	35	5	5838.67	5838.67	3120.67	3172.33	4.68	4.90	827	792	19.03	17.86	0.00	0.00	80.97	82.14	15.74	14.15	14.94
19	10	35	5	5652.78	5652.78	3171.67	3043.33	4.89	4.85	860	835	19.23	17.71	0.00	0.00	80.77	82.29	16.54	14.79	15.67
20	10	35	5	5838.67	5838.67	3634.29	3611.43	5.13	5.38	849	851	19.43	18.18	0.00	0.00	80.57	81.82	16.50	15.47	15.99

Table C2: Results showing various conversions of production rates and yields of hydrogen

Run/STD	BT (h)	Temp (°C	pH in	Hydrogen Prod rate (mL/h)			(mL/h)/gC	mL/gCOD/	mL/gCOD	mmol/gC(	L/h/L	mL/L/h
				1	2	Average						
1	6	33	3.5	3.24	2.72	2.98	30.35	17.34	182.09	7.45	0.000284	0.28382
2	14	33	3.5	2.37	2.24	2.30	10.47	13.96	146.53	5.99	0.000219	0.219428
3	6	37	3.5	4.72	4.08	4.40	38.46	21.98	230.76	9.44	0.000419	0.418807
4	14	37	3.5	3.98	3.59	3.79	14.99	19.99	209.88	8.58	0.000361	0.360759
5	6	33	6.5	9.03	8.09	8.56	99.31	56.75	595.89	24.37	0.000815	0.814987
6	14	33	6.5	5.57	5.51	5.54	19.87	26.49	278.16	11.38	0.000528	0.527709
7	6	37	6.5	14.42	12.99	13.70	67.06	38.32	402.39	16.46	0.001305	1.305153
8	14	37	6.5	13.61	12.92	13.26	39.22	52.29	549.08	22.46	0.001263	1.263135
9	3.3	35	5	2.10	2.11	2.11	23.29	7.32	76.87	3.14	0.000201	0.200776
10	16.7	35	5	7.47	7.47	7.47	25.01	39.78	417.71	17.08	0.000711	0.711298
11	10	32	5	6.79	6.65	6.72	35.04	33.37	350.40	14.33	0.000640	0.639989
12	10	38	5	12.68	11.45	12.07	38.36	36.53	383.58	15.69	0.001149	1.14911
13	10	35	2.5	1.00	0.88	0.94	6.78	6.45	67.75	2.77	0.000090	0.089714
14	10	35	7.5	6.09	5.38	5.73	26.83	25.56	268.33	10.97	0.000546	0.54586
15	10	35	5	18.22	16.19	17.20	72.81	69.35	728.15	29.78	0.001638	1.638381
16	10	35	5	17.91	15.34	16.63	74.60	71.05	745.99	30.51	0.001584	1.583517
17	10	35	5	18.60	17.72	18.16	65.44	62.33	654.45	26.76	0.001729	1.729339
18	10	35	5	15.74	14.15	14.94	58.28	55.50	582.78	23.83	0.001423	1.423082
19	10	35	5	16.54	14.79	15.67	64.63	61.55	646.28	26.43	0.001492	1.492038
20	10	35	5	16.50	15.47	15.99	75.75	72.14	757.52	30.98	0.001522	1.52247

Table C3: Raw data for COD and yields base of COD removed

Run/STD	COD in		COD out		Absolute COD removal (mg/L)			pH out	%CO2		Hydrogen Prod rate (		mL/gCOD/L	mL/gCOD	mmol/gCOD
	1	2	1	2	1	2	Average	1	1	2	1	2			
1	5838.67	5838.67	4856.67	4758.50	982.00	1080.17	1031.08	3.91	96.07	96.46	3.24	2.72	17.34	182.09	7.45
2	5742.22	5742.22	3335.00	3526.67	2407.22	2215.56	2311.39	4.47	94.23	94.69	2.37	2.24	13.96	146.53	5.99
3	5742.22	5742.22	4500.00	4583.33	1242.22	1158.89	1200.56	3.64	94.89	95.39	4.72	4.08	21.98	230.76	9.44
4	5742.22	5742.22	3171.67	3006.67	2570.56	2735.56	2653.06	4.98	91.83	92.46	3.98	3.59	19.99	209.88	8.58
5	5742.22	5742.22	4805.56	4869.44	936.67	872.78	904.72	5.23	90.85	91.70	9.03	8.09	56.75	595.89	24.37
6	5742.22	5742.22	2820.00	2808.00	2922.22	2934.22	2928.22	6.12	59.33	60.90	5.57	5.51	26.49	278.16	11.38
7	5742.22	5742.22	3660.75	3532.50	2081.47	2209.72	2145.60	4.98	87.48	88.40	14.42	12.99	38.32	402.39	16.46
8	5838.67	5838.67	2266.67	2309.17	3572.00	3529.50	3550.75	5.76	76.21	77.02	13.61	12.92	52.29	549.08	22.46
9	5652.78	5652.78	4757.50	4647.50	895.28	1005.28	950.28	4.41	97.10	97.36	2.10	2.11	7.32	76.87	3.14
10	5652.78	5652.78	2485.83	2549.17	3166.94	3103.61	3135.28	6.30	65.22	67.37	7.47	7.47	39.78	417.71	17.08
11	5838.67	5838.67	3892.50	3757.50	1946.17	2081.17	2013.67	5.23	90.90	91.27	6.79	6.65	33.37	350.40	14.33
12	5838.67	5838.67	2516.67	2555.00	3322.00	3283.67	3302.83	5.07	85.19	86.36	12.68	11.45	36.53	383.58	15.69
13	5652.78	5652.78	4205.00	4180.83	1447.78	1471.94	1459.86	3.62	98.14	98.31	1.00	0.88	6.45	67.75	2.77
14	5652.78	5652.78	3440.00	3380.00	2212.78	2272.78	2242.78	6.98	78.92	80.08	6.09	5.38	25.56	268.33	10.97
15	5652.78	5652.78	3220.00	3124.17	2432.78	2528.61	2480.69	5.38	78.42	80.52	18.22	16.19	69.35	728.15	29.78
16	5652.78	5652.78	3229.17	3395.83	2423.61	2256.94	2340.28	4.91	78.60	80.65	17.91	15.34	71.05	745.99	30.51
17	5838.67	5838.67	2932.33	2918.40	2906.33	2920.27	2913.30	4.93	78.20	79.56	18.60	17.72	62.33	654.45	26.76
18	5838.67	5838.67	3120.67	3172.33	2718.00	2666.33	2692.17	4.68	80.97	82.14	15.74	14.15	55.50	582.78	23.83
19	5652.78	5652.78	3171.67	3043.33	2481.11	2609.44	2545.28	4.89	80.77	82.29	16.54	14.79	61.55	646.28	26.43
20	5838.67	5838.67	3634.29	3611.43	2204.38	2227.24	2215.81	5.13	80.57	81.82	16.50	15.47	72.14	757.52	30.98

Table C4: COD as measured by the Spectrophotometer as for each reactor effluent.

16R1 means run number 16 in reactor 1

5R2 means run number 5 in reactor 2

	Absorbance(y) vs COD (x) curve		y = 0.0003x - 0.049			R^2 = 0.9815		Dilution factor						
		Absorban	Dilution factc	COD (mg/L)			Absorban	Dilution factor	COD (mg/L)			Absorban	Dilution fa	COD (mg/L)
Raw (S1)	1	0.041	18.5	5550.0	Raw (S2)	1	0.052	17.4	5858.0	Raw (S3)	1	0.061	16.0	5866.7
	2	0.043	18.5	5673.3		2	0.048	17.4	5626.0		2	0.059	16.0	5760.0
	3	0.044	18.5	5735.0		3	0.055	17.4	6032.0		3	0.056	16.0	5600.0
	Average	0.043	18.5	5652.8		Average	0.052	17.4	5838.7		Average	0.059	16.0	5742.2
16R1	1	0.028	12.5	3208.3	20R2	1	0.028	13.7	3520.0	3R2	1	0.031	16.7	4444.4
	2	0.029	12.5	3250.0		2	0.033	13.7	3748.6		2	0.033	16.7	4555.6
	Average	0.029	12.5	3229.2		Average	0.031	13.7	3634.3		Average	0.032	16.7	4500.0
16R4	1	0.032	12.5	3375.0	20R3	1	0.029	13.7	3565.7	3R3	1	0.034	16.7	4611.1
	2	0.033	12.5	3416.7		2	0.031	13.7	3657.1		2	0.033	16.7	4555.6
	Average	0.033	12.5	3395.8		Average	0.030	13.7	3611.4		Average	0.034	16.7	4583.3
19R1	1	0.037	11.0	3153.3	18R2	1	0.027	12.4	3141.3	5R2	1	0.037	16.7	4777.8
	2	0.038	11.0	3190.0		2	0.026	12.4	3100.0		2	0.038	16.7	4833.3
	Average	0.038	11.0	3171.7		Average	0.027	12.4	3120.7		Average	0.038	16.7	4805.6
19R4	1	0.033	11.0	3006.7	18R3	1	0.027	12.4	3120.7	5R3	1	0.038	16.7	4850.0
	2	0.035	11.0	3080.0		2	0.029	12.4	3224.0		2	0.039	16.7	4888.9
	Average	0.034	11.0	3043.3		Average	0.028	12.4	3172.3		Average	0.039	16.7	4869.4
15R1	1	0.042	10.5	3185.0	17R1	1	0.044	9.5	2945.0	7R1	1	0.033	13.5	3681.0
	2	0.044	10.5	3255.0		2	0.043	9.5	2919.7		2	0.032	13.5	3640.5
	Average	0.043	11.0	3220.0		Average	0.044	9.5	2932.3		Average	0.032	13.5	3660.8
15R4	1	0.032	11.5	3105.0	17R4	1	0.042	9.5	2881.7	7R4	1	0.029	13.5	3510.0
	2	0.033	11.5	3143.3		2	0.044	9.5	2955.1		2	0.030	13.5	3555.0
	Average	0.033	11.5	3124.2		Average	0.043	9.5	2918.4		Average	0.030	13.5	3532.5

Table C4 continued

	Absorbance(y) vs COD (x) curve			y = 0.0003x - 0.049		R^2 = 0.9815		Dilution factor						
		Absorban	Dilution factc	COD (mg/L)			Absorban	Dilution factor	COD (mg/L)			Absorban	Dilution fa	COD (mg/L)
10R1	1	0.028	9.5	2438.3	12R2	1	0.026	10.0	2500.0	2R2	1	0.037	11.5	3296.7
	2	0.031	9.5	2533.3		2	0.027	10.0	2533.3		2	0.039	11.5	3373.3
	Average	0.030	9.5	2485.8		Average	0.027	10.0	2516.7		Average	0.038	11.5	3335.0
10R4	1	0.029	9.5	2470.0	12R3	1	0.028	10.0	2566.7	2R3	1	0.043	11.5	3526.7
	2	0.034	9.5	2628.3		2	0.027	10.0	2543.3		2	0.043	11.5	3526.7
	Average	0.032	9.5	2549.2		Average	0.028	10.0	2555.0		Average	0.043	11.5	3526.7
9R1	1	0.037	16.5	4730.0	8R2	1	0.031	8.5	2266.7	4R2	1	0.037	11.0	3153.3
	2	0.038	16.5	4785.0		2	0.031	8.5	2266.7		2	0.038	11.0	3190.0
	Average	0.038	16.5	4757.5		Average	0.031	8.5	2266.7		Average	0.038	11.0	3171.7
9R4	1	0.036	16.5	4675.0	8R3	1	0.034	8.5	2351.7	4R3	1	0.033	11.0	3006.7
	2	0.035	16.5	4620.0		2	0.031	8.5	2266.7		2	0.033	11.0	3006.7
	Average	0.036	16.5	4647.5		Average	0.033	8.5	2309.2		Average	0.033	11.0	3006.7
14R1	1	0.036	12.0	3400.0	1R1	1	0.044	15.5	4805.0	6R1	1	0.047	9.0	2880.0
	2	0.038	12.0	3480.0		2	0.046	15.5	4908.3		2	0.043	9.0	2760.0
	Average	0.037	12.0	3440.0		Average	0.045	15.5	4856.7		Average	0.045	9.0	2820.0
14R4	1	0.037	12.0	3440.0	1R4	1	0.044	15.5	4815.3	6R4	1	0.043	9.0	2766.0
	2	0.034	12.0	3320.0		2	0.042	15.5	4701.7		2	0.046	9.0	2850.0
	Average	0.036	12.0	3380.0		Average	0.043	15.5	4758.5		Average	0.045	9.0	2808.0
13R1	1	0.039	14.5	4253.3	11R2	1	0.038	13.5	3915.0					
	2	0.037	14.5	4156.7		2	0.037	13.5	3870.0					
	Average	0.038	14.5	4205.0		Average	0.038	13.5	3892.5					
13R4	1	0.036	14.5	4108.3	11R3	1	0.034	13.5	3735.0					
	2	0.039	14.5	4253.3		2	0.035	13.5	3780.0					
	Average	0.038	14.5	4180.8		Average	0.035	13.5	3757.5					

Table C5: Volatile solids for every run in the ABR

VS	Brewery vwastewater + seed sludge				
Run	Volume (mL)	C+F (g)	After 105	After 550 (g)	VS (mg/L)
1	10	48.4935	48.5624	48.4814	8100
	10	48.8744	48.9659	48.8803	8560
Average					**8330**
2	10	48.5092	49.5825	49.5098	7270
	10	50.9451	49.9870	49.9171	6990
Average					**7130**
3	10	48.8487	50.0595	49.9946	6490
	10	50.8012	50.9076	50.8414	6620
Average					**6555**
4	10	48.5092	48.9953	48.9236	7170
	10	51.6887	48.9041	48.8314	7270
Average					**7220**
5	10	48.9942	48.6295	48.5564	7310
	10	50.7432	49.0943	49.0164	7790
Average					**7550**
6	10	48.9942	48.9310	48.8537	7730
	10	51.3328	50.6488	50.5695	7930
Average					**7830**
7	10	48.7032	49.0273	48.9560	7130
	10	50.8217	50.7475	50.6748	7270
Average					**7200**
8	10	48.9942	49.5893	49.5162	7310
	10	49.9676	49.3556	49.2817	7390
Average					**7350**
9	10	48.9457	50.7803	50.6905	8980
	10	51.0364	50.1609	50.0736	8730
Average					**8855**
10	10	48.5921	51.3039	51.2260	7790
	10	51.2808	50.7380	50.6581	7990
Average					**7890**

VS	Brewery vwastewater + seed sludge				
Run	Volume (mL)	C+F (g)	After 105	After 550 (g)	VS (mg/L)
11	10	48.5106	48.9978	48.9236	7420
	10	50.9183	49.4448	49.3692	7560
Average					**7490**
12	10	49.9640	49.1005	49.0250	7550
	10	50.9387	49.0145	48.9395	7500
Average					**7525**
13	10	50.2200	48.6339	48.5621	7180
	10	50.9451	49.0190	48.9475	7150
Average					**7165**
14	10	48.5302	48.5915	48.5146	7690
	10	52.5027	49.0200	48.9395	8050
Average					**7870**
15	10	48.9183	48.4993	48.4254	7390
	10	51.9482	48.3181	48.2468	7130
Average					**7260**
16	10	48.7247	48.4436	48.3692	7440
	10	51.9956	48.8517	48.7804	7130
Average					**7285**
17	10	51.4188	48.5614	48.4696	9180
	10	51.3813	49.0347	48.9495	8520
Average					**8850**
18	10	49.4344	49.0454	48.9658	7960
	10	52.4538	48.4789	48.4012	7770
Average					**7865**
19	10	49.9640	51.1424	51.0714	7100
	10	50.9387	50.4117	50.3375	7420
Average					**7260**
20	10	49.9640	46.9328	46.8430	8980
	10	50.9983	48.7695	48.6827	8680
Average					**8830**

Appendix D: Calibration curve for COD determination

Table D1: KHP working concentration and working volumes

Concentration (mgO_2/L)	KHP volume	Distilled water volume	Total volume
100	10ml	90ml	100ml
250	25ml	75ml	100ml
500	50ml	50ml	100ml
750	75ml	25ml	100ml
1000	0.425g ($C_8H_5KO_4$)	500ml	500ml

Table D2: Absorbance values for various KPH concentrations

Concentration	Absorbance			Selected		Average	
	1	2	3				
100	0	0.001	0.026	0	0.001	0.0005	0.000707
250	0.022	0.031	0.02	0.022	0.02	0.021	0.001414
500	0.135	0.101	0.108	0.101	0.108	0.1045	0.00495
750	0.245	0.226	0.225	0.226	0.225	0.2255	0.000707
1000	0.285	0.285	0.285	0.285	0.285	0.285	0

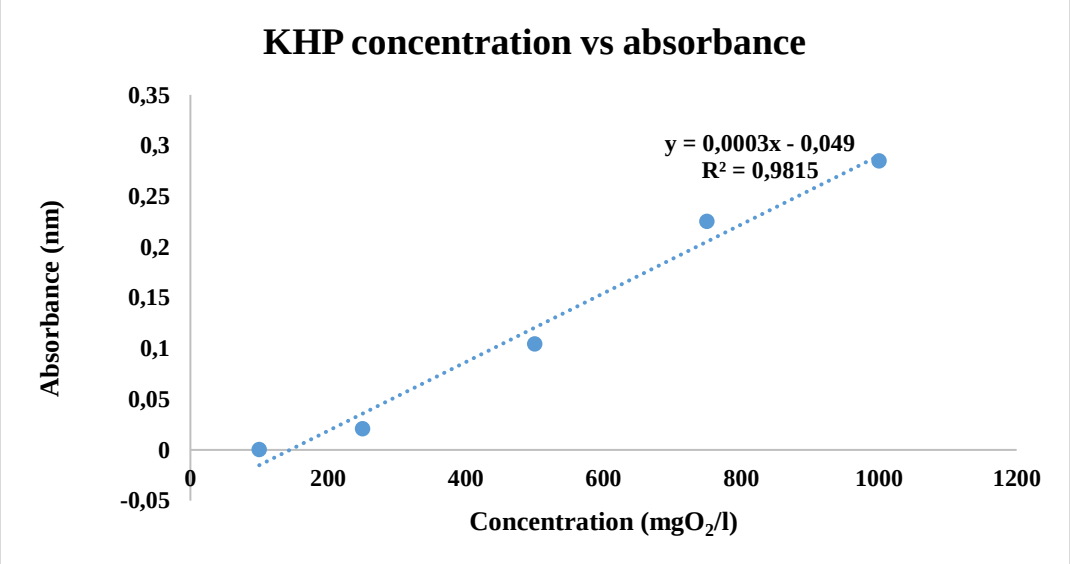

Figure D3: Plot of the KHP concentration with respect to absorbance

Appendix E: Results on nanoparticles system

Table E1: Volumetric and compositional representation of systems with and without magnetite nanoparticles

	nano			no nano			nano			no nano		
	reactor 1			reactor 2			hydrogen %, reactor 1			hydrogen %, reactor 2		
Time	V1	V2	Average	V1	V2	Average	C1	C2	Average	C1	C2	Aver
0	0	0	0	0	0	0	0	0	0	0	0	
1	237	201	219	196	205	200.5	0	0	0	0	0	
2	539	493	516	489	504	496.5	9.87	10.73	10.30	6.74	5.94	
3	617	598	607.5	561	550	555.5	16.87	17.99	17.43	14.46	13.96	
4	707	682	694.5	647	669	658	19.32	20.11	19.72	16.7	15.58	
5	866	842	854	728	741	734.5	22.03	23.21	22.62	16.57	17.93	
6	904	902	903	794	782	788	24.37	23.55	23.96	18.02	19.32	
7	943	913	928	821	813	817	23.69	24.77	24.23	19.56	18.86	
8	951	926	938.5	843	830	836.5	23.14	25.76	24.45	21.23	18.95	
9	951	928	939.5	848	842	845	25.84	24.18	25.01	22.03	20.85	
10	955	928	941.5	850	842	846	24.77	25.85	25.31	22.24	21.18	
10.2	955	928	941.5	852	844	848	25.02	25.72	25.37	22.66	21.04	

	nano	ml/h		no nano		ml/h
	hydrogen production rate, reactor 1			hydrogen production rate, reactor 2		
Time	C1	C2	Average	C1	C2	Average
0	0.00	0.0	0.00	0.00	0.00	0.00
1	0.00	0.0	0.00	0.00	0.00	0.00
2	26.60	26.4	26.52	16.48	14.97	15.72
3	34.70	35.9	35.28	27.04	25.59	26.32
4	34.15	34.3	34.22	27.01	26.06	26.53
5	38.16	39.1	38.62	24.13	26.57	25.35
6	36.72	35.4	36.06	23.85	25.18	24.51
7	31.91	32.3	32.11	22.94	21.90	22.42
8	27.51	29.8	28.66	22.37	19.66	21.02
9	27.30	24.9	26.12	20.76	19.51	20.13
10	23.66	24.0	23.82	18.90	17.83	18.37
10.2	23.43	23.4	23.41	18.93	17.41	18.17

Table E2: COD removal in systems with magnetite and without magnetite nanoparticles

COD						
	1	2	3	Ave		Removal
R 1	2637	2661	2709	2669		2954
R 2	2723	2704	2778	2735	2702	2888
R 3	2897	2942	2957	2932		2691
R 4	2910	2847	2856	2871	2901.5	2752
VFA						
	1	2	3	**Ave**		
R 1	751	763	745	**753**		
R 2	805	814	847	**822**	787.5	
R 3	641	665	644	**650**		
R 4	701	716	701	**706**	678	

Appendix F: Sample of chromatograms

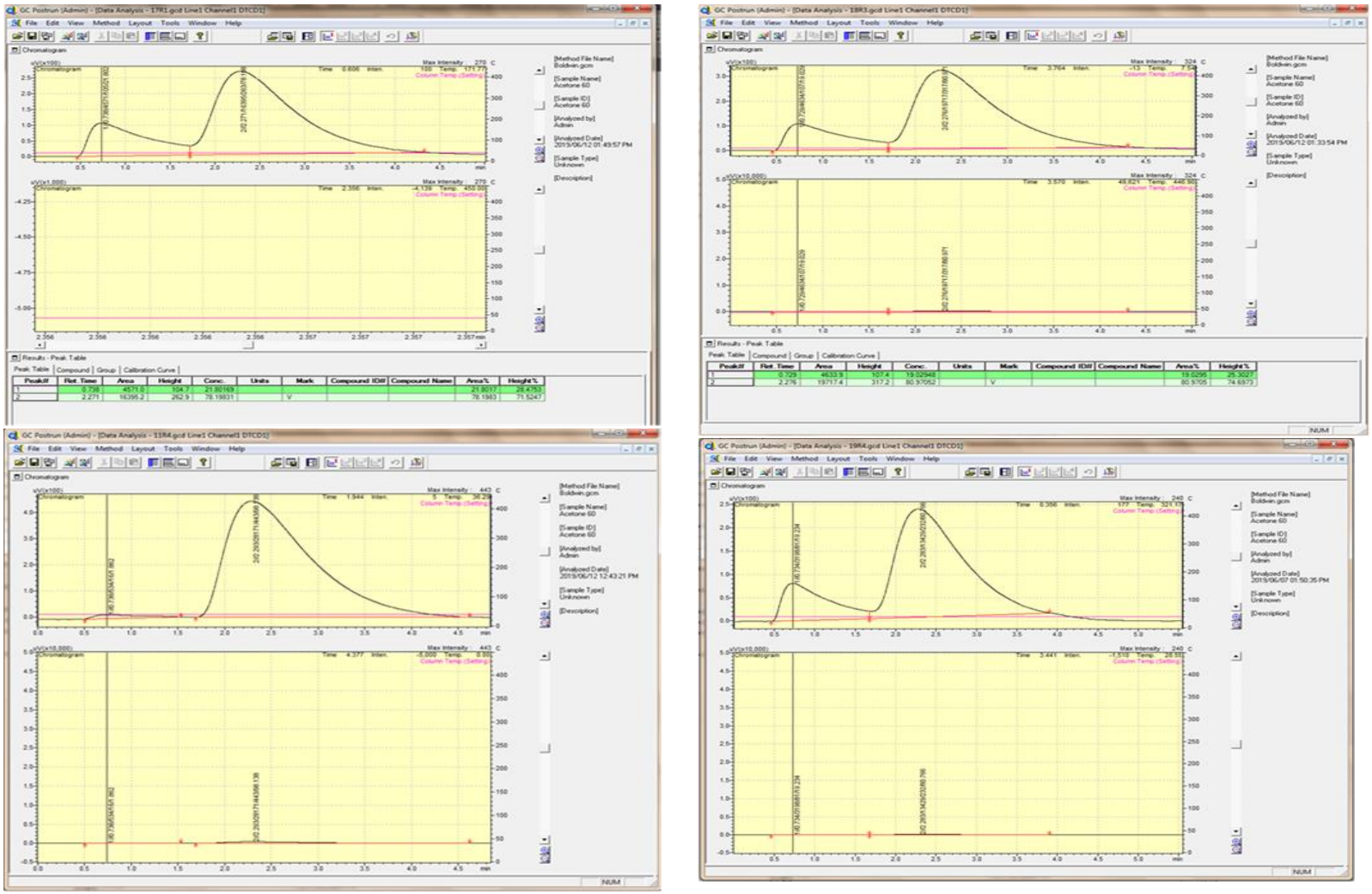

Figure F1: Sample chromatogram

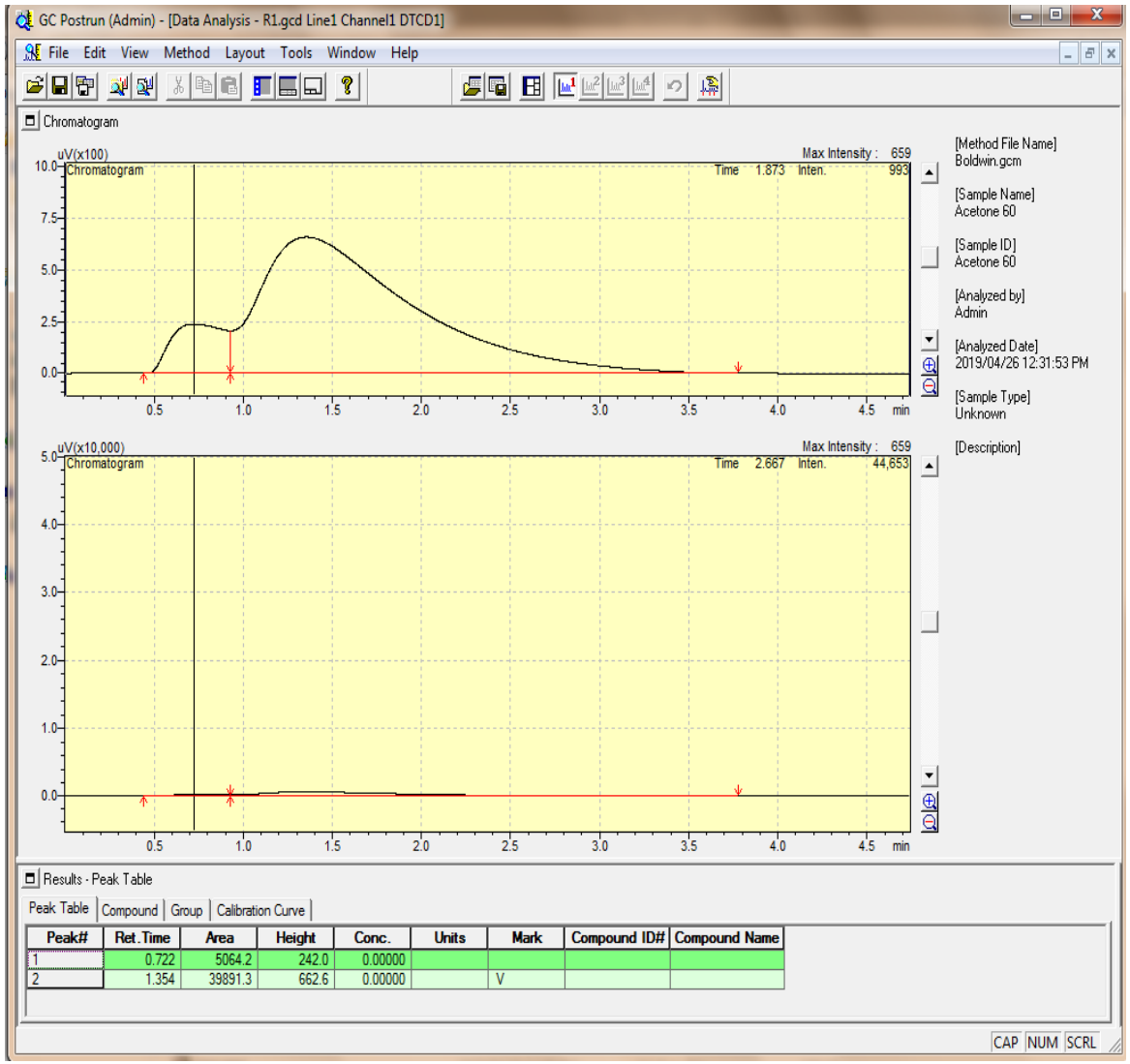

Peak#	Ret.Time	Area	Height	Conc.	Units	Mark	Compound ID#	Compound Name
1	0.722	5064.2	242.0	0.00000				
2	1.354	39891.3	662.6	0.00000		V		

Figure F2: Sample chromatogram

Appendix G: Calibration curve for the GC

Table G1: Different composition of standard gases and the corresponding GC areas

		GC AREAS											
		H2	0.753 MINS			CH4	1.441 MINS			CO2	2.229 MINS		
COMPO	1	2	3	AVERAGE	1	2	3	AVERAGE	1	2	3	AVERAGE
0%	0	0	0	0	0	0	0	0	0	0	0	0
20%	58140.9	57827.6	57734.3	57900.93	45636.3	46102.3	45424.9	45721.17	31919.2	30019.2	32034.6	31324.33
40%	117799.4	117843.2	117861.8	117834.8	78773.2	78427.2	79003.7	78734.7	54812.5	53982.3	55097.9	54630.9
60%	167717.7	166917.5	167298.6	167311.3	108617.5	109063.2	108487.3	108722.7	69776.3	70103.4	69227.5	69702.4
80%	225339.7	226327.3	225873.5	225846.8	122631.7	122237.1	122627.4	122498.7	86617.2	87076.8	86293.6	86662.53
100%	272688.6	273403.5	273056.1	273049.4	165126.1	164454	165778.2	165119.4	97349.7	96248.2	96494.7	96697.53

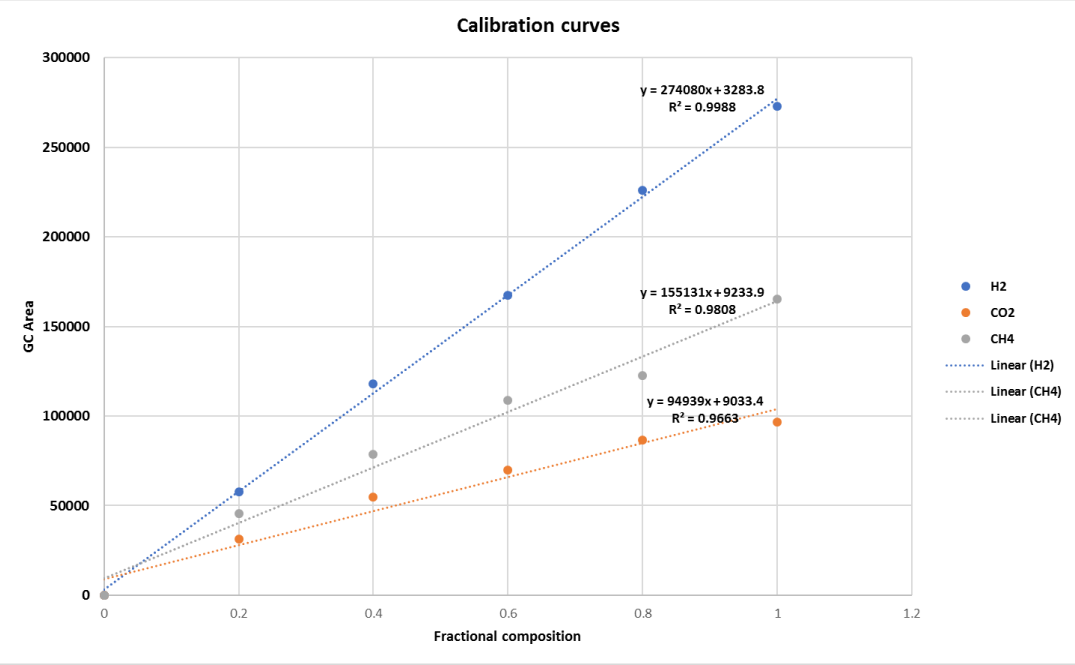

Figure G2: Calibration curve for the GC

Table G3: Areas on GC with respect to the gases composing biogas

	H2				CO2				CH4			
	area	%			area	%			area	%		
Pure	272688.6	100			96494.7	100			165964.7	100		
Run	A	A	B	B	A	A	B	B	A	A	B	B
1	1705.1	3.9	1739.2	3.5	41670.9	96.1	47333.6	96.5	0.0	0.0	0.0	0.0
2	1758.9	5.1	1794.1	4.6	32683.4	94.9	37124.8	95.4	0.0	0.0	0.0	0.0
3	1380.4	9.1	1408.0	8.3	13709.8	90.9	15563.2	91.7	0.0	0.0	0.0	0.0
4	2850.5	12.5	2968.0	11.6	19917.1	87.5	22623.7	88.4	0.0	0.0	0.0	0.0
5	1132.6	5.8	1179.3	5.3	18497.8	94.2	21021.1	94.7	0.0	0.0	0.0	0.0
6	1013.2	8.2	1055.0	7.5	11382.6	91.8	12929.4	92.5	0.0	0.0	0.0	0.0
7	2667.9	10.5	2777.9	10.3	15006.3	59.3	16348.6	60.9	7620.4	30.1	7716.4	28.7
8	7534.5	23.8	7845.2	23.0	24139.9	76.2	26299.2	77.0	0.0	0.0	0.0	0.0
9	1445.4	9.1	1505.0	8.7	14445.1	90.9	15730.5	91.3	0.0	0.0	0.0	0.0
10	3040.1	14.8	3008.0	13.6	17487.5	85.2	19051.7	86.4	0.0	0.0	0.0	0.0
11	534.4	1.9	528.8	1.7	28170.9	98.1	30690.8	98.3	0.0	0.0	0.0	0.0
12	2133.8	8.7	2111.3	8.0	19424.7	78.9	21160.3	80.1	3055.0	12.4	3152.6	11.9
13	1750.9	2.9	1732.4	2.6	58533.2	97.1	63865.3	97.4	0.0	0.0	0.0	0.0
14	4928.0	12.6	4876.0	11.5	25434.2	65.2	28551.0	67.4	8636.1	22.1	8949.2	21.1
15	8812.9	21.6	8720.0	19.5	32018.9	78.4	36039.0	80.5	0.0	0.0	0.0	0.0
16	9000.6	21.4	8905.7	19.4	33065.2	78.6	37117.2	80.6	0.0	0.0	0.0	0.0
17	4571.0	21.8	4727.6	20.4	16395.2	78.2	18404.3	79.6	0.0	0.0	0.0	0.0
18	4633.9	19.0	4792.6	17.9	19717.4	81.0	22037.3	82.1	0.0	0.0	0.0	0.0
19	3198.0	19.2	3307.5	17.7	13429.0	80.8	15363.6	82.3	0.0	0.0	0.0	0.0
20	5143.2	19.4	5319.4	18.2	21323.1	80.6	23936.1	81.8	0.0	0.0	0.0	0.0

Table G4: GC results for the preliminary runs is Schott bottles

		Alcohols				Brewery			
		1	2	3	Average	1	2	3	Average
GC area	H2	18474.5	19632.4	19869.9	19325.6	32565.9	33929.4	31362.3	32619.2
	CH4	0.0	0.0	0.0	0.0	0.0	0.0	0.0	0.0
	CO2	69457.3	72003.4	71482.0	70980.9	48645.8	50682.5	46847.9	48725.4
Retention Time	H2	0.721	0.724	0.724	0.723	0.737	0.768	0.710	0.738
	CH4	1.128	0.000	0.000	0.000	0.000	0.000	0.000	0.000
	CO2	1.836	1.862	1.831	1.843	1.794	1.869	1.728	1.797

		Yeast				Dairy				Sugar			
		1	2	3	Average	1	2	3	Average	1	2	3	Average
GC area	H2	22574.7	22398.7	21925.4	22299.6	27009.6	26447.8	26821.0	26759.5	29709.7	30296.2	28745.2	29583.7
	CH4	0.0	0.0	0.0	0.0	0.0	0.0	0.0	0.0	0.0	0.0	0.0	0.0
	CO2	67364.2	66839.2	65426.8	66543.4	47192.7	46211.0	46863.1	46755.6	60593.4	61789.5	58626.3	60336.4
Retention Time	H2	0.735	0.729	0.714	0.726	0.721	0.706	0.716	0.714	0.722	0.736	0.699	0.719
	CH4	0.000	0.000	0.000	0.000	0.000	0.000	0.000	0.000	0.000	0.000	0.000	0.000
	CO2	1.826	1.812	1.774	1.804	1.850	1.812	1.837	1.833	1.835	1.871	1.775	1.827

Appendix H: DOE plots

Design-Expert® Software

Hydrogen production rate

Color points by value of
Hydrogen production rate:
0.94 18.16

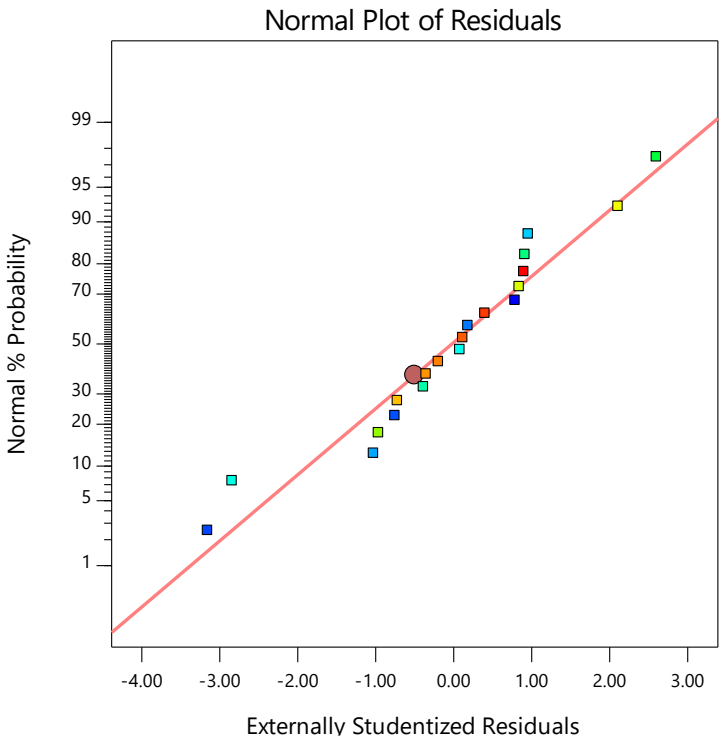

Figure H1: Normal Plot of residuals for the HPR

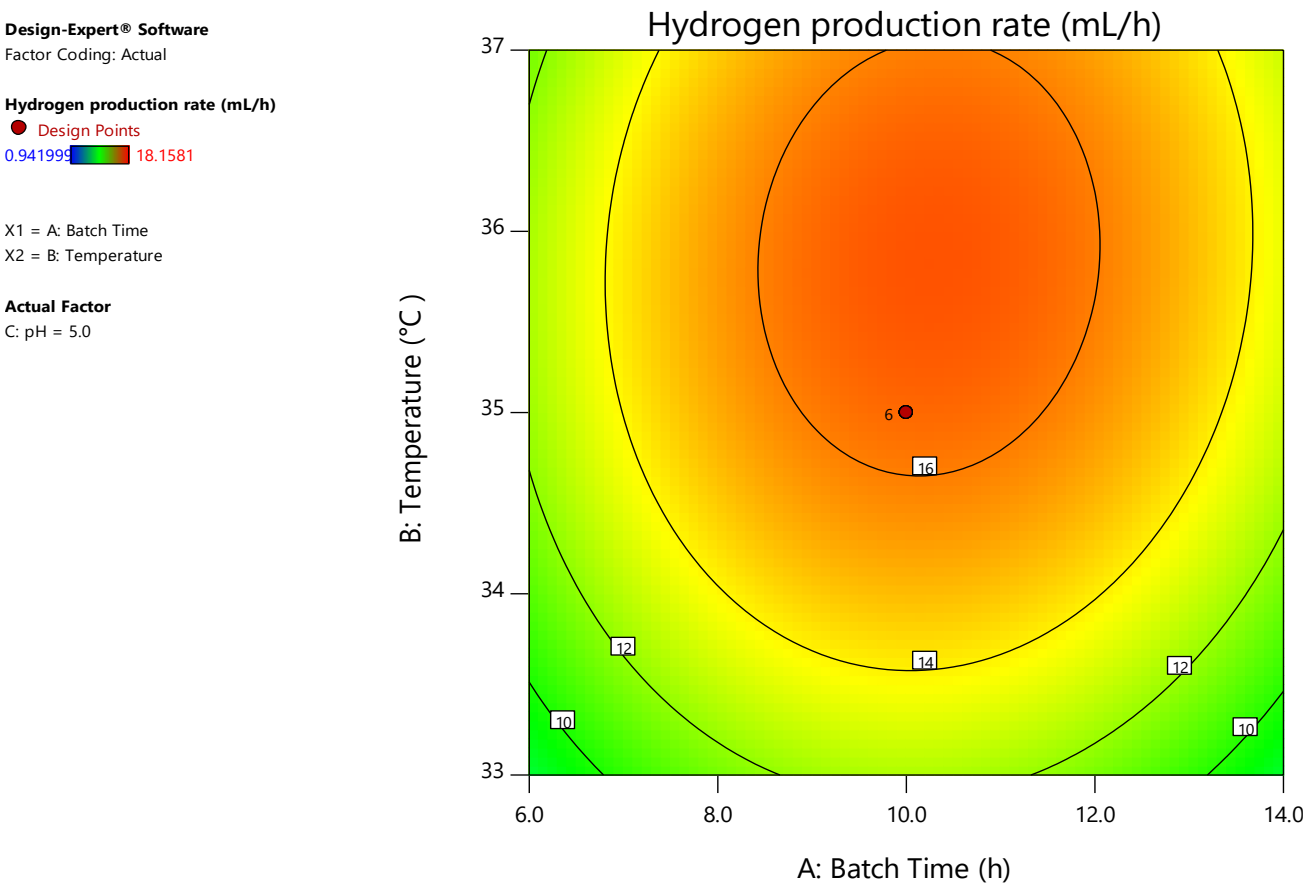

Figure H2: Graphical representation for the Hydrogen Production Rate

Table H3: ANOVA for Reduced Cubic model

Response 2: COD removal efficiency

Source	Sum of Squares	df	Mean Square	F-value	p-value	
Model	3352.35	12	279.36	20.38	0.0003	significant
A-Batch Time	700.78	1	700.78	51.13	0.0002	
B-Temperature	243.76	1	243.76	17.79	0.0040	
C-pH	292.48	1	292.48	21.34	0.0024	
AB	10.32	1	10.32	0.7532	0.4142	
AC	14.58	1	14.58	1.06	0.3367	
BC	61.78	1	61.78	4.51	0.0714	
A^2	125.43	1	125.43	9.15	0.0192	
B^2	0.3458	1	0.3458	0.0252	0.8783	
C^2	274.29	1	274.29	20.01	0.0029	
ABC	26.25	1	26.25	1.92	0.2089	
A^2B	7.32	1	7.32	0.5338	0.4887	
AC^2	15.92	1	15.92	1.16	0.3169	
Residual	95.94	7	13.71			
Lack of Fit	12.31	2	6.16	0.3680	0.7094	not significant
Pure Error	83.63	5	16.73			
Cor Total	3448.29	19				

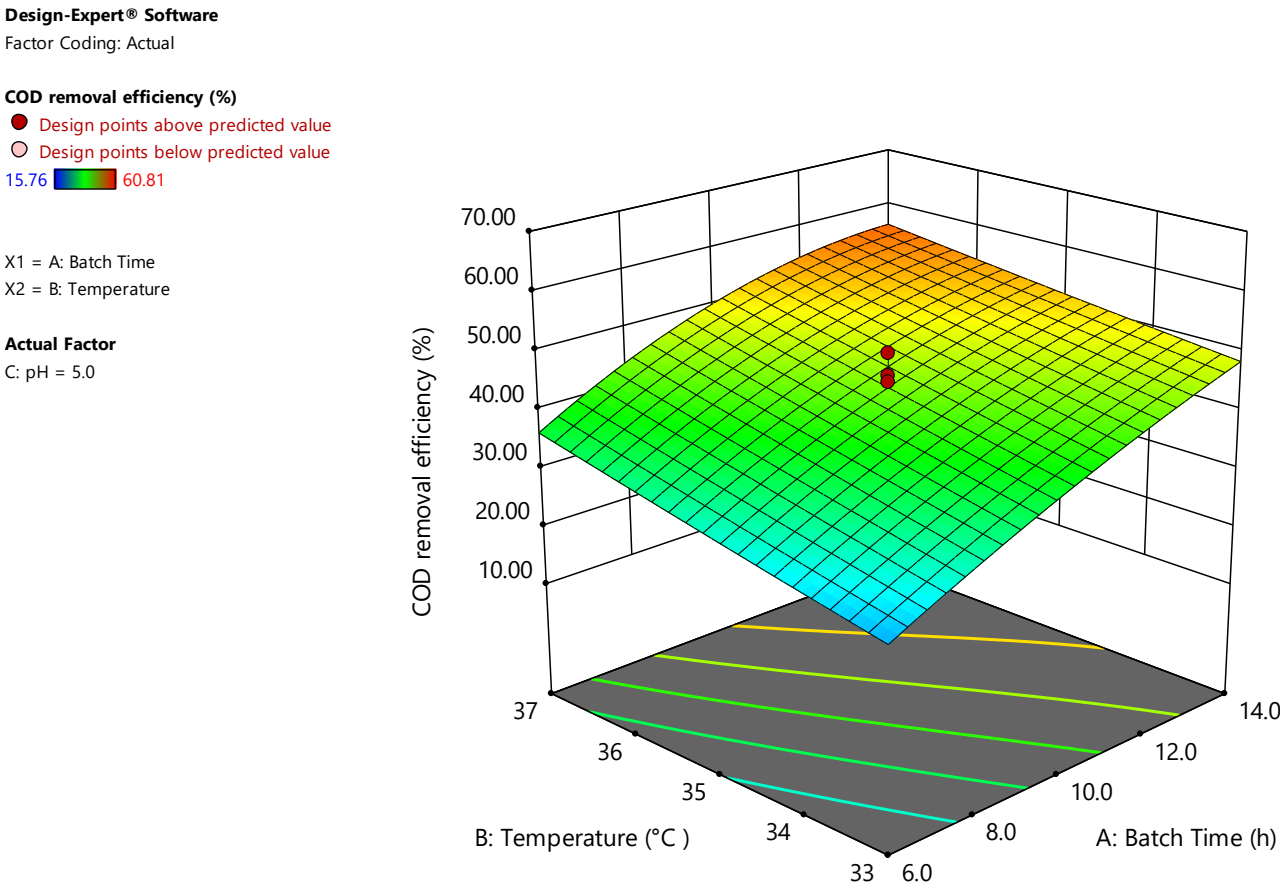

Figure H4: Surface plot for COD removal efficiency

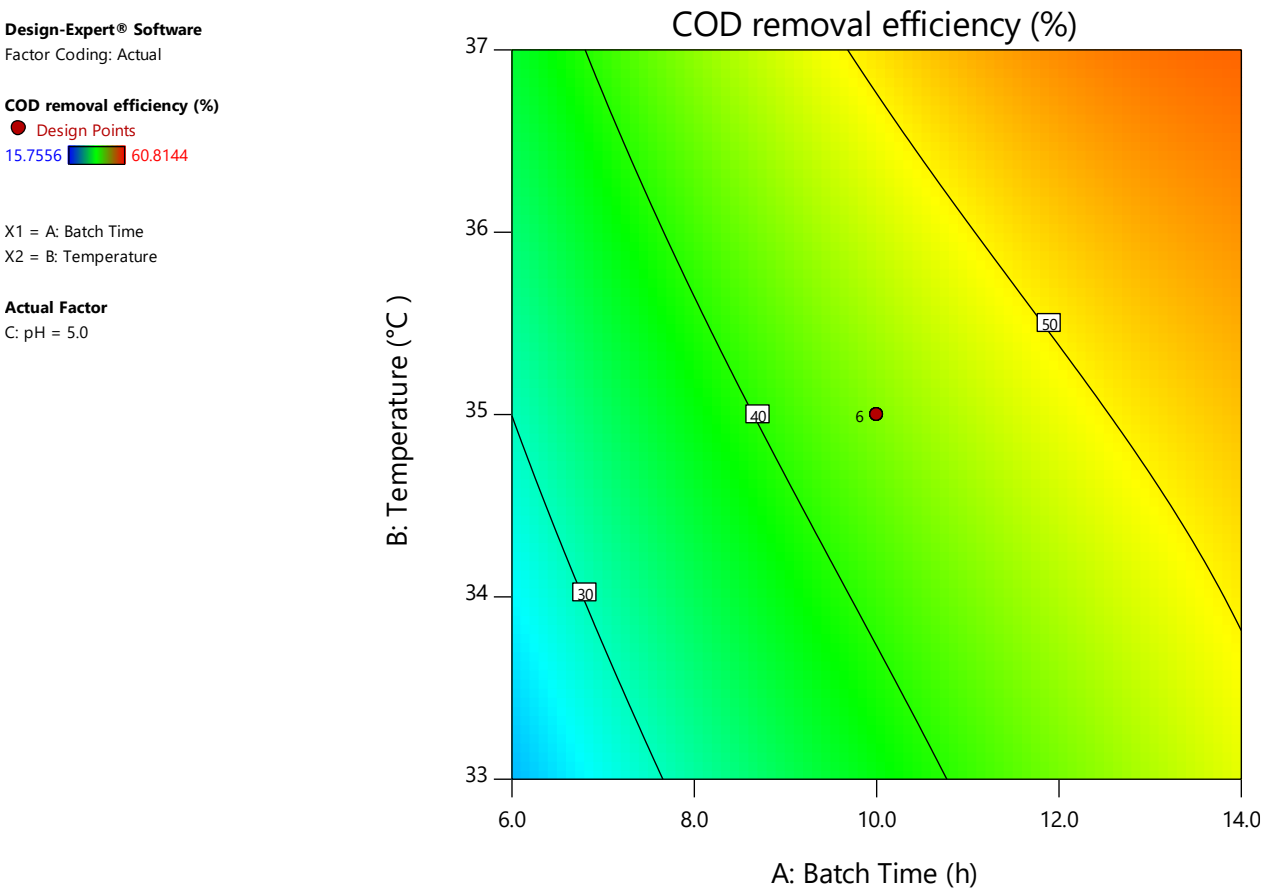

Figure H5: Contour plot for COD removal efficiency

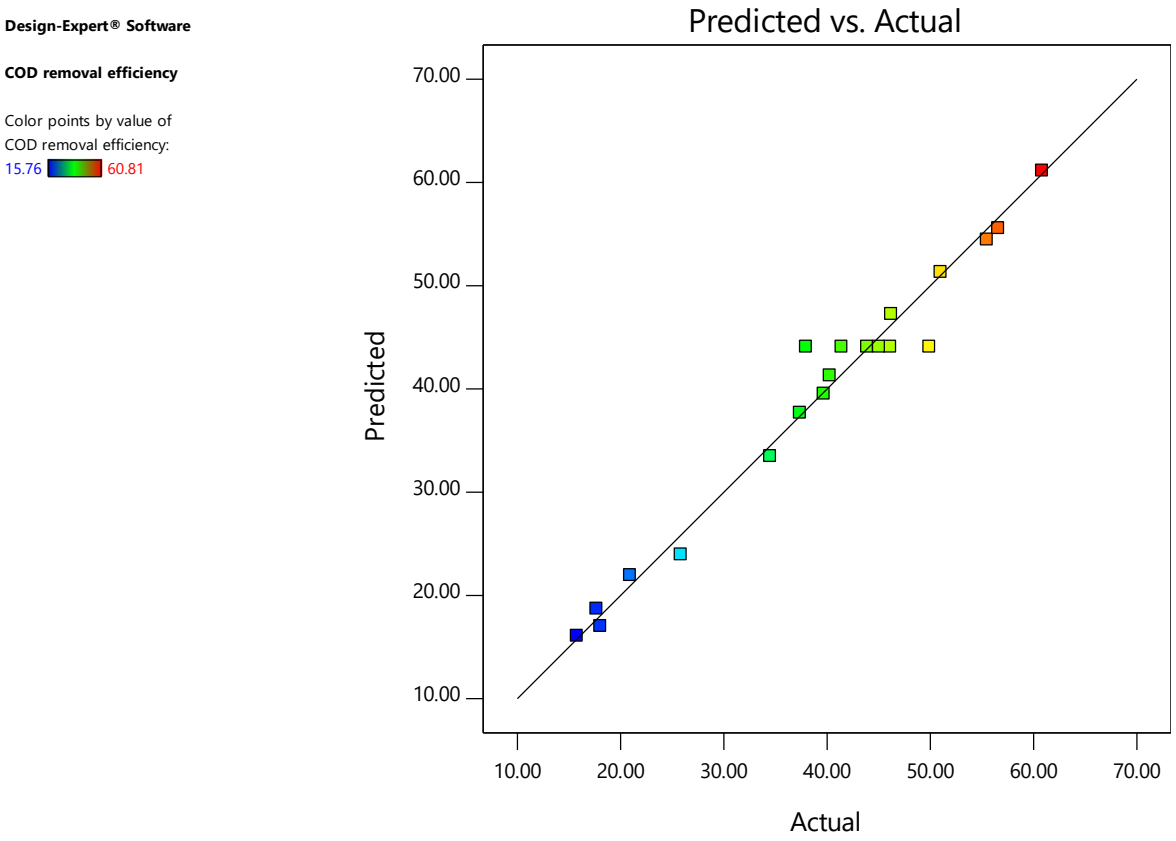

Figure H6: Predicted vs Actual COD removal efficiency

Table H7: ANOVA for Quadratic model

Response 3: VFA

Source	Sum of Squares	df	Mean Square	F-value	p-value	
Model	6.116E+05	9	67959.91	5.35	0.0075	significant
A-Batch Time	30780.79	1	30780.79	2.42	0.1507	
B-Temperature	34233.92	1	34233.92	2.69	0.1318	
C-pH	3877.42	1	3877.42	0.3051	0.5928	
AB	4950.13	1	4950.13	0.3896	0.5465	
AC	3042.00	1	3042.00	0.2394	0.6352	
BC	6612.50	1	6612.50	0.5204	0.4872	
A^2	2.536E+05	1	2.536E+05	19.95	0.0012	
B^2	42470.34	1	42470.34	3.34	0.0975	
C^2	3.131E+05	1	3.131E+05	24.64	0.0006	
Residual	1.271E+05	10	12707.17			
Lack of Fit	1.206E+05	5	24116.07	18.58	0.0030	significant
Pure Error	6491.33	5	1298.27			
Cor Total	7.387E+05	19				

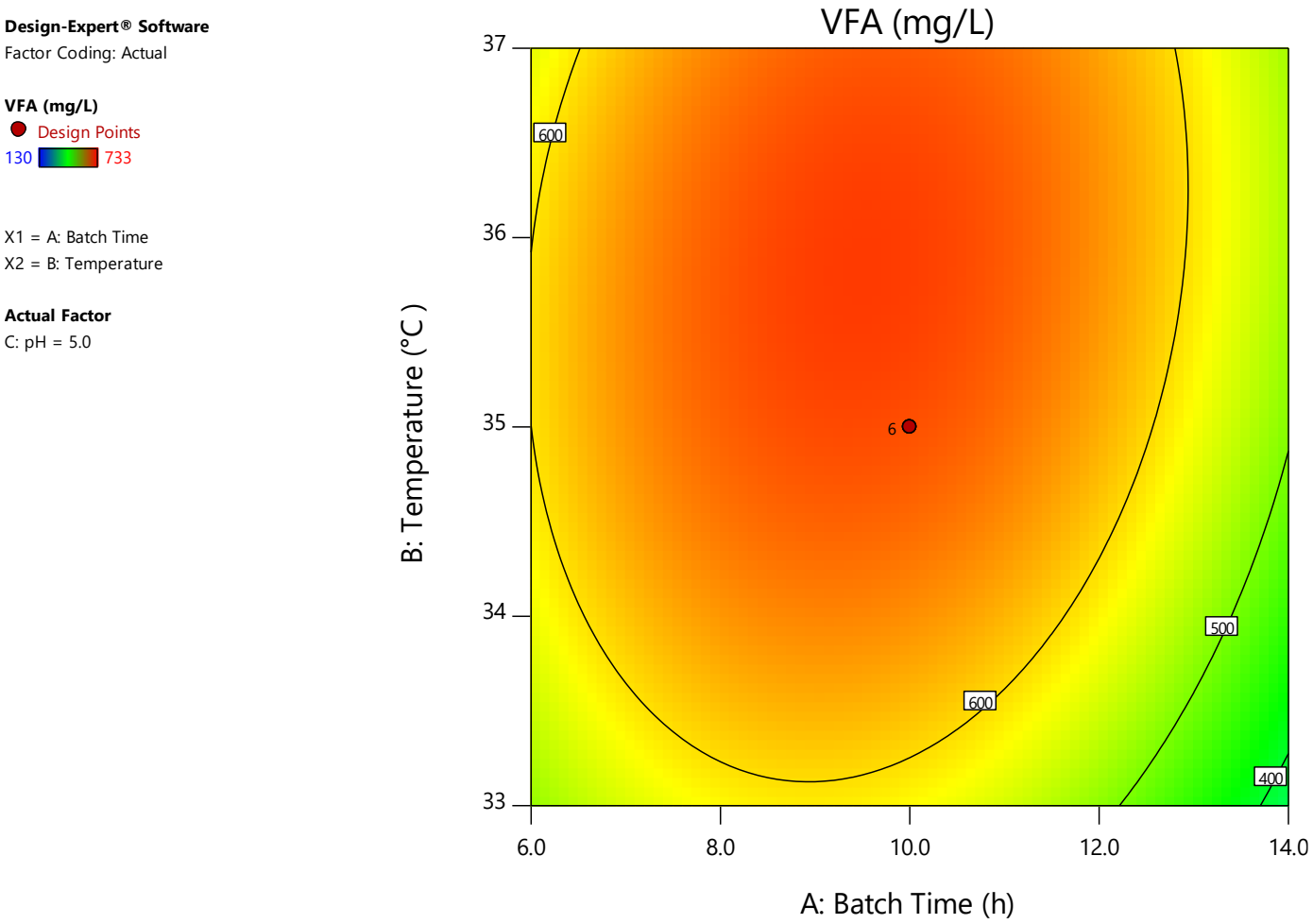

Figure H8: Contour plots for COD removal efficiency

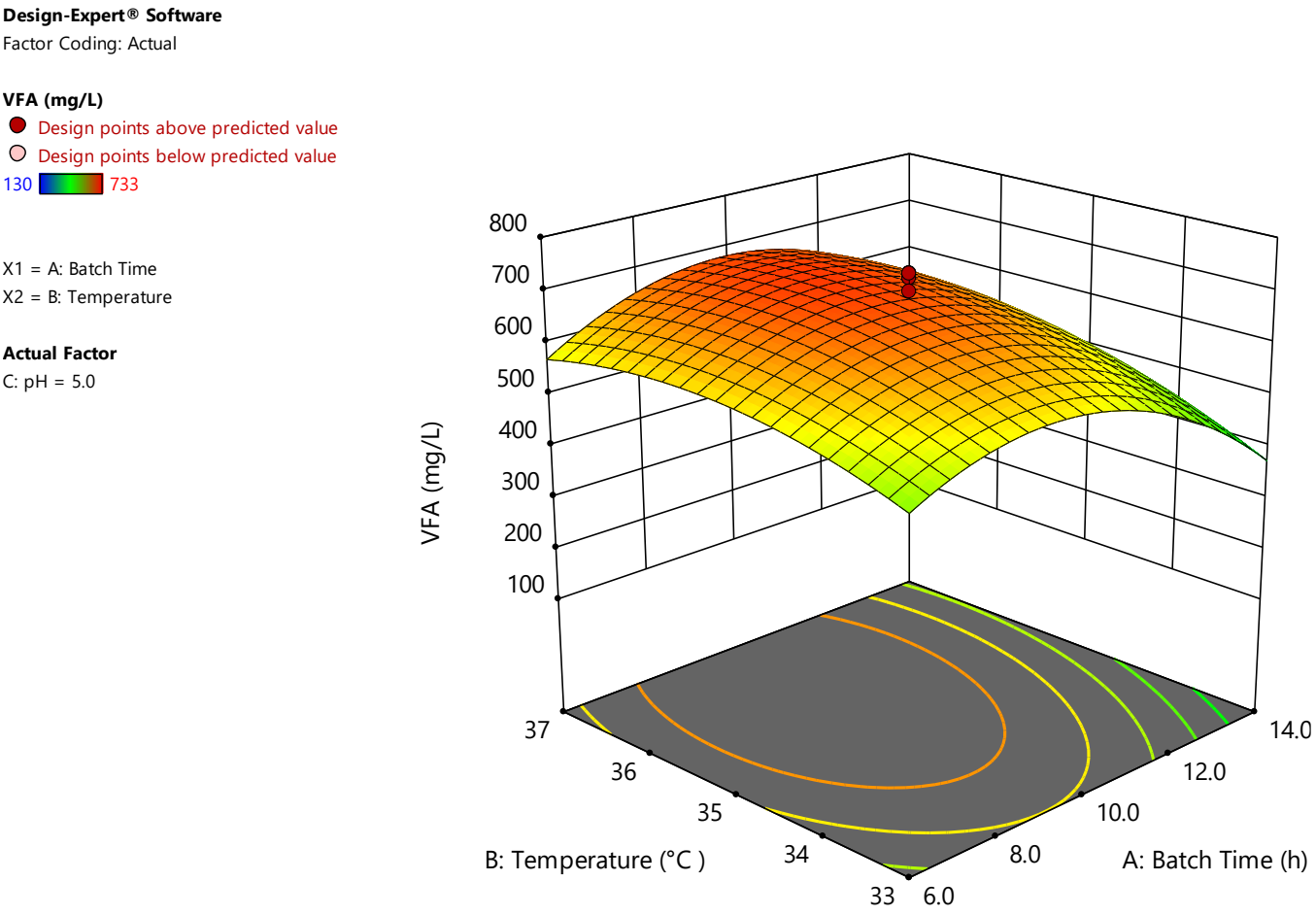

Figure H9: Surface Plot for the VFA concentration in the effluent

Table H10: Coefficients Table for predictive models of all responses

	Intercept	A	B	C	AB	AC	BC	A^2	B^2	C^2	ABC	A^2B	AC^2
Hydrogen production rate	16.3781	0.312809	**1.81305**	**2.61047**	0.330229	-0.271501	1.24592	**-3.77423**	**-2.14633**	**-4.28745**			
p-values		0.6005	**0.0106**	**0.0011**	0.6715	0.7269	0.1303	**<0.0001**	**0.0034**	**<0.0001**			
COD removal efficiency	44.1013	**11.1302**	**6.56437**	**4.62777**	-1.13596	1.35001	2.77893	**-2.95024**	0.154906	**-4.36271**	-1.8115	-1.48593	2.19183
p-values		**0.0002**	**0.0040**	**0.0024**	0.4142	0.3367	0.0714	**0.0192**	0.8783	**0.0029**	0.2089	0.4887	0.3169
VFA	685.109	-47.475	50.0672	16.8499	24.875	-19.5	28.75	**-132.643**	-54.2865	**-147.404**			
p-values		0.1507	0.1318	0.5928	0.5465	0.6352	0.4872	**0.0012**	0.0975	**0.0006**			

Appendix I: Turnit in report

turnitin

Digital Receipt

This receipt acknowledges that Turnitin received your paper. Below you will find the receipt information regarding your submission.

The first page of your submissions is displayed below.

Submission author:	Boldwin Mutsvene
Assignment title:	Publication
Submission title:	Boldwin Final
File name:	Final_Thesis_Boldwin_M.docx
File size:	14.63M
Page count:	188
Word count:	45,092
Character count:	252,467
Submission date:	12-Dec-2019 01:42AM (UTC+0200)
Submission ID:	946369705

DUT DURBAN UNIVERSITY OF TECHNOLOGY

ENHANCED BIOHYDROGEN PRODUCTION FROM CARBOHYDRATE-RICH INDUSTRIAL WASTEWATER THROUGH DARK FERMENTATION

Submitted in fulfilment of the requirements for Master of Engineering degree in Chemical Engineering at the Durban University of Technology

By
Boldwin Mutsvene (21649785)

December 2019

Supervisor..... Date.....

Co-Supervisor..... Date.....

Co-Supervisor..... Date.....

Boldwin Final

ORIGINALITY REPORT

9%	6%	2%	5%
SIMILARITY INDEX	INTERNET SOURCES	PUBLICATIONS	STUDENT PAPERS

PRIMARY SOURCES

1	Submitted to University of KwaZulu-Natal Student Paper	1%
2	link.springer.com Internet Source	<1%
3	academicjournals.org Internet Source	<1%
4	hdl.handle.net Internet Source	<1%
5	Abhijit Gadhe, Shriram S. Sonawane, Mahesh N. Varma. "Kinetic analysis of biohydrogen production from complex dairy wastewater under optimized condition", International Journal of Hydrogen Energy, 2014 Publication	<1%
6	Submitted to Caledonian College of Engineering Student Paper	<1%
7	acikerisim.deu.edu.tr Internet Source	<1%
	Submitted to Universiti Malaysia Pahang	